An Investigation into Plasticiser Compatibility and the Development of Novel Bio-based Plasticisers for Polyvinyl Chloride.

Katharine Burns

Doctor of Philosophy (PhD)

2023

An Investigation into Plasticiser Compatibility and the Development of Novel Bio-based Plasticisers for Polyvinyl Chloride.

Katharine Burns

A thesis submitted in partial fulfilment of the requirements of Manchester Metropolitan University for the degree of Doctor of Philosophy

Department of Natural Sciences

Manchester Metropolitan University

Collaborating Establishment – Alphagary Ltd.

2023

Abstract

Polyvinyl Chloride (PVC) is the world's third most commonly used polymer and accounts for 80% of all plasticiser usage worldwide. Plasticisers, such as phthalate esters, are added to PVC to increase flexibility and softness. A number of phthalate esters exhibit toxic and environmentally harmful properties, leading to rapid growth in the development of non-phthalate plasticisers. Compatibility between plasticiser and polymer is crucial for successful formulation of PVC compounds. Compatible plasticisers show permanence in the PVC compound, whereas incompatible plasticisers often exude from the surface. The ASTM D3291 Loop compatibility test is the primary industrial method for testing compatibility, but this relies on a subjective observation of plasticiser exudation which may be unreliable. Analytical techniques were evaluated to develop an improved method for testing plasticiser compatibility. GC-MS analysis was found to be specific and sensitive enough to determine the quantity and composition of plasticiser exudation at levels that were undetectable by the standard method. Quantification of exudation through GC-MS was compared to other methods of testing plasticiser compatibility such as glass transition by TGA, giving minimal correlation between the results. This demonstrates the importance of considering both plasticising ability and permanence in the PVC compound when describing plasticiser compatibility. Epoxidised soybean oil (ESBO) is widely used as a bio-based non-toxic plasticiser for PVC but does not show the same plasticising ability as phthalates and so cannot fully replace these plasticisers. To improve the compatibility of ESBO with PVC, a selection of bio-based molecules were reacted with ESBO by epoxide ring-opening to introduce different functional groups to the plasticiser through ether linkages. Four derivatives of ESBO were prepared and evaluated as bio-based plasticisers for PVC. ESBO functionalised with methoxy-terminated poly(ethylene glycol) (mPEG) showed excellent plasticising ability, with tensile strength increased by 3% and elongation at break by 6.9%, as well as almost 2 °C lower glass transition temperature compared to ESBO. The novel plasticiser mPEG-ESBO offers for the first time a bio-based ESBO derivative which could be used as a true replacement for phthalate plasticisers, giving comparable mechanical performance and compatibility with PVC.

Acknowledgements

I would like to thank Duncan Makin and Frank Johnson for starting me upon my PhD journey. I would also like to thank my former colleagues from Alphagary - Anna, Alan, Kate, Dave, Matty, Daniel, Collie and Scott - for their support and friendship along the way.

My biggest thanks go to my supervisors, Professor Herman Potgieter, Dr Ian Ingram, Dr Sanja Potgieter-Vermaak and Dr Chris Liauw, for all of their mentorship and guidance. Their encouragement has been invaluable through the many challenges that seemed impossible. I would also like to thank all of the support staff at MMU, particularly Hayley Andrews for her help with the SEM imaging.

Finally, I would like to thank my family, and most of all Greg for being there for me throughout. I couldn't have made it this far without you.

Contents

List of Figures

List of Schemes

List of Tables

Abbreviations

ASTM – American Society for Testing and Materials

ATBC – Acetyl Tributyl citrate

ATR – Attenuated Total Reflectance

BMB – Biomass Balance

COSY – Correlated Spectroscopy

CPSIA – Consumer Product Safety Improvement Act

d – doublet

dd – doublet of doublets

ddd – doublet of doublet of doublets

DBP – Dibutyl phthalate

DCM – Dichloromethane

DDP – Di decyl phthalate

DEPi – Diethyl pimelate

DiDP – Di Isodecyl phthalate

DINP – Di isononyl phthalate

DMA – Dynamic Mechanical Analysis

DMPi – Dimethyl pimelate

DnOP – Di n-octyl phthalate

DOP or DEHP – Di Octyl (or Ethyl Hexyl) phthalate

DOSY – Diffusion–Ordered Spectroscopy

DOTP or DEHT – Di Octyl (or Ethyl Hexyl) terephthalate

DPHP – Di Propyl heptyl phthalate

DSC – Differential Scanning Calorimetry

EFAME – Epoxidised Fatty Acid Methyl Ester

EN – Ethyl naphthalene

ESBO – Epoxidised Soybean Oil

ESO – Epoxidised Sunflower Oil

EU – European Union

FDA – United States Food and Drugs Administration

FTIR – Fourier Transform InfraRed spectroscopy

FWHM – Full Width at Half Maximum

GC-FID – Gas Chromatography - Flame Ionisation Detection

GC-MS – Gas Chromatography - Mass Spectrometry

HSP – Hansen Solubility Parameters

ID – Inner Diameter

IEEP – Isosorbide Ether ESBO Polyol

IR – Interaction Radius

IRE – Internal Reflection Element

ISO – International Organization for Standardization

LC-MS – Liquid Chromatography - Mass Spectrometry

LN – Liquid Nitrogen

m – multiplet

MEEP – Methyl Ether ESBO Polyol

MEFE – Methyl ESBO Furoic Ester

mPEG – Methoxy Polyethylene

MTBE – Methyl tert-Butyl Ether

m/z – Mass to Charge ratio

NMR – Nuclear Magnetic Resonance

PEG – Polyethylene Glycol

PHR – Per Hundred Resin

PPM – Parts Per Million

pPVC – Plasticised Polyvinyl Chloride

PTFE – Polytetrafluoroethylene

PTSA – p-Toluene Sulfonic Acid

PVC – Polyvinyl Chloride

q – quartet

REACH – Registration, Evaluation, Authorisation and Restriction of Chemicals

(European Union Regulation)

s – singlet

S-PVC – Suspension PVC

SEM – Scanning Electron Microscopy

SIM – Selected Ion Monitoring

t – triplet

TBC – Tributyl Citrate

TEM – Transmission Electron Microscopy

THF – Tetrahydrofuran

TIC – Total Ion Current

TGA – Thermogravimetric Analysis

USA – United States of America

UTM – Universal Testing Machine

VCM – Vinyl Chloride Monomer

Research Contributions

The work presented in this thesis has been presented and published in the following formats:

ACI European PVC Industry Summit oral presentation (2019, London) – Evaluating plasticiser compatibility through analytical techniques.

PVC 2021 Conference oral presentation (online) – Analytical Techniques for Determining Plasticiser Compatibility.

SCI Early Career Materials Annual Conference, poster presentation (2022, London) – Improving sustainability in the PVC Industry – Replacing Phthalate Plasticisers with Bio-based Alternatives from Soybean Oil

K. Burns, H. Potgieter, S. Potgieter-Vermaak, I. Ingram, C. M. Liauw 'A Comparative Assessment of the Use of Suitable Analytical Techniques to Evaluate Plasticiser Compatibility' – Journal of Applied Polymer Science, 10.1002/app.54104

K. Burns, I. Ingram, H. Potgieter, S. Potgieter-Vermaak. 'Synthesis and performance evaluation of novel soybean oil-based plasticisers for polyvinyl chloride (PVC).' –Journal of Applied Polymer Science, 10.1002/app.54656

1 Introduction

1.1 History of PVC

The synthesis of vinyl chloride monomer (VCM) was first reported in 1835, and the light-induced polymerisation of VCM to polyvinyl chloride (PVC, Scheme 1.1) was first reported in 1872 by Baumann.[1] The first patent for PVC was obtained in 1913 by Klatte,[2] who discovered the use of peroxides to initiate polymerisation of VCM.[3] Klatte successfully processed PVC using heat and pressure with the aim to use PVC as a replacement for natural fibres and lacquers, however this was not commercially successful.[3]
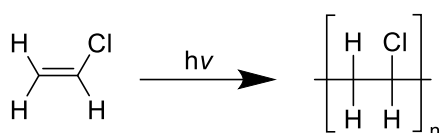
Scheme 1.1: Light-induced polymerisation of vinyl chloride monomer (VCM) to polyvinyl chloride (PVC).

Early commercial use of PVC was in the form of copolymers such as PVC-vinyl acetate copolymer to overcome the difficulties in processing and thermal stability that PVC presents. In 1930 the use of metal salts to stabilise PVC was reported, followed by alkaline earth soaps and lead salts in 1934.[3] Many other stabiliser systems were subsequently developed, including cadmium, barium-zinc, calcium-zinc and tin compounds. Due to toxicology concerns, cadmium and lead stabilisers have since been phased out in the EU under the voluntary commitment scheme Vinyl 2010.[4] PVC is now one of the most commonly used plastics in the world, with around 50 million tonnes produced annually.[5, 6] The largest sector for PVC usage is in construction, which mainly uses rigid (unplasticised) PVC. However, flexible, plasticised PVC has a much more diverse range of applications, due to the many different properties that can be introduced through choice of additives. These include medical tubing, blood bags, footwear, cables, flooring and toys.[5] The plasticiser composition used in a PVC formulation can be specifically tailored to give rise to properties such as oil resistance,

flame retardancy, low temperature flexibility, resistance to high temperatures and products with a wide range of softnesses.[7]

1.2   PVC Production

The polymerisation of vinyl chloride is carried out through radical reactions as shown in Schemes 1.1-1.4.[8] The majority of commonly used initiators are peroxides such as cumyl peroxyneodecanoate and benzoyl peroxide. These initiators form radicals upon heating, which react with the vinyl chloride monomer as shown in Scheme 1.2. The resulting radicals then continue to react with further monomer in the propagation step, growing the polymer chain through subsequent reaction steps (Scheme 1.3). Head-to-tail addition of vinyl chloride is the predominant mode of reaction due to steric factors. However, head-to-head addition is also possible and can lead to defect structures in the polymer as shown in Scheme 1.4 through 1,2-chloro migration.[9]
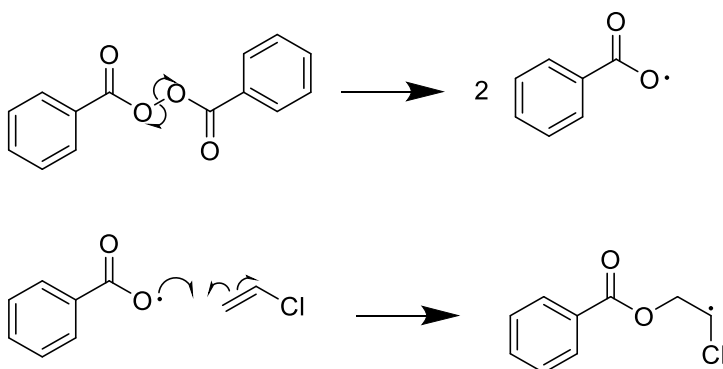
Scheme 1.2: Activation of benzoyl peroxide to form radical initiators and initiation reaction between benzoyl peroxide fragment and VCM.
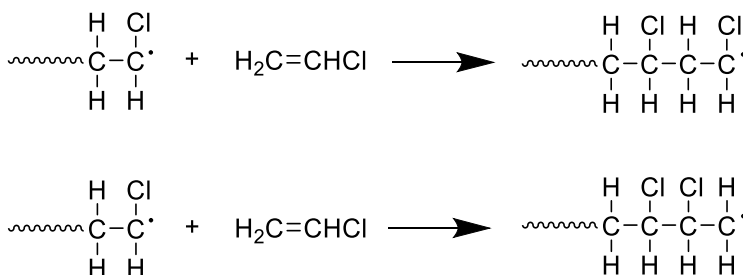
Scheme 1.3: Head-to-Tail and Head-to-Head propagation reactions between the growing polymer chain radical and VCM.
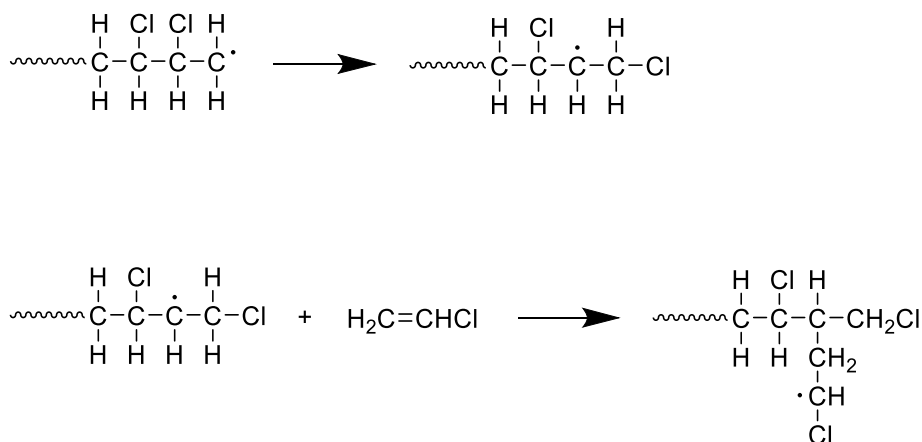
Scheme 1.4: 1,2-chloro migration and subsequent reaction with VCM leading to a branched structural defect in the polymer chain.

Termination can occur through a number of different processes, but the most common are combination (wherein two radicals react to form a single polymer chain) and disproportionation (the transfer of a hydrogen atom from one radical chain to another, forming two polymer chains) as shown in Scheme 1.5.
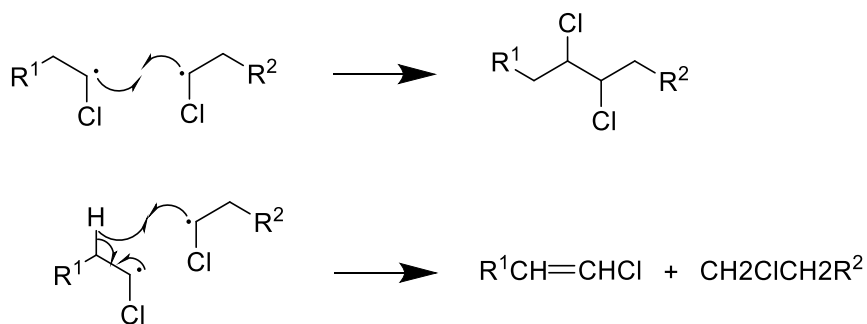
Scheme 1.5: Combination and disproportionation mechanisms for termination of PVC polymerisation.

The polymerisation of VCM leads to an overall atactic (disordered) arrangement of the chlorine atoms on the polymer backbone, although segments of isotactic and syndiotactic arrangements (Figure 1.1) do occur. Syndiotactic addition has a lower activation energy than isotactic addition as this conformation is less sterically hindered. As such, at lower reaction temperatures there is a greater prevalence of syndiotactic segments in the PVC structure.[9]
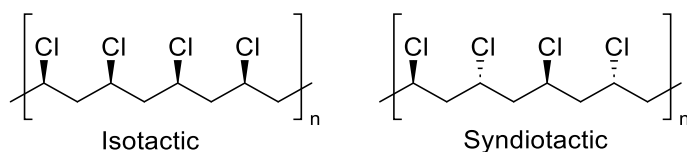
Figure 1.1: Structures of isotactic and syndiotactic PVC.

PVC resins are produced industrially by three main processes: suspension polymerisation (80% of total production), emulsion polymerisation and bulk polymerisation.[10] In the suspension process, vinyl chloride monomer (VCM) is suspended in small droplets (50 – 150 µm diameter) in an aqueous solution with suspending agents (e.g. vinyl acetate/vinyl alcohol copolymers or cellulose) and an initiator (typically a peroxide), which are reacted by mixing under heat and pressure.[5] Polymerisation occurs within these droplets, which form a semi-permeable membrane through copolymerisation of VCM and the suspension agents.[10] This membrane defines the 'subgrain' structure of the PVC, which can either remain as a single grain in the final product or may coalesce with other subgrains to form a larger agglomerate grain. Grains produced by suspension polymerisation are typically of the order of 100 µm diameter, with internal structures consisting of primary particles ($\sim$ 1 µm), which have been examined by scanning electron microscopy (SEM) as well as smaller structures known as microdomains (10 nm) which were observed by transmission electron microscopy (TEM).[5] Grains of PVC resin produced by suspension polymerisation are irregularly shaped and porous. The porosity allows plasticiser to be absorbed by the grains prior to gelation of the PVC-plasticiser blend. The reaction conditions as well as the choice of suspension agents and initiators control the morphology and molecular weight of the resulting PVC molecules.[10] As the polymerisation reaction proceeds mainly through chain transfer steps, temperature is the main factor controlling chain length, and thus molecular weight.

Emulsion PVC uses emulsifying agents to mix the VCM with water before polymerisation occurs. This generally gives a finer particle size, but the resultant PVC may contain residual emulsifiers which cause poor clarity in the finished products.[5] Emulsion and suspension polymerisation are carried out in water to control the heat released from the exothermic polymerisation reaction. However, VCM can be

polymerised in the absence of water using the Bulk polymerisation process. This is a two-stage process with high-speed mixing of the liquid VCM initially, before transferring it to a slower mixer as the viscosity increases due to the growth of PVC chains.[5]

Vinyl chloride monomer is most often produced from ethylene from petrochemical sources. However, a process for the production of VCM from biomass-based acetylene has been patented.[11] This process has been commercialised by PVC producers such as Ineos and Vynova, who report a 90% reduction in carbon dioxide emissions relative to conventional PVC production.[12, 13] This development shows that PVC products can form a part of a circular economy and so reinforces the importance of sourcing the other components of the PVC formulation from biomass.

Plasticised PVC is mainly supplied in one of two forms - as a PVC "compound" or as a plastisol. The term PVC compound is used to describe a mixture of PVC resin and a number of additives such as plasticiser, filler (typically calcium carbonate), and heat stabiliser, which are mixed together and then usually extruded through a die and cut into small pellets of material. This process melts the PVC particles to form a homogeneous product and is known as compounding. Compounding can be used for plasticised and unplasticised PVC products, and the resulting pellets can be used to produce finished articles by processes such as extrusion, injection moulding or calendaring. Plastisols are mixtures of PVC and additives that creates a free-flowing suspension through the use of low viscosity plasticisers.[5] These are either poured or spread to the required shape, and then cured to melt the PVC particles and form a solid product. This is often used to coat fabrics by screen printing, or as a dip-coating. PVC compounding typically uses PVC resin produced by suspension polymerisation, while emulsion PVC resins are used in the production of plastisols.[7]

PVC molecular weight is most often expressed as the Fikentscher K-value, a function of the viscosity of the polymer in a dilute solution Equation 1-1),

$$\log \frac{\eta_c}{\eta_0} = \left(\frac{75k^2}{1 + 1.5kc} + k \right) c$$

Equation 1-1

where the η_c is the viscosity of the solution, η_0 is the viscosity of the solvent, c is the concentration of the polymer solution and k is a constant.[8] The Fikentscher K-value is related to the constant k as shown in Equation 1-2.

$$K = 1000 \, k$$

Equation 1-2

The choice of K-value for PVC resin influences many of the properties of the PVC formulation. Higher K-values give rise to increased tensile strength, impact strength and melt viscosity. As such, plasticised PVC formulations typically use resins with a K-value of 70-100, while unplasticised PVC formulations use resins with a K-value 50-68. This range (K50 to K100) is equivalent to a weight average molecular weight of 40-200 x10^3 Da.[14]

1.3 Plasticisation of PVC

Plasticisers are high boiling point solvents that increase the flexibility of polymers by reducing the intermolecular interactions between the polymer chains. This allows the chains to move more freely and so imparts flexibility to the polymer matrix. A compound will solvate a polymer successfully if the intermolecular forces between the polymer and solvent are stronger than those of polymer-polymer and solvent-solvent. If this is not the case, the polymer and solvent will tend towards forming separate domains within the material.[2]

The global plasticiser market was estimated at nearly 10 million tons in 2020, of which 80% are used in the production of flexible PVC.[6] The first plasticisers to be used in PVC were phthalates (e.g. diethylhexyl phthalate **1**, Figure 1.2) and phosphates (**2**), reported in 1933 by Semon.[15] Dibutyl phthalate was the first phthalate to be used in

PVC.[5] Diethylhexyl phthalate (often abbreviated to DEHP or DOP[*]) replaced this as the most common plasticiser for PVC by 1950 and remained so until recent years, when concerns over the safety of phthalates have led to a reduction in use.[16] Toxicological investigations in the 1980s suggested a possible carcinogenic effect of DOP exposure, as liver cancer was observed in rodents exposed to DOP *in vivo*.[17] Whilst no evidence has been found that DOP is carcinogenic in humans, it does show endocrine-disrupting and reprotoxic effects, and so there was public pressure to reduce usage and find alternative plasticisers.[18] The mechanism is not fully understood, however molecular modelling shows that DOP and its metabolites can bind to androgen receptors with a 91-100% similarity to testosterone, and thus disrupt hormone regulation.[19]
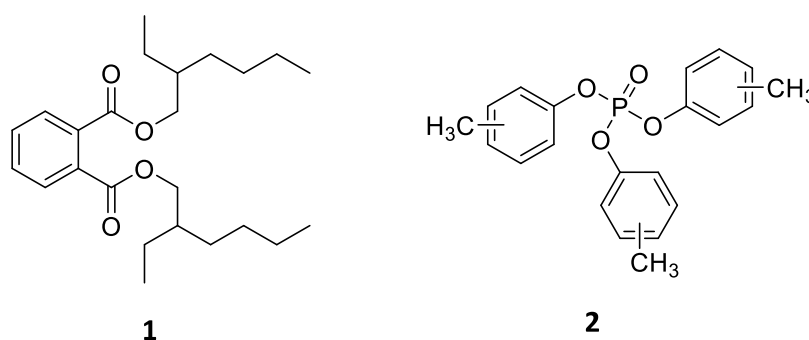
*Figure 1.2: Chemical structure of early plasticisers diethylhexyl phthalate (DEHP/DOP **1**) and tricresyl phosphate **2**.*

As of 2015, DOP represented only 13% of the EU plasticiser market.[20] DOP and other low molecular weight phthalates have been added to the REACH Annex XIV "Authorisation List", which restricts the manufacture and use of these substances within the EU. Other phthalates that are not restricted under REACH, such as diisononyl phthalate (DINP) and dipropyl heptyl phthalate (DPHP), are also considered a toxicity risk and so are prohibited from use in products designed to be placed in children's mouths.[16] In spite of this, phthalates still make up the majority of the

---

[*] The linear di n-octyl phthalate is often referred to as DnOP to distinguish this from the use of DOP to refer to diethylhexyl phthalate.

plasticiser market, with over 50% of the total EU market in 2020.[20] Phthalates have also been restricted from use in the USA by CPSIA and Proposition 65 in California.[21, 22] Despite these restrictions, many phthalates and alternative plasticisers have been detected in samples of dust and airborne particles in studies of homes and childcare facilities across Europe, the USA and Asia.[23, 24]

Due to these restrictions and public pressure, many alternative plasticisers have been developed. The majority of these plasticisers are esters such as adipates (**3,** Figure 1.3), azelates (**4**), sebacates (**5**), terephthalates (**6)** and citrates (**7**). The most widely used terephthalate, DEHT or DOTP **6**, is the *para* isomer of DOP. However, it has been shown that DOTP does not pose the same health risks as DOP. This is due to the difference in metabolites formed by the two compounds in the body - DOTP metabolises completely to terephthalic acid and 2-ethylhexanol, while DOP is metabolised to mono-ethylhexyl phthalate (MEHP), which is thought to cause the observed toxicity of DOP.[18]
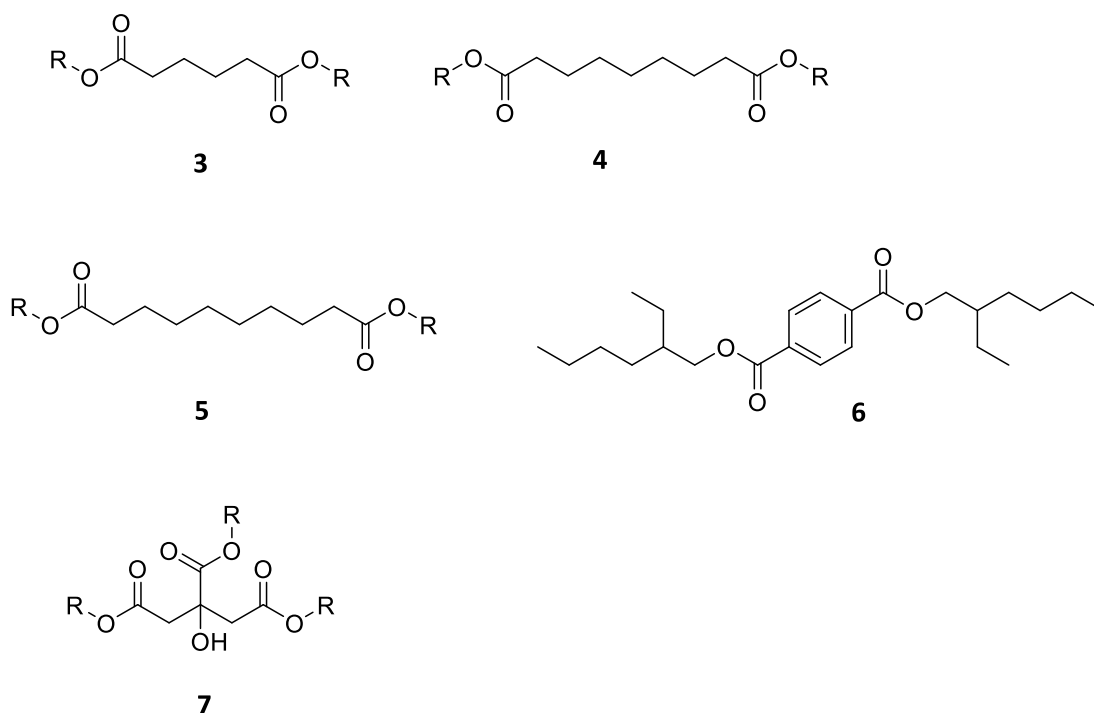
*Figure 1.3: Chemical structures of common plasticiser types - adipate ester **3**, azelate ester **4**, sebacate ester **5**, diethylhexyl terephthalate (DEHT/DOTP, **6**) and citrate ester **7**.*

While lower toxicity plasticisers have largely replaced the more hazardous phthalates in the EU and USA, these are primarily still petrochemical plasticisers.[20] As such, there remains the need to develop plasticisers based on renewable bio-based raw materials such as vegetable and plant oils. Oils such as sunflower, soybean, castor and linseed have been epoxidised for use as plasticisers for PVC.[16] The degree of potential epoxidation will depend upon the unsaturation present in the oil. A typical composition of soybean oil is 53% 18:2 (fatty acid chain length: unsaturation), 22% 18:1, 12% 16:0, 8% 18:3, 5% other, thus giving approximately 5 epoxide groups in the resulting ESBO.[25] The structure of epoxidised soybean oil (ESBO, **8**) shown in Figure 1.4 is based on a triglyceride of linoleic (18:2) and oleic (18:1) acids as an example of a typical major component of ESBO.[26] The conversion of double bonds to epoxides is considered to correlate with greater compatibility as the more polar epoxide group can interact with the polar PVC chain to a greater extent than the C=C bond.[27] Residual unsaturation, as measured by iodine number, following the epoxidation of these plasticisers has been shown to increase migration from PVC.[27]
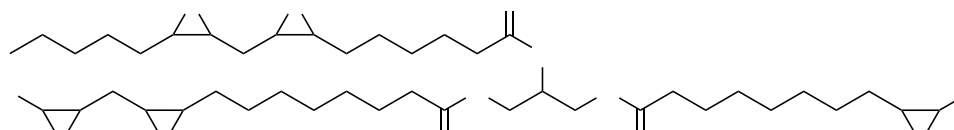
8

*Figure 1.4: A representative structure of epoxidised soybean oil **8** based on the typical fatty acid composition.*

Plasticisers for PVC are categorised as primary and secondary. Primary plasticisers have good solubility in the polymer and can be used at high concentrations, while secondary plasticisers are less soluble and must be used in combination with a primary plasticiser.[2] Secondary plasticisers often impart useful properties such as increased thermal stability, flame retardancy, or simply reduced cost.[7] However, these plasticisers can only be successfully combined with primary plasticisers in certain ratios, outside of which exudation of the plasticisers occurs.[16] It has been observed

from common practice that reduced compatibility occurs when the secondary plasticiser ESBO is used in combination with DOTP, compared to DOP. However, where binary plasticiser systems have been examined in the literature, reports frequently investigate the compatibility of novel bio-based plasticisers with DOP, despite the restrictions on its use.[28, 29] Functionalisation of ESBO and other similar bio-based plasticisers has received much interest lately, due to the reactive nature of the epoxide ring.[16, 30] The ring-opening reaction of ESBO has most commonly been investigated to form polyols which are then used in the synthesis of bio-based polyurethanes.[31-33]

The presence of plasticisers in flexible PVC compounds presents a significant challenge for recycling these materials. The VinyLoop project was launched in 2002 using a solvent-based process to separate the additives from post-consumer PVC waste. This waste contained high levels of hazardous plasticisers that needed to be separated from the recycled product. In 2018 the project was closed as it was no longer economically feasible.[34] Other recycling initiatives are ongoing, such as RecoMed which aims to increase recycling of single-use medical equipment such as oxygen masks in hospitals.[35] This project focuses on ensuring a controlled waste stream and so does not face the same challenges as the VinyLoop project.

1.4 Measurement of Compatibility

The compatibility of plasticisers is defined by a number of different properties. Some works focus on the ability of the plasticiser to lower the glass transition temperature of the PVC polymer.[36]. Other works measure plasticiser extraction into test liquids such as solvents and oils, or volatility on heating.[37] Theoretical calculations of plasticiser compatibility have also been carried out based on the treatment of the plasticiser-polymer interaction as a solvation mechanism.[38]

In the PVC industry, the ASTM D3291 Loop spew test is frequently used as a measure of compatibility.[39] This test involves stressing samples of plasticised PVC in a 180° bend and evaluating the level of plasticiser exudation that occurs in response to this

stress. Measuring plasticiser compatibility in this way provides useful information to PVC compounders as any tendency for plasticiser to exude under stress in this manner can lead to noticeable degradation of the finished product. This can be observed as a reduction in clarity, a sticky surface or accumulation of dust and dirt on the product. If enough plasticiser is lost from the PVC in this fashion, then the material will become harder and brittle, reducing the lifespan of the product. However, this method relies on a subjective rating of the level of plasticiser exudation on a scale from 0 (no exudation) to 3 (saturated). As such, this method could give different results depending on the judgement of the operator and so has potential for poor reliability and repeatability. The duration of the test is not fixed, but the tests are often carried out over weeks or months.

1.5 Summary

Plasticised PVC is used in a wide range of applications where there are no current alternative materials that are technically and commercially equivalent. A number of the plasticisers used in these materials are known or suspected to have negative impacts on human health. The PVC plasticiser market is currently dominated by petrochemical plasticisers. As such, replacing these petrochemical plasticisers with bio-based alternatives will have a significant impact on the sustainability of PVC products. Alongside the replacement of petrochemical production of PVC with production from biomass, this would contribute significantly towards the circular economy.[11, 40] Bio-plasticisers are a growing market sector and find many uses in PVC production, however these plasticisers are usually not a direct replacement for the phthalates historically used.[16] ESBO is a bio-based plasticiser that is widely used in the PVC industry in combination with other plasticisers but does not match the performance of current petrochemical plasticisers such as DOP and DOTP. Therefore, a need exists for a new generation of bio-derived plasticisers with higher compatibility with PVC which are more able to entirely replace their petrochemical antecedents.

The benefits of using such bio-based plasticisers include lower toxicity, more sustainable and renewable precursors, and lower environmental impact than existing

plasticisers.[16] However, these alternative plasticisers must be evaluated by the manufacturers to ensure the PVC product meets the requirements. The current industry-standard loop spew test is not adequate to fully evaluate the suitability of, and inform formulation with, newer generations of bio-plasticisers. Instead, there is a need for an improved, more quantitative, method which can be implemented with instrumentation available to PVC compounders, such as FTIR and GCMS.

1.6 Aims and Objectives

The first aim of this work will be to evaluate alternative techniques for determining plasticiser exudation during the ASTM D3291 loop spew test and develop a quantitative method for measuring this exudation. This will improve the assessment of new plasticisers for use in PVC. To develop an improved compatibility test for PVC plasticisers, spectroscopic mapping will be evaluated using FTIR-ATR, micro-ATR FTIR, and micro-Raman spectroscopy. The plasticiser exudation will also be measured by GC-MS. The GC-MS and FTIR results will be compared alongside the ASTM standard method to determine the effectiveness of these techniques at improving the test to give a quantitative, analytical measurement of plasticiser compatibility. These results will also be compared with DMA analysis of the glass transition temperature of the PVC compounds, which is another metric of plasticiser compatibility.

The second aim of this work is to synthesise a group of novel plasticisers through ring-opening reactions at the epoxide ring of ESBO. Bio-based chemicals with structural similarities to current plasticisers will be chosen to react with ESBO to introduce functional groups that improve the interaction between the PVC chain and the plasticiser molecule. The catalysts and reaction conditions will be evaluated to give efficient conversion with a minimum of undesired side products. The structure of the products will be evaluated by ^{1}H and ^{13}C NMR, as well as DOSY NMR techniques. FTIR spectroscopy and thermogravimetric analysis (TGA) will also be used to analyse the plasticisers.

Finally, these plasticisers will be evaluated in PVC compounds. The novel plasticisers will be evaluated in a PVC formulation alongside the biobased plasticiser ESBO, and commercial petrochemical plasticisers DOTP and DOP. The plasticised PVC samples will be analysed by DMA, TGA, scanning electron microscopy (SEM) and tensile testing. DMA will be used to determine the glass transition temperature of the samples, as well as any signs of phase separation which may indicate incompatibility between the PVC and plasticiser. TGA will be used to determine the effect of the novel plasticisers on the PVC heat degradation. SEM will be used to examine the microstructure of the plasticised PVC. This can show any areas of phase separation and indicate how well the plasticisers solvate the polymer. Tensile testing will be used to show how well the plasticisers soften the PVC polymer, reducing the tensile strength of the material and increasing the elongation.

1.7 Hypothesis

This work has two hypotheses. The first is that analytical techniques can be used to improve upon the ASTM D3291 Loop spew test, by providing repeatable, objective, and quantitative measures of the amount of plasticiser exuded by PVC samples under compression.

The second is that through the synthesis of a small library of biomass-derived ESBO derivatives a more compatible bio-based "green" plasticiser can be obtained.

1.8 Impact and Contribution

The development of an improved compatibility test will be of value to those connected to the PVC industry, both PVC compounders and the plasticiser suppliers who are developing and marketing green plasticisers for PVC. This would allow more specific comparisons of exudation behaviour between different plasticisers. It would give PVC compounders confidence when testing a novel plasticiser that they can accurately assess the exudation behaviour of the plasticisers in comparison with the plasticisers currently in use. Furthermore, a more quantitative method for testing

plasticiser compatibility that reflects industry requirements would be of value to researchers in the field of novel plasticisers. Exudation is rarely measured in these works but is of high significance to PVC compound manufacturers.

The development of a more compatible green plasticiser would have a number of positive outcomes. Plasticisers can comprise more than 50% of the total weight of a PVC product, and thus if PVC compounders could use a green bio-based plasticiser to replace petrochemical plasticisers, this would reduce the environmental footprint of the PVC product. If this plasticiser is also less toxic than the petrochemical plasticiser, then the resulting PVC products will also be safer for the customers to use. Developing a plasticiser that has a lower tendency to migrate would also benefit the environment, as plasticisers can leach into their surroundings and contaminate waterways. These improvements could add value to the product for the manufacturer by widening the markets in which the product could be used, or by meeting a consumer demand for sustainability in their purchases.

2 Literature Review

This chapter will discuss the interactions between PVC and plasticisers, and theories put forward to explain this relationship. Following this is a discussion of plasticiser exudation, and the development of novel plasticisers to replace the current, largely petrochemical plasticisers. Finally, the analytical techniques used in this thesis are detailed, including the ways in which these techniques have been used in the development and testing of plasticisers for PVC.

2.1 Theories of Plasticisation

There are three primary theories of polymer plasticisation - the free volume theory, lubricity theory and gel theory. In general, the theories describe how plasticiser molecules allow the polymer chains to move more freely by reducing the interactions between the chains. Lubricity theory was developed by Kirkpatrick, Houwink and Clark, and describes the plasticiser behaving as a lubricant to reduce friction between polymer chains, allowing them to move past one another to create flexibility.[41] This requires that the plasticiser contain groups that solvate sections of the polymer chain and groups that lubricate the movement of the chain. Successful solvation of the polymer by the plasticiser was related back to the polarities of the two components, under the principle of "like dissolves like". Clark and Houwink described the polymer-plasticiser system forming a layered structure of polymer and plasticiser planes that could slide past one another.[41]

The gel theory describes the polymer in terms of a large 3-dimensional structure formed by the polymer chains linked at intervals due to loose interactions.[42] In this gel structure, the polymer chains can move randomly to a small degree but are limited by the interactions between the chains. Plasticisers interrupt these linkages by solvating the polymer and allowing greater free motion of the polymer chains. This can be considered as a dynamic equilibrium of solvation and desolvation which allows the plasticiser molecules to move within the polymer structure. This freedom of movement would explain why the softening effect of external plasticisers (which are

not chemically bonded to the polymer) increases with temperature but does not for internal plasticisers, as they are bonded to a certain site.[42] Additionally, this explains the softening effect of non-solvent secondary plasticisers, which have weaker interactions with the polymer than primary plasticisers. These plasticisers reduce the number of linkages between polymer chains due to steric effects.

The Free Volume theory was developed to explain a number of phenomena within plasticised and unplasticised polymers. It was observed that the temperature dependence of the specific volume of polymers undergoes a change at the glass transition temperature T_g, with much greater temperature dependence in the rubbery state above T_g. It was also shown that the viscosity of polymers at their T_g was of similar magnitude for all polymers regardless of the chemical structure, of the order of 10^{12} Pa s.[2] This relationship between the volume of the polymer and the freedom of movement as measured by the viscosity was related to the level of "free volume" within the polymer structure. Free volume is the space within the plastic material that is not occupied by the molecules of polymer or plasticiser and as such is available for molecular movement of the structure. At temperatures above T_g, the polymer has sufficient energy to allow greater freedom of movement than in the glassy state, such that segmental rotation of the polymer chains can occur. The summary of free volume theory by Sears and Darby concludes that the free volume in a polymer is created by the motions of end groups, side chains and the main chain.[43] As such, the free volume can be increased by increasing these motions. Polymers of lower molecular weight (and thus chain length) will have a greater number of chain-ends by mass. The role of external plasticisation is introduced as a "compatible compound of lower molecular weight" that causes an increase in free volume by allowing greater freedom of movement to the main chain by reducing steric hindrance and intermolecular attractions.[43] In the case of most plasticisers, this is due to the flexible alkyl chains, which increase free volume and thus cause a reduction in T_g.

2.2 Theories of Compatibility

A plasticiser is compatible with a polymer if the two remain combined as a homogenous system after mixing, and do not separate for the required lifespan of the resulting product.[2] Models have been proposed to describe this mixing from thermodynamic principles, such as the Flory-Huggins solution theory. This treatment modifies the Gibbs free energy of the mixing equation (Equation 2-1) to account for the large difference in molecular size between a polymer and plasticiser (or solvent). It introduces the Huggins interaction parameter χ_1 as shown in Equation 2-2. This parameter represents the difference in interaction for a plasticiser molecule in the polymer versus in the pure plasticiser.[2]

$$\Delta_{mix}G = \Delta_{mix}H - T\Delta_{mix}S$$

Equation 2-1

$$\frac{\Delta G}{RT} = x_1 \ln \phi_1 + x_2 \ln \phi_2 + \chi_1 \phi_1 \phi_2 \left(x_1 + x_2 \frac{V_2}{V_1} \right)$$

Equation 2-2

Where:

ΔG Gibbs free energy of mixing

x_1, x_2 plasticiser and polymer mole fractions

ϕ_1, ϕ_2 plasticiser and polymer volume fractions

V_1, V_2 plasticiser and polymer molar volumes

χ_1 Huggins interaction parameter.

In general, if $\chi_1 < 0.5$, the plasticiser and polymer will be compatible. This parameter can be estimated experimentally through observations of swelling and dissolution behaviour of the plasticizer and polymer, as well as techniques such as inverse gas chromatography.[2] Herein, the polymer is deposited in the column to form the stationary phase and a solvent 'probe' passed through.[2, 44] From the retention time

of the probe molecule, the volume of carrier gas required to elute the probe molecule (known as the specific retention volume V_g) can be calculated. This can be used to determine the enthalpy of interaction between the stationary phase and the probe, and thus the Huggins interaction parameter for the polymer-solvent pair.[44, 45]

Another treatment of the interactions between plasticiser and polymer is through the use of the Hildebrand solubility parameters. These parameters represent the difference in energy between the liquid and ideal vapour states of a substance, and thus is a measure of the intermolecular attraction in a single liquid.[2] Hildebrand solubility parameters can be used to predict which plasticisers will not dissolve a polymer, as substances with a large difference in solubility parameter will show poor solubility. However, compatibility between a polymer and plasticiser with similar solubility parameters is not guaranteed. The molecular structures of the polymer and plasticiser must also contain suitable functional groups that can interact with one another.[2] The solubility parameter δ is related to the latent heat of vaporisation ΔH_{vap}, the molecular mass M and the density of the substances ρ as shown in Equation 2-3.

$$\delta = \left(\frac{\Delta H_{vap} - RT}{M/\rho}\right)^{1/2}$$

Equation 2-3

Solubility parameters for mixtures of plasticisers can be found by simply multiplying the solubility parameters of the components by their mole fractions in the plasticiser mixture. If the resulting solubility parameter is sufficiently similar to PVC, then the mixture will most likely be compatible.[2]

The solubility parameters of plasticisers can be predicted in a number of ways. The most common method is to sum the contributions of each part of the chemical structure, as developed by Small (Equation 2-4).[46]

$$(EV)^{1/2} = \sum_i F_i$$

V = molar volume of solvent.

E = cohesion energy.

F_i = molar attraction constants.

As the solubility parameter δ is the square root of the cohesion energy E, this can be rearranged to Equation 2-5.

$$\delta = \frac{\sum_i F_i}{V^{1/2}}$$

A number of authors have compiled tables of molar attraction constants for typical organic groups, and these numbers do not necessarily agree with one another. This simple additive method of calculating solubility parameters has been criticised as it does not consider the overall molecular structure of the solvents.[41] This is clearly a factor in this work, as the observed compatibility of DOP (**1**) is greater than that of DOTP (**6**) which, as isomeric compounds, would give the same calculated solubility parameters by Small's method. An improved method of predicting solubility parameters was developed by Askadskii to consider the reduction in molar volume due to neighbouring atoms (Equation 2-6).[2] The contribution of each atom or to the overall volume, ΔV_i, is calculated by subtracting part of the volume of overlapping neighbouring atoms from the spherical volume of the atom (Equation 2-7). The height of the subtracted segments, h_i is calculated from the bond lengths (Equation 2-8).

$$\delta = \sqrt{\frac{\sum_i \Delta E_i}{N_A \sum_i \Delta V_i}}$$

N_A = Avogadro's Constant.

ΔE_i = cohesion energy for atoms or groups.

ΔV_i = Contribution of atom/group to the Van der Waals volume.

$$\Delta V_i = \frac{4}{3}\pi R^3 - \sum_i \frac{1}{3}\pi h_i^3 (3R - h_i)$$

$$h_i = R - \frac{R^2 + d_i^2 - R_i^2}{2d_i}$$

R = van der Waals radius of the atom

d_i = atomic bond length to atom i

R_i = radius of adjacent covalently bonded atom i

Methods for determining solubility parameters continued to develop to include further physical properties of polymers and solvents. An initial approach by Blanks and Prausnitz described the components of polar and non-polar interactions.[47] However, this method did not account for hydrogen bonding and as such is not suitable for the polar systems of PVC and its plasticisers. Methods to take into account the hydrogen bonding were developed by Beerbower, Lieberman, Crowley and Nelson, using various methods, but the current predominant method was developed by Hansen.[41] This splits the cohesive energy, and thus solubility parameter δ into dispersion δ_D, polar δ_P and hydrogen bonding δ_H components:

$$\delta^2 = \delta_D^2 + \delta_P^2 + \delta_H^2$$

Equation 2-9

These components can be used as axes to define a 3-dimensional plot of solubility parameters (known as the Hansen Solubility Parameter, HSP), with each solvent occupying a point corresponding to the dispersive, polar and hydrogen bonding characteristics of that solvent. From this, solubility spheres can be defined, such that other solvents sufficiently similar in each component fall within the spheres and therefore the free energy of mixing will be negative. The minimum distance between the positions of the polymer and plasticiser/solvent is called the Interaction Radius (IR).

The IR can be used to predict plasticiser compatibility as the lower the interaction radius of the polymer and plasticiser, the greater solubility and thus compatibility of the mixture.[48] The IR values for PVC with a range of plasticisers and solvents was calculated by Krauskopf using the CO-ACT service, with values largely correlating to reported plasticiser efficiencies.[48] In phthalate plasticisers, the IR values corresponded mainly to molecular weight, with little difference found between isomeric phthalates such as L9P (linear dinonyl phthalate) and DINP (di isononyl phthalate). Krauskopf also found little difference in IR between DOP (diethylhexyl phthalate) and the meta- and para- isomers DOIP (diethylhexyl isophthalate) and DOTP (diethylhexyl terephthalate). This discrepancy with reported experimental properties of these plasticisers is acknowledged and attributed to a limitation of the calculation method.

Methods of calculating HSPs have developed over time through the use of software such as HSPiP (Hansen Solubility Parameters in Practice), as employed by Kwansa *et al.*[49] Differences in the values for total HSP (δ_t) as a result of different versions of the software used to calculate the HSPs for DOP and DOTP were stated. Notably, the values calculated using HSPiP V1.01.7 ($\delta_{t(DOP)}$ = 17.457 MPa$^{1/2}$ and $\delta_{t(DOTP)}$ = 17.603 MPa$^{1/2}$) were much more alike than the values used in the further evaluation of plasticiser exudation. The value for DOP used throughout the work was

taken from a reference dataset ($\delta_{t(DOP)}$ = 18.28 MPa$^{1/2}$) while the value for DOTP was calculated using HSPiP V5.0.04, giving $\delta_{t(DOTP)}$ = 17.86 MPa$^{1/2}$.[49, 50] These values are taken alongside further molecular dynamics simulations to explain the observed differences in migration between DOP and DOTP, as discussed further in section 2.5.

Hansen solubility parameters were applied to an evaluation of cardanol and its derivatives for use as PVC plasticisers.[51] Cardanol is a phenolic lipid derived from cashew nut shells and has been used in the synthesis of a number of potential bio-based plasticisers for PVC.[52-54] Through examination of the HSPs of cardanol, cardanol acetate and epoxidised cardanol acetate, Greco *et al.* suggested that the phenolic hydroxyl group of cardanol leads to an excessively high value of the hydrogen bonding term in the HSP calculation and thus reduces miscibility with PVC.[51] Epoxidised cardanol acetate was shown to have a lower PVC Interaction Radius than DOP, indicating enhanced miscibility. This was also reflected in the improved gelation properties shown by rheological testing.

2.3   Plasticiser Movement Within the PVC Matrix

Plasticisers in PVC can move through the structure by diffusion. For amorphous polymers above their glass transition temperatures, this diffusion obeys Fick's Law, such that vapours or low molecular weight liquids will tend to migrate from areas of high concentration to areas of low concentration, for example from plasticised polymer to the surface.[2] Fick's law (Equation 2-10) relates the flux, *J*, of the penetrant, to the diffusivity constant *D*, the difference in concentration between the region of high and low concentration d*c* and the distance d*x*.

$$J = -D\frac{\mathrm{d}c}{\mathrm{d}x}$$

Equation 2-10

This equation describes systems with a constant concentration gradient, while Fick's second law (Equation 2-11) describes the diffusion in a system wherein the concentration gradient changes over time.

$$\frac{\mathrm{d}c}{\mathrm{d}t} = -D\frac{\mathrm{d}^2c}{\mathrm{d}x^2}$$

Equation 2-11

For diffusion of a plasticiser through a polymer, there are a number of physical processes which can lead to non-Fickian behaviour, such as changes in crystallisation with a change in plasticisation, swelling of the polymer or evaporation of the diffusing substance from the surface.[2]

Coughlin *et al*. published a series of papers on diffusion in PVC and described a number of trends based on the properties of the diffusant, i.e. plasticiser.[55-57] Conformational analysis was used on a series of phthalates to predict their diffusion behaviour and found to be in good agreement with experimental data. This was an improvement on previous models which approximated the plasticiser as a spheroid shape, which is not necessarily a good fit for the lowest energy conformations of plasticiser molecules. Instead, these molecules were shown to be much more irregular in shape. This paper also showed that for a series of phthalates, the cross-sectional areas did not increase to the same degree in all coordinates, and for longer chain length phthalates, the cross sections were more elongated in the *x* coordinate as defined by the authors. The effect of the polymer on the lowest energy conformations of the plasticiser was described as "reverse solvation", treating the polymer as small segments of the chain which solvate the plasticiser.[57] Plasticiser diffusion through the polymer then must overcome an activation energy due to this solvation. Energies of interaction were calculated for each chemical group of a series of phthalates and scaled by the accessible surface area of that group in the molecule as a whole. The main contributor to the interaction energy was the benzene ring, followed by the ester groups. This is attributed to the polarisable (benzene) or polar (ester) nature of these groups. The effect of the ester groups is diminished as they are not easily accessible in the phthalate structure. Including the effect of interactions between the polymer and plasticiser gave a much closer fit to the experimental diffusion data than the model that considered only the shape and size of the plasticiser molecule, both for the effect of phthalate chain length and the effect of temperature.[57]

2.4   Alternative Approaches to Plasticisation

Plasticiser exudation from flexible PVC can be prevented through the use of internal plasticisation. [2] This can either take the form of copolymers of vinyl chloride and other monomers such as vinyl acetate, or through reacting the PVC chain to introduce new groups.[58, 59] Jia *et al*. modified PVC through reaction with sodium azide to form PVC-N_3 by replacing chlorine in the polymer. This was then reacted with propargyl ether triethyl citrate to form triethyl citrate-modified PVC.[58] This modified polymer showed effective plasticisation through tensile testing (greater elongation and lower tensile strength) and reduced T_g relative to pure PVC, however the degree of conversion was not reported and thus comparisons to these properties in the conventionally plasticised PVC sample tested alongside cannot be made.

Vinyl chloride – vinyl acetate copolymers are commonly used in PVC formulations, with typically 5-15% vinyl acetate content.[7] This is produced through polymerisation of a mixture of the monomers, giving a largely random distribution of the two monomers. The presence of the acetate groups disrupts crystallinity in the PVC polymer structure and so produces a more flexible polymer.[5] Internal plasticisation has also been achieved through block copolymerisation of PVC with poly (n-butyl acrylate).[60] The resulting polymer behaved as a single material, displaying one glass transition by DMA.

Internal plasticisers give some advantages over the more common externally plasticised PVC, such as greatly improved permanence, however there are also disadvantages. Plasticised PVC formulations are often finely tuned to meet the softness requirements of the customer and changing this is a simple matter of altering a formulation. However, if the plasticiser must be reacted with the PVC, or specific copolymer ratios used, this becomes a much more extensive task as reaction conditions and other factors must be considered. Additionally, plasticisers that are chemically bound to the polymer chain show a reduced plasticising effect, requiring higher addition levels of the plasticiser to achieve the same softness.[61]

2.5 Plasticiser Exudation

The vast majority of studies on plasticiser loss from PVC are concerned with evaporative loss at elevated temperatures, or loss to a liquid extractant medium.[62-65] Djilani et al. investigated the migration of DOP from PVC discs into a range of food-simulant oils in comparison to mathematical models of diffusion.[66] After immersion in the test liquid, the samples were frozen with liquid nitrogen, then sliced into very thin (0.2 mm) sections and each slice weighed to determine the depth profile of plasticiser loss, as well as GC-FID on the resulting simulant liquid - plasticiser mixture. This showed that the greatest plasticiser loss occurred nearest the outer faces of the samples, with a gradient through to the most central sections.[66]

Ekelund found that the rate of evaporation of DOP at 100 °C was the same for liquid samples as for PVC plasticised with DOP.[63] From this it was deduced that the samples of pPVC had a thin layer of DOP present at the surface without any applied stress, and this was then confirmed by FTIR measurements. Competition between evaporation-controlled and diffusion-controlled plasticiser loss was examined in the work by Audouin et al., who showed that below a critical temperature the process was controlled by evaporation kinetics (linear with time), and above this temperature it was controlled by diffusion kinetics.[64] The work was carried out on unstressed didecyl phthalate (DDP) plasticised PVC samples from 85 to 120°C. Fickian diffusion led to a weight loss proportional to the square root of time. In experiments of plasticiser diffusion into n-heptane, DOTP **6** showed a much higher diffusion constant than DOP **1**.[67] This work also showed that using a binary blend of primary plasticisers - DOP combined with either DOTP or dibutyl phthalate, lead to reduced rates of migration overall. This difference was explained by the concept of the two plasticisers solvating each other more strongly than each solvates the PVC.

Plasticiser depth distribution was further examined by Audouin in samples with a range of phthalate plasticisers.[65] Samples were microtomed following thermal ageing and plasticiser content was quantified by FTIR. Comparison of FTIR with rate of mass loss showed that in samples where the plasticiser loss was diffusion controlled, the

plasticiser content was heterogenous throughout the sample, whereas in evaporation-controlled samples the plasticiser content was mostly homogenous. It was also shown that thermal plasticiser loss tends towards a diffusion-controlled process at lower plasticiser levels (between 20-25%).[65] Atek investigated the migration of DOP and epoxidised sunflower oil (ESO) into food simulants and found that ESO migration was slowed when DOP concentration was increased.[68] However, DOP migration was not measured in samples without ESO present and so the effect of ESO on DOP migration was not examined.

Kwansa *et al.* carried out molecular modelling of PVC-plasticiser interactions and correlated this with gravimetric measurements of plasticiser exudation under compression through transfer to an absorbent paper.[49] The plasticisers used were DOP, DOTP and DnBT (di n-butyl terephthalate), and experimental results were compared with computer models of plasticiser distribution and exudation under stress as well as Flory-Huggins and Hansen solubility parameters. Of these plasticisers, DOTP showed the greatest phase separation in the simulated plasticiser distributions, while DnBT showed the least. The experimental results for exudation showed the same trends as the modelled data but a smaller difference between the plasticisers. Both sets of data showed a reduction in plasticiser exudation in samples of mixed DOTP-DnBT composition.[49] It was concluded that in these examples, the greater compatibility of DnBT was a stronger factor in the exudation behaviour than the relative viscosity and mobility of the smaller molecule, leading to lower migration than the larger but less compatible plasticisers.

2.6 Methods of Testing Plasticiser Compatibility

The compatibility of PVC and plasticisers has been studied and defined in a number of ways throughout the literature. The effect of plasticiser on T_g measured by DMA (discussed in further detail in section 2.7.4),[37, 69, 70] the effect of PVC-plasticiser interactions on the FTIR spectra (section 2.7.1),[71, 72] and solid-gel transition temperatures have all been used as measures of compatibility.[5] These are useful

measurements and give information on the interactions between the plasticiser and polymer molecules. However, from an industrial perspective the primary concern raised by incompatibility of plasticisers is the tendency to exude from the PVC compound. Two standards set out methods of testing this property of a PVC formulation - ASTM D2383 (Plasticizer compatibility in poly (vinyl chloride) (PVC) under humid conditions) and ASTM D3291 (Standard Practice for Compatibility of Plasticizers in Poly(Vinyl Chloride) Plastics Under Compression, Figure 2.1).[39, 69] These tests stress the material, either mechanically or with heat and humidity, to accelerate the exudation of incompatible plasticisers. These methods are rarely referenced in the literature concerning PVC-plasticiser compatibility, and correlations between these measures of compatibility and others such as T_g or FTIR are not often examined. These tests have some limitations, as the measurement of exudation is a subjective judgement of how much plasticiser has exuded based on the transfer to an absorbent paper. A more quantitative analytical method would allow PVC compounders to compare and record useful information about the compatibility of different plasticisers. This would facilitate the evaluation of novel plasticisers for PVC in the drive to substitute toxic and petrochemical additives with novel bio-based additives.
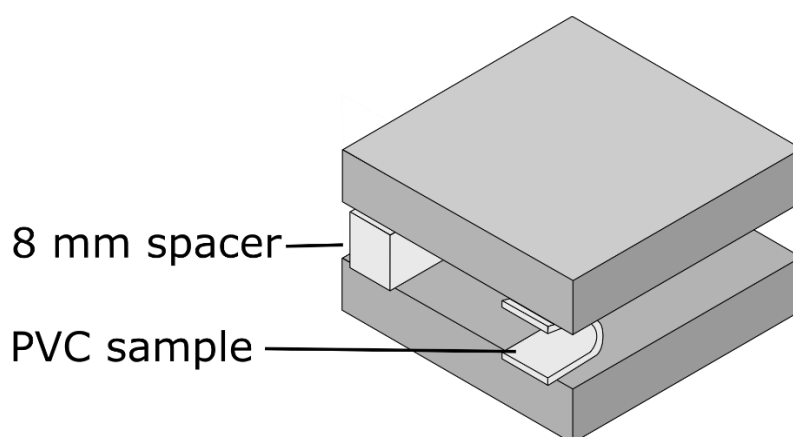
Figure 2.1: Diagram of the ASTM D3291 Loop spew test for plasticiser compatibility in PVC.[39]

2.7   Analytical Techniques

2.7.1 FTIR Spectroscopy

Fourier Transform Infrared spectroscopy (FTIR) is a widely used analytical technique throughout chemistry and other sciences. The technique is based on the interaction of molecules with infra-red light, which is absorbed at characteristic wavelengths due to the vibrational frequencies of the chemical bonds in the sample. To be IR-active, the vibration of the bond must change the dipole moment of the molecule. FTIR can be carried out in transmission or reflectance mode depending upon the properties of the sample.

Attenuated Total Reflectance FTIR (FTIR-ATR) is a reflectance technique whereby the sample is in direct contact with a crystal (typically diamond or germanium) known as an internal reflection element (IRE). The IR beam contacts the IRE surface at greater than the critical angle and so reflects back into the crystal by total internal reflectance. Some energy penetrates a small distance into the sample in the form of the evanescent wave, which is attenuated by absorption at the characteristic wavelengths of the bonds present in the sample.[73] The penetration depth d_p of the evanescent wave depends upon the wavelength of light (λ), the angle of incidence (ϑ) and the refractive indices of the IRE and sample (n_1 and n_2) as shown in Equation 2-12. Penetration depths are typically of the order of 100-1000 nm.[73]

$$d_p = \frac{\lambda_1}{2\pi n_1 \sqrt{\sin^2\theta - \left(\frac{n_2}{n_1}\right)^2}}$$

Equation 2-12

FTIR has been used to examine the interaction between plasticiser and PVC in the works by Tabb and Koenig, Beltran, Garcia, and Marcilla and Gonzalez and Fernandez-Berridi.[71, 74, 75] Tabb first showed that in samples of PVC plasticised with DOP, the FTIR absorption wavelengths differed between pure DOP and PVC/DOP blends of differing composition. Tabb suggested that this would be due to complexes forming between

the carbonyl groups in DOP and the carbon-chlorine bonds within PVC, changing the characteristic absorption of the carbonyl stretch.[75]

Beltran *et al*. compared three phthalate plasticisers (dibutyl phthalate, diethylhexyl phthalate (DOP, **1**) and diisodecyl phthalate) by FTIR spectra *in situ* during the gelation and fusion process of their PVC plastisols.[71] The spectrum of the plasticiser was subtracted from the spectrum of the mixture, and compared to that of the pure PVC resin. Dibutyl phthalate and DOP showed larger differences in the subtracted spectrums than did diisodecyl phthalate. This was interpreted as greater compatibility of dibutyl phthalate and DOP with PVC, due to stronger intermolecular interactions of the plasticisers and polymer.

Gonzalez and Fernandez-Berridi compared the FTIR spectra of eight plasticisers with the theoretical FTIR spectra using the same principles, examining both the carbonyl stretching region and the C–Cl tactic and atactic bands.[74] As PVC is formed through radical polymerisation, the structure is overall atactic, i.e. the chlorine atoms are distributed randomly on both sides of the polymer chain (Figure 2.2). However, regions of syndiotactic arrangement (chlorine atoms located on alternating sides of the PVC chain) can occur, giving rise to localised crystallinity. The atactic band corresponds to the amorphous regions of the PVC structure, which are the regions that interact with the plasticisers most readily. The crystalline regions, corresponding to the tactic band in the FTIR spectra, are not easily solvated.
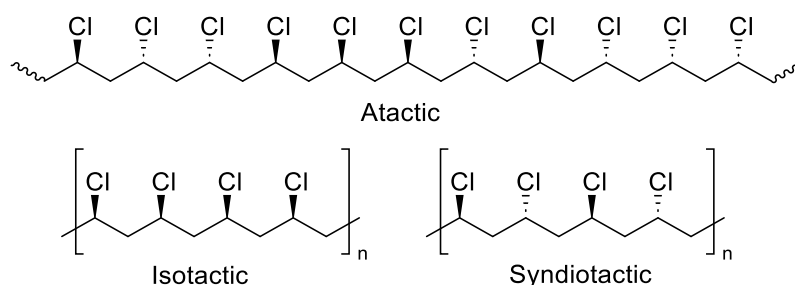
Figure 2.2: Atactic, isotactic and syndiotactic conformations of PVC.

The order of compatibility was then compared with the chemical structures of the plasticisers to identify the relationship between compatibility and properties such as chain length and degree of substitution of the aromatic ring. The results showed that shorter, branched alkyl chains gave a stronger interaction with PVC than longer linear alkyl chains, while greater substitution of the aromatic ring reduced the interaction with PVC. This was attributed to steric hindrance reducing the ability of the plasticiser to interact with the polymer chain.

2.7.2 Raman Spectroscopy

Raman Spectroscopy is often used in conjunction with FTIR spectroscopy, as they are complimentary techniques. While only chemical bonds with a dipole moment are FTIR active, this is not required for Raman activity, which instead relies on the polarisability of the bonds. Raman spectroscopy was used in conjunction with FTIR to investigate molecular orientation in uniaxially drawn PVC.[76] The conjugated polyene chains formed by the degradation of PVC were examined by Raman spectroscopy while FTIR was used to investigate C-Cl bond orientation. These techniques gave complimentary results for the orientation of the PVC chains in the drawn samples. Methods of quantifying adipate, phthalate and terephthalate plasticisers in PVC samples through Raman spectroscopy have been reported in a number of works.[77-79] While Berg and Otero reported successful quantification of plasticisers by Raman spectroscopy, they noted that specific identification of adipate plasticisers was limited due to the abundance of aliphatic diesters with similar spectra.[78] Phthalates were more easily identifiable by the strong band at 1060 cm^{-1} due to the aromatic ring. This highlights that while FTIR and Raman spectroscopy have many uses in the analysis of plasticisers in PVC, in the case of complex mixtures (such as PVC with binary or ternary plasticiser systems) chromatographic methods may allow for more specific identification.

2.7.3 Gas Chromatography - Mass Spectrometry

Gas Chromatography - Mass Spectrometry (GC-MS) provides a detection method that can both detect the concentration and elution time and determine the identity of the compounds present based on the chemical structure. In the mass spectrometry detector, the sample is ionised and then passed through a magnetic field to separate the ionised fragments by their *m/z* (mass to charge) value. The total molecular weight of each compound can be identified, and the structure can be elucidated from the fragmentation pattern shown by the fragment ions. Depending on the requirements of the analysis, MS detectors can be used in total ion current (TIC) or selected ion monitoring (SIM) modes. In TIC, the detector scans across a range of m/z values to measure all ions within that range. SIM is used when particular ions are of interest and can give greater resolution by reducing noise and increasing the collection time for the target ions.

GC-MS is widely used for the identification and quantification of plasticisers and additives in PVC [23, 80, 81]. This method is suitable for testing the majority of medium-volatility plasticiser groups such as phthalates, adipates and trimellitates. However, low volatility plasticisers such as ESBO cannot be tested directly by GC-MS as they cannot be volatilised and passed through the GC-MS column. These plasticisers can be tested by LC-MS (liquid chromatography - mass spectrometry) since this method does not require the analytes to be volatile, or through derivatisation of the ESBO prior to GC-MS analysis. The two methods have been compared by Suman *et al.*,[82] using the derivatisation procedure described by Castle *et al.*[83] Both methods were able to quantify ESBO **8** migration from PVC seals into various food products, although there was some variation between the results from the two methods. The derivatisation described by Castle *et al.* is a multistep process involving two reaction steps and two evaporation steps and so is more complicated and time-consuming than testing the sample directly by LC-MS. An alternative derivatisation method is used by Biedermann-Brem *et al.*[81] This method involves a single reaction step to

transesterify ESBO and other high molecular-weight plasticisers using sodium ethoxide. The full procedure and its use in this work is described in Chapters 3 - 5.

2.7.4 Dynamic Mechanical Analysis

As PVC is a largely amorphous polymer, it does not have a precise melting point. Instead, the structure exists as either a glassy or rubbery material, depending on the temperature and composition of the PVC blend. The temperature at which it changes from a glassy to rubbery state is known as the glass transition temperature T_g. Glass transition temperatures of polymers are often measured using Differential Scanning Calorimetry (DSC), however for plasticised PVC this technique often does not show a clear glass transition. Dynamic Mechanical Analysis (DMA, also known as DMTA) is commonly used instead.[69, 84, 85]

DMA measures the response of a material to a cyclic applied deformation over a range of temperatures. The deformation can be a bending motion, as in the cantilever mode, a stretching motion as in the tensile mode, or a shearing/compression motion. The change in the stress-strain response of the material over a range of temperatures can be used to determine the glass transition temperature by examining the storage (E') and loss (E'') moduli of the material. The storage and loss moduli reflect the elastic and inelastic components respectively of the material's response to an applied stress. The glass transition can be identified by the reduction in the elastic "glassy" behaviour of the material, shown by the reduction in storage modulus, and the increase in the inelastic "rubbery" behaviour shown by an increase in the loss modulus. These two variables are combined in the tan delta:

$$tan\, \delta = \frac{E''}{E'}$$

Equation 2-13

Measurement of the glass transition temperature by DMA is widely used as a compatibility metric.[69] As discussed in section 2.1 (Theories of Plasticisation),

plasticisers lower the glass transition of PVC by lubrication of the polymer chains, allowing rotation of the chain segments and increasing free volume. This is aided by solvation of PVC by the plasticiser through polar groups that interact with the polar polymer. As noted by Daniels, in addition to the glass transition temperature DMTA can also be used to measure the width of the glass transition curve.[69] Multiple separate transition points can be measured in PVC due to regions of differing crystallinity in the polymer. These transitions can occur at different temperatures due to poor solvation behaviour of the plasticiser, broadening the glass transition curve. In a series of phthalate plasticisers, increasing the alkyl chain length was observed to decrease compatibility while increasing lubrication. Daniels notes the complexity of interpreting these results, as from their observations the plasticisers used for low temperature flexibility show different glass transition behaviour to general purpose plasticisers.[69] As such, the glass transition temperature alone is not sufficient to determine if a plasticiser can be successfully used in a PVC compound.

2.8   Synthesis of Novel Non-Phthalate Plasticisers

Investigations into the synthesis of novel plasticisers are numerous, and primarily focus on the use of bio-based chemistry to produce "green" plasticisers. Green chemistry encompasses a number of principles that aim to minimise harm to human health and the environment. This includes consideration of the hazards of all parts of the chemical process, such as chemical feedstocks, by-products, solvents and reagents as well as the target product.[86] The 12 principles of green chemistry as set out by Anastas and Warner provides a framework for designing greener processes within chemistry.[87] While the use of renewable feedstocks is one of these principles, it is a limited definition of a green product without consideration of the other factors such as energy efficiency, atom economy and waste prevention.

Plant oils such as soybean oil, castor oil, and palm oil are commonly used in the development of biobased plasticisers, as well as citrates and derivatives of sugars.[16,]

[28, 88-90] In spite of this, petrochemical plasticisers still predominate, constituting more than 95% of the total European plasticiser market in 2020.[20] Esters of citric acid such as acetyl tributyl citrate (ATBC) and tributyl citrate (TBC) have been used in PVC compounding for some time. These esters show good performance in the polymer but have not achieved widespread use due to high cost.[16] These plasticisers are generally considered to have low-toxicity, and many are FDA-approved. However, ATBC has shown potential concerns as an endocrine disruptor and possible interactions with steroid metabolism.[91, 92]

Epoxidised soybean oil is widely used in the PVC industry as a secondary plasticiser, with production globally of over 2 million tonnes per year.[93] As stated previously, secondary plasticisers are generally used in combination with a primary plasticiser that shows greater solubility in the polymer.[7] The epoxidation of unsaturated oils was described as early as 1949, in a two-step process using acetic acid and hydrogen peroxide to form peroxyacetic acid, which is then combined with the unsaturated compound to form the epoxide.[94] This combination of peroxide and carboxylic acid remains the primary method industrially, although other routes include acid ion exchange resins, enzymatic methods and metal catalysts.[95] The industrial method has been refined over time and some producers claim near complete conversion of the double bonds, with approximately 0.04 residual double bonds per ESBO molecule.[27]

Epoxidised fatty acid methyl esters (EFAMEs) have been investigated in numerous studies, as they show improved low-temperature plasticisation over triglycerides such as ESBO. However, these plasticisers are susceptible to volatilisation and solvent extraction due to their low molecular weight.[96]

2.9   Reactions of the ESBO Epoxide Ring

The epoxide ring opening reaction of ESBO is well established with a range of nucleophiles such as alcohols, diols and amines, with reports going as far back as 1995.[97-99] These reactions have been used to produce polyols for applications such as the synthesis of polyurethanes and other bio-based polymer alternatives.[31-33]

These polyols have been shown to oligomerise through side reactions, as the hydroxyl groups formed in the reaction can then act as nucleophiles.[100] When a diol is used as the nucleophile, the unreacted hydroxyl can also react to form oligomeric structures. Propylene glycol was shown to form gel-like polymeric structures with ESBO and zinc triflate catalyst, which could be crosslinked to form hard polymeric coatings.[32]

Guo *et al*. tested a number of different acid catalysts for the methanolysis of the ESBO epoxide ring for use in polyurethane synthesis. They found fluoroboric acid to give the highest conversion to the methyl ether polyol, compared with perchloric acid, p--toluene sulfonic acid, sulfuric acid, and formic acid.[33]

Erhan *et al*. reacted ESBO with a series of acid anhydrides to produce diesters for use as industrial lubricants.[101] This mechanism for producing diesters from the epoxide ring could be used to introduce a wide range of groups into the ESBO structure. The production of acid anhydrides often involves large amounts of hazardous oxidants, although more environmentally-friendly methods have also been reported.[102] Reactions of epoxidised fatty acids with PEGs have also been reported in the production of non-ionic surfactants.[103] This work in particular focuses on the sustainable synthesis of these compounds, utilising heterogenous catalysis and solventless processes.

Despite the utility of the epoxide ring as a target for synthetic modification, retaining some epoxide functionality could be desirable, due to the benefits to both compatibility and stability. The effect of epoxide rings on plasticiser compatibility and stability was shown in an evaluation of eleostearic acid eugenol esters, where the presence of the epoxide group led to lower T_g values and higher onset of decomposition by DSC and TGA respectively.[104] ESBO is often used as a heat stabiliser in PVC, as the epoxide ring scavenges the hydrochloric acid produced by PVC decomposition. This prevents the acid from promoting further degradation of the PVC chain.[16] This is discussed in further detail in Chapter 7.

The reactivity of the epoxide ring was exploited to synthesise novel plasticisers as described in the following chapters, incorporating the bio-based reactant molecules shown in Figure 2.3.
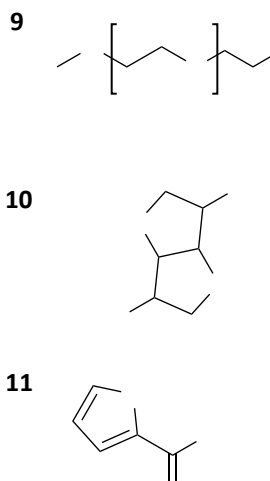
Figure 2.3: Bio-based reactants used to modify the structure of epoxidised soybean oil to produce novel plasticisers for PVC: methoxy polyethylene glycol (mPEG, 9), isosorbide 10 and 2-furoic acid 11.

2.10 The Use of DOSY-NMR in the Analysis of Complex Mixtures

As ESBO is derived from a natural vegetable oil, it is typically a mixture of components of varying chain length and epoxide number. As such, when reacting at the epoxide functionality a complex mixture of products is formed. This poses a challenge for analysis, as these closely related products are not easily separated through chromatographic methods. Diffusion-ordered NMR spectroscopy (DOSY) separates the NMR signals of different molecules in a mixture on the basis of the diffusion behaviour. This is achieved by using pulsed field gradient experiments and examining the signal decay as the samples move under Brownian motion. Molecules that are more mobile will show a greater signal attenuation as described by the Stejskal-Tanner equation (Equation 2-14).[105]

$$S = S_0 e^{-bD}$$

Where S is the signal strength, S_0 is the signal strength without the diffusion gradient, D is the diffusion coefficient and b is related to the field gradient G, pulse duration δ and time delay τ as shown in Equation 2-15.

$$b = \gamma^2 G^2 \delta^2 \left(\tau - \frac{\delta}{3}\right)$$

As well as allowing for more accurate analysis of the composition of mixtures, DOSY can also be used to estimate diffusion coefficients as well as molecular weights of large molecules such as polymers, as described by Groves.[106]

DOSY has also been used in the analysis of biodiesel to determine mono-, di- and triacylglycerols in the methylated reaction products formed from vegetable oils.[107]

2.11 Summary

In conclusion, the work presented in the following chapters aims to address the needs of the PVC industry as described, in the drive to replace toxic petrochemical plasticisers with bio-based alternatives. The lack of a quantitative method for testing plasticiser exudation from PVC samples limits the evaluation of novel plasticisers. A more reliable test method could increase the confidence of the PVC industry when approving novel plasticisers for use. Furthermore, the synthesis of novel plasticisers from epoxidised soybean oil presents the possibility of a bio-based plasticiser with enhanced compatibility, from a low-cost starting material that is familiar to PVC compounders.

3 Experimental

3.1 Introduction

This chapter describes the procedures and analytical techniques evaluated in Chapter 5for the development of an improved method of testing plasticiser compatibility in PVC samples. Furthermore, it describes the synthesis procedures of the modified ESBO compounds evaluated as new or alternative plasticisers for PVC. The techniques for evaluation of these plasticisers and the PVC samples prepared from them are also described here.

3.2 Materials

All materials used to produce the PVC samples were provided by Alphagary Ltd and were industrial grade. These materials were PVC resin (suspension grade, K70), diethylhexyl phthalate (DOP), diethylhexyl terephthalate (DOTP), epoxidised soybean oil (ESBO), calcium-zinc stabiliser (proprietary) and barium-zinc liquid stabiliser. Chemicals used were ethanol (absolute, VWR), 1-Ethyl Naphthalene (≥97%, Aldrich), sodium citrate (99%, Aldrich), dimethyl pimelate (99%, Aldrich), sodium ethoxide (21% in ethanol, Alfa Aesar), methyl tert-butyl ether (MTBE, 99.8%, Sigma Aldrich), n-hexane (>97%, Honeywell), magnesium sulfate (Laboratory reagent grade, Fisher Scientific, polyethylene glycol methyl ether (average molecular weight 350, Alfa Aesar), p-toluene sulfonic acid (PTSA, 99%, Acros Organics), zinc trifluoromethane sulfonate (98%, Acros Organics), methanol (≥ 99.9%, Fisher Scientific), D-isosorbide (98%, Alfa Aesar), L-phenylalanine (99%, Alfa Aesar), vanillin (99%, Alfa Aesar), 4-hydroxy-3-methoxybenzyl alcohol (vanillyl alcohol, 99%, Alfa Aesar), 2-furoic acid (98%, Acros Organics), THF (Fisher Scientific, PureSolv purification system), chloroform (Fisher Scientific, >99% lab reagent grade), DCM (Fisher Scientific, >99% lab reagent grade), deuterated chloroform (Sigma Aldrich), diethyl ether (Fisher Scientific, laboratory reagent grade), sodium hydrogen carbonate (Fisher Scientific

Laboratory reagent grade), and toluene (Fisher Scientific, PureSolv purification system).

3.3 Sample Preparation for Compatibility Testing

Samples of plasticised PVC were prepared by cold mixing of plasticisers, PVC resin and heat stabiliser additives, followed by compounding with a Farrel two-roll mill at 155 °C. The samples were then compression moulded in a heated hydraulic press (Mackey-Bowley) at 170 °C and 200 bar pressure for 4 minutes to give plaques of uniform 2 mm thickness with smooth surfaces. The plasticisers selected to evaluate the compatibility methods were DOP, DOTP and ESBO. PVC formulations were prepared as shown in Table 3.1.

Table 3.1: Formulations of samples used to evaluate compatibility test methods in PHR (parts per hundred resin) and percentage by weight.

	1	2	3	4	5
Formulation	PVC-DOTP	PVC-DOP	PVC-ESBO	PVC-DOTP-ESBO	PVC-DOP-ESBO
PVC K70 resin (PHR)	100	100	100	100	100
(percentage)	58.6%	58.6%	58.6%	58.6%	58.6%
Ca/Zn heat stabiliser	0.6 0.4%	0.6 0.4%	0.6 0.4%	0.6 0.4%	0.6 0.4%
DOTP	70 41.0%	-	-	35 20.5%	-
DOP	-	70 41.0%	-	-	35 20.5%
ESBO	-	-	70 41.0%	35 20.5%	35 20.5%

3.4 Development of an Analytical Method for Testing Plasticiser Compatibility

The compatibility testing was based upon the ASTM D3291 method *Standard Practice for Compatibility of Plasticizers in Poly(Vinyl Chloride) Plastics Under Compression.*[39] The procedure for mechanically stressing the samples was followed, whereby a loop is made in a 2 mm thick piece of PVC compound between two metal plates separated by 8 mm spacers, as shown in Figure 3.1. Various methods were evaluated to measure the exudation over time in a quantitative manner.
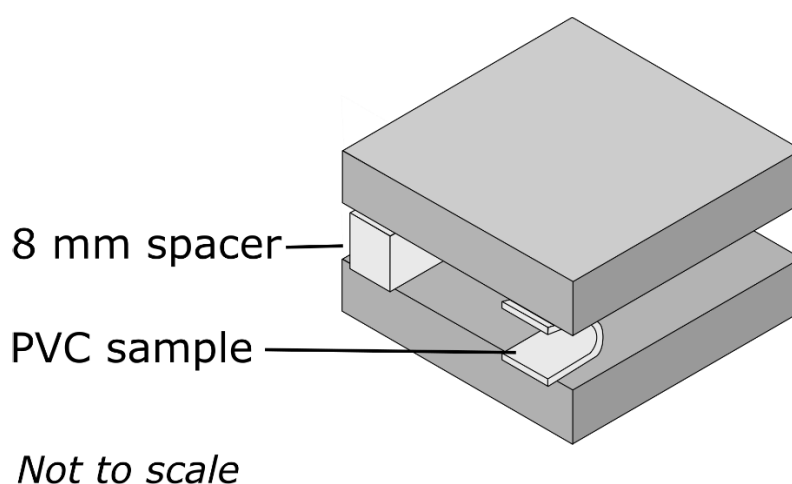
Figure 3.1: Diagram of the Loop spew test for plasticiser compatibility in PVC.

3.4.1 FTIR Spectroscopy

FTIR spectra were measured on a Nicolet iS5 with iD5 ATR attachment and a Perkin Elmer Spectrum Two with Spotlight 200i microscope accessory using ATR mode. The use of transmission and reflection modes were investigated on the Perkin Elmer FTIR. Both single point and mapping techniques were tested on the samples. Samples were mounted on a moving stage and optical microscopy images were collected to identify the areas for FTIR measurement. Grid and line maps were tested on these samples at various resolutions, typically 100 μm. The maps were analysed using the SpectrumIMAGE Viewer software in ChemiMap and Compare Correlation modes. The ChemiMap function compares the intensity of the bands at certain wavenumbers for known functional groups, in this case the ester C=O stretch at 1780-1665 cm^{-1} and C-O

stretch at 1300-1220 cm^{-1}. These regions were adjusted from the program default to better fit the peak positions in the tested samples. The Compare Correlation mode compares the map data to known standards. Spectra for the pure plasticisers were also collected for this use.

The Nicolet iS5 FTIR was used to measure the surfaces of the samples stressed by the compatibility test in the area where plasticiser would exude i.e., the compressed face of the looped sample, Figure 3.2. The sample was removed from the compression plates, the centre of the stressed area was placed on the ATR internal reflection element (IRE) and clamped in place to ensure good contact with the IRE. Five samples of each formulation were measured for each time point. 16 scans were collected for each spectrum, the spectral resolution was set to 4 cm^{-1} and the data spacing was 0.482 cm^{-1}.
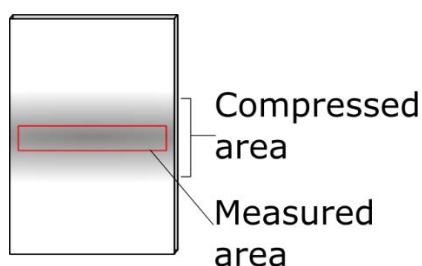
Figure 3.2: Diagram of compressed PVC sample showing the stressed portion and the target area for FTIR measurement.

The penetration depth was calculated for this experiment using Equation 3-1, through employing the primary wavelength investigated (1725 cm^{-1}) for a situation of maximum and minimum values of refractive index possible with the plasticisers and plasticised PVC samples (θ= 42°, $n_{diamond}$ = 2.42, n_{DOP}, n_{DOTP} = 1.49, n_{ESBO} = 1.47 and n_{PVC}= 1.55).[108-110] This gave a penetration depth (d_p) range of 4.0-4.9 μm.

$$d_p = \frac{\lambda_1}{2\pi n_1 \sqrt{\sin^2 \theta - \left(n_2/n_1\right)^2}}$$

Equation 3-1

3.4.2 Raman Spectroscopy

Raman spectra were measured on a ThermoScientific DXR Raman, using a 532 nm laser and 10x microscope objective. The method used was 1-minute photobleaching, 10 mW laser power, 25 µm pinhole and five exposures of 5 seconds. Both flat-pressed and cut surfaces were tested to attempt to map the distribution of plasticiser on the exuding surface, as well as throughout the sample. Optical microscope images were also collected prior to Raman measurement.

3.4.3 Gas Chromatography - Mass Spectrometry

GC-MS analysis was used to quantify plasticiser exudation following the loop spew compatibility test. The inner surface of each sample, where the exudation occurs, was wiped with an analytical cotton swab in a set pattern covering the surface of the sample. The swabbing procedure ensured that every part of the compressed area was swabbed twice in each of two perpendicular directions. The swab was then immersed in 3 ml ethanol and mechanically agitated for 20 s to dissolve any substances transferred from the sample to the swab. This solution was then analysed directly to quantify DOTP and DOP, as well as transesterified to quantify ESBO, as described by Biedermann-Brem *et al*. and detailed below.[81] The ethanol contained 5 ppm 1-ethyl naphthalene (EN) and 5 ppm dimethyl pimelate (DMPi) as internal standards. Three samples were tested for each time interval and were discarded after swabbing.

3.4.3.1 Transesterification of esters

To analyse ESBO, samples were derivatised using a 21% sodium ethoxide/ethanol solution to convert the triglyceride functionality to ethyl esters. The internal standard DMPi also undergoes transesterification in these conditions, and this is used to monitor the reaction.

1 ml of the ethanol solutions was added to 0.325 ml of sodium ethoxide/ethanol solution, shaken, and allowed to react for 5 min. 2 ml MTBE/hexane (60/40%) and 2 ml disodium citrate solution was added. The organic phase was then separated and

dried over excess magnesium sulfate and filtered using pipette filters (Fisherbrand, PTFE 0.2 μm) into vials for GC-MS analysis.

3.4.3.2 Quantification of Plasticisers by GC-MS

GC-MS analysis was carried out on an Agilent 7890B gas chromatograph system coupled to a 5977B mass spectrometer. The injection volume was 1 μl and an inlet temperature of 300 °C was used in splitless mode, under helium gas at 1 ml/min column flow. The column was an Agilent HP-5MS UI, length 30 m, ID 0.25 mm, and the temperature program was 60 °C to 100 °C at 7 °C/min, then 15 °C/min to 300 °C followed by a 5-minute hold.

Samples of known concentration were prepared and used as calibration standards. A total of 6 concentration levels were prepared, and 3 repeats were tested. A quadratic fit was used, giving an R^2 value of 0.995 for DOTP and 0.996 for DOP. Method blank samples were prepared by immersing clean swabs in 3 ml ethanol containing the internal standard and were tested alongside the samples and standards. This confirmed that the swabs did not release any substances that would interfere with the results. These standards were also derivatised as described to quantify ESBO. The peak corresponding to ethyl 9-epoxystearate (Et 9-ES) was chosen for quantification, giving an R^2 of 0.994 with a quadratic fit.

3.4.4 Dynamic Mechanical Analysis

DMA was used to investigate the low temperature properties of the PVC samples tested for exudation (Chapter 5) and to evaluate the novel plasticisers derived from ESBO (Chapter 7). This analysis was carried out using a Perkin Elmer DMA 8000. Experiments were carried out in both tensile and cantilever modes. Samples were tested from −130 °C to 70 °C at a rate of 5 °C min^{-1}, under a 0.5 mm strain at a rate of 1 Hz.

3.5 Synthesis of Novel Bio-based Plasticisers Derived from Epoxidised Soybean Oil

The reaction of the ESBO epoxide functionality with alcohols was carried out under acidic conditions. The effect of varying the catalyst choice and quantity was examined for the methanolysis reaction. All starting materials and products were characterised by ^{1}H and ^{13}C NMR spectroscopy using a Jeol ECS 400 MHz FT-NMR and CDCl$_3$ solvent. NMR integrations were carried out and normalised to the six α-carbonyl protons in the triglyceride structure. FTIR-ATR measurements were taken using a Perkin-Elmer Spectrum Two as described in section 3.4.1. Structures are depicted based on a diepoxide fatty acid chain in which one epoxide has reacted to represent the functionality present in a concise format.

3.5.1 Synthesis of ESBO methyl ether polyol (MEEP, 12)
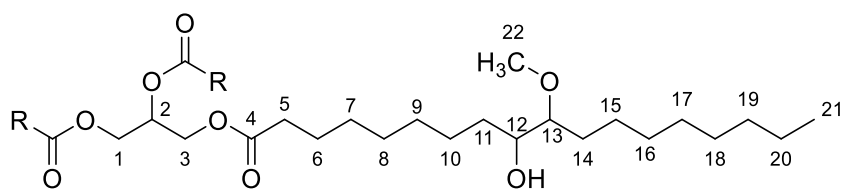
Methyl Ether ESBO Polyol, **9**

ESBO (53.67 g) was reacted with excess methanol (90 mL) with zinc triflate catalyst (0.25 g). The reaction mixture was stirred at reflux (65 °C) under argon for 20 h. The reaction mixture was cooled to room temperature and the solvent removed *in vacuo*. The crude product was dissolved in chloroform (50 mL), washed with 1 M sodium bicarbonate solution (50 mL) and deionised water (2 x 50 mL). The organic fraction was dried over magnesium sulfate and concentrated *in vacuo* to give a yellow oil (53.02 g).

^{1}H NMR (400 MHz, CHLOROFORM-*D*) δ 5.26 (1H, m, H2), 4.29 (2H, dd, *J* = 11.8, 4.2 Hz, H1/3), 4.14 (2H, dd, *J* = 11.9, 5.9 Hz, H1/3), 3.52 – 3.42 (3H, m, H12,13), 3.41 (3H, s, H22), 2.99 (1H, q, J = 5.7 Hz, H15,16) 2.31 (6H, t, *J* = 7.6 Hz, H5), 1.61 - 1.26 (64H, m, H6-11, 14, 17-20), 0.88 (9H, m, H21).

^{13}C NMR (101 MHz, CHLOROFORM-D) δ 173.43, 173.01 (C4), 84.46, 72.74 (C13), 68.98 (C2), 62.21 (C1, C3), 58.25 (C22), 56.75 (C15,16), 50.97, 39.14, 38.83, 38.05, 34.30, 33.63, 33.51, 32.19, 32.05, 32.01, 30.11, 30.02, 29.88, 29.82, 29.60, 29.49, 29.40, 29.24, 29.18, 26.11, 25.90, 25.16, 24.98, 24.93, 22.81, 22.74, 14.25, 14.20 (C21).

FTIR-ATR (v_{max} cm^{-1}) – 3456 (O-H stretch), 2926, 2855 (sp^3 C-H stretch), 1742 cm^{-1} (C=O stretch).

3.5.2 Synthesis of ESBO-mPEG ether polyol (13)
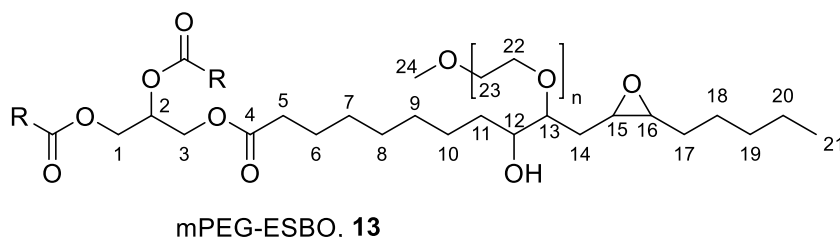
mPEG-ESBO, **13**

MPEG (methoxy polyethylene glycol, 52.15 g, 0.15 mol) of average molecular weight 350 Da was reacted with ESBO (15.08 g, 0.015 mol) and zinc triflate catalyst (0.022 g, 0.06 mmol) at 150 °C under argon with stirring for 2 h. The reaction mixture was cooled to room temperature and triturated with deionised water (3 x 50 mL). The resulting yellow oil was dissolved in chloroform, dried over anhydrous magnesium sulfate, and concentrated *in vacuo,* giving a mass of 15.32 g.

1H NMR (400 MHz, CHLOROFORM-D) δ 5.25 (1H, m, H2), 4.29 (4H, m, H1, H3), 3.65 (34H, s, H22, H23), 3.55 (4H, m, H12, H13), 3.38 (5H, s, H24), 2.31 (6H, t, J = 7.6 Hz, H5), 1.76-1.13 (74 H, m, H6-11, 14, 17-20), 0.88 (9H, m, H21).

^{13}C NMR (101 MHz, CHLOROFORM-D) δ 173.36, 172.95 (C4), 104.95, 104.88, 72.02 (C13), 70.65 (C12), 70.38 (C22, C23), 68.96 (C2), 62.18 (C1, C3), 61.79, 59.13 (C24),

42.94, 42.85, 42.80, 36.10, 34.25, 34.14, 34.08, 32.02, 31.96, 31.91, 31.69, 31.51, 29.79, 29.75, 29.57, 29.46, 29.37, 29.21, 29.16, 29.10, 28.98, 28.17, 28.12, 27.91, 24.95, 24.90, 23.98, 23.89, 23.83, 22.78, 22.67, 22.52, 14.22 (C21).

FTIR-ATR (ν_{max} cm^{-1}) – 3476 (O-H stretch), 2925, 2856 (sp^3 C-H stretch), 1742 (C=O stretch).

3.5.3 Synthesis of Furoic Acid Ester of Methoxylated ESBO (MEFE, 14)
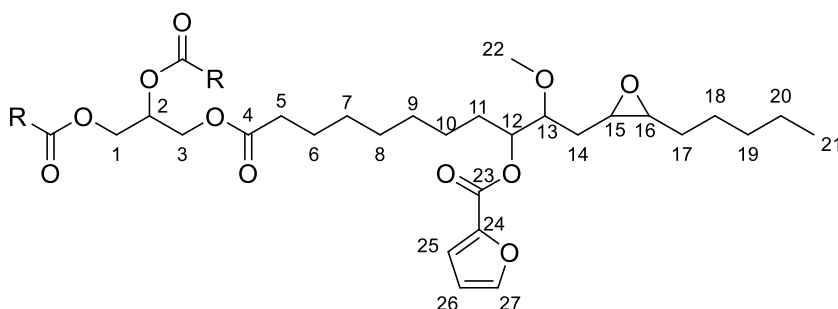
Methoxylated ESBO Furoic Ester, **14**

Methyl Ether ESBO Polyol (MEEP, 10.00 g) was reacted with furoic acid (6.28 g) in dry toluene (100 mL) with PTSA catalyst (0.964 g) in a round bottomed flask with a Dean-Stark condenser trap. The mixture was stirred at reflux (110 °C) for 18 h and cooled to room temperature and the solvent removed *in vacuo*. The crude product was dissolved in chloroform (50 mL), washed with 1 M sodium bicarbonate solution (50 mL) and deionised water (2 x 50 mL). The organic fraction was dried over magnesium sulfate and concentrated *in vacuo* to give a brown oil (11.21 g).

^{1}H NMR (400 MHz, CHLOROFORM-*D*) δ 7.88 – 7.49 (2H, m, H25, H27), 6.51 (1H, m, H26), 5.25 (1H, m, H2) 4.34 – 4.08 (4H, m, H1, H3), 3.44 (1H, s, C22), 3.41 (2H, s, C22), 2.99 (<1H, m, H15, H16), 2.35 (3H, s), 2.31 (6H, t, J = 7.6 Hz, H5), 2.09 (s, 5H) 1.72 – 1.16 (72H, m, H6-11, H14, H17-20), 0.87 (9H, t, J = 6.9 Hz, H21).

^{13}C NMR (101 MHz, CHLOROFORM-D) δ 173.42, 130.14, 129.44, 129.17, 128.36, 128.15, 126.67, 125.43, 111.93, 68.99, 65.20, 62.21, 34.18, 32.06, 29.84, 29.79, 29.64, 29.50, 29.41, 29.25, 25.82, 24.97, 22.82, 21.59, 14.26, 14.17.

FTIR-ATR (v_{max} cm^{-1}) 3020 (sp^2 C-H stretch), 2927, 2856(sp^3 C-H stretch), 1735 (C=O stretch), 1661 (C=C stretch).

3.5.4 Synthesis of Isosorbide Ether ESBO Polyol (IEEP, 15)
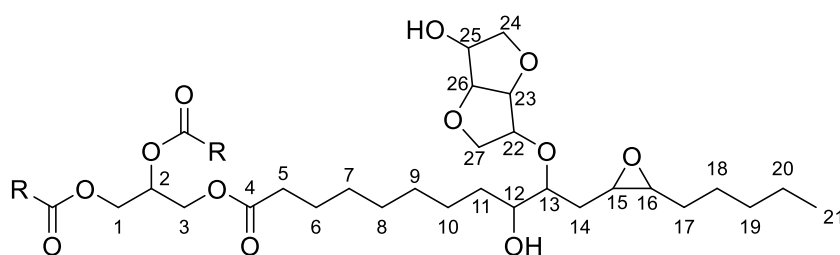
Isosorbide Ether ESBO Polyol, **15**

ESBO (15.01 g) was reacted with an excess of isosorbide (33.83 g) in THF (175 ml) with zinc triflate catalyst (0.279 g). The chemicals were dissolved in THF and dried with excess magnesium sulfate, then filtered into a dry round bottomed flask. The mixture was heated to reflux (75 °C) under argon for 20 h with stirring. The reaction mixture was cooled to room temperature and the solvent removed *in vacuo*. The crude product was dissolved in diethyl ether (50 mL), washed with 1 M sodium bicarbonate solution (50 mL) and deionised water (2 x 50 mL). The organic fraction was dried over magnesium sulfate and concentrated *in vacuo* to give a yellow oil (19.33 g).

^{1}H NMR (400 MHz, CHLOROFORM-D) δ 5.25 (1H, m, H2), 4.7-4.4 (1H, m), 4.21 (4H, ddd, J = 59.9, 11.7, 5.1 Hz, H1, H3), 4.05 − 3.53 (6H, m, H22-H27), 3.49 − 3.37 (7H, m,), 2.55 (2H, t, J = 7.6 Hz), 2.38 (1H, t, J = 7.4 Hz), 2.31 (6H, t, J = 7.6 Hz, H5), 1.70 − 1.20 (70, m), 0.88 (9H, m, H21).

^{13}C NMR (101 MHz, CHLOROFORM-D) δ 173.46, 104.91, 70.76, 68.98, 62.22, 43.01, 34.29, 34.14, 32.06, 29.84, 29.80, 29.61, 29.51, 29.41, 29.22, 28.18, 26.61, 24.98, 24.02, 22.81, 22.73, 14.28.

FTIR-ATR (v_{max} cm^{-1}) – 3457 (O-H stretch), 2926, 2855 (sp^3 C-H stretch), 1741 (C=O stretch).

3.5.5 Diffusion-Ordered NMR Spectroscopy

Diffusion-Ordered NMR Spectroscopy (DOSY) was used to analyse the products further and confirm that the reactions had occurred. A matrix of pulsed field gradients from 10 to 240 mT m^{-1} was used with a 50 ms diffusion time. The settings were chosen to give a signal reduction of 70-90% at the higher field gradient compared to the lower, to give an appropriate range of data.

MestreNova software was used to analyse the data. The data was transformed to give a 2D graph of ^{1}H-NMR against diffusion rate f1. The parameters used for the transformation were Bayesian method, Resolution factor 0.1, 1 repetition, DOSY spectrum range 1x10^{-14} – 1x10^{-12}, 32 points in the diffusion dimension.

3.6 Evaluation of Novel Plasticisers

3.6.1 Solvent Casting of Plasticised Films

The novel plasticisers were incorporated into PVC films using solvent casting. Plasticiser (2.5 g) was dissolved in 50 ml THF in a 100 ml round bottomed flask with stirrer bar. 0.05 µl liquid barium-zinc stabiliser was added with stirring, followed by 5 g PVC resin (K70 suspension resin). A condenser was attached, and the mixture was heated to reflux (66 °C) under argon for 2 hours until the polymer was fully dissolved. The mixture was allowed to cool to room temperature and then poured into a dry glass petri dish and loosely covered to allow gradual evaporation of the THF for 7 days.

The films were removed from the petri dishes and dried under vacuum at 40 °C for 2 hours to remove residual THF.

3.6.2 Tensile Properties Testing

For the tensile properties testing, 1 mm thickness plaques were prepared using a heated hydraulic press. The cast films were placed in a steel mould which was subjected to 200 bar at 160 °C for 4 minutes and cooled under pressure. Dumbbell shaped pieces in accordance with ISO 37:2017 (E) Type 2 (Figure 3.3) were cut from the moulded sheets. The thickness of the central narrow portion of each sample was measured to 0.01 mm and recorded. Five test pieces were prepared for each plasticised PVC formulation.
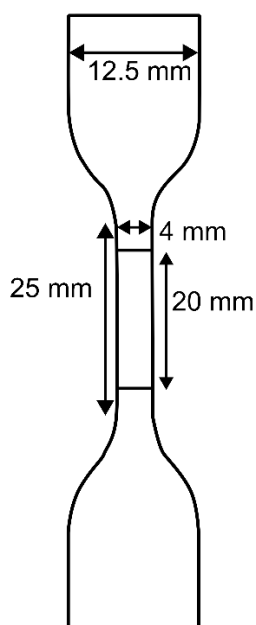
Figure 3.3: Type 2 dumbbell test piece in accordance with ISO 37:2017 (E).

The tensile properties of the moulded films were tested using a Hounsfield H10KS UTM equipped with a 1000 N load cell and laser extensometer. Load and extension were measured, and stress and strain calculated from the sample dimensions. Samples were secured in the tensiometer grips and a small preload applied (0.3 N) to remove any slack from the sample prior to testing. The crosshead speed was set to 100 mm min^{-1}.

3.6.3 Scanning Electron Microscopy

Plasticised PVC samples were analysed by scanning electron microscopy to examine the microscopic structure of the polymer. Samples were prepared by cryogenic fracture of samples cut from the solvent-cast films. Pieces of film were cooled in liquid nitrogen and manually broken. The samples were sputter coated with 10 nm gold-palladium using a Leica EM ACE200. The samples were examined using a Zeiss Supra 40VP SEM (2 kV acceleration voltage) at 5000-20,000 x magnification to investigate the internal structure.

3.6.4 Thermogravimetric Analysis

Samples of the novel plasticisers and plasticised films were tested by TGA using a Mettler Toledo TGA 1 to investigate the volatility of the plasticiser as well as the effect of the plasticiser on the thermal stability of the resulting PVC sample. Samples of approximately 15 mg were weighed into aluminium pans (plasticisers) or alumina crucibles (PVC samples) and heated at 20 °C min^{-1} to 600 °C (plasticisers) or 1000 °C (PVC samples) under a nitrogen atmosphere.

4 Experimental Rationale

4.1 Compatibility Test Method Development

To develop the test method for quantitative analysis of plasticiser compatibility in PVC, five formulations were chosen, comprising three plasticisers and their mixtures. These plasticisers were chosen to represent three main groups of plasticisers in use within the PVC industry – phthalate esters (DOP), non-(ortho-)phthalate petrochemical plasticisers (DOTP) and bio-based secondary plasticisers (ESBO). The samples for testing plasticiser compatibility were produced using industry-standard lab-scale procedures (Section 3.3), which replicate the conditions used in manufacturing to produce PVC compounds. DOP and DOTP are isomers with a known and well reported difference in plasticisation behaviour.[2, 111] DOP was the dominant plasticiser for PVC prior to REACH regulation, while DOTP is widely used as a replacement for phthalate plasticisers.[16] ESBO is typically used for its properties as both a secondary plasticiser and heat stabiliser in combination with primary plasticisers such as phthalates and so the mixed plasticiser formulations were chosen to evaluate the effect of mixing petrochemical and bio-based plasticisers.

A PVC formulation was chosen for the evaluation samples to include only necessary additives besides the polymer and plasticiser. Typical PVC formulations can contain many additives such as fillers (most often calcium carbonate), flame retardants and antimicrobial additives, however these were omitted to prevent the influence of other additives on the plasticiser-polymer interaction. A heat stabiliser additive based on calcium and zinc stearate was included to prevent decomposition of the polymer during processing, as PVC will decompose readily to produce HCl gas on heating without additives to prevent this.[112] The amount of plasticiser was chosen to give a 'medium softness' flexible PVC. Suspension PVC resin with a K-value of 70 was chosen as this is the most common PVC resin used for flexible PVC compounds produced through thermomechanical methods (emulsion PVC resins being more common in solvent-based PVC production).[111]

The ASTM D3691 method for testing plasticiser compatibility was chosen as the basis of the compatibility test method as this is well known in the industry and plasticiser exudation under this test is well established. The analytical techniques were mainly chosen to be within the capabilities of PVC industry laboratories, which often have access to FTIR and GC-MS. Raman spectroscopy is less common but was also evaluated after FTIR spectroscopy was found to be unsuitable for mapping of plasticiser exudation.

In the evaluation of different methods of FTIR measurement, reflectance and transmission FTIR were found to be unsuitable for use in these plasticised PVC samples. The samples were not sufficiently reflective and absorbed the IR beam too strongly at the thicknesses tested to give good quality data. As such, micro-ATR was chosen for this investigation.

The aim of the mapping techniques was to create a depth profile of the samples which would show the movement of plasticiser from the bulk to the surface where it was exuding. The suitability of the micro-ATR FTIR mapping technique for identifying changes in the composition of a plasticised PVC sample was evaluated by creating a sample with a known change in composition. This was prepared by moulding a plaque of two differing PVC-plasticiser compositions (PVC-DOTP and PVC-ESBO) alongside one another to create a boundary where the composition changes. While the change in composition could be identified (as shown in Section 5.3.1), this experiment showed the technical challenges in using a contact mapping technique on the flexible sample, as the sample would deform under the required pressure of the ATR probe and surfaces showing plasticiser exudation would lead to contamination of the probe.

Mapping of the exuding samples was also investigated through Raman spectroscopy (Section 5.4). Initially, measurements were attempted on both cross-sectional cut surfaces and the exuding surfaces of samples. However, the cut samples posed a problem as irregularities in the cut surface made it difficult to reliably focus the Raman laser, giving poor quality maps. As such, the surface distribution of exuded plasticiser was chosen for the continuing work.

4.2 Synthesis of Bio-based Plasticisers from Epoxidised Soybean Oil

The target compounds studied in this work aim to improve the compatibility between the plasticiser and PVC. The reactant molecules (Figure *4.1*) were chosen to introduce more polarity into the structure of the plasticiser relative to ESBO, thus increasing the intermolecular attraction between the plasticiser and the PVC polymer. Additionally, phthalate plasticisers in part owe their compatibility to the aromatic ring in their structure, and the introduction of aromaticity into bio-based plasticisers intended to replace phthalates has therefore also been the subject of investigation.[89] In a computational analysis of a series of phthalate plasticisers, the aromatic ring was found to have the largest contribution towards the polymer-plasticiser interaction.[57] This was attributed to the large amount of accessible surface area of the group, as well as the polarisability of the disubstituted ring. The ester groups also provided a large contribution to the intermolecular interactions, but this was diminished by the comparatively smaller accessible surface area when considered as part of the whole phthalate ester molecule.
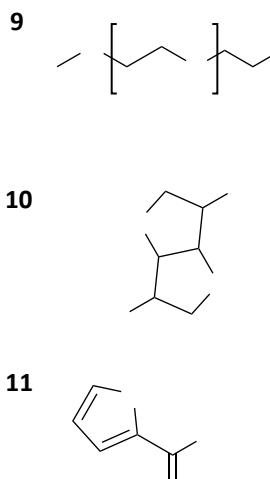
Figure 4.1*: Bio-based reactants used to modify the structure of epoxidised soybean oil to produce novel plasticisers for PVC: methoxy polyethylene glycol (mPEG, 9), isosorbide 10 and 2-furoic acid 11.*

Furans can be produced from biomass and are a significant area of renewable chemistry.[113] Furan esters have been investigated for use as a replacement for the aromatic benzene group present in phthalates and similar plasticisers, showing promising characteristics for successful replacement of current petrochemical plasticisers, such as low migration.[84, 114] As such, the reaction of a soybean oil-based polyol with 2-furoic acid **11** is described herein, with the aim of introducing aromaticity into the ESBO derivative structure. Furoic acid is produced by the oxidation of furfural, which has been produced commercially from biomass for decades.[115]

Isosorbide **10**, derived from glucose, has shown potential as a bio-based starting material for novel plasticisers.[90] Lee *et al*. evaluated a series of diesters of isosorbide with fatty acids, as well as the effect of epoxidation on the resulting diesters, and found a positive correlation of shorter chain lengths with greater compatibility, measured by plasticiser absorption.[116] Converting the alkene of oleic acid to an epoxide also promoted compatibility in the resulting epoxidised isosorbide diester. Yang *et al*. reacted isosorbide with acyl chlorides to investigate the effect of alkyl chain length on the resulting diester plasticisers, and also found greater compatibility of plasticisers with shorter alkyl chains.[117] The role of the isosorbide structure has been compared to the aromatic ring of phthalates and the heterocyclic functionality should introduce polarity into the resulting compound.[116]

Polyethylene glycol and compounds thereof have also been investigated in PVC plasticisation and have the interesting property of both adding a higher-volume morphology to the ESBO backbone, as well as additional polarity.[84, 118, 119] Methoxy polyethylene glycol **9** was chosen so that only one alcohol group remained in the PEG structure, thus preventing the crosslinking that could occur in a PEG molecule with alcohol functionalities at both ends of the chain.

4.3 Characterisation of Bio-based Plasticisers

4.3.1 Diffusion-Ordered NMR Spectroscopy

Purification of the products was limited by the mixed composition of the ESBO starting material. Diffusion-Ordered NMR Spectroscopy (DOSY) can be used to determine the composition of mixtures of samples by separating the 1H-NMR signals based on the diffusion properties of the molecules. This analysis is carried out by constructing a matrix of pulsed field gradient strengths and measuring the signal decays - molecules with a faster diffusion coefficient will decay more rapidly than those with a slower diffusion coefficient. If multiple substances are present in the mixture, and have sufficiently different diffusion coefficients, these can be resolved into their separate 1H-NMR spectra.

A matrix of pulsed field gradients from 10 to 240 mTm^{-1} was used with a 50 ms diffusion time. The settings were chosen to give a signal reduction of 70-90% at the higher field gradient compared to the lower, to give an appropriate range of data.

4.4 Evaluation of Bio-based Plasticisers

The methods chosen to evaluate the bio-based plasticisers in PVC compounds were selected as the most effective methods to demonstrate plasticisation for the quantity of plasticised PVC that was produced. The samples were produced by solvent casting as there was insufficient quantities for two-roll milling or extrusion. Test methods such as British Standard Softness (BSS) or Shore A Hardness were considered but there was insufficient quantities of each material to produce a suitable sample. Tensile strength and elongation are closely correlated to BSS in the absence of other differences in formulation, and so the tensile properties were evaluated to determine the effectiveness of the plasticiser candidates.[79] The glass transition behaviour was examined by DMA to further investigate the suitability of the plasticiser candidates. A successful plasticiser must lower the glass transition temperature of the polymer, and not display signs of phase separation which would be observed as multiple or

poorly-defined glass transitions. In this evaluation, the properties of PVC-DOP were considered to be those of a well-plasticised PVC compound, and thus were the target for the novel plasticiser candidates. The successful plasticiser candidate would show a change in plasticisation properties relative to PVC-ESBO, such that the resulting plasticised PVC is more similar to PVC-DOP.

5 Development of an Improved Test Method for Plasticiser Compatibility

5.1 Introduction

Plasticiser compatibility in PVC formulations is crucial for creating stable PVC-plasticiser blends that can maintain the properties of flexibility and softness over the lifespan of the plastic product, which is often many years. Plasticiser exudation leads to undesirable properties such as tackiness, as well as environmental pollution. The current industry standard method for testing plasticiser compatibility is the ASTM D3291 'Loop Spew' compatibility test, wherein plasticised PVC samples are compressed in a loop and exudation is judged by a visual assessment of a test paper wiped across the sample surface. This test relies on a subjective determination of the extent of plasticiser exudation on a scale from 0 – no exudation to 3 – heavy exudation. This method cannot distinguish between different plasticisers in a mixture and is dependent on the judgement of the operator. The recommended duration of the exposure to the compatibility loop in the ASTM standard is 4 h, 24 h and 7 days, followed by continuing 7-day intervals over an extended period if required.

A number of analytical techniques are explored in this chapter as potential methods to improve upon the ASTM D3291 'Loop Spew' compatibility test. A maximum of 1 h compression has been used in this work to investigate if the test could be accelerated by using techniques with greater sensitivity. The work presented in this chapter has been published in the Journal of Applied Polymer Science.[120]The techniques evaluated herein were chosen with consideration for the typical capabilities of an industrial PVC compounding laboratory. FTIR and to a lesser extent GC-MS are widely available techniques within the PVC compounding industry, while Raman spectroscopy is rarely used. However, Raman spectroscopy allows for an investigation into microscopic mapping that was not possible by FTIR. The samples tested in this chapter consist of single plasticisers DOP **1**, DOTP **6** and ESBO **8**, as well as mixtures of DOTP-ESBO and

DOP-ESBO, with a total plasticiser content in each sample of 41%. Full formulations are shown in Chapter 3 (Table 3.1).

5.2 Visual Exudation Evaluation

Samples were tested in the compatibility loop for 60 minutes, then removed and wiped with a dry test paper. The paper was examined for exudation visually and rated from 0-3 in accordance with the ASTM D3291 standard. All samples showed no visible exudation, and so would be given a grading of 0 by the ASTM D3291 scale under these conditions.

5.3 FTIR Spectroscopy

5.3.1 Micro-FTIR Spectroscopy

The suitability of the micro-ATR FTIR mapping technique for identifying changes in the composition of a plasticised PVC sample was evaluated by creating a sample with a known change in composition (PVC-DOTP to PVC-ESBO) as described in section 4.1. An FTIR map of this sample was measured and evaluated using the Perkin Elmer SpectrumIMAGE Viewer software. Plots of correlation to DOTP (Figure 5.1) and ESBO (Figure 5.2), the two plasticisers used, were created using this software, as well as a plot of the ester intensity using the ChemiMap function (Figure 5.3). This function measures the peak area for two FTIR regions known to correlate with certain bonds – in this case the areas were 1780-1665 cm^{-1} (C=O stretch) and 1300-1220 cm^{-1} (C-O stretch). All three methods showed a gradient of composition change from one formulation to the other, indicating that the samples mixed to a degree at the boundary, located approximately at the horizontal midpoint on the maps. This confirms that the micro-ATR mapping can measure a change in composition for these plasticised PVC samples.
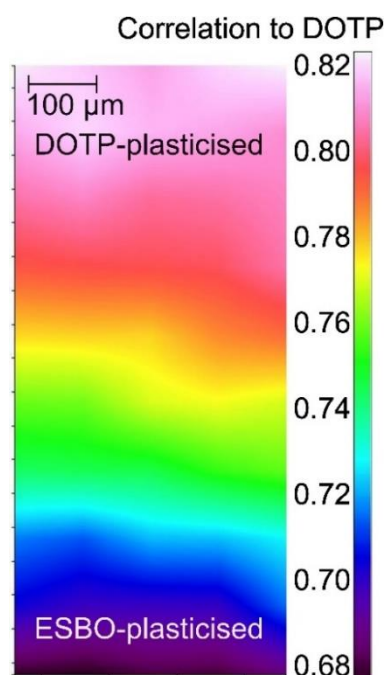
Figure 5.1: FTIR map of the surface of a plasticised PVC sample with a change in composition from DOTP (top) to ESBO (bottom) plasticisation. Scale (right) shows the correlation to the DOTP FTIR spectrum, which for this map ranges from 0.68 to 0.82 (exact match equals 1). The change in composition from DOTP to ESBO plasticisation is shown by the change in correlation to DOTP.
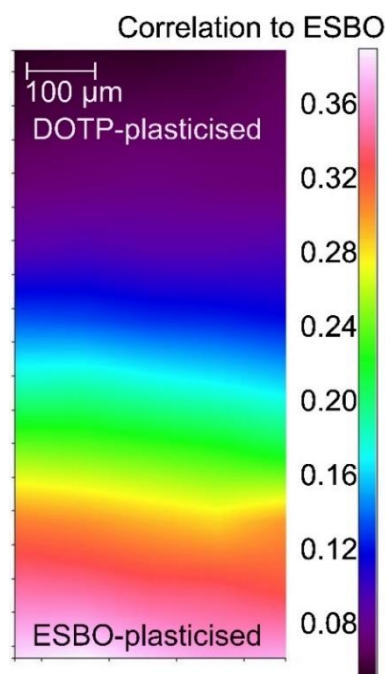
Figure 5.2: FTIR map of the surface of a plasticised PVC sample with a change in composition from DOTP to ESBO plasticisation. Scale (right) shows the correlation to the ESBO FTIR spectrum, which for this map ranges from <0.08 to >0.36 (exact match equals 1). The DOTP-plasticised region shows minimal correlation to the ESBO spectrum as indicated by the blue-purple region on the map.
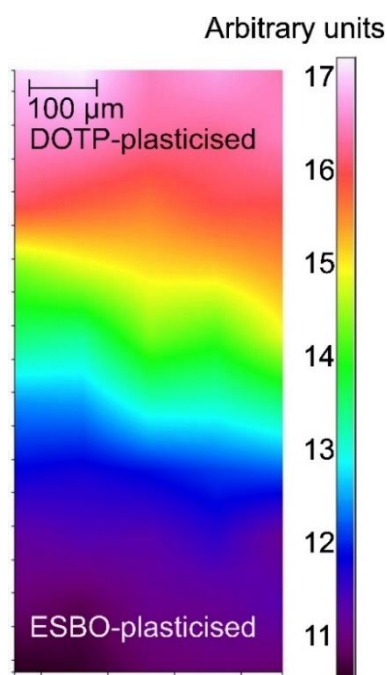
Figure 5.3: FTIR map of the surface of a plasticised PVC sample with a change in composition from DOTP to ESBO plasticisation by ChemiMap correlation to the ester functionality. This scale is in arbitrary units, and shows that the DOTP-plasticised area contains a greater intensity of the band associated with ester groups.

The measurement of cross sections of samples which showed visible exudation in the compatibility loop test was then attempted. Measurements could not be carried out on the exuding surfaces since the plasticiser would transfer to the ATR IRE (crystal). The IRE would then require cleaning after each measurement, which would be inefficient and time consuming.

For the cross sections, the exuding surface was first cleaned with a dry paper cloth and then cut into slices with a scalpel. The cleaning was to prevent transfer of plasticiser to other areas of the sample during cutting.

The maps of these cross sections were analysed as described, and an example is shown in Figure 5.4. It was predicted that as plasticiser migrates from the inner surface of the loop, a gradient of plasticiser distribution would develop through the bulk of the sample. However, the data did not support this. Some variation can be seen throughout the sample, but no structure or pattern of plasticiser distribution was

noted. Furthermore, the individual FTIR spectra did not show any significant differences between the outer and inner edge of the compressed sample, as illustrated in Figure 5.5.
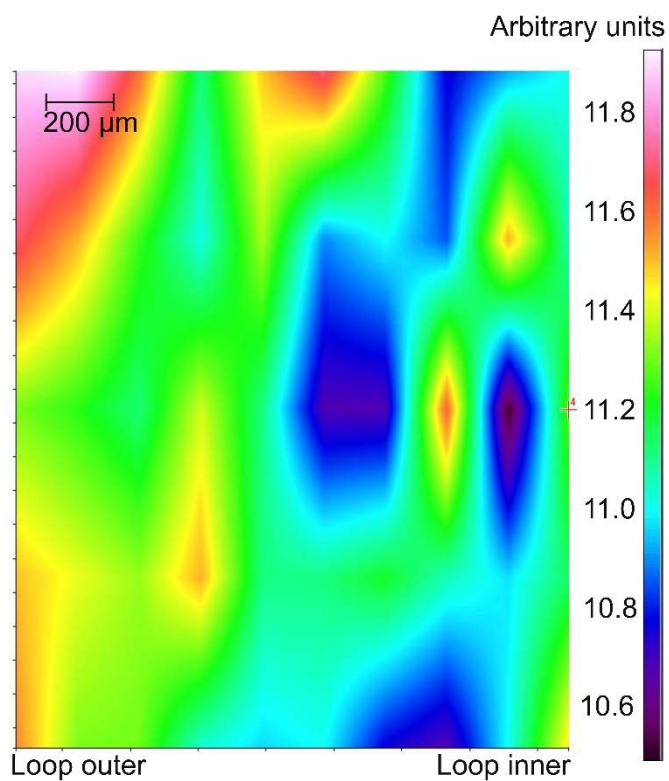
Figure 5.4: ChemiMap Ester correlation to a cross-sectional map of a plasticised PVC sample following compression in the ASTM D3291 loop.
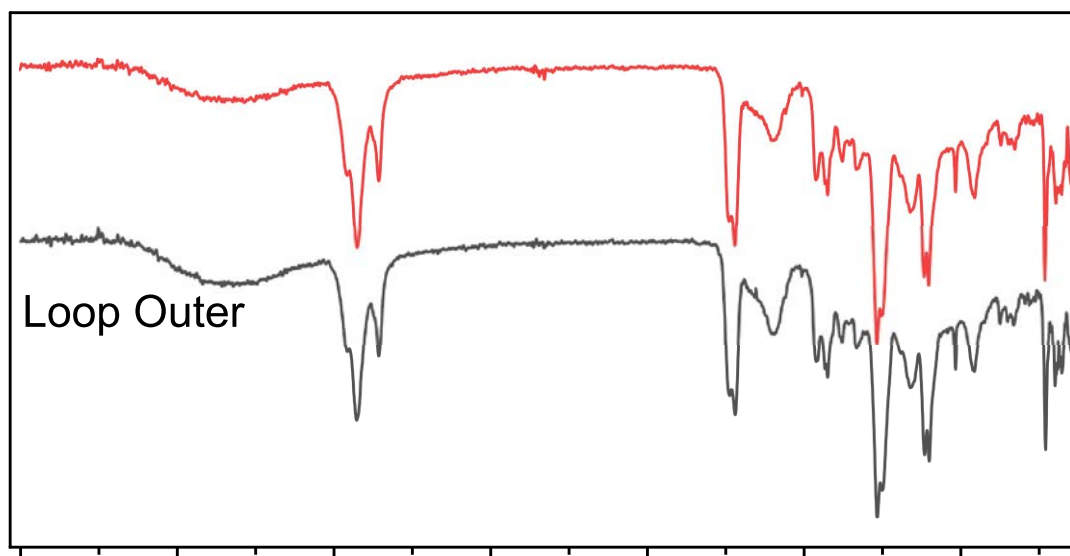
Figure 5.5: FTIR spectra from micro-ATR mapping of a compressed PVC sample, showing no significant differences between the outer and inner edges.

There could be a number of explanations for this observation. Firstly, that plasticiser exudation occurs from a very thin layer at the PVC surface and so the inner measurement was not representative of this depletion. Secondly, the level of plasticiser lost to exudation may be so low that it does not create a significant change in the FTIR spectrum of the plasticised PVC sample. Finally, plasticiser diffusion within the PVC sample could replace any plasticiser lost at the inner edge and so no difference would be detected throughout the bulk of the sample.

It was observed during this experiment that the contact from the IRE towards the edges of the sample caused the sample to deform due to its flexibility. This meant that the position of the scan may not have been exact and scans very close to the edge of the sample were not possible as the required contact pressure could not be achieved without greatly deforming the sample. Another drawback was the difficulty of preparing a clean straight cut through the sample. As such, this method was not investigated further.

5.3.2 Macro-scale FTIR Spectroscopy

The FTIR carbonyl stretch peak position (1700-1800 cm^{-1}, Figure 5.6) has been used for qualitative identification of the different plasticisers used in this study. It is has been shown that interaction of the plasticiser with the PVC matrix will lead to a change in carbonyl peak position, due to weakening of the carbonyl bond as a result of the interaction with the polar PVC chain.[71, 72, 74, 90, 121] To that end, the peak positions for individual plasticisers, plasticiser mixtures, plasticised PVC samples prior to the loop compression test, and plasticised PVC samples after compression were measured. The measurement following compression was taken in the region expected to show any exudation that was occurring, i.e., the portion of the sample that was bent in the loop during compression (Figure 5.7).
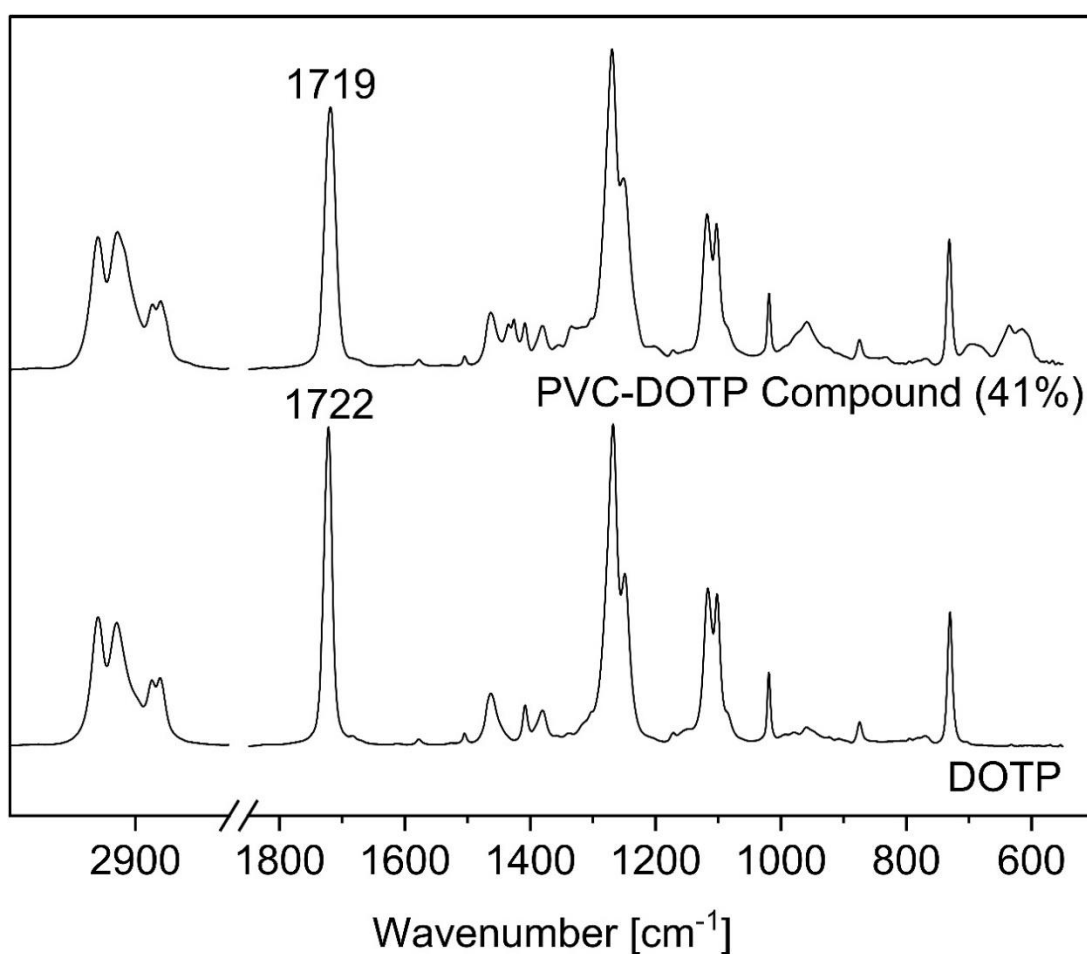
Figure 5.6: FTIR spectra of DOTP and a DOTP-plasticised PVC sample (Formulation 1), with the carbonyl symmetric stretching band position indicated.

8 mm spacer

PVC sample

Not to scale

Compressed area

Measured area
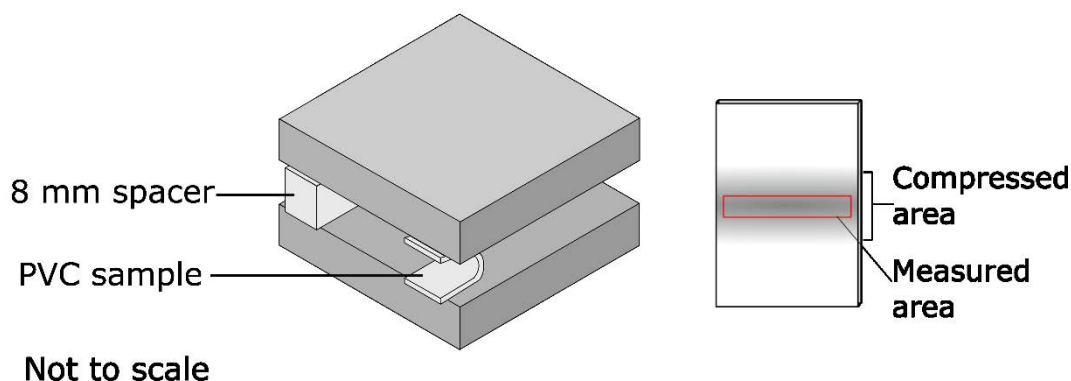
Figure 5.7: Diagram of the compatibility compression loop test and the PVC sample following compression with the FTIR testing location indicated.

It can be seen in Figure 5.6 that the carbonyl peak in the plasticiser shifts to a lower wavenumber in the plasticised PVC sample. The difference between the carbonyl peak positions in the plasticisers and respective plasticised PVC samples are shown in Table 5.2.

The carbonyl peaks of the individual plasticisers in the plasticiser mixtures (either as free liquids (1:1 DOTP-ESBO and 1:1 DOP-ESBO) or in the PVC compound) overlapped and therefore deconvolution was used to identify peak positions. The WIRE® software package of the Renishaw Invia Raman spectrometer was used to perform the deconvolution. The optimum deconvolution was achieved by manually providing boundaries for peak positions and a maximum of 3000 iterations, with a tolerance value of 0.001. The model provided a best fit using a mixture of Gaussian and Lorentzian peak shapes.

The peaks found by this method for the plasticiser mixtures were shifted relative to the single plasticisers, as shown in Table 5.1. These data suggest an interaction between the plasticisers in the mixtures leading to a change in the carbonyl bond stretching frequency following mixing. In DOTP and DOP individually, the carbonyl groups will interact most strongly with other carbonyl groups due to the electronegativity of the carbonyl oxygen. However, these groups are relatively sterically hindered by their position next to the aromatic ring, particularly so for DOP

where the carbonyl groups are in the ortho position. ESBO contains epoxide groups in addition to ester groups, and these are located on long alkyl chains which are more mobile and may be more able to interact with the para- and ortho-phthalate ester groups. This could explain the corresponding increase in the ESBO carbonyl position in the DOTP-ESBO mixture, if this interaction reduces the number of epoxide groups interacting with ESBO carbonyl groups. However, it would not explain the negative shift of the ESBO carbonyl bond position in the mixture with DOP.

Table 5.1: Carbonyl peak positions of each plasticiser individually and in the mixtures (DOTP-ESBO) and (DOP-ESBO) investigated.

Plasticiser	DOTP carbonyl position	DOP carbonyl position	ESBO carbonyl position
Single plasticiser	1722.5	1728.5	1742.4
DOTP-ESBO mixture	1720.7 (-1.8)	-	1744.3 (+1.9)
DOP-ESBO mixture	-	1724.8 (-3.7)	1739.8 (-2.6)

The carbonyl peaks in all formulations tested showed a shift between the free plasticiser(s) and the plasticised PVC samples (Table 5.2). However, following 60 minutes compression, the carbonyl peak positions changed very little – a maximum of 1 cm^{-1} as shown in Figure 5.8. As such, the difference in the carbonyl peak position between the plasticiser and the PVC-plasticiser blend prior to the compression test was identified as the most significant measurement from this analysis.

Table 5.2: Carbonyl peak positions in PVC formulations, and shift in carbonyl peak position between the free plasticiser (or plasticiser mixtures for Formulations 4 and 5) and the plasticised PVC samples before compression testing.

Sample	Carbonyl peak position (cm^{-1})	Carbonyl shift relative to free plasticiser (cm^{-1})
Formulation 1 – DOTP	1719.2	-3.4
Formulation 2 – DOP	1724.6	-4.0
Formulation 3 - ESBO	1739.9	-2.5
Formulation 4 – DOTP	1719.2	-1.6
ESBO	1742.0	-2.2
Formulation 5 – DOP	1723.0	-1.8
ESBO	1739.2	-0.6

The carbonyl shift in the PVC compound corresponds to the strength of the interaction between the PVC and the carbonyl group of the plasticiser.[71] By this measure, in the single plasticiser formulations DOP would be considered the most compatible (strongest interaction) and ESBO the least compatible (weakest interaction). In Formulation 4 (PVC-DOTP-ESBO) the carbonyl shift was substantially smaller for DOTP compared to Formulation 1 (PVC-DOTP), while the ESBO carbonyl shift was similar to that of Formulation 3 (PVC-ESBO). This would suggest that the compatibility of DOTP is reduced when mixed with ESBO. In Formulation 5 (PVC-DOP-ESBO) both the DOP and ESBO carbonyl shifts are significantly lower compared to each plasticiser alone. ESBO in particular changed by only 0.6 cm^{-1}. However, comparing the absolute carbonyl peak position gives a different picture. In Formulation 4, the DOTP peak has the same wavenumber as in Formulation 1 while the ESBO peak is at a similar wavenumber to free ESBO (1742.4 cm^{-1}). DOP is shifted to lower wavenumber in

Formulation 5 compared with Formulation 2, while the ESBO peak position is similar to that of ESBO in Formulation 3. This suggests that the DOTP carbonyl group is in a similar state of solvation whether in PVC-DOTP or in PVC-DOTP-ESBO. Likewise, the DOP carbonyl bond is weakened further by interactions in PVC-DOP-ESBO versus PVC-DOP. These interactions would require further investigation to investigate the relationship of solvation of each plasticiser pair and their effects on the extent of exudation.

As discussed previously, the observed carbonyl peak positions following the compression test showed very minimal changes compared to the unstressed PVC samples, however some small differences between the samples can be seen. PVC-DOTP appears to show the greatest change in carbonyl peak position over time (Figure 5.8), and the other single plasticiser samples and mixed plasticiser samples (Figure 5.9) showed weaker trends. While the peak positions show a slight indication that they are changing over time, this is not sufficiently large to make robust conclusions from the data. These changes are considered negligible relative to the resolution of the FTIR instrument. For these samples and conditions, it appears that the level of plasticiser exudation is below the detection limit of the method. This method could potentially be used as a qualitative indicator of plasticiser compatibility and does show some improvement above the visual observation method as it does identify PVC-DOTP as having higher exudation than the other samples, as confirmed by GC-MS in section 5.5.
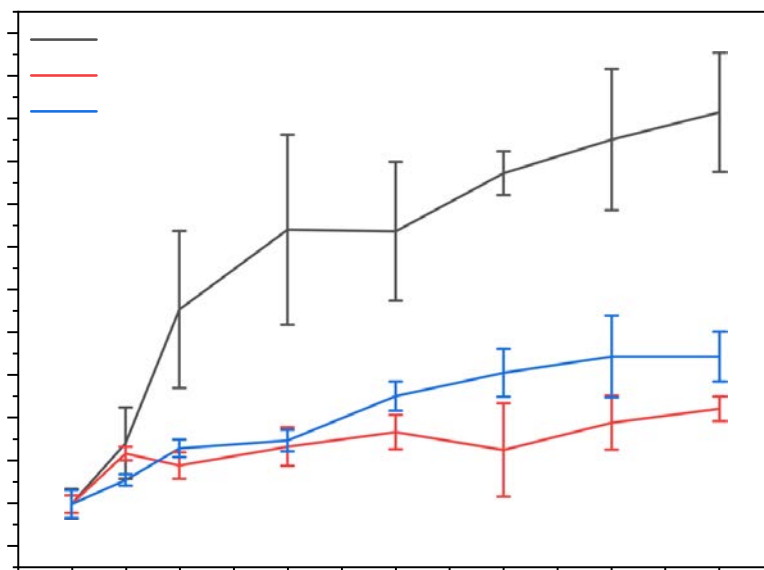
Figure 5.8: Carbonyl peak position change for the single plasticiser samples.
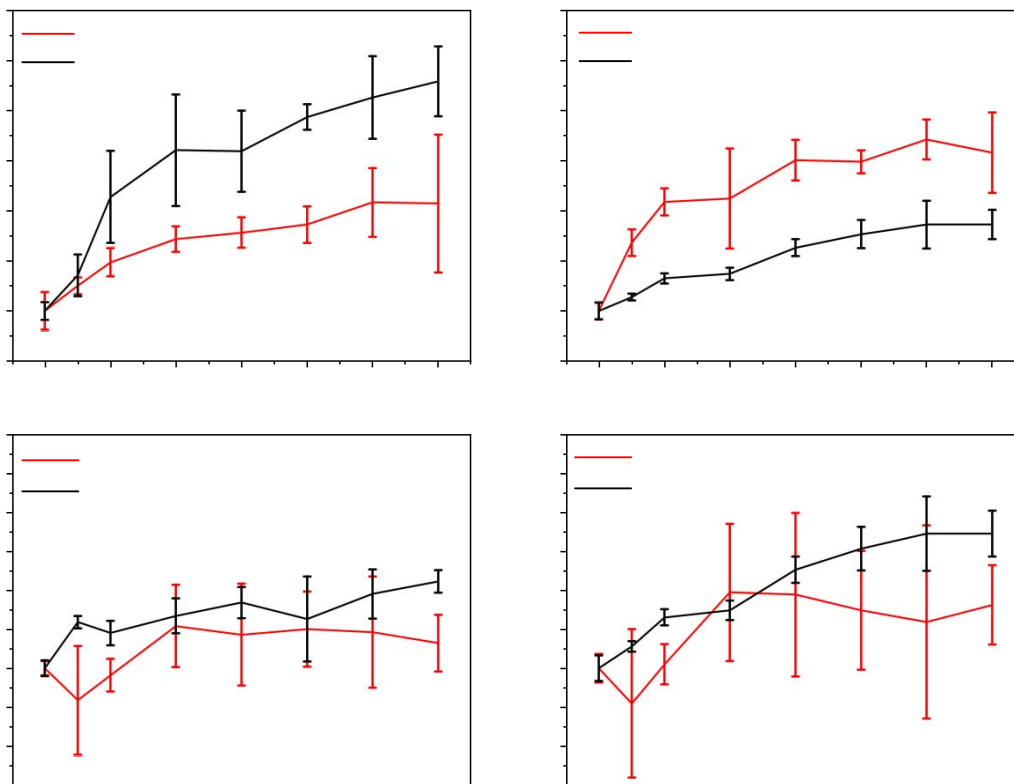
Figure 5.9: Carbonyl peak position changes for the mixed plasticiser samples in comparison with the respective single plasticiser samples.

Furthermore, the peak width at half height was analysed for the three single-plasticiser samples (Figure 5.10). It was thought that as plasticiser exuded from the sample, the environment measured at the IRE would consist of free plasticiser on the surface as well as the plasticised PVC. The carbonyl peak would thus be comprised of two peaks at slightly different wavenumbers, and this could be observed as an increase in the peak width. The mixed plasticiser samples were not investigated at this time due to the complication of the overlapping peaks from each plasticiser.
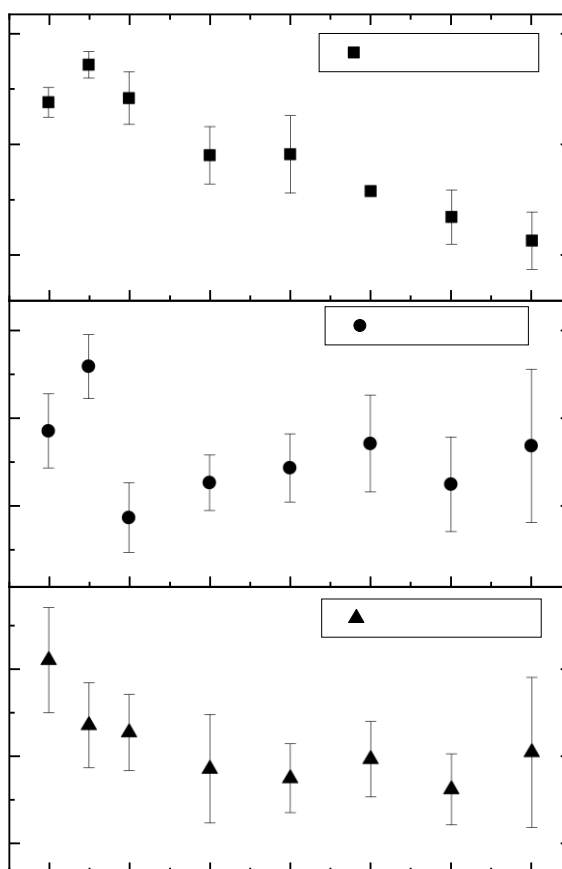
Figure 5.10: FTIR carbonyl C=O peak width measurements for PVC-DOTP, PVC-DOP and PVC-ESBO.

As with the carbonyl peak position, the most significant change in peak width over time was observed for PVC-DOTP, where a trend towards a smaller peak width can be seen. For PVC-DOP and PVC-ESBO, no trend in peak width is observed. The peak width for PVC-DOTP prior to compression was measured to be 20.2 cm^{-1}, while the peak

width for DOTP was measured to be 15.3 cm^{-1}. By contrast, the change in the peak position is approximately 3 cm^{-1}. As such, any broadening of the peak due to multiple carbonyl environments would be masked by the larger broadening due to the initial interaction with PVC. Instead, the peak width is seen to narrow, as a larger proportion of the measured sample is composed of DOTP alone, and so the narrower peak width of the free plasticiser has a larger influence on the overall measured width.

Spectra of the residue left on the IRE after the sample was removed were also collected. These spectra largely resembled the plasticiser(s) present in the PVC sample; however, the intensity was weak, and the signal-noise ratio was low due to poor coverage of the IRE. As such, this was not investigated further.

A limitation of the ATR-FTIR method is that it requires good contact between the sample and the IRE to obtain high quality data, as the evanescent wave penetrates the sample to only a few microns (calculated in section 3.4.1 as 4.0-4.9 μm at a wavenumber of 1725 cm^{-1}).[109] The ATR attachment clamps the sample to the IRE, ensuring close contact. This could be affecting the FTIR results, since the pressure applied by the ATR clamp could force the liquid plasticiser on the sample surface to flow away from the point of contact of the IRE. This would limit the amount of plasticiser that could accumulate between the solid PVC sample and the IRE, and so could affect the accuracy of the results. This method of determining compatibility is also limited by considering only the interactions of the ester carbonyl group. This may not directly correlate to the overall strength of the plasticiser-polymer solvation, as other parts of the plasticiser molecule may also interact with the polymer.

5.4 Raman Spectroscopy

Raman Spectroscopy mapping was investigated to measure the extent of exudation across the exuding surface. Unlike micro-ATR FTIR, Raman spectroscopy is a non-contact technique and so direct examination of the exuding surfaces was possible. Optical microscope images were first collected which showed the distribution of exuded droplets across the surface of the samples, and which were used to determine the sampling area for the Raman mapping (Figure 5.11). Examination of PVC-DOTP

under the 10x optical objective of the Raman microscope showed visible evidence of exudation after as little as 2 minutes in the compression loop. Spectra were collected for the raw materials as well as for the plasticised PVC samples before compatibility testing to determine the change in spectra in areas that were displaying exudation. The individual spectra showed little difference between the exuding areas and non-exuding areas as shown by Figure 5.12, however the slight differences are highlighted in Figure 5.13. These differences are due to stronger contributions from DOTP in the exuding areas and PVC in the non-exuding areas, corresponding to the bands assigned in Table 5.3.

Figure 5.11: Optical microscopy image of exudation on a plasticised PVC sample.
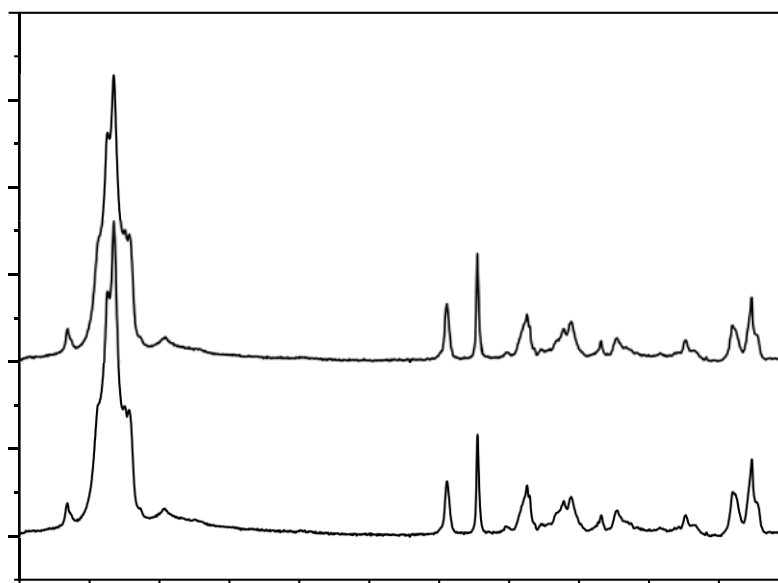
Figure 5.12: Raman spectra for PVC-DOTP in areas of no exudation and high exudation, showing that the spectra are largely similar.
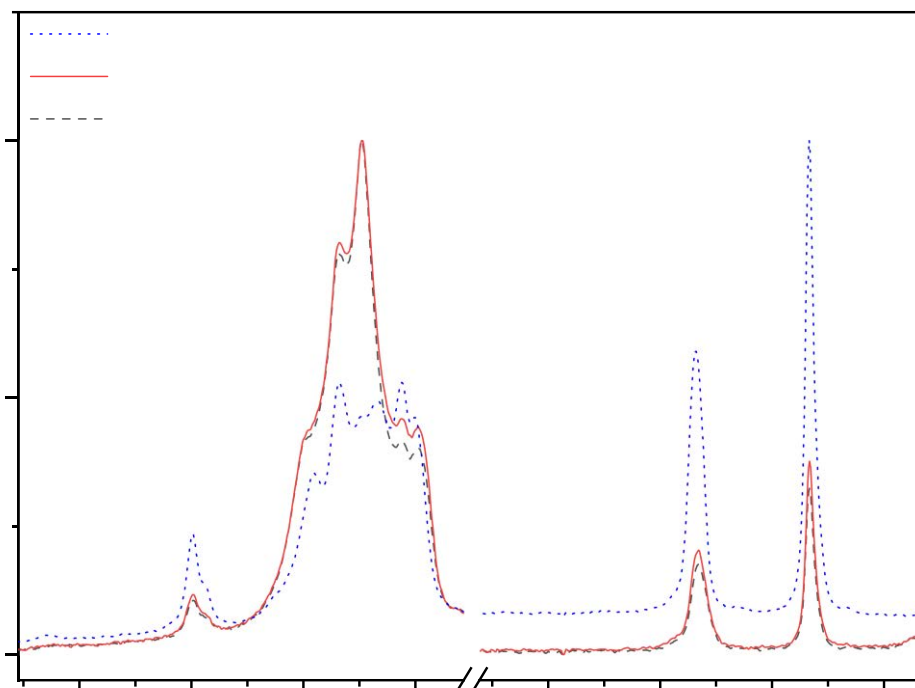
Figure 5.13: Raman spectra for PVC-DOTP taken from areas of no exudation and high exudation as well as DOTP plasticiser, showing a small increase in intensity for the peaks due to DOTP in the exuding area.

Table 5.3: Raman shift assignments for PVC and DOTP corresponding to the differences in intensity in the spectra shown in Figure 5.13.

PVC		DOTP	
Raman Shift (cm^{-1})	Assignment	Raman Shift (cm^{-1})	Assignment
2915.9	CH$_2$ stretching	1614.2	Aromatic C–C
2939.7	CH$_2$ stretching	1725.6	C–O stretching
2973.1	C–H stretching		

A map of Raman spectra was collected for the sample shown in Figure 5.11, with measurements taken at 100 µm intervals. These maps were processed by correlation to spectra of the individual plasticisers DOTP (Figure 5.14) and ESBO (Figure 5.15) using ThermoScientific Omnic software. The colour scale used in these figures is normalised to the maximum and minimum correlation found across all data points in

the map, and the values shown on the respective scales are a calculation of similarity to the reference spectra of each plasticiser from 0 (no correlation) to 1 (exact match).

It can be seen in these images that the regions identified as plasticiser droplets by optical microscopy show greater correlation to both of the individual plasticisers. The intense point shown as the highest correlation to DOTP and lowest correlation to ESBO at the top edge of each map does not correspond to any visible liquid present in the optical microscopy image. This may be due to contamination in the sample or an erroneous measurement, but this was not investigated further. Overall, this technique was thought to provide a potential method of mapping plasticiser exudation on PVC surfaces with the aim of quantifying this exudation, for example by calculating the percentage of the sample surface covered by exudation.
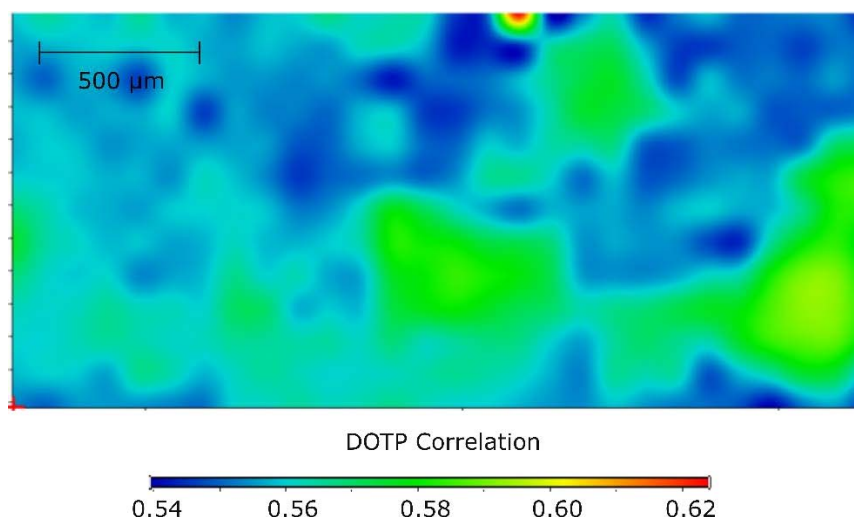
Figure 5.14: Raman map of an exuding sample of PVC-DOTP-ESBO showing correlation to a reference sample of DOTP. Greatest correlation occurs in areas identified as exuded plasticiser droplets through microscopy imaging.
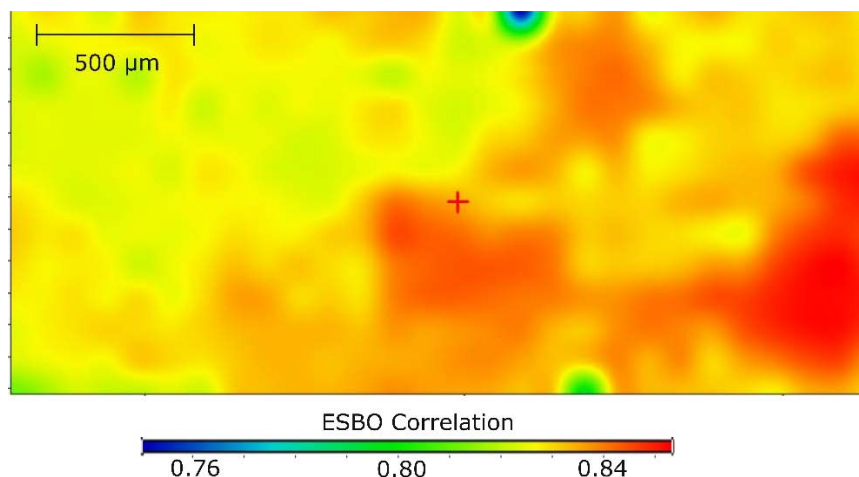
Figure 5.15: Raman map of an exuding sample of PVC-DOTP-ESBO showing correlation to a reference sample of ESBO. Greatest correlation occurs in areas identified as exuded plasticiser droplets through microscopy imaging.

An issue was identified with using the Raman mapping technique for this application, following observations from the optical microscope when testing a sample of PVC-DOTP after compression. The microscope images showed that in the time taken to collect a small map of 9 points, the previously visible plasticiser droplets had disappeared - an interval of approximately 20 minutes. Two optical microscope images are shown in Figure 5.16, which shows the sample surface initially and after this 20-minute delay. Raman spectroscopy can cause heating of the sample due to the power of the laser, which could cause evaporation of volatile samples. However, this would be unlikely to cause of the observed effect as the boiling point of DOTP is approximately 400 °C, while the sample would likely show signs of burning above 200 °C.[108] The observed disappearance of the droplets was also uniform across the sample, while only a small area was exposed to the laser. As such, the most likely explanation for this would be that the exuded plasticiser has reabsorbed into the sample. Reabsorption of exuded plasticiser is known to happen and is noted in the ASTM D3291 standard.[39] This would be a significant hindrance to developing a method of quantifying exudation using Raman mapping, as the observed exudation would not reliably last long enough to gather enough data points before reabsorption. However, plasticiser compatibility may be related to the rate of this reabsorption, which could be measured by a time-resolved study of exudation.
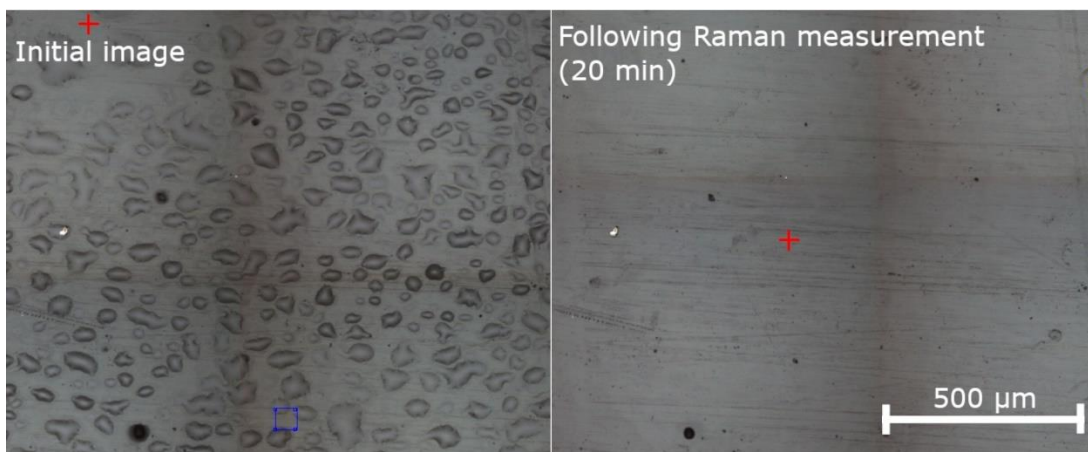
Figure 5.16: Optical microscope images of the same area of an exuding sample of PVC-DOTP before and after a Raman map collection.

5.5 Gas Chromatography - Mass Spectrometry

GC-MS was used to detect, identify, and quantify the compounds present on the surface of samples following the loop compression test. The surfaces were swabbed in a fixed pattern, and the swabs then immersed in solvent to extract the compounds from the swab. The resulting solutions were tested by GC-MS directly, as well as transesterified with sodium ethoxide to investigate ESBO (Scheme 5.1). This allows for analysis of ESBO by GC-MS under standard conditions due to the increased volatility of the resulting esters compared with ESBO. Base-catalysed epoxide ring opening reactions are well documented and may also occur under the conditions used in the transesterification procedure.[122, 123] However, the reaction products were not rigorously examined in this case, since the repeatability of conversion to the quantification target was acceptable (R^2=0.994 for the calibration curve of transesterified standard samples).

The internal standard dimethyl pimelate (DMPi) was used to monitor the transesterification reaction as described by Biedermann-Brem *et al.*[81] Sodium ethoxide can react with moisture from the air, forming sodium hydroxide and reducing the available ethoxide in the solution. DMPi undergoes transesterification to form diethyl pimelate (DEPi, Scheme 5.2) and thus confirms that the sodium ethoxide reagent is active.

Four peaks resulting from derivatisation products of ESBO were detected by GC-MS, as indicated in Figure 5.17. These peaks were attributed to ethyl esters of fatty acids with 0, 1 or 2 epoxide groups. Ethyl 9-epoxystearate (Et 9-ES, **16**) was chosen for quantification due to the intensity and minimal overlapping peaks.

Ethyl 9-epoxystearate (16)

+

Ethyl 9,12-diepoxystearate (17)
+ other fatty acid ethyl esters
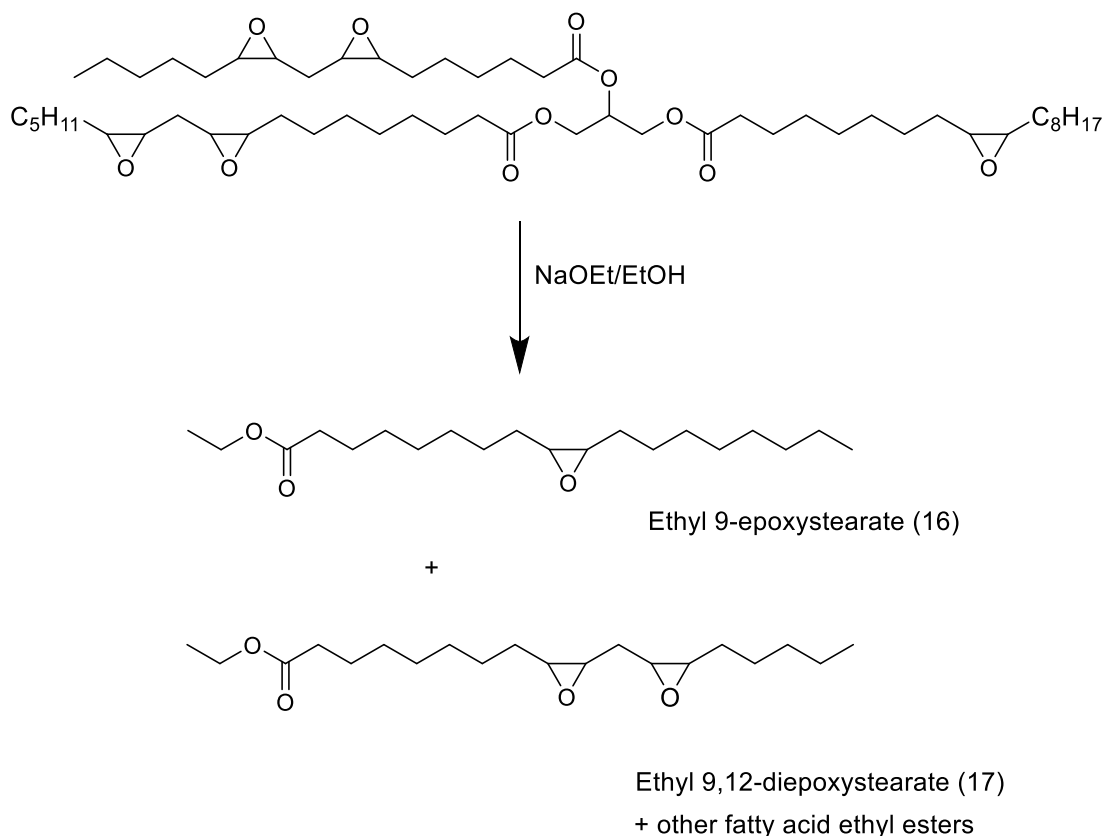
Scheme 5.1: Transesterification of ESBO with sodium ethoxide to form ethyl esters (two major components shown).
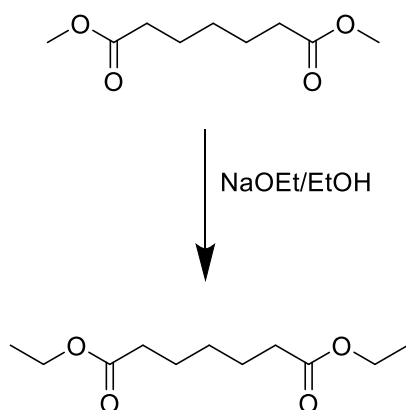
Scheme 5.2: Transesterification of dimethyl pimelate to diethyl pimelate.
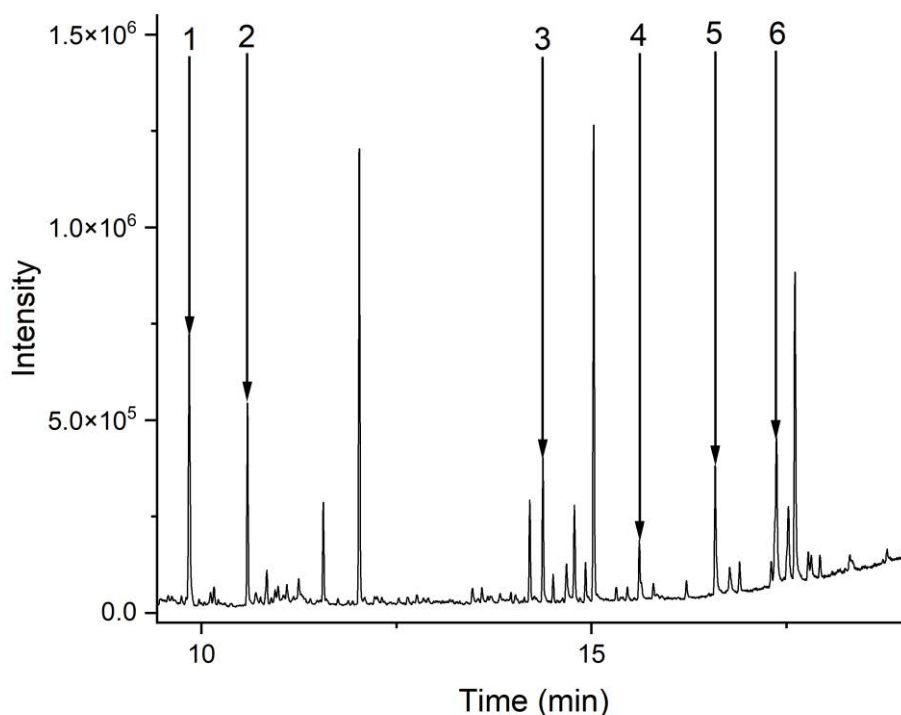
Figure 5.17: Gas chromatograph of a transesterified solution of the plasticiser standard containing 1-ethyl naphthalene (1), diethyl pimelate (2), ethyl hexadecanoate (3), ethyl octadecenoate (4), ethyl 9-epoxystearate (5) and ethyl 9,12-diepoxystearate (6) as well as transesterification products of DOP and DOTP.

The compounds present in the swab extracts and derivatised samples were quantified using the Agilent MassHunter software. Each plasticiser was quantified by an ion with high response, and qualifier ions were chosen to validate the results. The intensity of the qualifier is compared to the quantifier to confirm that the correct target molecule is being measured. For DOTP, the quantifier ion had an m/z value 167, qualifier 261, and for DOP the quantifier ion had an m/z value 149, qualifier 167. For the representative peak for ESBO, ethyl 9-epoxystearate (Et9-ES, Scheme 5.1, **16**), m/z 155 was chosen as quantifier and 69 as qualifier. The quantification was created from a solution of known concentration containing the three plasticisers and internal standards 1-ethyl naphthalene and dimethyl pimelate.

Table 5.4 shows the measured exuded plasticiser for each sample alongside the composition of the samples. The exudation of plasticiser was quantifiable for all

samples tested by GC-MS, which highlights the increased sensitivity of the method. As seen in Figure 5.18, DOTP (Formulation 1) gives the highest level of exudation of the single plasticiser samples – ten times more than DOP (Formulation 2) or ESBO (Formulation 3). The exudation appears to follow a non-linear pattern of a steep early gradient followed by a more gradual increase.

Table 5.4: Exuded plasticiser at t=60 min measured by GC-MS quantification, alongside the initial plasticiser type and percentage in the samples.

	Plasticiser (%)			Exudation (µg)		
	DOTP	DOP	ESBO	DOTP	DOP	ESBO
Formulation 1 PVC-DOTP	41.0 %			83.9	-	-
Formulation 2 PVC-DOP		41.0 %		-	7.6	-
Formulation 3 PVC-ESBO			41.0 %	-	-	9.8
Formulation 4 PVC-DOTP-ESBO	20.5 %		20.5 %	14.5	-	8.0
Formulation 5 PVC-DOP-ESBO		20.5 %	20.5 %	-	5.3	3.4
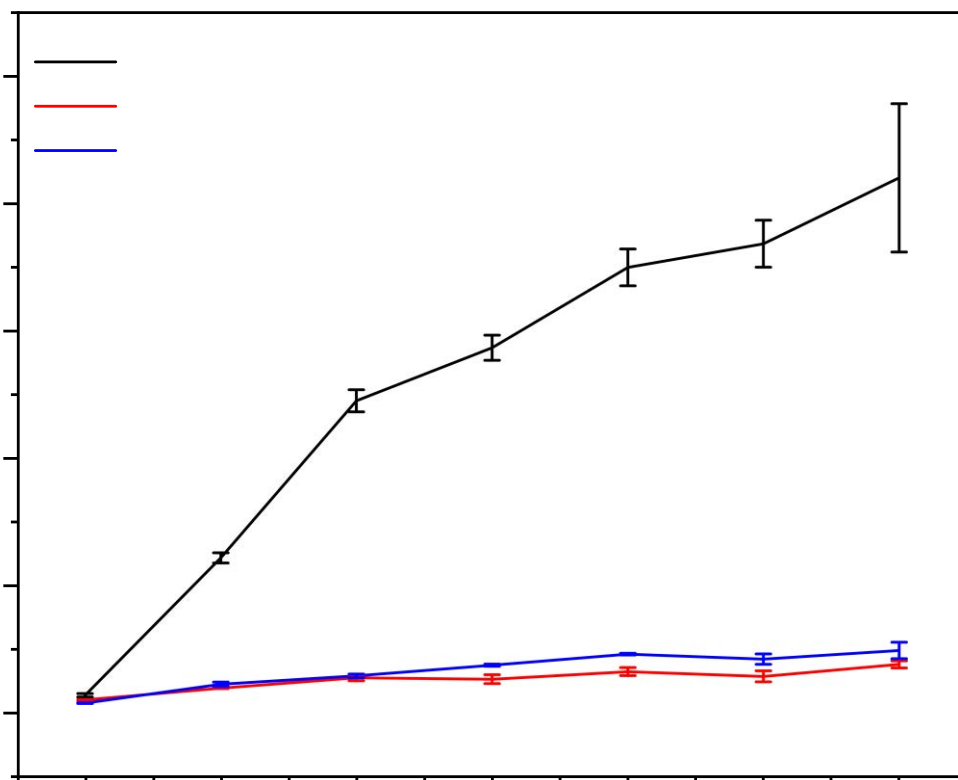
Figure 5.18: Plasticiser exudation by GC-MS for PVC samples containing DOTP, DOP and ESBO, following compression in the 'loop spew test'. Results are presented as the average of three individual test pieces swabbed separately, with error bars calculated as the standard deviation of the three results.

Figure 5.19 shows the exudation of plasticisers in the mixed plasticiser formulations, alongside the relevant single plasticiser formulation. The amount of DOTP that exuded from Formulation 4 after 60 minutes was 17% of that which exuded from Formulation 1. Relative to the amount of plasticiser present in the formulations, this means that the presence of ESBO reduced DOTP exudation to approximately 1/3 of the exudation shown by DOTP alone. This reduction in exudation contrasts with the FTIR analysis presented in section 5.3.2, which suggested that DOTP interacted less strongly with PVC when in a mixture with ESBO. Conversely, the mixture of plasticisers in Formulation 5 appears to increase the exudation of DOP and decrease the exudation of ESBO, relative to the concentrations in the PVC samples. In fact, while ESBO exuded more rapidly than DOP in the single plasticiser Formulations 2 and 3, when mixed in Formulation 5 this was reversed, with DOP exuding faster than ESBO.
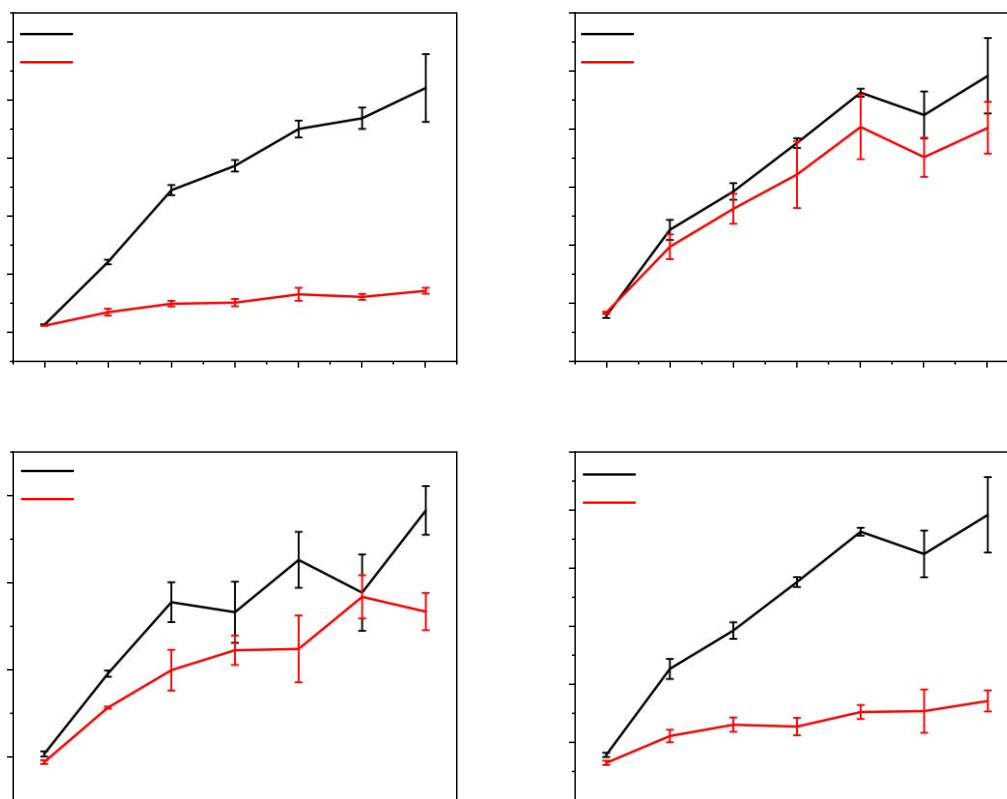
Figure 5.19: Plasticiser exudation from the mixed plasticiser formulations (shown in red) alongside the exudation of the component plasticisers from the single plasticiser formulations (black) following compression in the 'loop spew test'. Results are presented as the average of three individual test pieces swabbed separately, with error bars calculated as the standard deviation of the three results.

In addition to quantifying the amount of plasticiser exuded from the PVC matrix, an attempt was also made to determine the kinetics of the exudation for the various plasticisers and combinations thereof. An example is illustrated in Figure 5.20 for DOTP, where the amount of plasticiser exuded over time was fitted to a first order process with a reasonable degree of success (R^2 = 0.96). The other plasticisers and combinations yielded poorer fits to both zero and first order processes. The various attempts are summarised in Table 5.5 and illustrate that for all datasets, the exponential fit gives a higher R^2 than the linear fit.

Equation	y = A1*exp(-x/t1) + y0
y0	98.46 ± 9.29
A1	-96.19 ± 8.57
t1	33.82 ± 6.94
Reduced Chi-Sqr	33.44
R-Square (COD)	0.96
Adj. R-Square	0.96
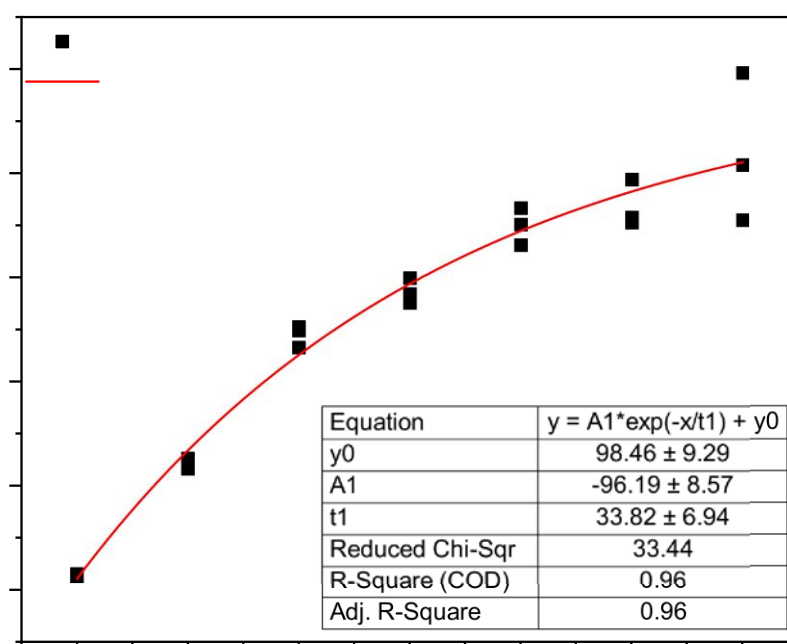
Figure 5.20: Exponential fit of DOTP exudation from Formulation 1 by GC-MS.

Table 5.5: R^2 values for exponential fits to the plasticiser exudation data as measured by GC-MS.

Formulation	Plasticiser	Linear Fit R^2	Exponential Fit R^2
Formulation 1 PVC-DOTP	DOTP	0.91	0.96
Formulation 2 PVC-DOP	DOP	0.69	0.72
Formulation 3 PVC-ESBO	ESBO	0.84	0.92
Formulation 4 PVC-DOTP-ESBO	DOTP	0.79	0.88
Formulation 4 PVC-DOTP-ESBO	ESBO	0.76	0.85
Formulation 5 PVC-DOP-ESBO	DOP	0.79	0.85
Formulation 5 PVC-DOP-ESBO	ESBO	0.79	0.84

The difference in compatibility (as determined by exudation) between DOTP and DOP has been noted in a number of works and is generally acknowledged within the PVC industry.[59, 67] Hansen solubility parameters have been reported for DOTP and DOP, and were noted to show only minor differences, in contrast to the observed difference in experimental measures of compatibility.[48] However, due to the difference in stereochemistry, DOP was shown to have greater miscibility with PVC in a computational model of plasticised PVC structures, with DOTP showing a greater tendency to form a separate phase and exude under compressive stress.[49]

5.6 Dynamic Mechanical Analysis

The DMA data was used to produce plots of storage modulus, loss modulus and tan delta for the samples. These plots were examined to determine the glass transition temperature as well as the presence of multiple glass transition temperatures within the samples. This can be caused by phase separation which would indicate incompatibility between the PVC and plasticisers. The storage modulus (E') represents the elastic (glassy) component of the material while the loss modulus (E'') represents the inelastic (rubbery) component. As the sample temperature is increased, the polymer changes from glassy behaviour to rubbery behaviour. The point at which this change occurs is the glass transition temperature. Storage and Loss modulus are related by the tan δ as shown in Equation 5-1.

$$tan\,\delta = \frac{E''}{E'}$$

Equation 5-1

The samples were tested using tensile and cantilever modes. Both modes gave comparable data, however at higher temperatures the samples could not be measured in cantilever mode as they became too soft for the instrument to apply a strain, which led to erroneous measurements.

All samples showed similar overall trends in both storage and loss modulus, producing profiles such as the example shown Figure 5.21. The samples gave a clear single glass

transition temperature, which can be measured by either the onset of the storage modulus decrease, or the peak of the loss modulus curve. These data are presented in Table 5.6.
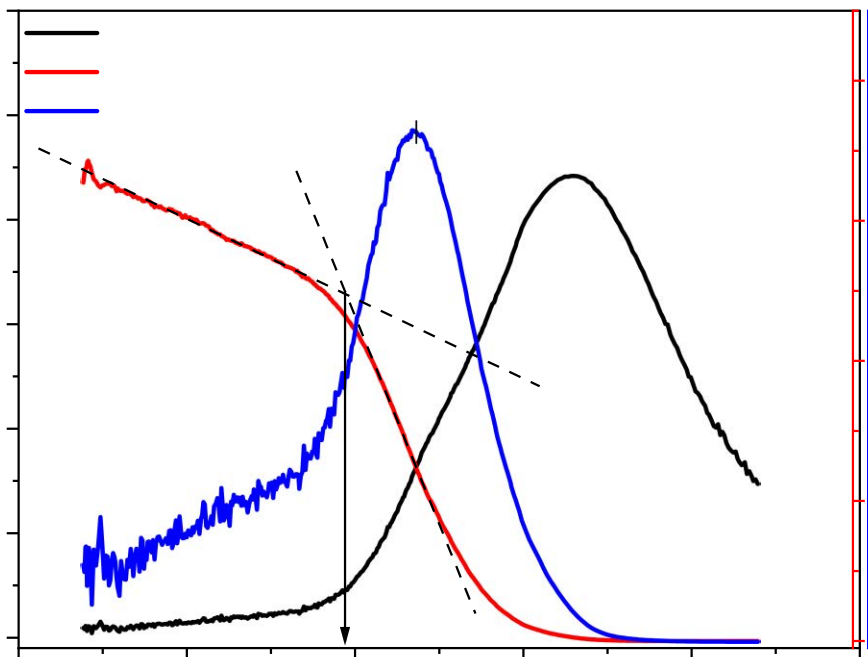
Figure 5.21: An example of the Storage Modulus, Loss Modulus and Tan Delta data produced by DMA analysis. Measurements of glass transition temperature include the onset of Storage modulus (intersection of tangents) and peak of Loss modulus as illustrated.

The storage modulus onset and loss modulus peak values both show the same trends between the plasticised samples – Formulation 1 (PVC-DOTP) and Formulation 2 (PVC-DOP) gave the lowest T_g values, and Formulation 3 (PVC-ESBO) the highest, with the T_g for the mixtures at approximately the midpoint of those values. This suggests that all of the plasticisers are equally able to solvate and lubricate the PVC chains whether used as single plasticisers or combined in the mixtures tested. Additionally, no evidence of phase separation (that would indicate poor compatibility) was detected in any sample by DMA. The tan δ peak values generally correlate with the observations from the storage and loss modulus. The value for PVC-DOTP is anomalously high, as this gave the lowest storage modulus onset and loss modulus peak temperatures but the second highest tan δ peak.

Table 5.6: Glass transition temperatures (and standard deviations) measured by Storage modulus onset and Loss modulus Peak.

Sample	Storage Modulus onset (°C)	Loss modulus peak (°C)	Tan δ peak (°C)
Formulation 1 – PVC-DOTP	-51.2 (0.2)	-32.7 (0.9)	12.6 (2.7)
Formulation 2 – PVC-DOP	-47.3 (2.5)	-29.9 (0.7)	5.0 (0.2)
Formulation 3 – PVC-ESBO	-29.8 (1.0)	-12.8 (0.3)	15.1 (0.7)
Formulation 4 – PVC-DOTP-ESBO	-38.2 (1.1)	-22.3 (0.2)	10.0 (1.5)
Formulation 5 – PVC-DOP-ESBO	-38.0 (2.7)	-20.9 (0.8)	9.4 (0.4)

Each test piece was only measured once, with new pieces used for repeat measurements. As such, the effect of repeated heat histories on the glass transition behaviour was not investigated. Rapid thermal decomposition of PVC typically occurs at temperatures above 200 °C.[124] As the maximum test temperature was 70 °C, thermal decomposition was not predicted to occur, and no signs of decomposition were observed. However, the samples showed some permanent deformation following the test, and so may not have been suitable for repeated testing as the dimensions of the test piece changed.

5.7 Comparison of methods for testing plasticiser compatibility

Table 5.7 summarises the methods evaluated for plasticiser compatibility testing. For all samples, the ASTM D3291 method of testing plasticiser exudation gave a result of 0 after one hour, and so the methods described to detect and quantify exudation through analytical techniques show much greater sensitivity. The ability to test plasticiser compatibility within hours rather than days or weeks would be of great

benefit to the development of new PVC compounds. The FTIR carbonyl peak position shift was substantially larger for PVC-DOTP than the other samples, and so PVC-DOTP was determined to be the least compatible by this method. Less significant differences were observed for the other PVC-plasticiser combinations. Exudation measured by GC-MS showed greater differences between the samples, and all three plasticisers tested could be reliably identified and quantified. Again, DOTP showed the greatest exudation, while DOP showed the least. However, the comparison between exudation behaviour and glass transition temperature (measured by DMA) showed little correlation.

While exudation behaviour suggests that DOTP is less compatible than DOP, it is more effective at reducing the glass transition temperature of the PVC, and so is classified as the most compatible by this measurement. This highlights the need to consider the way that compatibility is defined when developing new plasticisers for use in PVC, as clearly the glass transition behaviour is only one aspect of the relationship between the polymer and plasticiser.

Table 5.7: Summary of the outcomes for the four methods of compatibility testing - ASTM D3291, FTIR carbonyl shift, GC-MS of exudation and glass transition temperature by DMA.

Compatibility Measure	ASTM D3291 method	FTIR carbonyl shift	Exudation (GC-MS)	Glass Transition Temperature
Most compatible	n.d.	DOP	DOP	DOTP
Least compatible	n.d.	DOP-ESBO	DOTP	ESBO

The tendency of an external plasticiser to remain within the PVC matrix is controlled by both the strength of the attractive forces between the plasticiser and polymer, and the ability of the plasticiser to move through the structure. Thus, both intermolecular forces and the size and shape of the plasticiser will determine the exudation behaviour under the loop spew compression test. Larger, more bulky plasticisers will

have a lower tendency to migrate and so by exudation measures will be deemed compatible with the polymer. In contrast, smaller, more mobile plasticisers such as adipates are known to give greater suppression of the glass transition temperature and thus good flexibility of the polymer compound at lower temperatures.[7] Determining plasticiser compatibility by the measurement of T_g would suggest that these plasticisers are highly compatible. However, these plasticisers are also prone to migration (e.g. into foodstuffs) due to their high mobility.[125]

The test conditions also clearly influence the migration or exudation of plasticiser from PVC – for example in a study of plasticiser migration from films at elevated temperature, the film containing DOP showed significantly greater mass loss than with DOTP.[126] Conversely, in a study of migration of plasticiser into n-heptane the diffusion coefficient of DOTP was found to be three times higher than DOP.[67] Brouillet suggests that the higher boiling point of DOTP (400 °C) compared to DOP (384 °C) indicates stronger intermolecular interactions between the DOTP molecules, and thus a relatively less favourable interaction with PVC. This difference is attributed to the effect of the aromatic substitution positions in the two molecules. The *para-* orientation in DOTP allows each ester group to interact more easily with neighbouring molecules, while the *ortho-* position in DOP is more sterically hindered, and could also result in intramolecular interactions between the two ester groups within the molecule.[67] This somewhat correlates with the conclusions drawn from the FTIR investigation regarding the mixtures of DOTP-ESBO and DOP-ESBO, wherein DOP showed a larger change in the carbonyl position on mixing with ESBO than DOTP. If the DOTP ester groups are already able to interact freely then the addition of ESBO has a smaller impact on the carbonyl bond energy, compared to DOP where the ESBO is more able to interact with the hindered ester groups and so shows a larger change in carbonyl bond energy in the mixture. The effect of this interaction could be further investigated through thermogravimetric analysis of the plasticiser blends.

GC-MS appears to be the most suitable candidate as a method of improving the current ASTM D3291 compatibility test, since it is sufficiently sensitive to quantify very low levels of plasticiser exudation and can distinguish easily between plasticisers in a

mixture. The examination of the FTIR carbonyl peak showed limited potential as the changes observed here were close to or below the detection limit of the instrument. This method is also limited to plasticisers that contain a carbonyl group. While Raman spectroscopy was able to detect the plasticiser exudation on the surface and measure this in a map, the observed tendency of the plasticiser to reabsorb is a severe limitation on the potential of this method. Raman spectroscopy is also rarely seen within the PVC industry and so this would prevent many PVC compounders from engaging with this method.

6 Synthesis Of Derivatives of ESBO for Use as Bio-Based Plasticisers for PVC

6.1 Introduction

A group of potential bio-based plasticisers were synthesised from ESBO **8** through epoxide ring-opening reactions as detailed in Scheme 6.1. The target products were chosen to investigate different functional groups present in bio-based molecules, such as aromaticity in furoic acid, alcohol groups in isosorbide and polar chains in PEG. Plasticisers for PVC typically contain polar groups such as esters and aromatic rings, which interact with the polar PVC chains to keep the plasticiser and polymer bound together, and non-polar groups (typically branched or linear alkyl chains) that create free volume in the polymer matrix and allow movement of the polymer chains, imparting flexibility. ESBO is widely used as a secondary plasticiser for PVC, typically at levels below 5%.[127] The structure of ESBO contains three ester groups that make up the triglyceride as well as 4-6 epoxide groups which provide the polarity to interact with PVC, as well as long alkyl chains in the fatty acids, typically C18 (oleic and linoleic) and C16 (palmitic). Despite this, migration of ESBO into foods has been reported in a number of works, and it is generally considered to be less compatible with PVC than plasticisers such as phthalates.[16, 128, 129] The epoxide ring of ESBO provides potential routes for synthetic modification by ring-opening reactions, which have been used in both soy and other vegetable oil-based epoxides to develop novel plasticisers for PVC.[30, 33, 88]

As ESBO itself is a mixture with multiple possible reaction sites, the resulting products described herein were themselves mixtures. As such, options for purification of the products were limited since typical routes such as column chromatography were unsuitable. As noted by Moser, while the nucleophilic attack at the epoxide ring is regioselective to the less substituted site, in these compounds both sites are (effectively) equally likely due to the similar environments.[130] This leads to two possible products for each epoxide ring opening. Taking a typical ESBO molecule

comprising two linoleic (18:2) and one oleic (18:1) acid, one instance of nucleophilic attack has 10 possible reaction products. As such, all yields have been reported by mass. Furthermore, the reaction schemes shown in this chapter are depicted as one possible epoxide ring opening on an epoxidised oleic acid (18:1) group for simplicity.
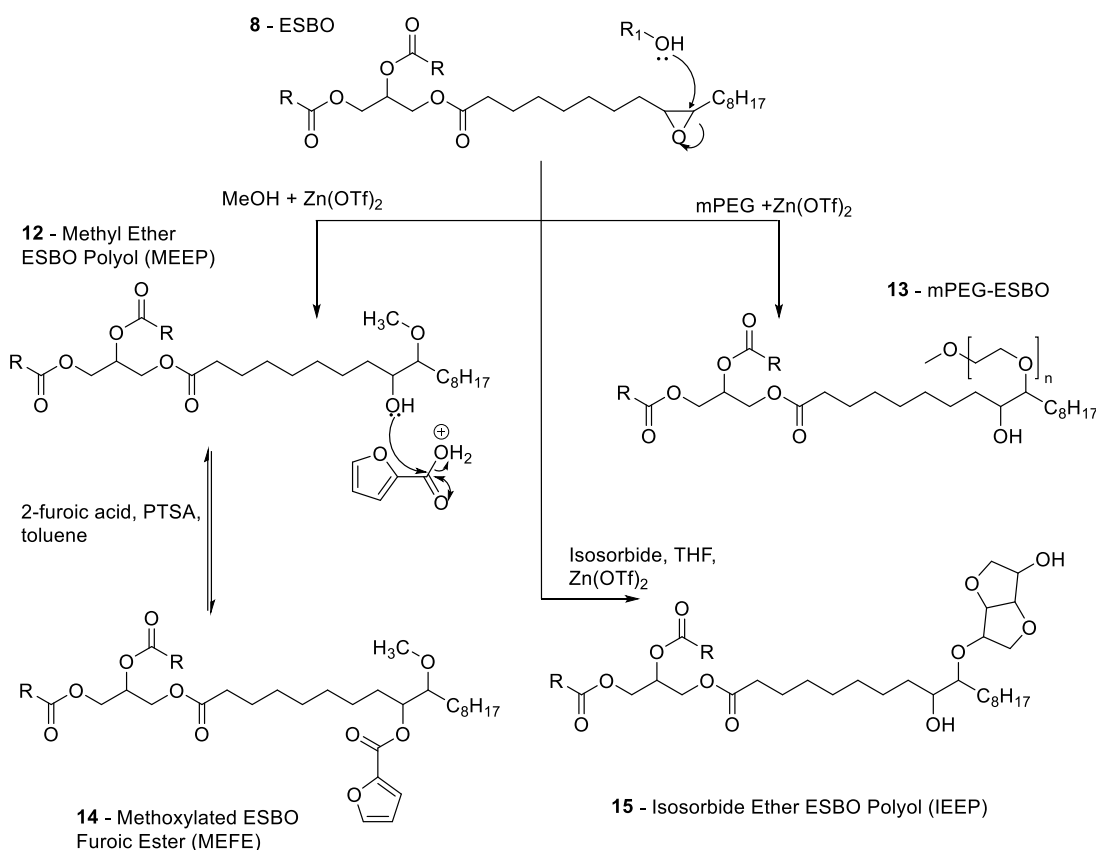
Scheme 6.1: Reaction scheme showing the synthesis routes for four bio-based derivatives of ESBO **8**, Methyl Ether ESBO Polyol (MEEP, **12**), mPEG-ESBO **13**, Methoxylated ESBO Furoic Ester (MEFE, **14**), Isosorbide Ether ESBO Polyol (IEEP, **15**).

6.2 Synthesis of Methyl Ether ESBO Polyol (MEEP, 12)

Methyl ether ESBO polyol (MEEP, **12**) has been reported in previous works[33, 131] as a precursor for polyurethanes and was primarily synthesised here as an intermediate. ESBO was reacted with methanol to convert the epoxide group to a methyl ether and an alcohol (Scheme 6.2), which can then be used in further reactions. To the best of

our knowledge this compound has not been evaluated for use as a plasticiser for PVC, so this was also carried out as described in Chapter 7. Lozada *et al*. evaluated six catalysts for the alcoholysis of the ESBO epoxide for use in the production of rigid polyurethane foams.[132] The reaction was carried out with a mixture of methanol and ethylene glycol, finding that PTSA gave the greatest conversion to the polyol ether. However, as noted by Lozada, both methanol and ethylene glycol can act as the nucleophile in this reaction and selectivity between the two reactions was not reported. Guo *et al*. used fluoroboric acid as the catalyst for epoxide ring opening of ESBO for use in polyurethanes.[33] Bailosky *et al*. evaluated methanesulfonic acid, boron trifluoride etherate and zinc triflate as catalysts for the epoxide opening reaction of ESBO with n-butanol and benzyl alcohol for the purposes of developing bio-based polymeric can coatings.[32] The study found that zinc triflate showed more rapid conversion than methanesulfonic acid or boron trifluoride etherate.
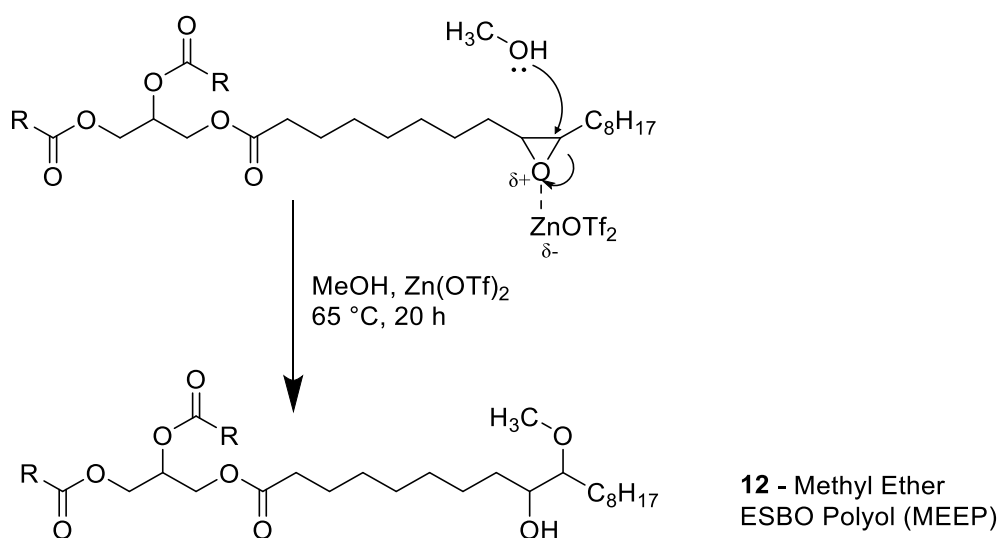
Scheme 6.2: Synthesis of methyl ester ESBO polyol (MEEP, *12*), note that the structure of ESBO is simplified here for clarity.

6.2.1 Evaluation of Catalysts for Methoxylation of ESBO

Zinc triflate, PTSA (p-toluene sulfonic acid) and sulfuric acid were evaluated for use as catalysts in the epoxide ring opening reaction, as each catalyst was reported to be effective for the methoxylation reaction in different works.[32, 132] It was found that the

selectivity of the reaction was strongly dependent on the choice of catalyst – sulfuric acid and higher concentrations of PTSA both led to transesterification of the glycerol esters with methanol. The reaction was monitored by ^{1}H NMR on samples taken over 5 hours. Figure 6.1 shows the ^{1}H NMR of samples taken after one hour reaction time. Formation of the methyl ether is shown by the reduction of the epoxide peaks (2.8-3.2 ppm, b) and appearance of the methyl ether peak at 3.4 (c). Transesterification was noted by the appearance of a peak at 3.6 ppm, corresponding to the methyl ester protons (d), and the reduction in the glycerol ester peaks at 4.1-4.3 ppm (a) and 5.2 ppm. No significant transesterification was observed with 0.1% (weight) zinc triflate or 1% (weight) PTSA. This is further illustrated in Figure 6.2 which shows the percentage conversion to the desired methyl ether and the undesired methyl ester for the different catalysts. 2.5% PTSA has comparable conversion after 1 h reaction time to 0.1% zinc triflate after 5 hours, however this level of PTSA led to greater transesterification with longer reaction time (not represented in this figure). As zinc triflate showed higher formation of the desired product and minimal side reaction, this catalyst was also used for further epoxide-opening reactions.

The structure was confirmed with FTIR-ATR spectroscopy which showed the broad alcohol O-H stretch at 3400-3500 cm^{-1}, as well as a reduction in the epoxide double peak (828 and 847 cm^{-1}).
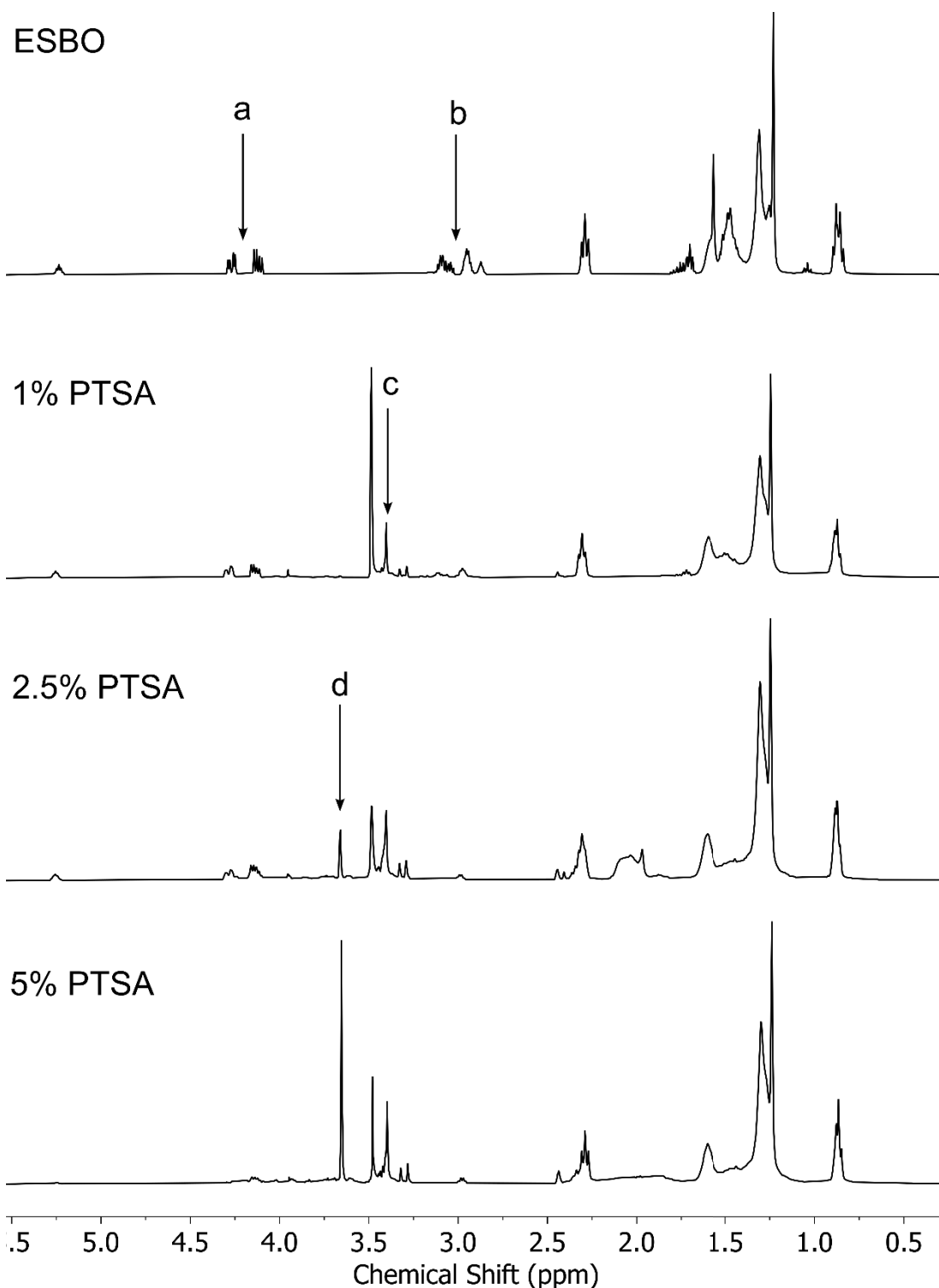
Figure 6.1: *^{1}H NMR of ESBO and the reaction product with methanol after 1 hour with 1, 2.5 and 5% PTSA catalyst, showing the reduction of the epoxy signal (b), the emergence of the desired methyl ether signal (c) and the transesterification side reaction leading to a reduction in the glycerol ester (a) and emergence of a methyl ester (d).*
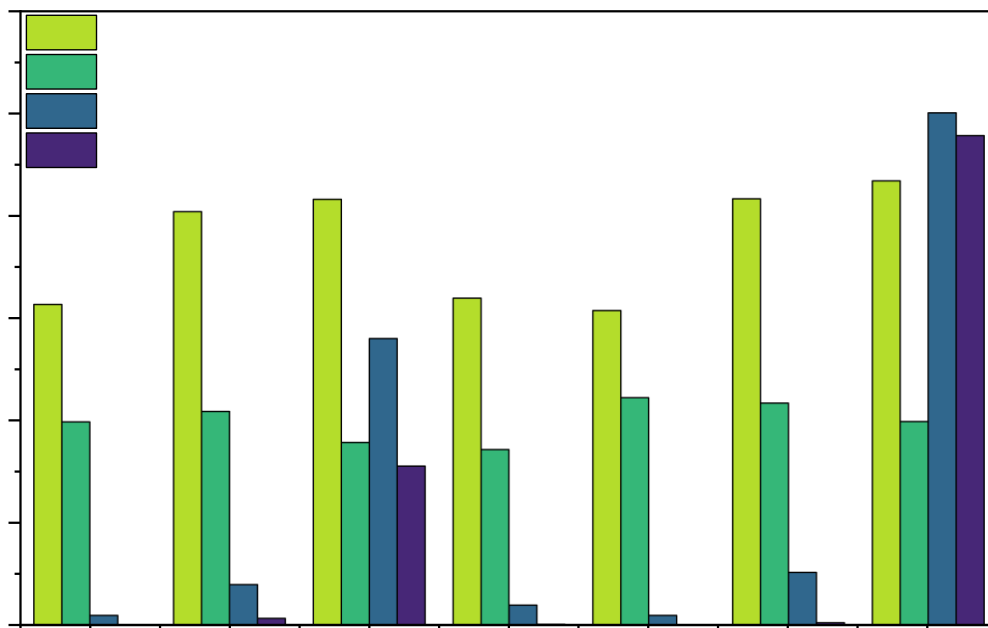
Figure 6.2: Evaluation of the selectivity of the methanolysis of ESBO with different catalysts and reaction times, by ^{1}H NMR peak integrals.

6.3   Synthesis of mPEG-ESBO (13)

Polyethylene glycol has been investigated as a potential bio-based plasticiser for PVC, showing some plasticising ability in the effect of PEG on the tensile strength and elongation.[118] Tan *et al*. produced a series of mPEG esters of varying chain length by reaction with a mixture of dimer acids from soy fatty acids, showing that longer PEG chains gave greater plasticisation, comparable with DOTP (6).[119] Glycol esters have also been used as plasticisers for a number of polymers including PVC.[16]

The synthesis of mPEG-ESBO **13** (Scheme 6.3) was carried out without additional solvent, as mPEG also functions as the solvent. An excess of mPEG was used to ensure the greatest possible reaction of the epoxide rings. Methyl capped PEG was used to prevent crosslinking between ESBO molecules, or between fatty acid chains within one triglyceride ESBO molecule, as uncapped PEGs have two alcohol functionalities

that could both react with the epoxide rings. This crosslinking was utilised by Bailosky *et al*. to synthesise ESBO polyether polyols with propylene glycol for can coatings.[32] As both ESBO and mPEG are mixtures, the resulting product will be a statistical mixture of composition and so precise structural determination is not possible. The ^{1}H NMR signal corresponding to the terminal methyl group (3.38 ppm) of the mPEG was used to determine the progress of the reaction. In the final product, the methyl group was measured as 4.85 protons, indicating that on average each molecule of ESBO has reacted with 1-2 mPEG molecules.
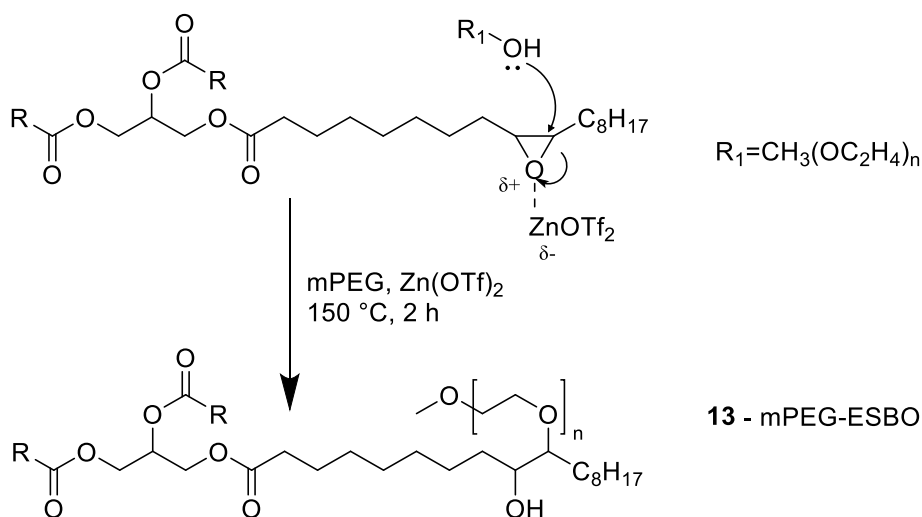
*Scheme 6.3: Synthesis of mPEG-ESBO (**13**), note that the structure of ESBO is simplified here for clarity.*

In the initial synthesis attempt, 1 g ESBO was reacted with 5.3 g mPEG (zinc triflate catalyst, 150 °C for 2 hours). Purification was first attempted by dissolving the reaction mixture in chloroform and washing with water. However, the measured yield following this method was 6.23 g, showing that the excess mPEG had not been removed by this purification. This was confirmed by ^{1}H NMR, which showed very large peaks for mPEG, integrating to 35 terminal methoxy protons (3.4 ppm) per ESBO, i.e., approximately 12 mPEG chains when the maximum theoretically attached by epoxide opening could be 6.

As separation of the mPEG through the liquid-liquid extraction was unsuccessful, trituration with water was attempted. ESBO is hydrophobic due to the long fatty acid chains. The addition of mPEG to the structure will increase the hydrophilicity of the molecule, as shown by HLB calculations using Davies group contribution method (see Appendices).[133, 134] For an mPEG-ESBO product with two reacted epoxide groups, the HLB value is 2.01. While the addition of mPEG has increased the HLB value, the molecule is remains hydrophobic and so will be poorly soluble in the aqueous phase. Methyl-capped PEG is hydrophilic (HLB value of 11.07) and readily dissolves in water. The reaction mixture was stirred with deionised water, then left to separate. The aqueous phase was then removed by pipette, and this was repeated three times. It was noted that the oily product was denser than water. This indicated that ESBO had reacted with mPEG since ESBO has a density of 0.994 g ml^{-1}, while mPEG has density 1.09 g ml^{-1}. Following trituration, the ^{1}H NMR showed approximately 5 terminal methoxy protons, i.e., 1-2 mPEG groups per ESBO.

To further investigate if the mPEG ether had formed, DOSY NMR experiments were carried out. Diffusion-Ordered NMR Spectroscopy (DOSY) can be used to determine the composition of samples by separating the ^{1}H-NMR signals based on the diffusion properties of the molecules. This was used to account for the limited purification options due to the inherently mixed composition of products from ESBO. While ESBO, mPEG and the reaction products are not of a single chemical composition, the components were expected to be of sufficiently similar diffusion behaviour that they can be resolved by the DOSY experiment, and this is shown to be the case in Figure 6.3. The analysis was carried out by constructing a matrix of pulsed field gradient strengths and measuring the ^{1}H signal decays. Molecules with a faster diffusion coefficient will decay more rapidly than those with a slower diffusion coefficient. If multiple substances are present in the mixture, and have sufficiently different diffusion coefficients, they can be resolved into their separate ^{1}H-NMR spectra. The NMR data was converted to a 2D plot using a Bayesian transformation that calculates the diffusion coefficient of each signal from the attenuation of the signal strength.

DOSY NMR spectra were collected for the products, as well as ESBO alone and in combination with the reactants to confirm that the technique was distinguishing between the starting molecules. The DOSY transform for a mixture of ESBO and mPEG is shown in Figure 6.3. Greater separation was observed between ESBO and the other reactants, as these are much smaller molecules and so have a greater difference in diffusion coefficient to ESBO than mPEG does. In spite of this, a clear difference is shown in the mPEG-ESBO product, where the DOSY transform shows the change to a single diffusion coefficient compared to the reactant mixture (Figure 6.4). This indicates that the peaks attributed to protons from the new functional groups were attached to the larger ESBO molecule.
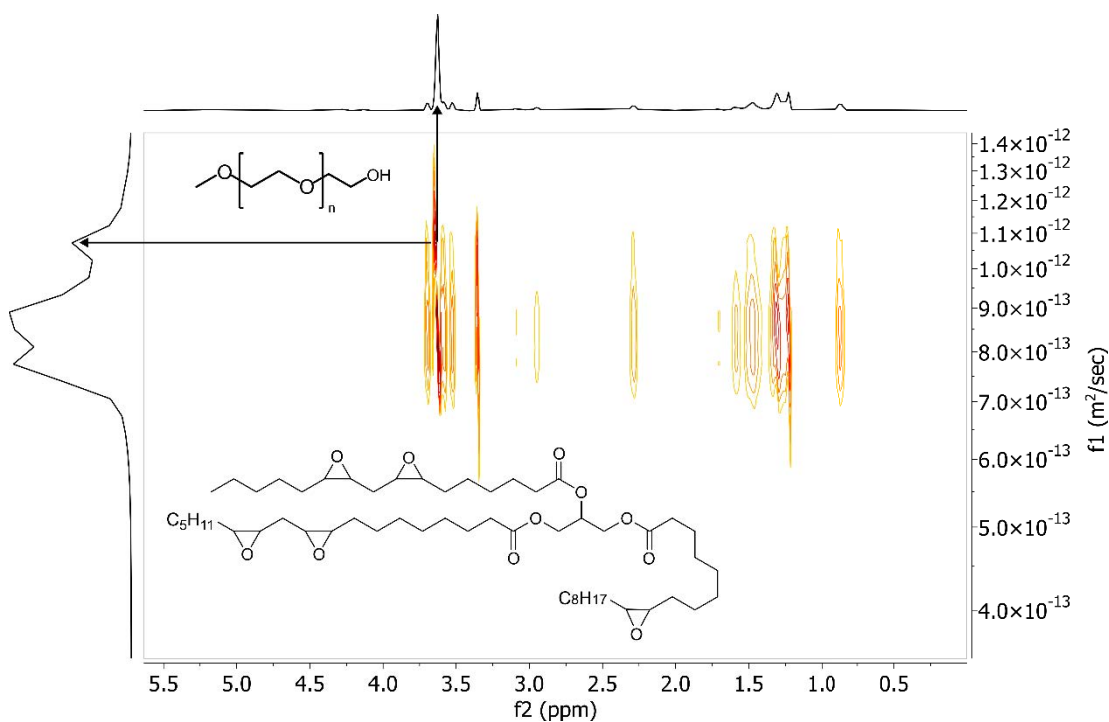
Figure 6.3: DOSY NMR for a mixture of ESBO and mPEG showing the separation of the signals for the components.
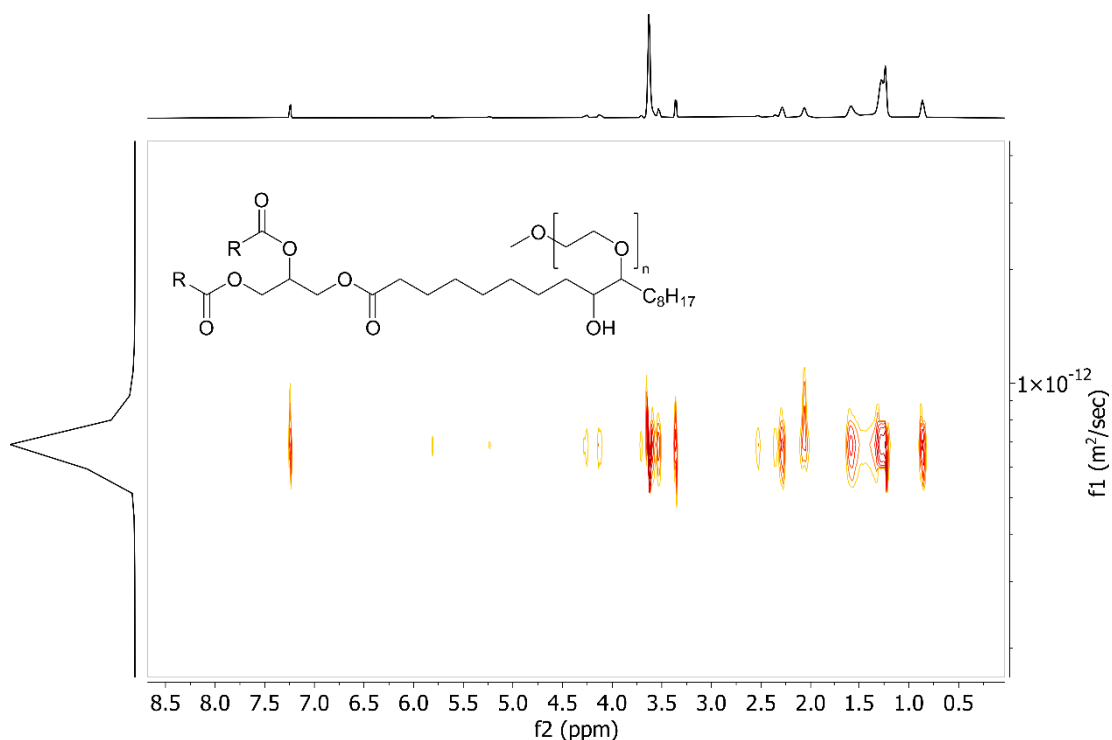
Figure 6.4: DOSY NMR for the product of ESBO and mPEG showing a single diffusion behaviour, indicating that the reaction has occurred.

FTIR-ATR also indicates that the product was formed, due to an alcohol O-H stretch at 3486 cm^{-1}, reduction in epoxide (828 and 847 cm^{-1}) and a peak at 1100 cm^{-1} corresponding to the C-O-C asymmetric stretch of the ether groups.

6.4 Synthesis of Isosorbide Ether ESBO Polyol (IEEP, 15)

Isosorbide **10** is a readily available bio-based compound derived from sugars which has been used to produce a number of bio-based plasticiser candidates for PVC.[90, 116, 117] In these studies, isosorbide was reacted with carboxylic acids to form diesters. The isosorbide diester structure somewhat mimics that of phthalates/terephthalates, with the heterocyclic isosorbide and diester providing polarity to promote interaction with PVC, and aliphatic chains providing lubrication for the polymer.[116] As such, isosorbide was chosen to introduce further polarity in the ESBO molecule.

As isosorbide is a solid (unlike mPEG and methanol), a solvent was required for this reaction (Scheme 6.4). Toluene was initially trialled as solvent and zinc triflate was

used as catalyst. Purification was attempted by dissolving the product in dichloromethane and washing with water, however after drying, crystals were observed in the resulting oil. The product was then triturated with water to remove residual isosorbide.

After two hours reflux in toluene (110 °C), it was observed that all epoxide groups had reacted, but it was unclear if isosorbide was present in the structure. The reaction was repeated at a lower temperature (80 °C), but results were similarly inconclusive. It was noted that the oil produced in the second reaction had separated from the solvent on cooling. Dry THF was then trialled as the solvent for this reaction, to reduce the possibility of hydrolysis side reactions and to improve the solubility of the reactants and products. All reactants were dissolved in THF and dried over magnesium sulfate prior to reaction, and glassware was dried under vacuum.
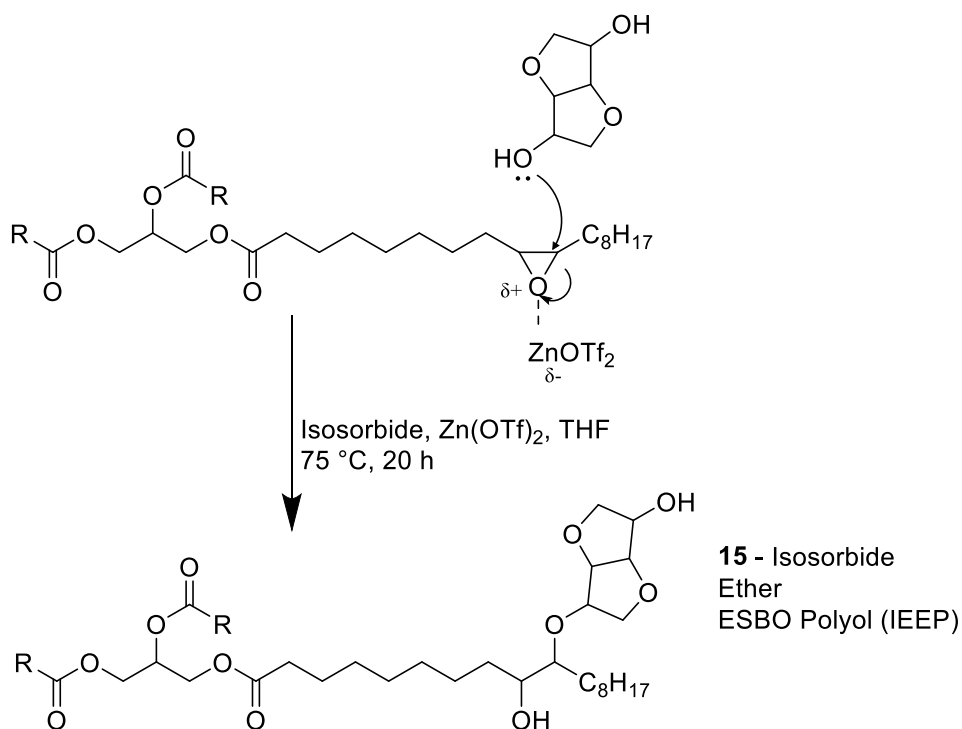
Scheme 6.4: Synthesis of isosorbide ether ESBO polyol (**15**), note that the structure of ESBO is simplified here for clarity.

Following reaction and trituration, peaks were noted in the ^{1}H NMR spectrum from 4-3.5 ppm that were attributed to isosorbide. DOSY NMR was used to confirm that these peaks were not due to residual isosorbide reactant. As shown in Figure 6.5, ESBO and isosorbide show distinct diffusion behaviour in the DOSY experiment, while the reaction product IEEP shows a single diffusion behaviour (Figure 6.6).
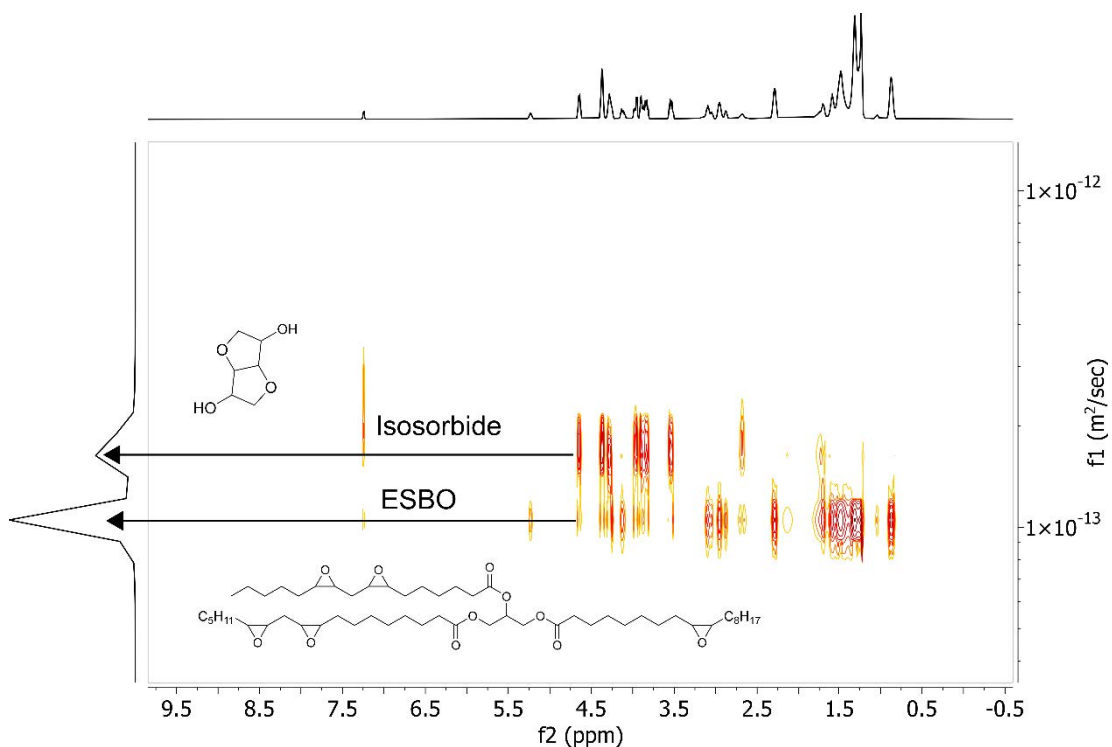
Figure 6.5: DOSY NMR of a mixture of ESBO and isosorbide showing the separation of the NMR peaks by the diffusion coefficient.
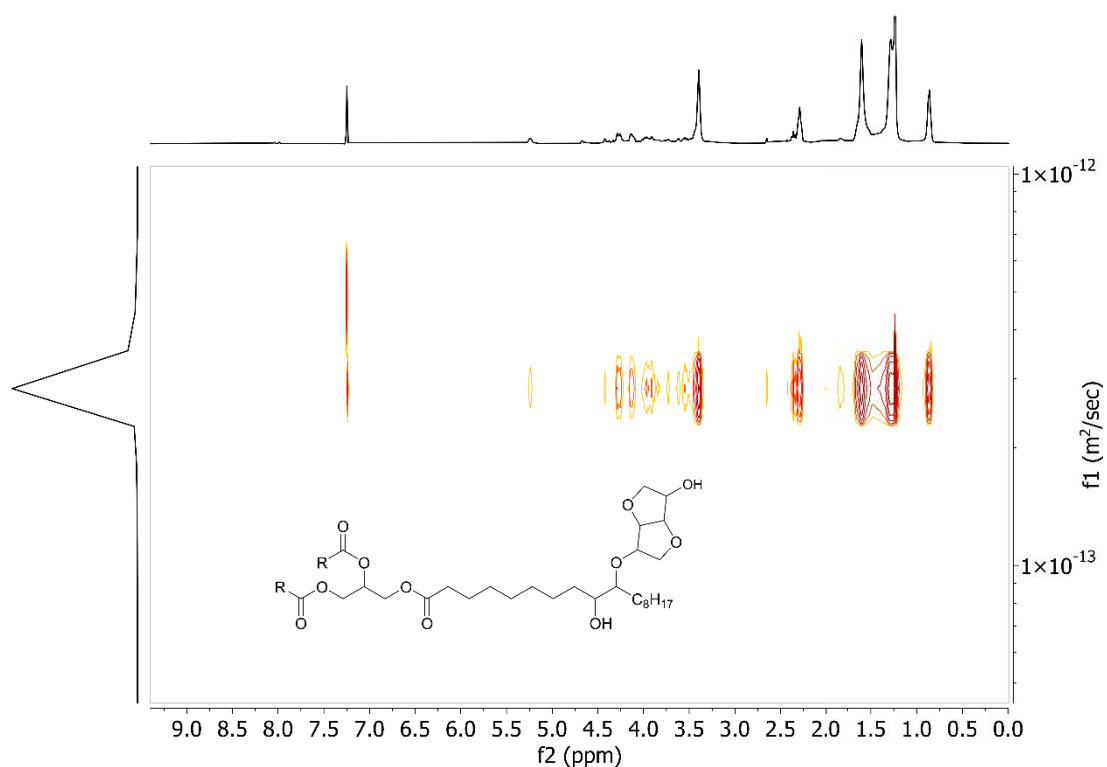
Figure 6.6: DOSY NMR of IEEP (product of ESBO and isosorbide) showing a single diffusion behaviour, indicating that all peaks are from the same molecule.

The isosorbide peaks in the region 4-3.5 ppm were used to determine the extent of the reaction (Figure 6.7). In isosorbide these account for 3 of the 8 C-H protons in the structure. Exact assignment of the protons was not possible due to low intensity combined with multiplet splitting, however integration over the region gave 6 protons (normalised to the α-carbonyl protons as in previous sections). This would suggest approximately two isosorbide molecules has reacted with every ESBO molecule. There is the possibility of both alcohol groups of isosorbide reacting either inter- or intramolecularly with other ESBO epoxides, however this was not specifically investigated.
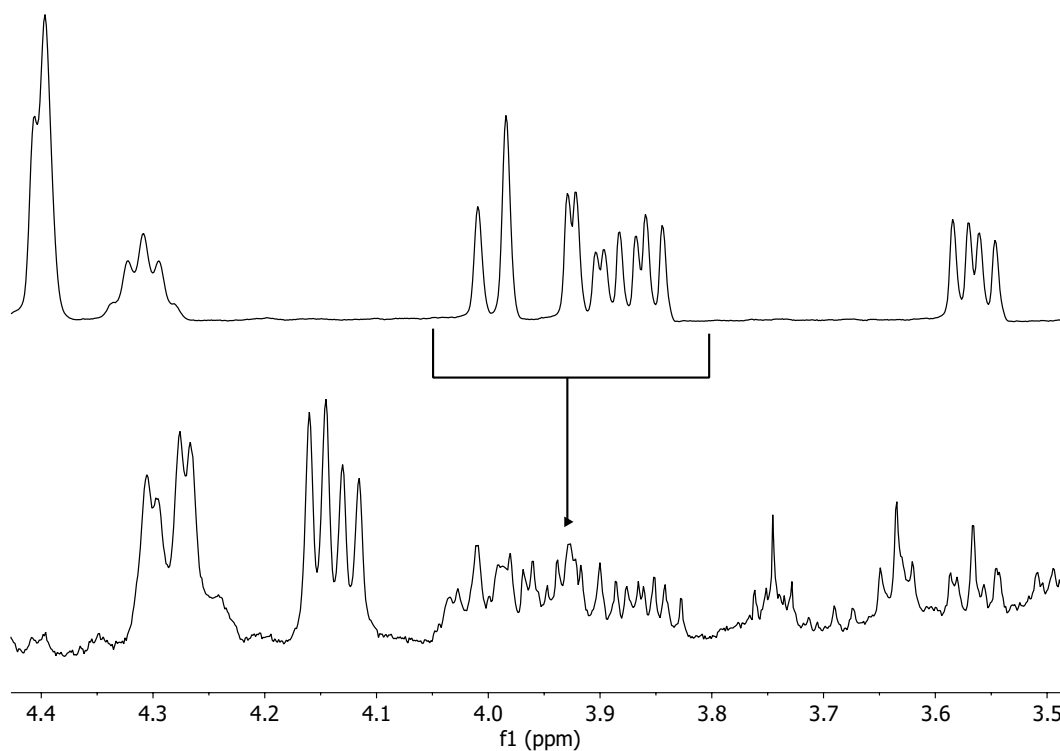
Figure 6.7: ^{1}H NMR of isosorbide and IEEP in the region used to determine the presence of the isosorbide group in the product.

6.5   Attempted Synthesis of Vanillin – ESBO Polyol

Vanillin and related compounds have been investigated as a source of both bio-based plasticisers and renewable polymers.[135, 136] These compounds are of particular interest because they can be produced through the depolymerisation of lignin, which is present in wood at up to 30%.[135] Despite this, as much as 85% of synthetic vanillin is produced from petrochemical resources, and yields from lignin are currently too low to be commercially competitive.[137] Zhu *et al.* synthesised a novel plasticiser for PVC from vanillic acid, making use of both the carboxylic acid and alcohol functional groups of the molecule to form two ester groups. This combination of an aromatic ring and two ester groups is very similar to that of phthalates, and the resulting products showed good plasticising ability in comparison with DOP.[136] As such, vanillin and vanillyl alcohol (section 6.6) were selected as candidates for further epoxide ring-opening reactions to investigate the effect of aromaticity on the compatibility of ESBO with PVC (proposed reaction as in Scheme 6.5).
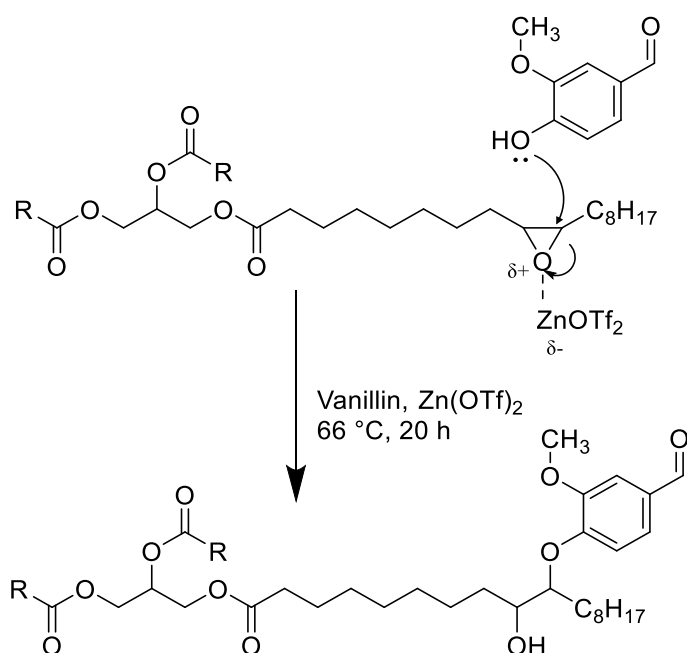
Scheme 6.5: Attempted reaction of ESBO and vanillin (ESBO structure simplified as previously described).

As in the synthesis of IEEP (section 6.4), toluene was used as the solvent initially, however the expected peaks in the ^{1}H NMR spectrum corresponding to vanillin were not found in the product, despite the observed loss of the epoxide groups. To reduce the possibility of hydrolysis, the reaction was repeated in dry THF, and all reactants were dried over magnesium sulfate prior to reaction. The product was triturated with a mixture of water and methanol (50:50) to remove any residual vanillin. Following this procedure however, the intended product did not appear to have been produced successfully. The methyl ether group of vanillin (3.9 ppm) was used to monitor the progress of the addition reaction, which was integrated to 0.6 H per ESBO molecule (normalised to the α-carbonyl as described previously). DOSY NMR did not show any separation of the diffusion coefficients present in the product, however this level of conversion to the desired product was decided to be too low for further evaluation.

6.6 Attempted Synthesis of Vanillyl Alcohol - ESBO Polyol

Vanillyl alcohol was chosen for reaction for similar reasons to vanillin, as described in section 6.5. As shown in Scheme 6.5, vanillyl alcohol has two alcohol groups which could each react with the epoxide to form an ether. As with vanillin, toluene was used

initially but replaced with dry THF as this was a better solvent for vanillyl alcohol and to reduce the possibility of hydrolysis from any water present. The reaction product was triturated with a mixture of water and methanol. The product showed signs of successful reaction, with the methyl ether group (3.9 ppm) integrating to 3 H relative to ESBO, indicating that one vanillyl alcohol group reacted. However, the DOSY plot (Figure 6.8) shows multiple peaks on the vertical axis, with the peaks attributed to vanillyl alcohol having a higher diffusion coefficient than those of ESBO. The observed vanillyl alcohol peaks are therefore due to residual starting material rather than the desired product and this reaction was unsuccessful.

ESBO + vanillyl alcohol
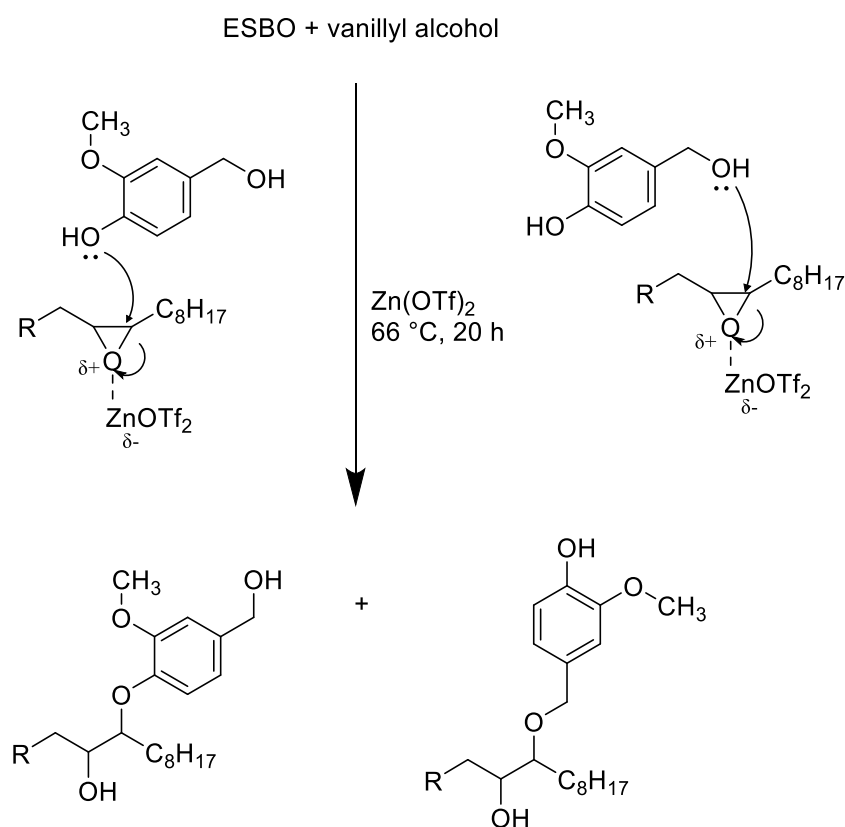
Scheme 6.6: Two potential synthetic routes predicted for the reaction of ESBO and vanillyl alcohol (ESBO structure simplified for clarity).
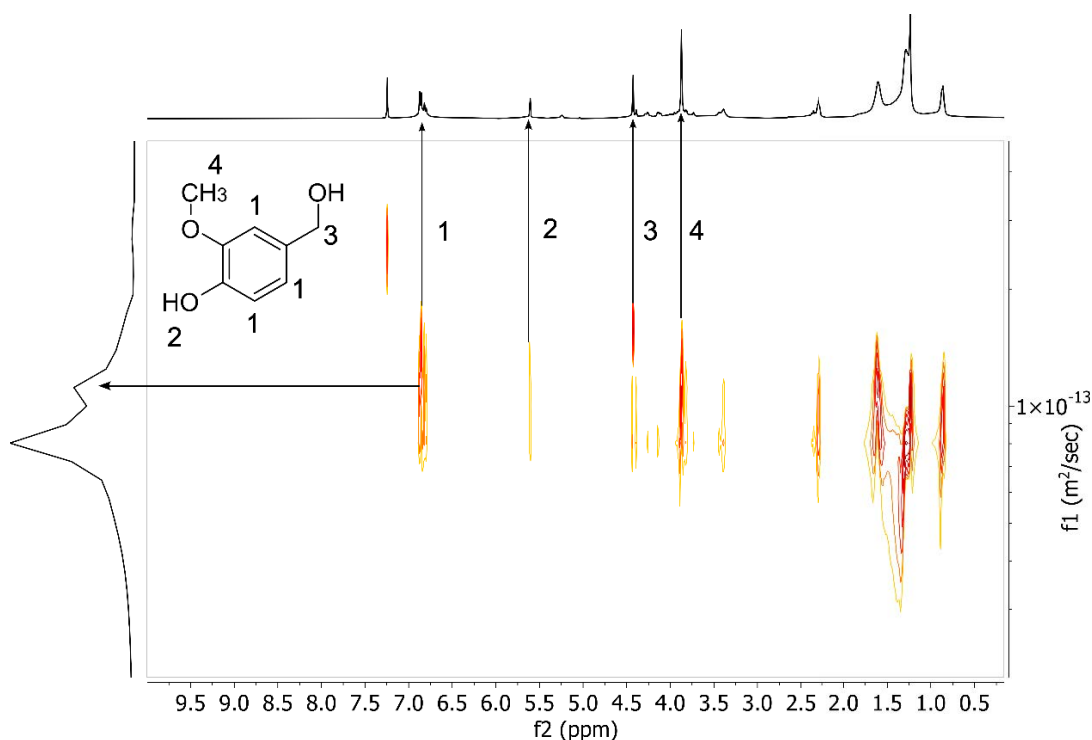
Figure 6.8: DOSY NMR spectrum of vanillyl alcohol-ESBO product showing multiple components.

6.7 Synthesis of Bio-based Esters of MEEP 12 with Furoic Acid (MEFE, 14) and Phenylalanine

The reaction of methanol with the ESBO epoxide ring (section 6.2) produces an alcohol group that can then be used to form esters when reacted with carboxylic acids. Kandula *et al*. investigated a similar synthetic route using soy fatty acid esters.[30] Epoxidised soy fatty acid esters were reacted with methanol to form a methyl ether and alcohol group, which was then reacted with acetic anhydride to convert the alcohol to an ethyl ester. This product as well as other soybean oil derivatives were evaluated as bio-based plasticisers for PVC.

The esterification reaction of MEEP **12** was attempted with both 2-furoic acid **11** (Scheme 6.7) and phenylalanine (Scheme 6.8). These reactants were chosen to investigate the effect of adding aromaticity to the ESBO structure, as this is present in phthalate plasticisers and is thought to contribute to plasticisation.[89] It was also

thought that if the reaction with phenylalanine was successful, a library of amino acid-based esters could be produced to investigate the wide range of functionality present in this family of bio-based chemicals.

The esterification reaction is reversible and produces water. The reaction of MEEP with 2-furoic acid was attempted initially over dried molecular sieves, with zinc triflate and PTSA each evaluated as catalyst. All glassware was dried under vacuum and the reaction was carried out under argon. However, under these conditions none of the reaction products showed signals in the ^{1}H NMR spectra corresponding to the furan group (6.5, 7.3 and 7.6 ppm in furoic acid). The procedure was repeated for phenylalanine with zinc triflate catalyst, but this was also unsuccessful.
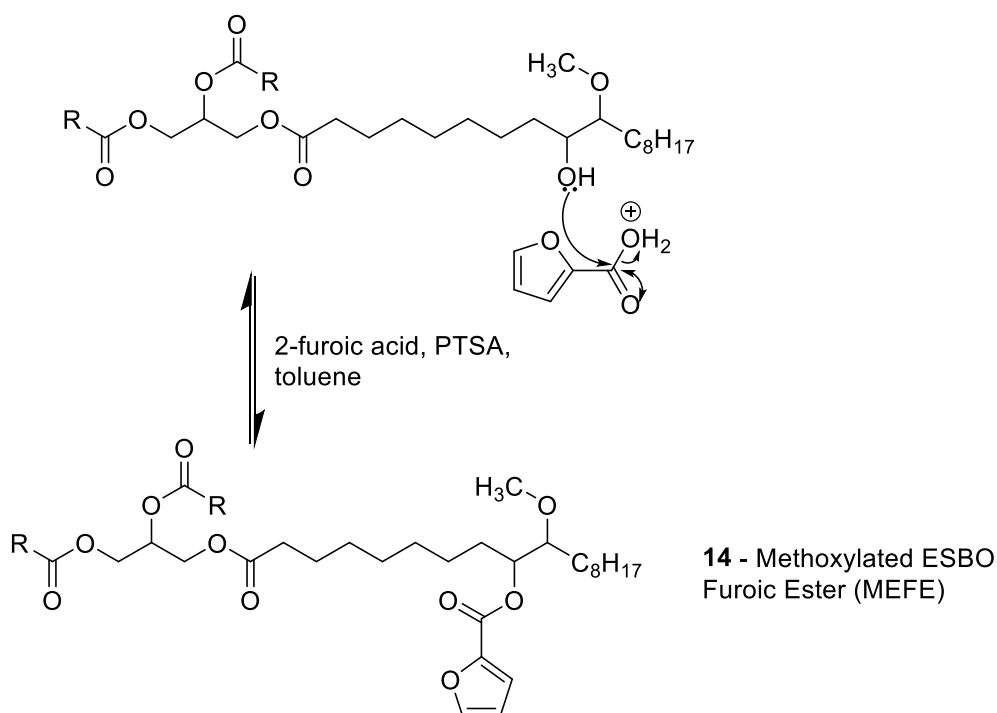
Scheme 6.7: Synthesis of Methoxylated ESBO Furoic Ester (MEFE, 14), structure simplified for clarity.

A Dean-Stark apparatus was then trialled to assist in the reaction by removing the water produced by esterification. This pushes the equilibrium towards completion, and the reaction progress can be monitored by observing the amount of water

collected in the trap. By using this method, methoxylated ESBO furoic ester (MEFE, **14**) was produced, however the reaction with phenylalanine remained unsuccessful. The MEFE product was confirmed by ^{1}H NMR, which showed peaks corresponding to the furan ring at 7.8 and 6.5 ppm. DOSY analysis showed a single diffusion behaviour confirming that the furan signals were attached to the larger molecule and FTIR showed the inclusion of an sp^2 C-H stretch at 3020 cm^{-1} as well as the disappearance of the O-H stretch observed in MEEP which confirms that the alcohol group has reacted.
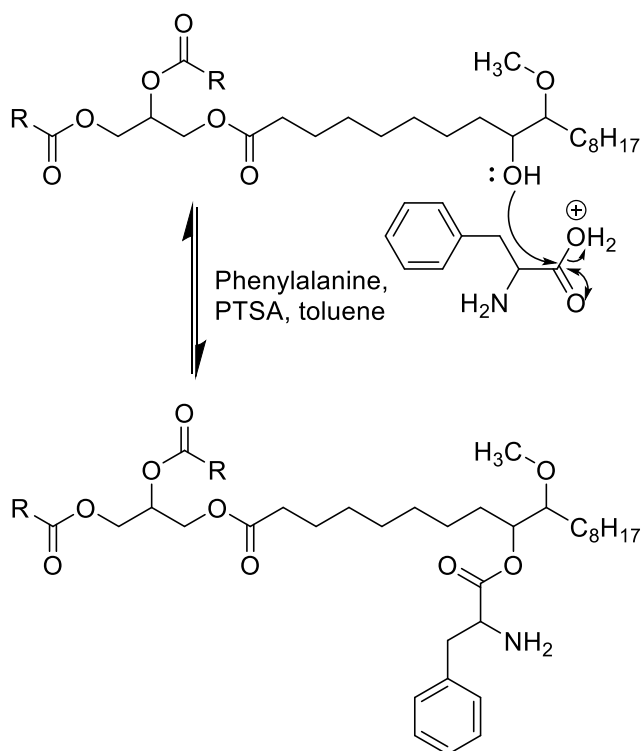
*Scheme 6.8: Attempted reaction of MEEP **12** with phenylalanine, structure simplified for clarity.*

6.8 Synthesis Mass Efficiency

Reducing waste is one of the 12 principles of green chemistry. As such, there are a number of metrics for determining the efficiency of a reaction method.[138] Atom economy (AE) is the simplest of these and is calculated from the expected molecular mass of the product divided by the molecular mass of the reactants (Equation 6-1).

$$Atom\ economy\ = \frac{Molar\ mass\ of\ product}{Molar\ mass\ of\ reactants}\ \%$$

Reaction mass efficiency (RME) is the percentage of the mass of the reactants remaining in the product. This metric accounts for the waste produced by using a reagent in excess but does not include other factors such as solvents or catalysts. These two metrics have been applied to the reactions carried out, and the results are presented in

Table 6.1.

$$Reaction\ mass\ efficiency\ = \frac{Mass\ of\ product}{Total\ mass\ of\ reactants}\ \%$$

Table 6.1: Green chemistry metrics for the plasticiser candidate molecules synthesised from epoxidised soybean oil.

Reaction	Atom economy (%)	Reaction mass efficiency (%)
MEEP **12** (Scheme 6.2)	100	42.4
mPEG-ESBO **13** (Scheme 6.3)	100	22.8
MEFE **14** (Scheme 6.7)	97.1	68.9
IEEP **15** (Scheme 6.4)	100	39.6

The addition reactions shown to form MEEP **12,** mPEG-ESBO **13** and IEEP **15** all have AE of 100%, as there is no waste product from the reaction. The AE of the synthesis of MEFE **14** depends upon the number of reactions that occur, and the molecular mass of the MEEP starting material. Assuming a MEEP molecule where two epoxide rings

were opened, and each resulting alcohol reacting with furoic acid (forming two molecules of water), the AE is 97.1%. While this relies on a number of assumptions, the true value will likely be similarly high since the reactants and products are relatively large and the only waste product (H_2O) is very low in mass.

In the reactions to form MEEP **12** *and* mPEG-ESBO **13***, the reactant also takes the role of the solvent. Of these two reactions, the RME for mPEG-ESBO is much lower than for MEEP. This is in spite of the fact that the stoichiometric excess used in the reaction with methanol was approximately 4 times greater than with mPEG. The RME for MEFE* **14** *was the highest of the synthesis products but this does not include any contribution from the solvents used in the process. Furthermore, the value for MEFE in*

Table 6.1 refers only for the reaction of MEEP with furoic acid, and so the overall efficiency of the process would include the RME for MEEP as well.

The Environmental factor (or E-Factor) and Process Mass Intensity are further metrics which consider all chemicals used in the process, such as solvents and drying agents. The reactions carried out herein were not optimised to reduce waste from solvents or reagent excesses, but this could be investigated in future works.

6.9 Conclusions

Four derivatives of ESBO were synthesised through epoxide ring opening reactions (and subsequent modification in the case of MEFE). Analysis of these products showed that the epoxide ring opening reaction did not go to completion, with typically 1-2 addition reactions occurring per ESBO molecule (of approximately 4-6 epoxide groups per molecule). Zinc triflate was found to catalyse the ring opening reaction of methanol to a greater degree with less transesterification of the glycerol esters compared to PTSA and sulfuric acid. The subsequent reaction of the alcohol present in MEEP was more difficult, requiring the removal of the water produced during the reaction. As this reaction was unsuccessful with phenylalanine, no further amino acids were trialled.

This is the first known production of mPEG-ESBO, MEFE and IEEP, and these compounds, as well as MEEP, will be evaluated as potential novel bio-based plasticisers for PVC in Chapter 7.

7 Evaluation of Novel Plasticisers for Use in PVC Compounds

7.1 Introduction

The four bio-based ESBO derivatives synthesised in Chapter 6 were compared against commercial petrochemical and bio-based plasticisers DOP **1**, DOTP **6** and ESBO **8** (Figure 7.1). DOP was chosen for the evaluation because it has been used as the most common plasticiser for PVC worldwide since the 1950s.[16] The use of DOP has declined in Europe and the USA following toxicological concerns, but it is still commonly used outside of these regions.[19] This plasticiser can therefore be considered the standard for general-purpose plasticiser performance in PVC. DOTP is the *para*-isomer of DOP and has been used as a replacement for DOP in many applications where phthalates are now prohibited.[16] Terephthalates make up the largest non-phthalate plasticiser group in European market trends, showing significant growth since 2008.[20] DOTP is approved for use in food-contact applications in Europe and USA and it is considered a suitable alternative to phthalates in medical devices.[18, 139] While this plasticiser is a safer alternative to phthalates, it is produced from petrochemicals and so replacement with a bio-based alternative would be beneficial to reducing the environmental impact of PVC products. As a secondary plasticiser, ESBO is rarely used at higher loadings in PVC compounds and is not considered to be a viable direct replacement for phthalates due to concerns over exudation.[16]

The novel bio-based plasticisers derived from ESBO in Chapter 6 were chosen in an attempt to improve the interaction between the plasticiser and PVC, and so to have better compatibility than ESBO. The novel plasticisers were compared against ESBO to investigate the effect of each chemical modification on the properties of the plasticiser, and thus identify improvements in compatibility with PVC. Comparison of the novel plasticiser candidates against commercial petrochemical plasticisers was carried out to look for similarities in the plasticising properties. The ideal bio-based plasticiser candidate in this investigation would replicate the plasticising properties of

DOP across all properties tested, as this plasticiser has been widely and successfully used throughout the PVC industry prior to regulations. However, any change in properties from the ESBO starting material towards that of DOP would indicate that the plasticiser candidate shows improved plasticising ability compared to ESBO, and thus has the potential to be used as a bio-based replacement for petrochemical plasticisers.
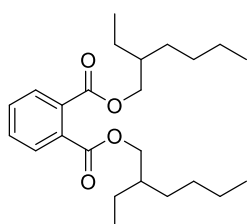
1 - Diethylhexyl phthalate (DEHP/DOP)   **6** - Diethylhexyl terephthalate (DEHT/DOTP)
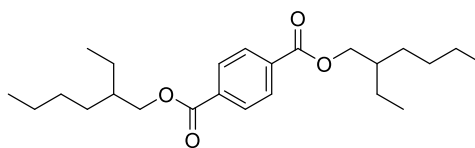
8 - Epoxidised soybean oil (ESBO)
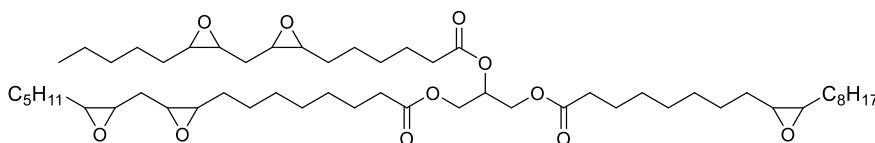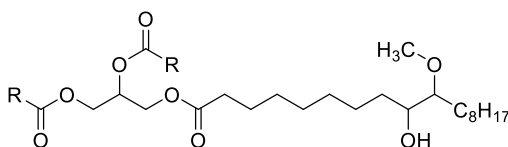
12 - Methyl Ether ESBO Polyol (MEEP)   **13** - mPEG-ESBO
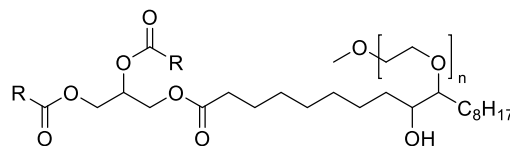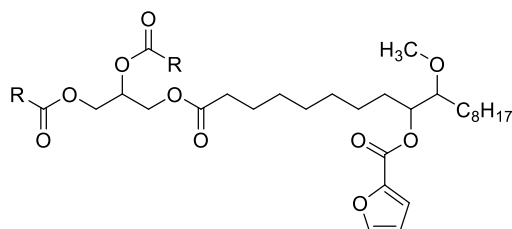
14 - Methoxylated ESBO Furoic Ester (MEFE)   **15** - Isosorbide Ether ESBO Polyol (IEEP)
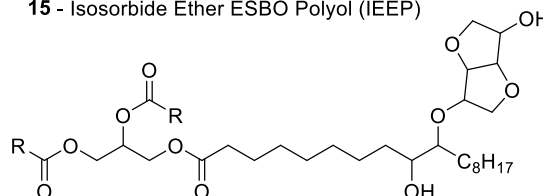
*Figure 7.1: Structure of commercial petrochemical plasticisers diethylhexyl phthalate (DOP, **1**) and diethylhexyl terephthalate (DOTP, **6**), bio-based plasticiser ESBO **8** and the novel bio-based plasticiser candidates MEEP **12**, mPEG-ESBO **13**, MEFE **14** and IEEP **15**.*

Plasticised PVC samples were prepared by solvent casting as described in Chapter 3, with plasticiser added at 50 phr (50 g plasticiser per 100 g PVC resin). The resulting PVC films were then tested by a number of techniques to evaluate the performance of the products as plasticisers for PVC. These techniques include those common to the PVC industry such as tensile testing, and less common such as DMA and SEM.

7.2   Tensile testing

Tensile testing is a core technique in PVC formulation development, as it provides information on the flexibility and toughness of the material.[2] Samples of PVC are typically cut or moulded into 'dumbbell' or 'dog-bone' shaped test pieces, where the wider ends provide area for the instrument to grip and the narrow portion is where the elongation of the material primarily takes place (Figure 7.2).
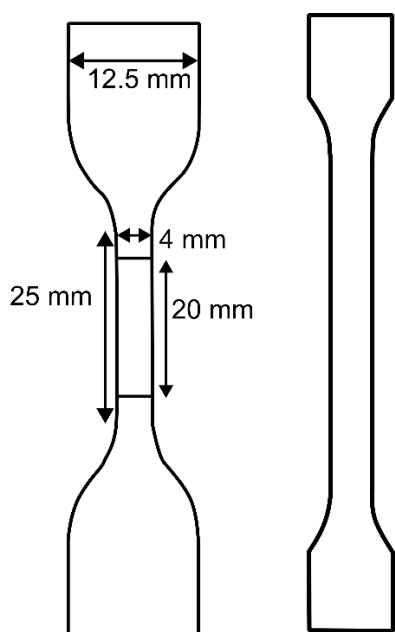
Figure 7.2: Examples of tensile dumbbell shapes used in tensile testing of polymeric materials. The Type 2 dumbbell of ISO 37:2017 used in this work is shown with dimensions labelled (left).

Test pieces are secured in grips attached to a Universal Testing Machine (UTM) or tensometer, which are attached to a stationary and moving head (crosshead) as shown in Figure 7.3. The UTM moves the crosshead at a set speed and measures the force experienced by the test piece under tension using a load cell connected to the

crosshead. This load is usually expressed as the tensile stress (σ, Equation 7-1) by dividing the load (F) by the cross-sectional area of the narrow portion of the test piece (A_0). This allows samples of different dimensions to be compared directly.

$$\sigma = \frac{F}{A_0}$$

Equation 7-1

Elongation can be measured with an extensometer. Contact extensometers attach directly to the sample, so may influence the test, and can only measure small extension ranges. Non-contact extensometers measure the elongation of the sample without direct contact, through video or laser measurement. An example of a laser extensometer is shown in Figure 7.3, where reflective tape is applied to the sample to specify the 'gauge length' (initial distance between the markers, L_0) to be measured. The elongation is expressed as a percentage of the gauge length, and is also known as strain (ε, Equation 7-2). The elongation and load data can be exported from the UTM to produce stress-strain plots for the samples.

$$\varepsilon = \frac{\Delta L}{L_0}$$

Equation 7-2
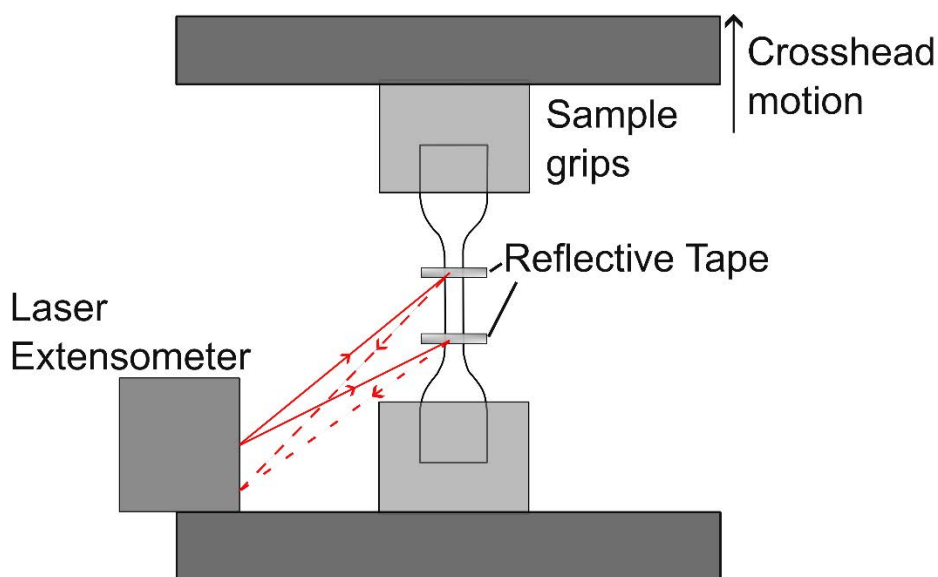
Figure 7.3: Diagram of Universal Testing machine used for tensile testing with laser extensometer.

The convention in PVC testing is to report the tensile stress (strength) and elongation at the break-point of the sample. The 100% modulus (the stress experienced by the sample at 100% elongation) is also often reported. Plasticised PVC rarely shows a linear elastic region in the stress-strain curve, instead yielding and undergoing plastic deformation. As such, calculation of the Young's modulus is not typically conducted.

Tensile testing can be used to compare the effectiveness of a plasticiser in PVC. As plasticisers lubricate the polymer chains and allow movement within the polymer matrix, this allows the test piece to elongate under the strain induced by the UTM. As such, PVC formulations that contain a more effective plasticiser (at a constant plasticiser loading) will have a higher elongation at break. Tensile stress at break is determined by two competing factors. A plasticiser that is poorly compatible with PVC may cause defects or inconsistencies within the polymer matrix that cause weakness, leading to breakage at lower loads. However, very effective plasticisers give a more ductile material that can stretch easily, reducing the load experienced by the sample. Interpretation of the results must therefore consider both elongation and tensile stress. The 100% modulus can give further information as breakage below 100% extension is rare. As such, a lower 100% modulus indicates a more ductile, well plasticised material.

The plasticised PVC films prepared by solvent casting were compression moulded prior to tensile testing to give an even sample thickness throughout. To fill the mould, pieces of cast film were cut and stacked together, then heated under pressure to fuse the material into a moulded sheet (section 3.6.2). However, both MEEP **12** and IEEP **15** showed delamination of the moulded PVC samples, where the material did not fuse together when moulded and instead separated into layers. This is an indication of poor compatibility, as delamination can be caused by plasticiser exudation which forms an oily layer on the surface, preventing fusion. As such, the sample thickness for the samples containing MEEP and IEEP were lower than the other samples. Tensile stress is calculated from the load and sample dimensions so this should have minimal impact on the results.

The tensile elongation and stress at the ultimate breakpoint for all samples are shown in Figure 7.4, and values including the 100% modulus are shown in Table 7.1. The three commercial plasticisers display similar properties, with DOP **1** giving marginally lower tensile stress and higher elongation than DOTP **6** or ESBO **8**. The mPEG-ESBO **13** product shows a higher elongation at breakpoint than ESBO, which suggests that mPEG-ESBO imparts greater flexibility and lubrication to the PVC structure than ESBO. This novel plasticiser also shows greater tensile stress at breakpoint than DOP (along with comparable elongation), which indicates that this novel plasticiser gives greater strength to the PVC product than the commercial plasticiser. The other novel plasticisers show signs of less effective plasticisation, with lower stress and elongation at break than the commercial plasticisers. In particular, the greatly reduced elongation at break shown in PVC-MEEP suggests that the epoxide rings of ESBO have a significant impact on the plasticiser compatibility, and that the conversion to an ether and alcohol group is detrimental to this interaction between plasticiser and polymer.

While MEFE **14** showed poor tensile properties in comparison with the commercial plasticisers, it does show a clear improvement over MEEP **12**, from which it is synthesised. This suggests that the inclusion of the furoic acid functionality has improved the plasticising ability. This could be because the furoic acid group increases

the solubility of the plasticiser within the PVC structure, leading to a more homogenous mixture and thus better plasticisation.
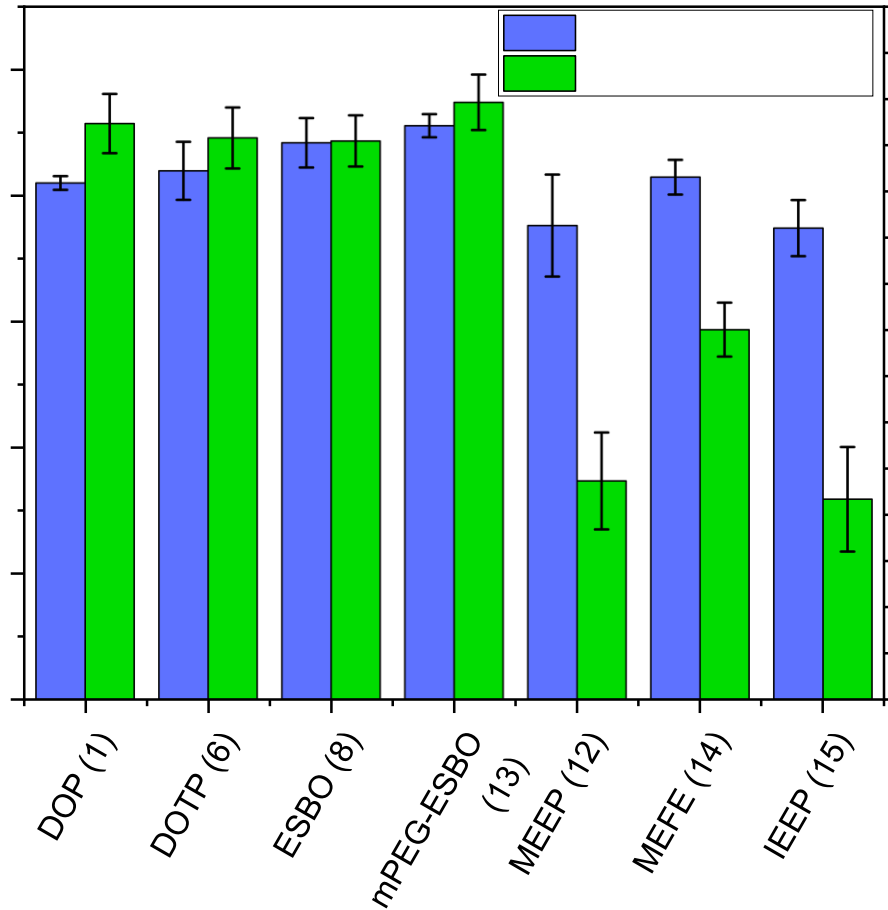
Figure 7.4: Tensile Stress and Elongation at breakpoint for PVC samples produced with commercial and novel plasticisers.

Table 7.1: 100% tensile modulus, tensile stress and elongation at breakpoint for the plasticised PVC samples (standard deviations).

Plasticiser	100% Modulus (MPa)	Stress at Breakpoint (MPa)	Elongation at Breakpoint (%)
DOP **1**	10.34 (0.33)	20.48 (0.27)	311.4 (16.0)
DOTP **6**	11.91 (0.19)	20.96 (1.15)	303.6 (16.5)
ESBO **8**	12.75 (0.13)	22.07 (0.98)	302.0 (13.9)
mPEG-ESBO **13**	12.61 (0.28)	22.75 (0.46)	322.9 (15.0)
MEEP **12**	18.19 (1.49)[a]	18.79 (2.02)	118.2 (26.2)
MEFE **14**	16.66 (0.26)	20.71 (0.69)	200.0 (14.5)
IEEP **15**	16.79 (0.21)[a]	18.69 (1.11)	108.3 (28.2)

[a] 100% modulus calculated from partial data as some samples fractured prior to 100% elongation.

Examples of the stress-strain curves for each PVC-plasticiser sample are shown in Figure 7.5, and illustrate that mPEG-ESBO **13** is the only novel plasticiser that gives a similar profile of stress-strain behaviour to the commercial PVC plasticisers. The other novel plasticisers show ductile deformation behaviour characterised by an early yield point leading to 'necking' of the sample.[140] This necking creates a region of very high stress as the cross-section narrows, and thus leads to fracture. This indicates poor plasticisation in these samples, which suggests that the synthetic modifications have reduced the plasticising ability relative to ESBO.
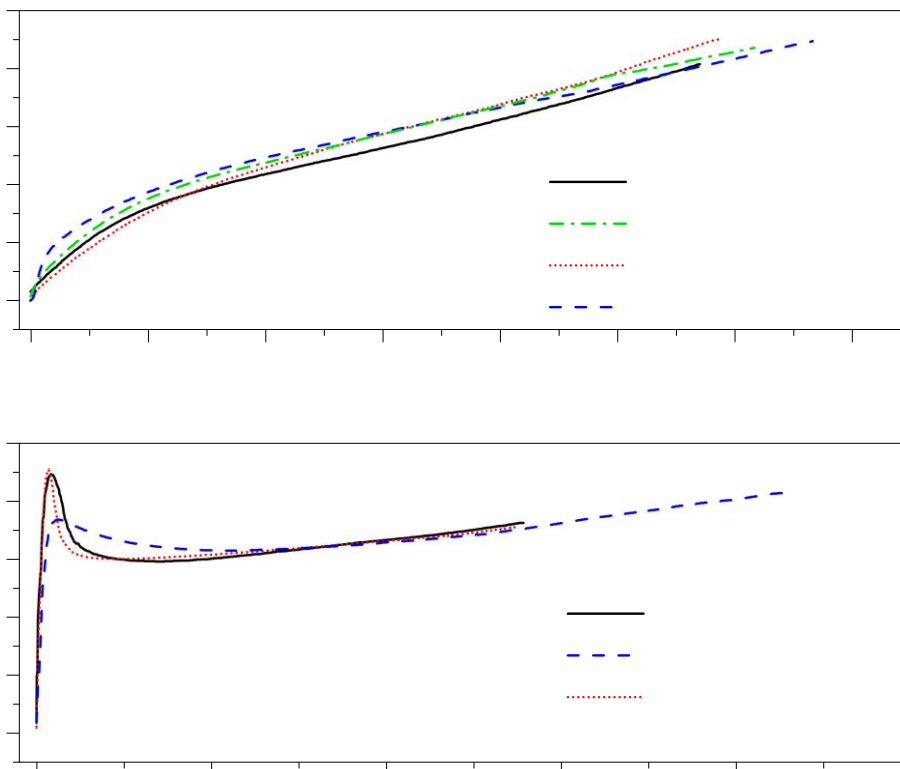
Figure 7.5: Stress-strain curves for tensile elongation of plasticised PVC samples.

7.3 Dynamic Mechanical Analysis (DMA)

The effect of the novel plasticisers on the glass transition temperature T_g of PVC was evaluated by DMA. As described in Chapter 5, DMA measures the response of the plasticised samples to an oscillating deformation over a temperature range. The material response can be described in terms of the elastic and inelastic components, represented by the storage and loss moduli, *E'* and *E"*. The glass transition temperature T_g of the material can be determined by the point at which the response changes from 'glassy' elastic behaviour to 'rubbery' inelastic behaviour. Unplasticised PVC has a T_g of approximately 80 °C, while plasticised PVC typically has T_g below the operating temperature of the product, such that the product is soft and flexible when in use. The ability of a plasticiser to reduce the glass transition temperature of PVC is a common metric of plasticiser compatibility and performance.[36, 69, 117] Effective

plasticisation leads to a lower T_g, while poor plasticisation can also give rise to phase separation which is shown through multiple or poorly defined glass transitions.

The T_g of plasticised PVC samples was determined by the peak of the loss modulus (Figure 7.6). All novel compounds gave a lower T_g than ESBO **8**, however the loss modulus peaks were much broader and less well defined (Table 7.2). IEEP **15** showed the lowest average T_g, but the peak width was more than double that of ESBO (FWHM of 82.2 °C compared with 39.7 °C) and appears irregular in shape, suggesting multiple phases present in the structure. The peak width of mPEG-ESBO **13** was also broader than that of ESBO, despite this plasticiser generally showing good performance in other material properties such as tensile strength and elongation. However, since it is comparable to the peak widths of the commercial petrochemical plasticisers, this increase does not necessarily indicate the presence of phase separation.
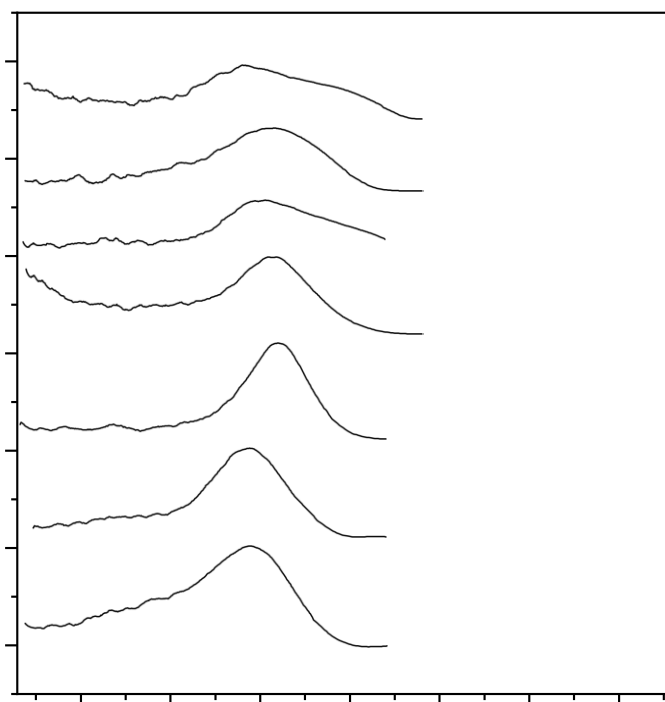
Figure 7.6: Loss modulus against Sample temperature by DMA for samples of plasticised PVC prepared by solvent casting.

Table 7.2: Glass transition temperatures (T_g) (Loss modulus peak) and peak width (FWHM of approximate peak fits).

Plasticiser	T_g (°C)	FWHM (°C)
DOP (**1**)	-2.0	54.2
DOTP (**6**)	-2.3	50.7
ESBO (**8**)	10.7	39.7
mPEG-ESBO (**13**)	7.9	46.1
MEEP (**12**)	2.9	68.8
MEFE (**14**)	10.1	66.8
IEEP (**15**)	-3.8	82.2

7.4 Thermogravimetric analysis (TGA)

Thermogravimetric analysis was carried out on the plasticisers and plasticised PVC samples. For the plasticisers alone, the data shows the volatility of the plasticiser, while for the plasticised PVC samples this technique also shows the effect of the plasticiser on the degradation of the PVC. The measurements were carried out under an inert atmosphere.

Figure 7.7 shows the mass loss of the plasticisers by TGA. All novel plasticisers showed an earlier onset of evaporation than ESBO. The mass loss also progressed in multiple distinct steps for MEEP **12**, MEFE **14** and IEEP **15**, whereas for mPEG-ESBO **13** the mass loss occurred gradually throughout the experiment. The composition of mPEG-ESBO is expected to be a more complex mixture than the other plasticiser candidates because both mPEG and ESBO are mixtures, which could account for the less defined boiling point of the resulting product. The temperatures of 5% and 50% mass loss ($T_{95\%}$ and $T_{50\%}$) are presented in Table 7.3. MEFE **14** showed the earliest onset of mass loss, losing 5% by 82 °C. This plasticiser may be undergoing a decomposition reaction leading to the mass loss at lower temperatures than the other plasticisers. The other

novel plasticisers showed a lower $T_{95\%}$ than ESBO, but comparable $T_{50\%}$ values. As such, while the major component of these plasticisers appears to have similar volatility to ESBO, these also contain more volatile or unstable minor components as well as some residual solvents.
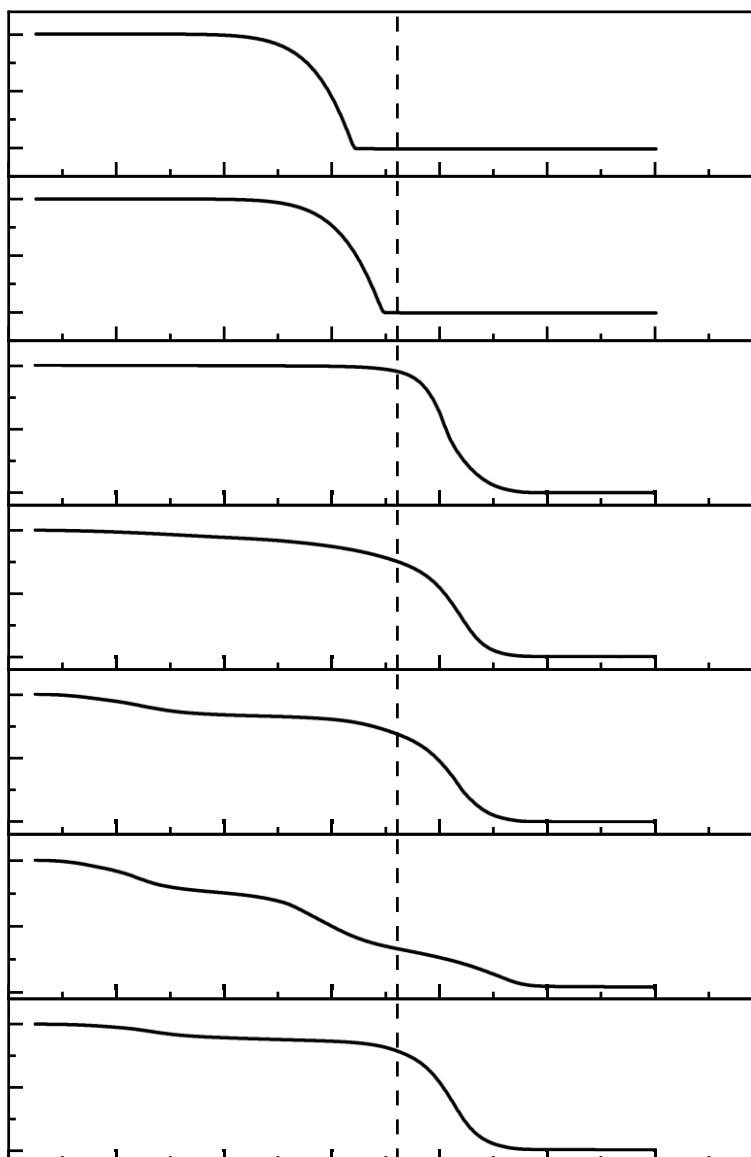
Figure 7.7: Thermogravimetric analysis of commercial and novel plasticisers.

Table 7.3: Temperature of 5% and 50% mass loss for plasticisers by TGA.

Plasticiser	$T_{95\%}$	$T_{50\%}$
DOP **1**	236	297
DOTP **6**	260	323
ESBO **8**	361	406
mPEG-ESBO **13**	185	405
MEEP **12**	95	397
MEFE **14**	82	300
IEEP **15**	126	403

The TGA results for the plasticised PVC samples (Figure 7.8) show the effect of the plasticiser on the decomposition of PVC. The thermal decomposition of PVC was described in detail by Starnes.[124] Structural defects such as tertiary and allylic chlorides are the most significant source of instability in the PVC structure as these increase the lability of the chlorine. Decomposition proceeds through an ionic (Scheme 7.1) or quasi-ionic (Scheme 7.2) loss of HCl, followed by polyene growth. The degradation can also be autocatalysed by the free HCl (Scheme 7.3). Free radical mechanisms are also thought to play a minor role in this degradation.[124]
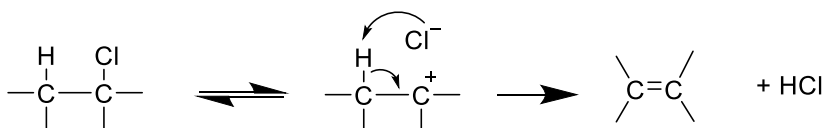
Scheme 7.1: Ionic mechanism of PVC thermal decomposition by loss of HCl.
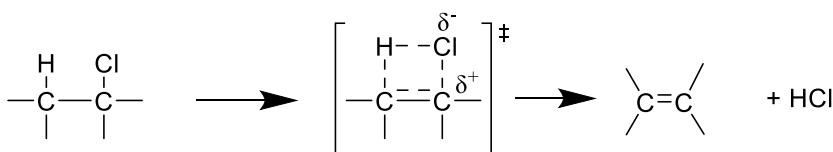
Scheme 7.2: Quasi-ionic mechanism of PVC thermal decomposition by loss of HCl.
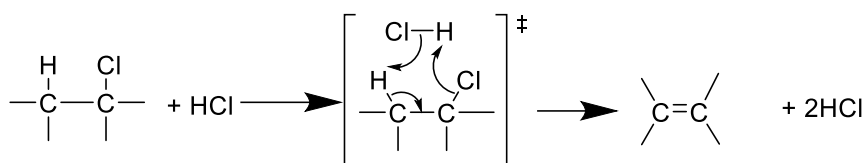
Scheme 7.3: PVC decomposition catalysed by free HCl (autocatalytic dehydrochlorination).

The polyene sequences formed by dehydrochlorination then undergo cyclisation to form benzene and other aromatic compounds.[112] Buddhiranon *et al.* measured the onset temperature of two mass loss steps in neat PVC as 260 °C and 410 °C, which correspond to dehydrochlorination and cyclisation respectively. Addition of ESBO was reported to increase the onset temperature of dehydrochlorination by 36 °C.[141]

Epoxides are thought to function as thermal stabilisers for PVC through multiple mechanisms.[142] The epoxide rings in ESBO react with chloride ions that are released during PVC decomposition (Scheme 7.4).[27] This slows the degradation of the polymer by reducing the autocatalytic dehydrochlorination. Substitution of labile chlorine atoms in the PVC structure (such as allylic chlorides) by the epoxide compound to give an α-chloro-ether was also proposed (Scheme 7.5).[142] The ether formed is more stable than the chloride, and so this prevents the growth of the polyene sequence. Further interactions of epoxides with other typical PVC stabiliser components are also thought to occur, although these depend on the nature of the stabiliser used.[142]
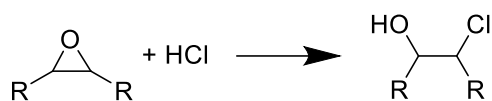
Scheme 7.4: Scavenging of hydrogen chloride by reaction with an epoxide.
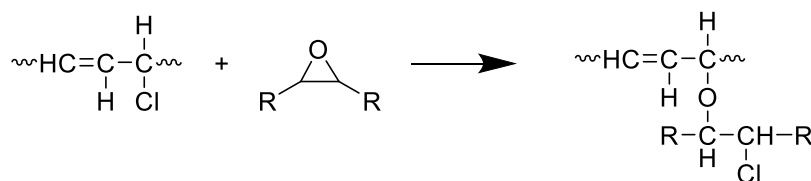
Scheme 7.5: PVC stabilisation by substitution of a labile chloride with an α-chloro-ether.

Two main mass loss steps were identified for all samples of plasticised PVC (Figure 7.8). Onset temperatures were calculated by the intersection of tangents using the Mettler Toledo STARe Evaluation software. As well as the PVC decomposition, these steps will also include volatilisation and decomposition of the plasticiser, however these processes could not be specifically identified in the data. The samples contain 33% plasticiser and 67% PVC (as well as < 1% liquid stabiliser). Complete loss of HCl from neat PVC with no other decomposition would give 58.4% loss of mass. Assuming all plasticiser (33%) is lost in the same step as complete dehydrochlorination (58.4% of 67%), expected mass loss is 72%, which is very similar to the measured mass loss for PVC-DOP (73.9%) and PVC-DOTP (73.7%). In PVC-ESBO however, the first mass loss step is 54.1%, which may indicate that the substitution reaction depicted in Scheme 7.5 is occurring, leading to a reduction in evaporation of ESBO as it reacts to form part of the polymer degradation products.

All novel plasticiser-based PVC samples retained some degree of the stabilisation behaviour observed with ESBO **8**, suggesting that some unreacted epoxide rings remain present in the compounds. ^{1}H NMR measurement of the epoxide signals gives less than one remaining epoxide per molecule, but the precision of this measurement is limited as the epoxide signals are spread over many peaks due to the mixed composition. The onset of degradation in the ESBO-plasticised sample is higher than all other samples, showing that the novel plasticisers produced from ESBO do not stabilise the PVC to the same extent. This is entirely expected, as the epoxide functionality that provides the stabilisation effect is also the functionality that has been exploited in this synthesis. As Table 7.4 shows, the $T_{95\%}$ for PVC combined with the novel plasticisers is comparable to the petrochemical plasticisers (with the exception of MEFE which is somewhat lower) and so these plasticisers are suitably non-volatile for use in PVC compounds. All samples contained the same amount of liquid heat stabiliser additive.
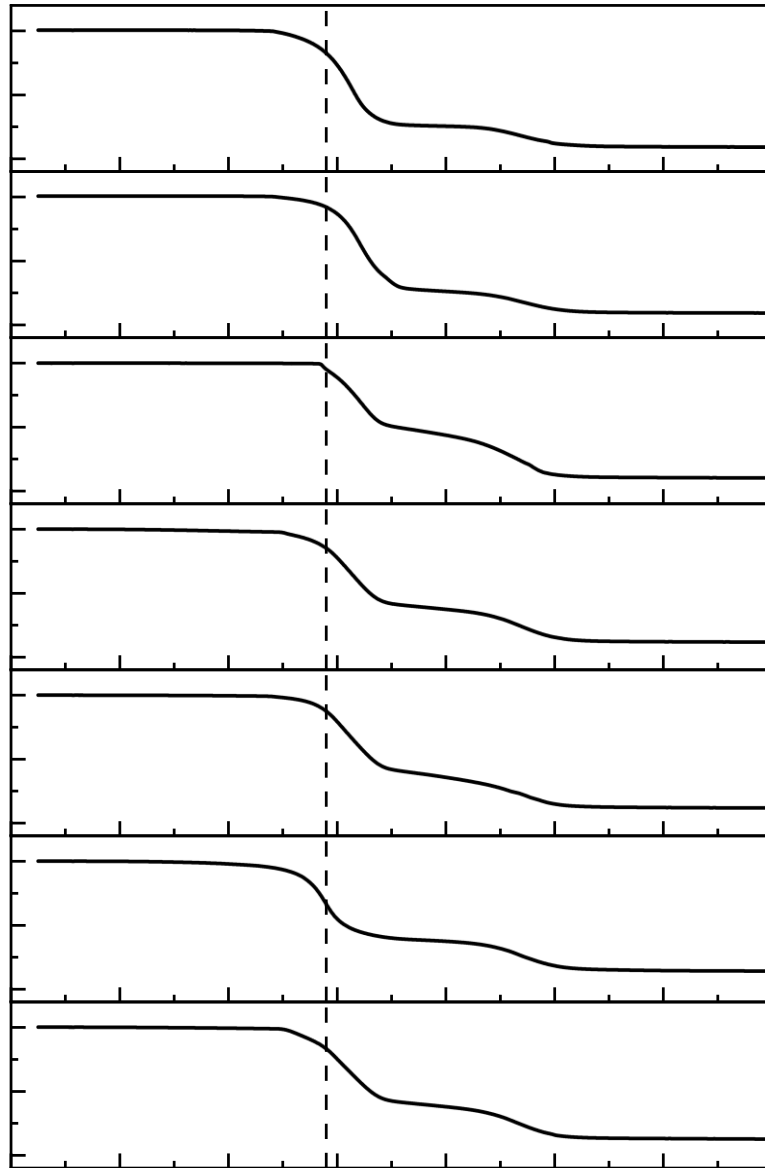
Figure 7.8: TGA of plasticised PVC samples.

Table 7.4: Mass loss steps for plasticised PVC samples by TGA.

Plasticiser	Step 1 Onset (°C)	Step 1 mass loss (%)	Step 2 Onset (°C)	Step 2 mass loss (%)	Final residue (%)	$T_{95\%}$
DOP **1**	284	73.9	452	15.9	8.2	262
DOTP **6**	296	73.7	442	16.7	8.3	278
ESBO **8**	291	54.1	447	34.5	7.2	290
mPEG-ESBO **13**	278	63.2	450	23.6	10.2	272
MEEP **12**	266	61.8	442	22.9	13.8	261
MEFE **14**	277	61.5	440	25.7	11.8	240
IEEP **15**	272	61.2	439	25.3	10.2	263

7.5 Scanning Electron Microscopy

SEM has been used to examine the morphology of PVC with novel plasticisers, typically on surfaces formed by tensile or cryogenic fracturing.[53, 143] It has also been used to examine the gelation and fusion of PVC plastisols by Nakajima *et al.*, who showed the change from a particulate structure to a continuous fused fracture surface.[144] If the PVC particulates are solvated effectively by the plasticiser, the resulting blend will show smooth features in the fracture surface, while poor solvation could lead to phase separation, showing as a rough, irregular fracture surface. The PVC-plasticiser films prepared by solvent casting were fractured under liquid nitrogen to produce fracture surfaces for SEM.

SEM images of plasticised PVC samples are shown in Figure 7.9. The samples containing commercial plasticisers DOP **1** and ESBO **8** both show smooth planes in the fractured surfaces, indicating good solvation of the PVC grains. There is no evidence of phase separation identifiable in these images. PVC-MEEP **12** shows mainly smooth plans with some inclusions observed. PVC-mPEG-ESBO **13** is the most similar in

appearance to the commercial plasticisers, however there are some features visible that appear fibrous. These could be caused by some localised crystallisation of the plasticiser.

PVC-MEFE **14** displays a very uneven microstructure, with large irregular regions visible. The surface of the fracture planes also appears to be rougher than in PVC-DOP or PVC-ESBO. PVC-IEEP **15** also shows signs of roughness on the fracture planes as well as voids which could be caused by areas of plasticiser accumulation due to poor compatibility with PVC.
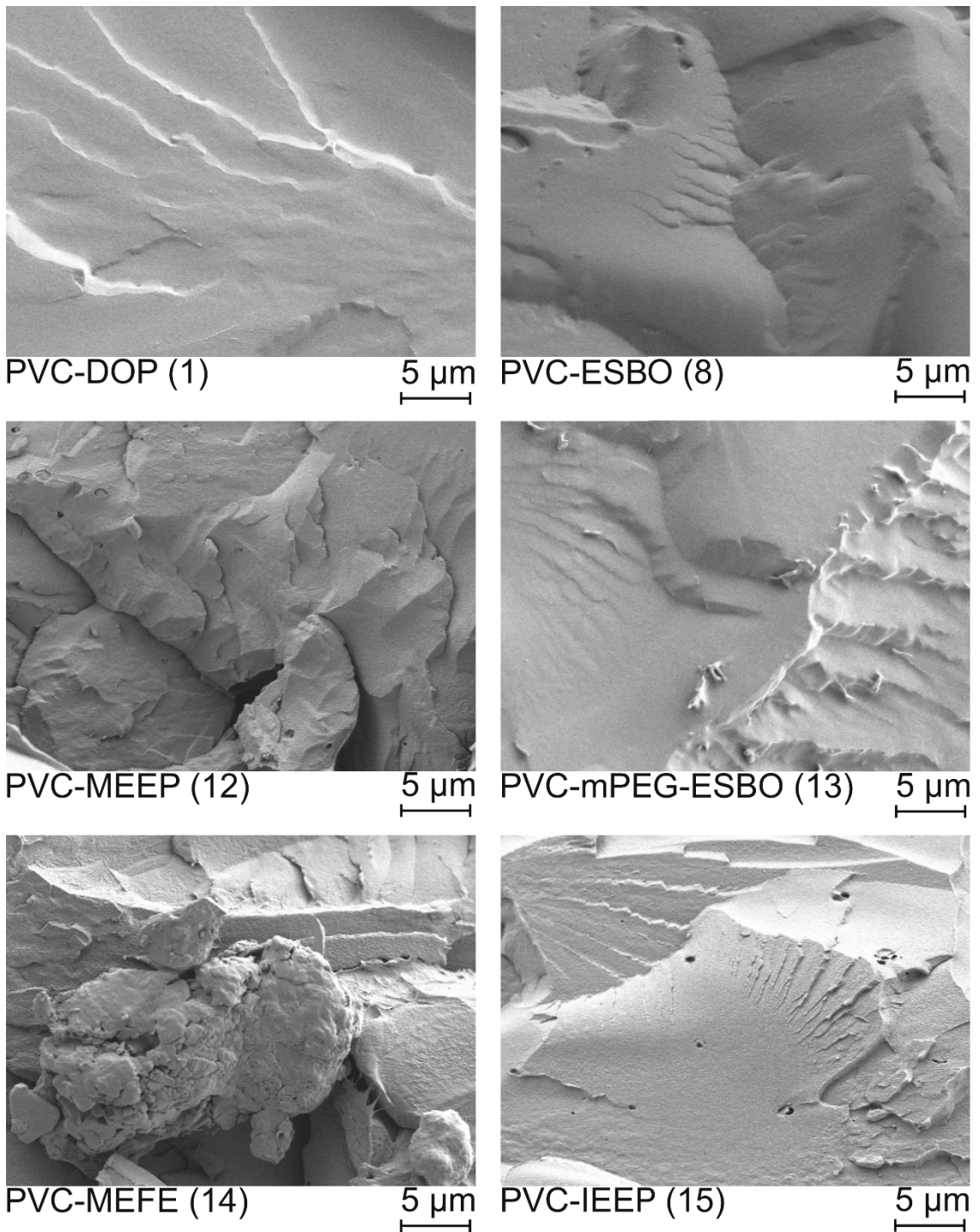
Figure 7.9: SEM images of cold fractured plasticised PVC sample surfaces, showing the effect of plasticiser on the morphology of the PVC-plasticiser blend.

7.6 Hansen Solubility Parameters

Hansen solubility parameters have been used to evaluate and describe the behaviour of plasticisers for PVC in a number of works.[49, 51] Calculations were performed using the HSPiP software package to examine the plasticisers evaluated herein. HSP values for the traditional petrochemical plasticisers were calculated using the Yamamoto – Molecular Break (Y-MB) method. This method was unsuccessful for the larger bio-based plasticisers, which were instead modelled as surfactants, using a group contribution approach based on the molecular volume of the hydrophilic and hydrophobic portion of the molecule.. The results are presented in Table 7.5.

Table 7.5: Hansen Solubility Parameters for the petrochemical and bio-based plasticisers.

Plasticiser	Dispersion δ_D	Polar δ_P	Hydrogen Bonding δ_H	Method
Diethylhexyl phthalate (DOP, 1)	16.0	4.9	2.3	Y-MB
Diethylhexyl terephthalate (DOTP, 6)	16.9	5.1	2.7	Y-MB
Epoxidised soybean oil (ESBO, 8)	16.6	4.5	1.7	Y-MB
MEEP (12)	16.6	5.1	2.7	Y-MB
mPEG-ESBO (13)	15.8	5.6	5.4	Surfactant
MEFE (14)	16.9	5.3	5.1	Surfactant
IEEP (15)	16.8	5.4	4.3	Surfactant

All of the plasticisers have similar solubility parameters, which is to be expected given that the synthesized bio-based plasticizers were designed to be compatible with PVC and therefore reflect the solubility properties of DOP and DOTP. However, it is apparent that solubility modelling does not fully explain the performance of

plasticisers, since this varied much more significantly than the differences in solvent parameters would suggest. Therefore whilst HSP calculations validate the selection of synthetic targets, and are a useful tool for the development of plasticisers, other factors may influence the interaction between polymer and plasticiser. This to some extent echoes the observations in Chapter 5 that the different metrics of plasticiser compatibility reflect different aspects of the polymer-plasticiser interaction.

7.7 Conclusions

The novel plasticisers synthesised in Chapter 6 were evaluated as plasticisers for PVC in comparison with commercial plasticisers DOP, DOTP and ESBO. All of the novel plasticisers showed some plasticising ability as determined by the glass transition temperatures measured by DMA, with MEEP **12** (2.9 °C)**,** mPEG-ESBO **13** (7.9 °C) and IEEP **15** (-3.8 °C) displaying greater suppression of T_g than ESBO (10.7 °C). However, these results indicated poor compatibility of MEEP **12**, MEFE **14** and IEEP **15** with PVC as the loss modulus peak was wide and poorly defined, particularly so in the case of IEEP. This behaviour suggests that there may be multiple glass transitions in PVC-IEEP due to phase separation in the material.

Tensile testing showed that mPEG-ESBO **13** gave enhanced tensile properties, including a 6.9 % increase in elongation at break. The tensile properties are comparable to the petrochemical plasticiser DOP, indicating an equivalent level of plasticisation. The results for the other novel plasticisers were substantially lower than ESBO, suggesting that these plasticisers lubricate the PVC chains poorly in comparison to ESBO.

The novel plasticisers all showed greater volatility than ESBO as measured by TGA. This was particularly pronounced for MEFE **14**. For mPEG-ESBO, MEEP and IEEP, the main mass loss step occurred at a similar temperature to ESBO and so the observed mass loss prior to this may be caused by impurities such as residual solvent. In the PVC blends, all of the novel plasticisers showed lower mass loss in the dehydrochlorination step (61-63 %) compared to PVC-DOP or PVC-DOTP (74 %). This

indicates that the bio-based plasticisers retain some degree of the PVC stabilisation properties of ESBO due to remaining epoxide functionality.

Examination of the morphology of the PVC-plasticiser blends by SEM showed irregularities in all samples produced with the novel plasticisers. PVC-MEFE showed a large irregular region indicating poor solvation of the polymer by the plasticiser, while the other novel plasticiser showed small inclusions. PVC-mPEG-ESBO showed the greatest similarity in structure to PVC-DOP and PVC-ESBO.

Overall, mPEG-ESBO **13** shows a number of properties comparable with the commercial petrochemical plasticisers and so should be considered a strong candidate for the replacement of petrochemical plasticisers in PVC compounds. The success of this plasticiser also indicates that further investigation into mPEG-ESBO ethers could lead to a number of suitable novel bio-based plasticisers for PVC.

8 Conclusions

8.1 Introduction

This chapter will summarise the findings of the investigation into plasticiser compatibility and the development of novel bio-based plasticisers for PVC.

The first aim of this work was to investigate analytical techniques to evaluate their use in the development of a new test method for determining plasticiser compatibility. The current industry standard method ASTM D3291 was chosen as an area of weakness in the evaluation of novel plasticisers as the method is subjective, which limits the reliability of the results.

The second aim was to synthesise a small library of novel bio-based compounds through the epoxide-opening reaction of ESBO, to improve interaction and compatibility with PVC. The third and final aim was to evaluate these novel plasticisers in comparison with commercial plasticisers across a number of metrics of plasticiser performance.

8.2 Methods of Testing Plasticiser Compatibility

In Chapter 5, the evaluation of analytical techniques for the improvement of the ASTM D3291 compatibility test was discussed. Mapping techniques were explored by micro-FTIR and Raman, however practical concerns prevented further development using these methods. Micro-FTIR was used to examine if a cross-sectional map of a compressed sample would show a change in plasticiser distribution due to the plasticiser migration, however no such change was observed. Possible reasons for this could be that under these conditions, the plasticiser exudation either occurs from a very thin layer that was not measured in the cross-sectional map, or is so minimal that it does not cause a significant measurable difference in the FTIR spectra of the plasticised PVC samples. Raman spectroscopy was shown to detect areas of plasticiser exudation on the surfaces of compressed PVC samples. However, subsequent

reabsorption of the plasticiser was also observed within a short timeframe. This effect prevents the reliable quantification of plasticiser exudation by Raman mapping, since the reabsorption took place over a similar timeframe to the collection of the Raman map.

FTIR-ATR was used to observe changes in the carbonyl peak position of the plasticisers in combination with PVC, which has been used in prior works as a measure of plasticiser compatibility.[90] The carbonyl peak position on the exuding surface of plasticised PVC samples showed some indication of plasticiser exudation, however this change was considered too small relative to the resolution of the FTIR measurement for reliable and quantitative interpretation to be possible. Despite this, it was noted that some indication of plasticiser exudation could be detected below the level observable from the ASTM D3291 standard method, and so this could still be used as a more sensitive measure of plasticiser exudation in a qualitative test. The FTIR measurements suggested that the sample plasticised with DOTP alone gave the greatest level of plasticiser exudation, while ESBO had the weakest interaction of carbonyl groups with the PVC chain. As such, the carbonyl peak position change due to incorporation into PVC does not appear to be strongly correlated to exudation behaviour within the parameters of this investigation.

The plasticiser compatibility test method developed using GC-MS was shown to have far greater sensitivity than FTIR, with some measurable exudation detected and quantified for all samples tested. This presents a significant improvement compared with the standard test method, which could not measure any plasticiser exudation at 60 minutes compression, with all samples tested rated "0 – no exudation" under these conditions. Ordinarily the ASTM D3291 test method takes a number of weeks to show differences in exudation. The ability to measure differences in compatibility of plasticisers on a much shorter timescale is of great value to the PVC industry, as rapid development of products is required to meet customer demands. These measurements confirmed the observation from FTIR that DOTP had the highest plasticiser exudation under the compatibility loop test. Variation in the results was high, possibly because the amount of plasticiser exudation was small and thus the

concentration in the solutions tested was low. However, for DOTP the data was of sufficient quality to examine the kinetics of plasticiser exudation, which presented as a first order kinetic process. This suggests that plasticiser diffusion through the PVC matrix occurs more slowly than the timescale of the compression test used in this work (60 min) and so the concentration of plasticiser at the exuding surface is depleted, leading to slower exudation over time.

These results showed no correlation to the observations of glass transition behaviour as measured by DMA, which showed that PVC-DOTP had the lowest T_g value, similar to PVC-DOP, while PVC-ESBO had a much higher T_g. As such, suppression of the glass transition temperature and the tendency of a plasticiser to exude in a loop spew compatibility test do not appear to be strongly linked in the plasticised PVC samples tested here. This highlights the potential importance of an improved 'loop spew' test as investigations of glass transition temperature cannot be used to replace this measure of exudation. The tendency of a plasticiser to exude is a more relevant measure of compatibility for industrial producers of PVC products, as exudation leads to many undesirable properties such as tackiness and hardening of the product. However, a plasticiser that can produce a greater suppression of glass transition temperature at an equivalent concentration in the PVC compound would be more efficient and thus more sustainable, as less would be required to produce a flexible PVC compound. A plasticiser that could be used at lower concentrations would also reduce the environmental impact from loss to the environment. Therefore, both glass transition temperature and permanence in the PVC compound are important considerations for the development of sustainable plasticisers.

8.3 Synthesis and Evaluation of Bio-Based Plasticisers for PVC

The synthesis of a small library of novel bio-based compounds was achieved in Chapter 6, introducing a range of functional groups into the ESBO structure by nucleophilic attack at the epoxide ring. Some attempted synthetic routes were unsuccessful, and purification of the resulting oils was challenging due to the mixed

composition of ESBO. Transesterification of the glycerol esters was a potential side reaction that was observed, and reaction conditions were chosen to limit this.

The evaluation of the novel bio-based plasticisers was described in Chapter 7, with tensile testing, DMA, TGA and SEM used to compare solvent-cast PVC films prepared with commercial plasticisers DOP **1**, DOTP **6** and ESBO **8**, and the four bio-based ESBO derivatives. From these results, mPEG-ESBO **13** presented excellent plasticisation of PVC, with an increase of 3% tensile strength and 6.9% elongation compared to material plasticised with the ESBO starting material. The other ESBO derivatives showed some plasticising properties in the suppression of T_g by DMA, but also showed stiff and brittle behaviour in the tensile test with fracture at much lower strain than the commercial plasticisers. As such, the synthetic modifications described in the unsuccessful plasticiser candidates have hindered their plasticising ability relative to ESBO. The calculations of the Hansen Solubility Parameters did not show significant differences between the more and less compatible plasticisers, and so could not be used to predict which of the plasticiser candidates would display good compatibility in the PVC compound.

The novel plasticiser mPEG-ESBO **13** shows improved mechanical properties in a PVC blend compared to ESBO, including a 6.9 % increase in elongation at break. This indicates greater plasticisation, comparable to the commercially dominant petrochemical plasticiser DOP **1,** and thus fulfils the objectives of synthesising and evaluating a bio-based plasticiser for PVC with enhanced properties.

8.4 Impact

The GC-MS method for testing plasticiser compatibility described here represents a significant improvement over the industry standard ASTM D3291 loop spew method, with a significantly lower limit of detection for exuded plasticiser, and is achievable in hours instead of weeks whilst providing quantitative data in place of a subjective scoring method. GC-MS is a widely available technique to PVC compounders, making this method suitable for immediate industry adoption without further capital

expense, to allow PVC compounders to evaluate new plasticisers for compatibility effectively and efficiently. Additionally, the composition of the exuded plasticiser can be determined by GC-MS analysis. This is of particular value as the use of mixed plasticiser systems is common in PVC formulation.[7] Through the use of this method, PVC compounders could evaluate the compatibility of novel plasticisers through a robust, quantitative method which would provide confidence in the use of these plasticisers in their products. This would aid industrial compounders in the replacement of toxic, petrochemical plasticisers with more sustainable alternatives without compromising the quality of the finished product. The use of more compatible plasticisers is not only beneficial to the material properties of the PVC item, but also reduces loss of plasticiser to the environment and so this method could be used to demonstrate reduction in pollution from PVC compounds.

The bio-based plasticiser candidate mPEG-ESBO shows comparable performance to the commercial petrochemical plasticisers in its tensile properties, while retaining some degree of PVC stabilisation from the unreacted epoxide groups remaining in the molecule, as shown by TGA. These properties mean that mPEG-ESBO has great potential for the replacement of petrochemical plasticisers in PVC compounds. The reaction between ESBO and mPEG requires no additional solvents and could be developed to improve the sustainability through the use of heterogenous catalysis and less harmful solvents in the purification. Plasticisers can account for as much as 50% of the total composition of a plasticised PVC compound, and so the replacement of harmful petrochemical plasticisers with a green alternative would significantly improve the sustainability of the resulting PVC compound. Approximately 8 million tonnes of plasticisers are used in PVC compounds annually, and so replacing these largely petrochemical plasticisers with less harmful and more sustainable alternatives such as mPEG-ESBO would reduce harm to the environment substantially.

8.5 Further Work

The method of testing plasticiser compatibility through GC-MS analysis shows clear advantages compared to the current industry standard method. This method could be improved further through experiments with a wider range of plasticisers and across a longer timescale. All of the samples tested herein were rated '0 (no exudation)' by the ASTM D3291 method. Thus, it would be of interest to quantify the plasticiser exudation in samples which show exudation in the 1-3 (slight to heavy exudation) rating categories. Further experiments could also investigate the kinetics of exudation over longer timescales that would allow for greater diffusion of plasticiser through the sample, since the exudation kinetics of DOTP presented here suggested that the exuded plasticiser mostly originated at the PVC surface as opposed to the bulk. This would further advance the method towards determining a numerical value for plasticiser exudation at which a plasticiser could be classed as 'compatible' or 'incompatible'. Determining this metric would advance the capabilities of the PVC industry in the evaluation of novel plasticisers by increasing the confidence in the plasticiser compatibility test.

There is significant scope for further development of the synthesis of bio-based plasticiser candidates through ESBO epoxide-opening reactions. Polyethylene glycols provide a wealth of options for further development, such as investigations into the effect of PEG chain length on the plasticising ability. Further work to evaluate the effect of PEG chain length, the use of capping-groups other than methyl, as well as other bio-based epoxide starting materials could expand upon this to develop a bio-based plasticiser for PVC that could replace toxic and petrochemical plasticisers. The methodologies used in the synthesis could also be improved upon in terms of sustainability through the use of less harmful solvents such as 2-methyl TMF (derived from sugars) to replace THF and TMO (2,2,5,5-tetramethyloxolane) to replace toluene. Through these developments and improvements, more compatible, bio-based plasticisers could be developed that would go some way to reducing the environmental impact of plasticised PVC materials.

References

(1) Baumann, E. Über einige Vinylverbindungen. *Ann. Chem. Pharm.* **1872**, *163*, 308-322.

(2) Wypych, G. *Handbook of Plasticizers (3rd Edition)*; ChemTec Publishing, 2017.

(3) Braun, D. PVC - Origin, growth, and future. *J. Vinyl Addit. Technol.* **2001**, *7* (4), 168-176, Article; Proceedings Paper. DOI: 10.1002/vnl.10288.

(4) Buekens, A.; Sevenster, A. Vinyl 2010-nearing the target date. *J. Mater. Cycles Waste Manage.* **2010**, *12* (2), 184-192. DOI: 10.1007/s10163-010-0286-9.

(5) Gilbert, M.; Patrick, S. Brydson's Plastics Materials (8th Edition). In *Brydson's Plastics Materials*, 8th ed.; Gilbert, M. Ed.; Elsevier, 2016.

(6) Zhang, Z. M.; Jiang, P. P.; Liu, D. K.; Feng, S.; Zhang, P. B.; Wang, Y. T.; Fu, J. H.; Agus, H. Research progress of novel bio-based plasticizers and their applications in poly(vinyl chloride). *J. Mater. Sci.* **2021**, *56* (17), 10155-10182. DOI: 10.1007/s10853-021-05934-x.

(7) Wypych, G. *PVC Formulary (3rd Edition)*; ChemTec Publishing, 2020.

(8) Wypych, G. *PVC Degradation and Stabilization*; ChemTec Publishing, 2015.

(9) Endo, K. Synthesis and structure of poly(vinyl chloride). *Prog. Polym. Sci.* **2002**, *27* (10), 2021-2054. DOI: 10.1016/s0079-6700(02)00066-7.

(10) Darvishi, R.; Esfahany, M. N.; Bagheri, R. S-PVC Grain Morphology: A Review. *Ind. Eng. Chem. Res.* **2015**, *54* (44), 10953-10963, Review. DOI: 10.1021/acs.iecr.5b02478.

(11) Dubois, J.-L. Manufacture of vinyl chloride monomer from renewable materials, vinyl chloride monomer thus-obtained, and use. France WO2010061152A1, 2009.

(12) INEOS. *Biovyn - Inovyn bio-attributed PVC*. 2020. https://biovyn.co.uk/ (accessed May 2023).

(13) VYNOVA. *Bio-Circular PVC*. https://www.vynova-group.com/bio-circular-pvc (accessed May 2023).

(14) Wypych, G. 2.3.1 Molecular Weight and its Distribution. In *PVC Formulary (3rd Edition)*, ChemTec Publishing, 2020.

(15) Semon, W. L. Synthetic rubber-like composition and method of making same. USA US1929453A, 1933.

(16) Bocque, M.; Voirin, C.; Lapinte, V.; Caillol, S.; Robin, J. J. Petro-Based and Bio-Based Plasticizers: Chemical Structures to Plasticizing Properties. *J. Polym. Sci., Part A: Polym. Chem.* **2016**, *54* (1), 11-33, Review. DOI: 10.1002/pola.27917.

(17) Doull, J.; Cattley, R.; Elcombe, C.; Lake, B. G.; Swenberg, J.; Wilkinson, C.; Williams, G.; van Gemert, M. A cancer risk assessment of di(2-ethylhexyl)phthalate: Application of the new US EPA risk assessment guidelines. *Regul. Toxicol. Pharm.* **1999**, *29* (3), 327-357. DOI: 10.1006/rtph.1999.1296.

(18) Wirnitzer, U.; Rickenbacher, U.; Katerkamp, A.; Schachtrupp, A. Systemic toxicity of di-2-ethylhexyl terephthalate (DEHT) in rodents following four weeks of intravenous exposure. *Toxicol. Lett.* **2011**, *205* (1), 8-14. DOI: 10.1016/j.toxlet.2011.04.020.

(19) Beg, M. A.; Sheikh, I. A. Endocrine Disruption: Structural Interactions of Androgen Receptor against Di(2-ethylhexyl) Phthalate and Its Metabolites. *Toxics* **2020**, *8* (4). DOI: 10.3390/toxics8040115.

(20) European Plasticisers. *Plasticisers Information Centre - Orthophthalates*. 2023. https://www.plasticisers.org/plasticiser/ortho-phthalates/ (accessed March 2023).

(21) Chemicals known to the State to cause cancer or reproductive toxicity. State of California Environmental Protection Agency, Ed.; 2017.

(22) Congress, U. S. *Consumer Product Safety Improvement Act, Public Law 110-314*; 2008.

(23) Subedi, B.; Sullivan, K. D.; Dhungana, B. Phthalate and non-phthalate plasticizers in indoor dust from childcare facilities, salons, and homes across the USA. *Environ. Pollut.* **2017**, *230*, 701-708. DOI: 10.1016/j.envpol.2017.07.028.

(24) Guo, Y.; Kannan, K. Comparative Assessment of Human Exposure to Phthalate Esters from House Dust in China and the United States. *Environ. Sci. Technol.* **2011**, *45* (8), 3788-3794. DOI: 10.1021/es2002106.

(25) Knothe, G.; Krahl, J.; Gerpen, J. V. 6.7 Soybean Oil Composition for Biodiesel. In *Biodiesel Handbook (2nd Edition)*, AOCS Press, 2010; p 248.

(26) Zhang, C. Q.; Garrison, T. F.; Madbouly, S. A.; Kessler, M. R. Recent advances in vegetable oil-based polymers and their composites. *Prog. Polym. Sci.* **2017**, *71*, 91-143. DOI: 10.1016/j.progpolymsci.2016.12.009.

(27) Karmalm, P.; Hjertberg, T.; Jansson, A.; Dahl, R. Thermal stability of poly(vinyl chloride) with epoxidised soybean oil as primary plasticizer. *Polym. Degrad. Stab.* **2009**, *94* (12), 2275-2281. DOI: 10.1016/j.polymdegradstab.2009.07.019.

(28) Jia, P. Y.; Zhang, M.; Hu, L. H.; Zhou, Y. H. A novel biobased polyester plasticizer prepared from palm oil and its plasticizing effect on poly (vinyl chloride). *Pol. J. Chem. Technol.* **2016**, *18* (1), 9-14, Article. DOI: 10.1515/pjct-2016-0002.

(29) Bouchareb, B.; Benaniba, M. T. Effects of epoxidized sunflower oil on the mechanical and dynamical analysis of the plasticized poly(vinyl chloride). *J. Appl. Polym. Sci.* **2008**, *107* (6), 3442-3450. DOI: 10.1002/app.27458.

(30) Kandula, S.; Stolp, L.; Grass, M.; Woldt, B.; Kodali, D. Functionalization of Soy Fatty Acid Alkyl Esters as Bioplasticizers. *J. Vinyl Addit. Technol.* **2017**, *23* (2), 93-105, Article. DOI: 10.1002/vnl.21486.

(31) Zhong, B.; Shaw, C.; Rahim, M.; Massingill, J. Novel coatings from soybean oil phosphate ester polyols. *J. Coat. Technol.* **2001**, *73* (915), 53-57. DOI: 10.1007/bf02730031.

(32) Bailosky, L. C.; Bender, L. M.; Bode, D.; Choudhery, R. A.; Craun, G. P.; Gardner, K. J.; Michalski, C. R.; Rademacher, J. T.; Stella, G. J.; Telford, D. J. Synthesis of polyether polyols with epoxidized soy bean oil. *Prog. Org. Coat.* **2013**, *76* (12), 1712-1719. DOI: 10.1016/j.porgcoat.2013.05.005.

(33) Guo, A.; Cho, Y. J.; Petrovic, Z. S. Structure and properties of halogenated and nonhalogenated soy-based polyols. *J. Polym. Sci., Part A: Polym. Chem.* **2000**, *38* (21), 3900-3910. DOI: 10.1002/1099-0518(20001101)38:21<3900::aid-pola70>3.0.co;2-e.

(34) *VinyLoop Closure of operation in Italy / Phthalates issue under REACH brings down European PVC recycling project*. PlastEurope, 2018. https://www.plasteurope.com/news/Closure_of_operation_in_Italy_Phthalates_issue_under_REACH_brings_do_t240095/ (accessed 2023 30.12.2023).

(35) PVC recycling branches out to medical products. In *Plastics Recycling World*, November/December 2020 ed.; AMI: 2020; pp 27-32.

(36) Ang, D. T. C.; Khong, Y. K.; Gan, S. N. Palm oil-based compound as environmentally friendly plasticizer for poly(vinyl chloride). *J. Vinyl Addit. Technol.* **2016**, *22* (1), 80-87, Article. DOI: 10.1002/vnl.21434.

(37) Omrani, I.; Ahmadi, A.; Farhadian, A.; Shendi, H. K.; Babanejad, N.; Nabid, M. R. Synthesis of a bio-based plasticizer from oleic acid and its evaluation in PVC formulations. *Polym. Test.* **2016**, *56*, 237-244, Article. DOI: 10.1016/j.polymertesting.2016.10.027.

(38) Li, D. Y.; Panchal, K.; Mafi, R.; Xi, L. An Atomistic Evaluation of the Compatibility and Plasticization Efficacy of Phthalates in Poly(vinyl chloride). *Macromolecules* **2018**, *51* (18), 6997-7012. DOI: 10.1021/acs.macromol.8b00756.

(39) ASTM International. *ASTM D3291-11, Standard Practice for Compatibility of Plasticizers in Poly(Vinyl Chloride) Plastics Under Compression*; 2011. DOI: 10.1520/D3291-11.

(40) Almeida, S.; Ozkan, S.; Goncalves, D.; Paulo, I.; Queiros, C.; Ferreira, O.; Bordado, J.; dos Santos, R. G. A Brief Evaluation of Antioxidants, Antistatics, and Plasticizers Additives from Natural Sources for Polymers Formulation. *Polymers* **2023**, *15* (1). DOI: 10.3390/polym15010006.

(41) Senichev, V. Y.; Tereshatov, V. V. Theories of Compatibility. In *Handbook of Plasticizers (3rd Edition)*, ChemTec Publishing, 2017; pp 135-164.

(42) Daniels, P. H. A Brief Overview of Theories of PVC Plasticization and Methods Used to Evaluate PVC-Plasticizer Interaction. *J. Vinyl Addit. Technol.* **2009**, *15* (4), 219-223, Article; Proceedings Paper. DOI: 10.1002/vnl.20211.

(43) Sears, J. K.; Darby, J. R. *The technology of plasticizers*; Wiley, 1982, 1982.

(44) Lloyd, D. R.; Ward, T. C.; Schreiber, H. P. *Inverse gas chromatography*; Washington, DC (USA); American Chemical Society, 1989.

(45) Mohammadi-Jam, S.; Waters, K. E. Inverse gas chromatography applications: A review. *Adv. Colloid Interface Sci.* **2014**, *212*, 21-44. DOI: 10.1016/j.cis.2014.07.002.

(46) Small, P. A. Some factors affecting the solubility of polymers. *J. Appl. Chem. (London, U. K.)* **1953**, *3* (2), 71-80. DOI: 10.1002/jctb.5010030205.

(47) Blanks, R. F.; Prausnitz, J. M. Thermodynamics of Polymer Solubility in Polar and Nonpolar Systems. *Ind. Eng. Chem. Fund.* **1964**, *3* (1), 1-8.

(48) Krauskopf, L. G. Prediction of plasticizer solvency using hansen solubility parameters. *J. Vinyl Addit. Technol.* **1999**, *5* (2), 101-106. DOI: 10.1002/vnl.10316.

(49) Kwansa, A. L.; Pani, R. C.; DeLoach, J. A.; Tieppo, A.; Moskala, E. J.; Perri, S. T.; Yingling, Y. G. Molecular Mechanism of Plasticizer Exudation from Polyvinyl Chloride. *Macromolecules* **2023**, *56* (13), 4775-4786. DOI: 10.1021/acs.macromol.2c01735.

(50) Hansen, C. M. *Hansen Solubility Parameters: A User's Handbook*; CRC Press, 2007. DOI: 10.1201/9781420006834.

(51) Greco, A.; Brunetti, D.; Renna, G.; Mele, G.; Maffezzoli, A. Plasticizer for poly(vinyl chloride) from cardanol as a renewable resource material. *Polym. Degrad. Stab.* **2010**, *95* (11), 2169-2174. DOI: 10.1016/j.polymdegradstab.2010.06.001.

(52) Chen, J.; Liu, Z. S.; Nie, X. A.; Zhou, Y. H.; Jiang, J. C.; Murray, R. E. Plasticizers derived from cardanol: synthesis and plasticization properties for polyvinyl

chloride(PVC). *Journal of Polymer Research* **2018**, *25* (5). DOI: 10.1007/s10965-018-1524-4.

(53) Li, X. Y.; Nie, X. A.; Chen, J.; Wang, Y. G.; Li, K. Synthesis and Application of a Novel Epoxidized Plasticizer Based on Cardanol for Poly(vinyl chloride). *J. Renewable Mater.* **2017**, *5* (2), 154-164. DOI: 10.7569/jrm.2017.634101.

(54) Yao, L. L.; Chen, Q. H.; Xu, W. Q.; Ye, Z. B.; Shen, Z. D.; Chen, M. J. Preparation of cardanol based epoxy plasticizer by click chemistry and its action on poly(vinyl chloride). *J. Appl. Polym. Sci.* **2017**, *134* (23), 7, Article. DOI: 10.1002/app.44890.

(55) Coughlin, C. S.; Mauritz, K. A.; Storey, R. F. A general free-volume based theory for the diffusion of large molecules in amorphous polymers above Tg .3. Theoretical conformational-analysis of molecular shape. *Macromolecules* **1990**, *23* (12), 3187-3192. DOI: 10.1021/ma00214a026.

(56) Coughlin, C. S.; Mauritz, K. A.; Storey, R. F. A general free-volume based theory for the diffusion of large molecules in amorphous polymers above Tg .5. Application to dialkyl adipate plasticizers in poly(vinyl chloride). *Macromolecules* **1991**, *24* (8), 2113-2116. DOI: 10.1021/ma00008a066.

(57) Coughlin, C. S.; Mauritz, K. A.; Storey, R. F. A general free-volume based theory for the diffusion of large molecules in amorphous polymers above Tg .4. Polymer penetrant interactions. *Macromolecules* **1991**, *24* (7), 1526-1534. DOI: 10.1021/ma00007a014.

(58) Jia, P. Y.; Hu, L. H.; Feng, G. D.; Bo, C. Y.; Zhang, M.; Zhou, Y. H. PVC materials without migration obtained by chemical modification of azide-functionalized PVC and triethyl citrate plasticizer. *Materials Chemistry and Physics* **2017**, *190*, 25-30. DOI: 10.1016/j.matchemphys.2016.12.072.

(59) Czogala, J.; Pankalla, E.; Turczyn, R. Recent Attempts in the Design of Efficient PVC Plasticizers with Reduced Migration. *Materials* **2021**, *14* (4). DOI: 10.3390/ma14040844.

(60) Coelho, J. F. J.; Silva, A.; Popov, A. V.; Percec, V.; Abreu, M. V.; Gonçalves, P.; Gil, M. H. Synthesis of poly(vinyl chloride)-*b*-poly(*n*-butyl acrylate)-*b*-poly(vinyl chloride) by the competitive single-electron-transfer/degenerative-chain-transfer-mediated living radical polymerization in water. *Journal of Polymer Science Part a-Polymer Chemistry* **2006**, *44* (9), 3001-3008. DOI: 10.1002/pola.21403.

(61) Navarro, R.; Perrino, M. P.; Tardajos, M. G.; Reinecke, H. Phthalate Plasticizers Covalently Bound to PVC: Plasticization with Suppressed Migration. *Macromolecules* **2010**, *43* (5), 2377-2381, Article. DOI: 10.1021/ma902740t.

(62) Ekelund, M.; Edin, H.; Gedde, U. W. Long-term performance of poly(vinyl chloride) cables. Part 1: Mechanical and electrical performances. *Polym. Degrad. Stab.* **2007**, *92* (4), 617-629. DOI: 10.1016/j.polymdegradstab.2007.01.005.

(63) Ekelund, M.; Azhdar, B.; Gedde, U. W. Evaporative loss kinetics of di(2-ethylhexyl)phthalate (DEHP) from pristine DEHP and plasticized PVC. *Polym. Degrad. Stab.* **2010**, *95* (9), 1789-1793. DOI: 10.1016/j.polymdegradstab.2010.05.007.

(64) Audouin, L.; Dalle, B.; Metzger, G.; Verdu, J. Thermal aging of plasticized PVC. 1. Weight-loss kinetics in the PVC didecylphthalate system. *J. Appl. Polym. Sci.* **1992**, *45* (12), 2091-2096. DOI: 10.1002/app.1992.070451204.

(65) Audouin, L.; Verdu, J. Thermal ageing of plasticized PVC - Effect of loss kinetics on plasticizer depth distribution. *Proceedings of the 4th International Conference on Properties and Applications of Dielectric Materials, Vols 1 and 2* **1994**, 262-265.

(66) Djilani, S. E.; Bouchami, T.; Krid, F.; Boudiaf, N.; Messadi, D. Comparison of chemical and mathematical simulations of DOP migration from plasticized PVC disks dipped into edible oils. *Eur. Polym. J.* **2000**, *36* (9), 1981-1987, Article. DOI: 10.1016/s0014-3057(99)00263-3.

(67) Brouillet, S.; Fugit, J. L. Solutions to reduce release behavior of plasticizers out of PVC-made equipments: binary blends of plasticizers and thermal treatment. *Polym. Bull.* **2009**, *62* (6), 843-854. DOI: 10.1007/s00289-009-0055-x.

(68) Atek, D.; Belhaneche-Bensemra, N.; Turki, M. Migration of Epoxidized Sunflower Oil and Dioctyl Phthalate from Rigid and Plasticized Poly(vinyl chloride). *Int. J. Polymer. Mater.* **2010**, *59* (5), 342-352. DOI: 10.1080/00914030903478909.

(69) Daniels, P. H.; Cabrera, A. Plasticizer Compatibility Testing: Dynamic Mechanical Analysis and Glass Transition Temperatures. *J. Vinyl Addit. Technol.* **2015**, *21* (1), 7-11. DOI: 10.1002/vnl.21355.

(70) Jia, P. Y.; Zhang, M.; Hu, L. H.; Zhou, Y. H. Green plasticizers derived from soybean oil for poly(vinyl chloride) as a renewable resource material. *Korean J. Chem. Eng.* **2016**, *33* (3), 1080-1087, Article. DOI: 10.1007/s11814-015-0213-9.

(71) Beltran, M.; Garcia, J. C.; Marcilla, A. Infrared spectral changes in PVC and plasticized PVC during gelation and fusion. *Eur. Polym. J.* **1997**, *33* (4), 453-462, Article. DOI: 10.1016/s0014-3057(96)00213-3.

(72) Gonzalez, N.; Fernandez-Berridi, M. J. Fourier transform infrared Spectroscopy in the study of the interaction between PVC and plasticizers: PVC/Plasticizer compatibility. *J. Appl. Polym. Sci.* **2008**, *107* (2), 1294-1300. DOI: 10.1002/app.26651.

(73) Mangolini, F.; Rossi, A. Attenuated total reflection-Fourier transform infrared spectroscopy: A powerful tool for investigating polymer surfaces and interfaces. In *Polymer Surface Characterisation*, Sabbatini, L. Ed.; De Gruyter, 2014; pp 113-151.

(74) Gonzalez, N.; Fernandez-Berridi, M. J. Application of Fourier transform infrared spectroscopy in the study of interactions between PVC and plasticizers: PVC/plasticizer compatibility versus chemical structure of plasticizer. *J. Appl. Polym. Sci.* **2006**, *101* (3), 1731-1737. DOI: 10.1002/app.23381.

(75) Tabb, D. L.; Koenig, J. L. Fourier-Transform Infrared Study Of Plasticized And Unplasticized Polyvinyl-Chloride). *Macromolecules* **1975**, *8* (6), 929-934. DOI: 10.1021/ma60048a043.

(76) Voyiatzis, G. A.; Andrikopoulos, K. S.; Papatheodorou, G. N.; Kamitsos, E. I.; Chryssikos, G. D.; Kapoutsis, J. A.; Anastasiadis, S. H.; Fytas, G. Polarized resonance Raman and FTIR reflectance spectroscopic investigation of the molecular orientation in industrial poly(vinyl chloride) specimens. *Macromolecules* **2000**, *33* (15), 5613-5623, Article. DOI: 10.1021/ma991772m.

(77) Norbygaard, T.; Berg, R. W. Analysis of phthalate ester content in poly(vinyl chloride) plastics by means of Fourier transform Raman spectroscopy. *Appl. Spectrosc.* **2004**, *58* (4), 410-413, Article. DOI: 10.1366/000370204773580248.

(78) Berg, R. W.; Otero, A. D. Analysis of adipate ester contents in poly(vinyl chloride) plastics by means of FT-Raman spectroscopy. *Vib. Spectrosc* **2006**, *42* (2), 222-225, Article; Proceedings Paper. DOI: 10.1016/j.vibspec.2006.05.031.

(79) Irvin, K. S.; Potgieter, J. H.; Liauw, C.; Sparkes, R.; Potgieter-Vermaak, S. The quantification of di-octyl terephthalate and calcium carbonate in polyvinyl chloride using Fourier transform-infrared and Raman spectroscopy. *J. Appl. Polym. Sci.* **2022**, *139* (24). DOI: 10.1002/app.52372.

(80) Al-Natsheh, M.; Alawi, M.; Fayyad, M.; Tarawneh, I. Simultaneous GC-MS determination of eight phthalates in total and migrated portions of plasticized polymeric toys and childcare articles. *Journal of Chromatography B-Analytical Technologies in the Biomedical and Life Sciences* **2015**, *985*, 103-109, Article. DOI: 10.1016/j.jchromb.2015.01.010.

(81) Biedermann-Brem, S.; Biedermann, M.; Fiselier, K.; Grob, K. Compositional GC-FID analysis of the additives to PVC, focusing on the gaskets of lids for glass jars. *Food Addit. Contam. Part A-Chem.* **2005**, *22* (12), 1274-1284, Article. DOI: 10.1080/02652030500309426.

(82) Suman, M.; La Tegola, S.; Catellani, D.; Bersellini, U. Liquid chromatography-electrospray ionization-tandem mass spectrometry method for the determination of epoxidized soybean oil in food products. *J. Agric. Food. Chem.* **2005**, *53* (26), 9879-9884, Article. DOI: 10.1021/jf052151x.

(83) Castle, L.; Jickells, S. M.; Nichol, J.; Johns, S. M.; Gramshaw, J. W. Determination of high-molecular-mass and low-molecular-mass plasticizers in stretch-type packaging films. *J. Chromatogr. A* **1994**, *675* (1-2), 261-266. DOI: 10.1016/0021-9673(94)85283-9.

(84) He, Z.; Lu, Y. Y.; Lin, C. Q.; Jia, H. H.; Wu, H. L.; Cao, F.; Ouyang, P. K. Designing anti-migration furan-based plasticizers and their plasticization properties in poly (vinyl chloride) blends. *Polym. Test.* **2020**, *91*. DOI: 10.1016/j.polymertesting.2020.106793.

(85) Tomaszewska, J.; Sterzynski, T.; Wozniak-Braszak, A.; Banaszak, M. Review of Recent Developments of Glass Transition in PVC Nanocomposites. *Polymers* **2021**, *13* (24). DOI: 10.3390/polym13244336.

(86) Anastas, P. T. Green chemistry and the role of analytical methodology development. *Crit. Rev. Anal. Chem.* **1999**, *29* (3), 167-175. DOI: 10.1080/10408349891199356.

(87) Anastas, P. T.; Warner, J. C. *Green chemistry: theory and practice*; Oxford University Press, 1998.

(88) Kandula, S.; Stolp, L.; Grass, M.; Woldt, B.; Kodali, D. Synthesis and Functional Evaluation of Soy Fatty Acid Methyl Ester Ketals as Bioplasticizers. *J. Am. Oil Chem. Soc.* **2014**, *91* (11), 1967-1974. DOI: 10.1007/s11746-014-2529-8.

(89) Mehta, B.; Kathalewar, M.; Sabnis, A. Benzyl ester of dehydrated castor oil fatty acid as plasticizer for poly(vinyl chloride). *Polym. Int.* **2014**, *63* (8), 1456-1464, Article. DOI: 10.1002/pi.4641.

(90) Yin, B.; Hakkarainen, M. Oligomeric Isosorbide Esters as Alternative Renewable Resource Plasticizers for PVC. *J. Appl. Polym. Sci.* **2011**, *119* (4), 2400-2407. DOI: 10.1002/app.32913.

(91) Takeshita, A.; Igarashi-Migitaka, J.; Nishiyama, K.; Takahashi, H.; Takeuchi, Y.; Koibuchi, N. Acetyl Tributyl Citrate, the Most Widely Used Phthalate Substitute Plasticizer, Induces Cytochrome P450 3A through Steroid and Xenobiotic Receptor. *Toxicological Sciences* **2011**, *123* (2), 460-470. DOI: 10.1093/toxsci/kfr178 (acccessed 3/16/2023).

(92) Sheikh, I. A.; Beg, M. A. Structural characterization of potential endocrine disrupting activity of alternate plasticizers di-(2-ethylhexyl) adipate (DEHA), acetyl tributyl citrate (ATBC) and 2,2,4-trimethyl 1,3-pentanediol diisobutyrate (TPIB) with human sex hormone-binding globulin. *Reprod. Toxicol.* **2019**, *83*, 46-53. DOI: 10.1016/j.reprotox.2018.11.003.

(93) de Quadros, J. V.; Giudici, R. Epoxidation of soybean oil at maximum heat removal and single addition of all reactants. *Chem. Eng. Process.* **2016**, *100*, 87-93. DOI: 10.1016/j.cep.2015.11.007.

(94) Terry, D. E.; Wheeler, D. H. Process of preparing epoxy derivatives from unsaturated aliphatic compounds. United States US-2458484, 1949.

(95) Madbouly, S. A.; Zhang, C.; Kessler, M. R. 6.3 Properties of Plant Oil-Based Polyethers. In *Bio-Based Plant Oil Polymers and Composites*, Elsevier, 2016.

(96) Pan, S. Y.; Hou, D. L.; Chang, J. M.; Xu, Z.; Wang, S. H.; Yan, S. X.; Zeng, Q.; Wang, Z. H.; Chen, Y. A potentially general approach to aliphatic ester-derived PVC plasticizers with suppressed migration as sustainable alternatives to DEHP. *Green Chem.* **2019**, *21* (23), 6430-6440. DOI: 10.1039/c9gc03077h.

(97) Dahlke, B.; Hellbardt, S.; Paetow, M.; Zech, W. H. Polyhydroxy fatty-acids and their derivatives from plant oils. *J. Am. Oil Chem. Soc.* **1995**, *72* (3), 349-353. DOI: 10.1007/bf02541095.

(98) Turco, R.; Tesser, R.; Vitiello, R.; Russo, V.; Andini, S.; Di Serio, M. Synthesis of Biolubricant Basestocks from Epoxidized Soybean Oil. *Catalysts* **2017**, *7* (10). DOI: 10.3390/catal7100309.

(99) Lin, B.; Yang, L. T.; Dai, H. H.; Yi, A. H. Kinetic studies on oxirane cleavage of epoxidized soybean oil by methanol and characterization of polyols. *J. Am. Oil Chem. Soc.* **2008**, *85* (2), 113-117. DOI: 10.1007/s11746-007-1187-5.

(100) Guo, Y. Z.; Hardesty, J. H.; Mannari, V. M.; Massingill, J. L. Hydrolysis of epoxidized soybean oil in the presence of phosphoric acid. *J. Am. Oil Chem. Soc.* **2007**, *84* (10), 929-935, Article. DOI: 10.1007/s11746-007-1126-5.

(101) Erhan, S. Z.; Sharma, B. K.; Liu, Z. S.; Adhvaryu, A. Lubricant base stock potential of chemically modified vegetable oils. *J. Agric. Food. Chem.* **2008**, *56* (19), 8919-8925. DOI: 10.1021/jf801463d.

(102) Liu, K. J.; Fu, Y. L.; Xie, L. Y.; Wu, C.; He, W. B.; Peng, S.; Wang, Z.; Bao, W. H.; Cao, Z.; Xu, X. H.; et al. Green and Efficient: Oxidation of Aldehydes to Carboxylic Acids and Acid Anhydrides with Air. *ACS Sustainable Chem. Eng.* **2018**, *6* (4), 4916-4921. DOI: 10.1021/acssuschemeng.7b04400.

(103) Ogunjobi, J. K.; Farmer, T. J.; Clark, J. H.; McElroy, C. R. Synthesis, Characterization, and Physicochemical Performance of Nonionic Surfactants via PEG Modification of Epoxides of Alkyl Oleate Esters. *ACS Sustainable Chem. Eng.* **2023**. DOI: 10.1021/acssuschemeng.2c06298.

(104) Ma, Y. F.; Song, F.; Yu, J.; Wang, N. N.; Jia, P. Y.; Zhou, Y. H. Combining Renewable Eleostearic Acid and Eugenol to Fabricate Sustainable Plasticizer and Its Effect of Plasticizing on PVC. *J. Polym. Environ.* **2021**. DOI: 10.1007/s10924-021-02341-w.

(105) Evans, R.; Day, I. J. Matrix-assisted diffusion-ordered spectroscopy. *RSC Adv.* **2016**, *6* (52), 47010-47022. DOI: 10.1039/c6ra05380g.

(106) Groves, P. Diffusion ordered spectroscopy (DOSY) as applied to polymers. *Polym. Chem.* **2017**, *8* (44), 6700-6708. DOI: 10.1039/c7py01577a.

(107) Socha, A. M.; Kagan, G.; Li, W. B.; Hopson, R.; Sello, J. K.; Williard, P. G. Diffusion Coefficient-Formula Weight Correlation Analysis via Diffusion-Ordered Nuclear Magnetic Resonance Spectroscopy (DOSY NMR) To Examine Acylglycerol Mixtures and Biodiesel Production. *Energy Fuels* **2010**, *24* (8), 4518-4521. DOI: 10.1021/ef100545a.

(108) Wypych, A. *Databook of Plasticizers (2nd Edition)*; ChemTec Publishing, 2017.

(109) Sabbatini, L. *Polymer Surface Characterization*; De Gruyter, 2014.

(110) Wiley, V. C. H. *Ullmann's Polymers and Plastics - Products and Processes*; John Wiley & Sons.

(111) Wypych, G. *PVC Formulary (2nd Edition)*; ChemTec Publishing, 2015.

(112) Pi, H.; Xiong, Y.; Guo, S. Y. The kinetic studies of elimination of HCl during thermal decomposition of PVC in the presence of transition metal oxides. *Polym. Plast. Technol. Eng.* **2005**, *44* (2), 275-288. DOI: 10.1081/pte-200048727.

(113) Bielski, R.; Grynkiewicz, G. Furan platform chemicals beyond fuels and plastics. *Green Chem.* **2021**, *23* (19), 7458-7487, 10.1039/D1GC02402G. DOI: 10.1039/D1GC02402G.

(114) Nguyen, T.; Kim, Y. J.; Park, S. K.; Lee, K. Y.; Park, J. W.; Cho, J. K.; Shin, S. Furan-2,5-and Furan-2,3-dicarboxylate Esters Derived from Marine Biomass as Plasticizers for Poly(vinyl chloride). *Acs Omega* **2020**, *5* (1), 197-206. DOI: 10.1021/acsomega.9b02448.

(115) Zeitsch, K. J. *The Chemistry and Technology of Furfural and its Many By-Products*; Elsevier, 2000.

(116) Lee, B. M.; Jung, J.; Gwon, H. J.; Hwang, T. S. Synthesis and Properties of Isosorbide-Based Eco-friendly Plasticizers for Poly(Vinyl Chloride). *J. Polym. Environ.* **2022**. DOI: 10.1007/s10924-022-02643-7.

(117) Yang, Y.; Huang, J. C.; Zhang, R. Y.; Zhu, J. Designing bio-based plasticizers: Effect of alkyl chain length on plasticization properties of isosorbide diesters in PVC blends. *Mater. Des.* **2017**, *126*, 29-36, Article. DOI: 10.1016/j.matdes.2017.04.005.

(118) Chen, L.; Sheng, C.; Duan, Y.; Zhang, J. Morphology, Microstructure and Properties of PEG-plasticized PVC. *Polym. Plast. Technol. Eng.* **2011**, *50* (4), 412-417. DOI: 10.1080/03602559.2010.543231.

(119) Tan, J. H.; Liu, B. W.; Fu, Q. H.; Wang, L. W.; Xin, J. N.; Zhu, X. B. Role of the Oxethyl Unit in the Structure of Vegetable Oil-Based Plasticizer for PVC: An Efficient Strategy to Enhance Compatibility and Plasticization. *Polymers* **2019**, *11* (5). DOI: 10.3390/polym11050779.

(120) Burns, K.; Potgieter, J. H.; Potgieter-Vermaak, S.; Ingram, I. D. V.; Liauw, C. M. A Comparative Assessment of the Use of Suitable Analytical Techniques to Evaluate Plasticiser Compatibility. *J. Appl. Polym. Sci.* **2023**, *140* (30).

(121) Lindstrom, A.; Hakkarainen, M. Environmentally friendly plasticizers for poly(vinyl chloride) - Improved mechanical properties and compatibility by using branched poly(butylene adipate) as a polymeric plasticizer. *J. Appl. Polym. Sci.* **2006**, *100* (3), 2180-2188. DOI: 10.1002/app.23633.

(122) Li, M. Q.; Tang, Z. H.; Wang, C.; Zhang, Y.; Cui, H. T.; Chen, X. S. Efficient side-chain modification of dextran via base-catalyzed epoxide ring-opening and thiol-ene click chemistry in aqueous media. *Chin. J. Polym. Sci.* **2014**, *32* (8), 969-974. DOI: 10.1007/s10118-014-1489-7.

(123) Isono, T.; Satoh, Y.; Kakuchi, T.; Satoh, T. Phosphazene Base-Catalyzed Living Ring-Opening Polymerization System for Substituted Epoxides. *Kobunshi Ronbunshu* **2015**, *72* (5), 295-305. DOI: 10.1295/koron.2014-0095.

(124) Starnes, W. H. Structural and mechanistic aspects of the thermal degradation of poly(vinyl chloride). *Prog. Polym. Sci.* **2002**, *27* (10), 2133-2170. DOI: 10.1016/s0079-6700(02)00063-1.

(125) Kondyli, E.; Demertzis, P. G.; Kontominas, M. G. Migration Of Dioctylphthalate And Dioctyladipate Plasticizers From Food-Grade Pvc Films Into Ground-Meat Products. *Food Chem.* **1992**, *45* (3), 163-168. DOI: 10.1016/0308-8146(92)90108-e.

(126) Demir, A. P. T.; Ulutan, S. Migration of phthalate and non-phthalate plasticizers out of plasticized PVC films into air. *J. Appl. Polym. Sci.* **2013**, *128* (3), 1948-1961. DOI: 10.1002/app.38291.

(127) Schiller, M. 2.3.3 Methods to Characterize and Test Plasticizers. In *PVC Additives - Performance, Chemistry, Developments, and Sustainability*, Hanser Publishers, 2015.

(128) Fankhauser-Noti, A.; Fiselier, K.; Biedermann, S.; Biedermann, M.; Grob, K.; Armellini, F.; Rieger, K.; Skjevrak, I. Epoxidized soy bean oil (ESBO) migrating from the gaskets of lids into food packed in glass jars. *Eur. Food Res. Technol.* **2005**, *221* (3-4), 416-422. DOI: 10.1007/s00217-005-1194-4.

(129) Biedermann-Brem, S.; Biedermann, M.; Fankhauser-Noti, A.; Grob, K.; Helling, R. Determination of epoxidized soy bean oil (ESBO) in oily foods by GC-FID or GC-MS analysis of the methyl diepoxy linoleate. *Eur. Food Res. Technol.* **2007**, *224* (3), 309-314. DOI: 10.1007/s00217-006-0424-8.

(130) Moser, B. R.; Cermak, S. C.; Doll, K. M.; Kenar, J. A.; Sharma, B. K. A review of fatty epoxide ring opening reactions: Chemistry, recent advances, and applications. *J. Am. Oil Chem. Soc.* **2022**, *99* (10), 801-842. DOI: 10.1002/aocs.12623.

(131) Campanella, A.; Bonnaillie, L. M.; Wool, R. P. Polyurethane Foams from Soyoil-Based Polyols. *J. Appl. Polym. Sci.* **2009**, *112* (4), 2567-2578. DOI: 10.1002/app.29898.

(132) Lozada, Z.; Suppes, G. J.; Tu, Y. C.; Hsieh, F. H. Soy-Based Polyols from Oxirane Ring Opening by Alcoholysis Reaction. *J. Appl. Polym. Sci.* **2009**, *113* (4), 2552-2560. DOI: 10.1002/app.30209.

(133) Guo, X.; Rong, Z.; Ying, X. Calculation of hydrophile–lipophile balance for polyethoxylated surfactants by group contribution method. *J. Colloid Interface Sci.* **2006**, *298* (1), 441-450. DOI: https://doi.org/10.1016/j.jcis.2005.12.009.

(134) Davies, J. Proc. Intern. Congr. Surface Active Substances. *2nd (London)* **1957**, *1*, 426.

(135) Zhang, C. Q.; Madbouly, S. A.; Kessler, M. R. Renewable Polymers Prepared from Vanillin and Its Derivatives. *Macromol. Chem. Phys.* **2015**, *216* (17), 1816-1822. DOI: 10.1002/macp.201500194.

(136) Zhu, H. C.; Yang, J. J.; Wu, M. Y.; Wu, Q. Y.; Liu, J. Y.; Zhang, J. A. Vanillic Acid as a New Skeleton for Formulating a Biobased Plasticizer. *ACS Sustainable Chem. Eng.* **2021**, *9* (45), 15322-15330. DOI: 10.1021/acssuschemeng.1c05885.

(137) Isola, C.; Sieverding, H. L.; Numan-Al-Mobin, A.; Rajappagowda, R.; Boakye, E. A.; Raynie, D. E.; Smirnova, A. L.; Stone, J. J. Vanillin derived from lignin liquefaction: a sustainability evaluation. *International Journal of Life Cycle Assessment* **2018**, *23* (9), 1761-1772. DOI: 10.1007/s11367-017-1401-0.
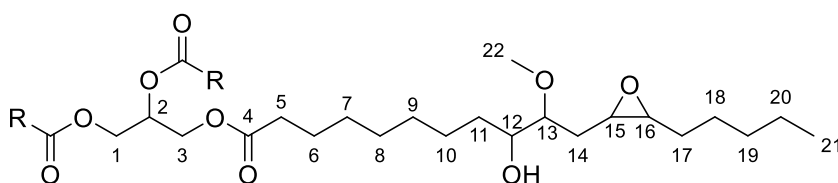
(138) Constable, D. J. C.; Curzons, A. D.; Cunningham, V. L. Metrics to 'green' chemistry - which are the best? *Green Chem.* **2002**, *4* (6), 521-527. DOI: 10.1039/b206169b.

(139) Chiellini, F.; Ferri, M.; Morelli, A.; Dipaola, L.; Latini, G. Perspectives on alternatives to phthalate plasticized poly(vinyl chloride) in medical devices applications. *Prog. Polym. Sci.* **2013**, *38* (7), 1067-1088, Review. DOI: 10.1016/j.progpolymsci.2013.03.001.

(140) Grellmann, W.; Seidler, S. 4.3.2.2 Conventional Tensile Tests. In *Polymer Testing (2nd Edition)*, Hanser Publishers, 2013.

(141) Buddhiranon, S.; Chang, T.; Tang, K. L.; Kyu, T. Stabilization of epoxidized soybean oil-plasticized poly(vinyl chloride) blends via thermal curing with genistein. *J. Appl. Polym. Sci.* **2018**, *135* (31). DOI: 10.1002/app.46472.

(142) Wypych, G. 11.3.5.1 Epoxidized Compounds. In *PVC Degradation and Stabilization (4th Edition)*, ChemTec Publishing, 2020.

(143) Chen, J.; Liu, Z. S.; Li, K.; Huang, J. R.; Nie, X. A.; Zhou, Y. H. Synthesis and application of a natural plasticizer based on cardanol for poly(vinyl chloride). *J. Appl. Polym. Sci.* **2015**, *132* (35). DOI: 10.1002/app.42465.

(144) Nakajima, N.; Isner, J. D.; Harrell, E. R.; Daniels, C. A. Dependence Of Gelation and Fusion Behavior of Polyvinyl-Chloride) Plastisols Upon Particle-Size and Size Distribution. *Polym. J.* **1981**, *13* (10), 955-965. DOI: 10.1295/polymj.13.955.

Appendices

Synthetic Characterisation Data

Methyl Ether ESBO Polyol - MEEP 12

^{1}H NMR (400 MHz, CHLOROFORM-*D*) δ 5.26 (1H, m, H2), 4.29 (2H, dd, *J* = 11.8, 4.2 Hz, H1/3), 4.14 (2H, dd, *J* = 11.9, 5.9 Hz, H1/3), 3.52 – 3.42 (3H, m, H12,13), 3.41 (3H, s, H22), 2.99 (1H, q, J = 5.7 Hz, H15,16) 2.31 (6H, t, *J* = 7.6 Hz, H5), 1.61 - 1.26 (64H, m, H6-11, 14, 17-20), 0.88 (9H, m, H21).

^{13}C NMR (101 MHz, CHLOROFORM-D) δ 173.43, 173.01 (C4), 84.46, 72.74 (C13), 68.98 (C2), 62.21 (C1, C3), 58.25 (C22), 56.75 (C15,16), 50.97, 39.14, 38.83, 38.05, 34.30,

33.63, 33.51, 32.19, 32.05, 32.01, 30.11, 30.02, 29.88, 29.82, 29.60, 29.49, 29.40, 29.24, 29.18, 26.11, 25.90, 25.16, 24.98, 24.93, 22.81, 22.74, 14.25, 14.20 (C21).

FTIR-ATR (v_{max} cm^{-1}) – 3456 (O-H stretch), 2926, 2855 (sp^3 C-H stretch), 1742 cm^{-1} (C=O stretch).

*Figure A 1: ^{1}H NMR spectrum of methyl ether ESBO polyol **12***
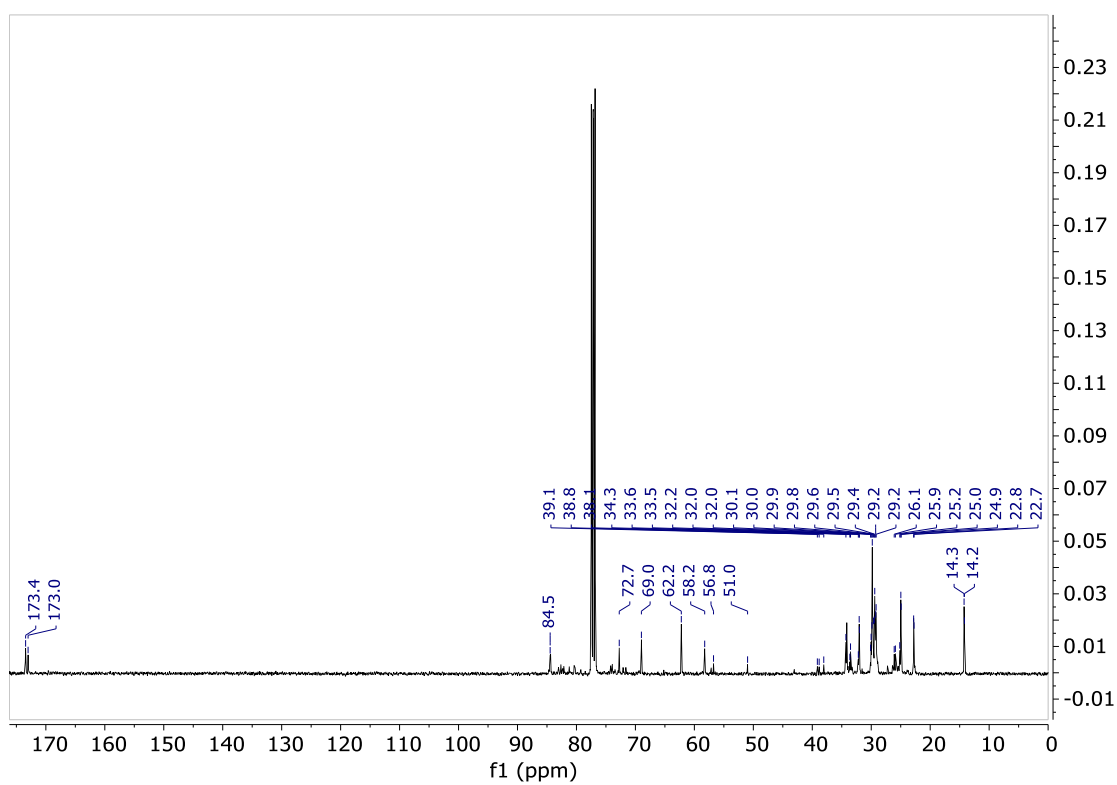
*Figure A 2: ^{13}C NMR spectrum of methyl ether ESBO polyol **12**.*
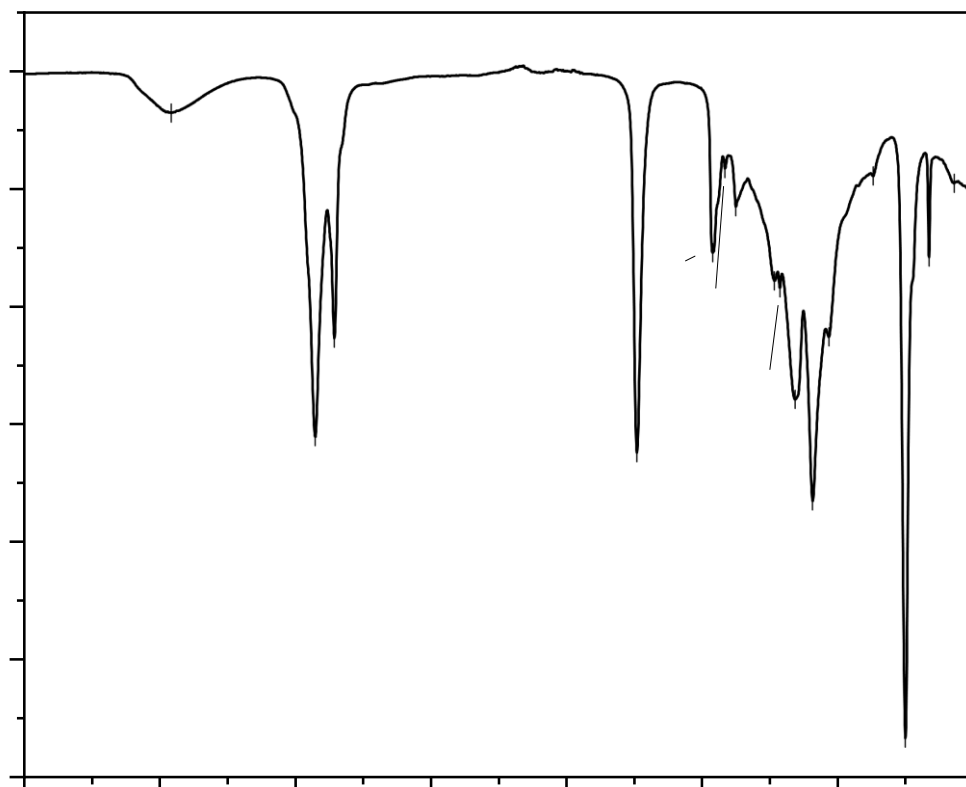
*Figure A 3: FTIR-ATR spectrum of methyl ether ESBO polyol **12**.*

Methoxy polyethylene glycol ESBO ether - mPEG-ESBO, 13
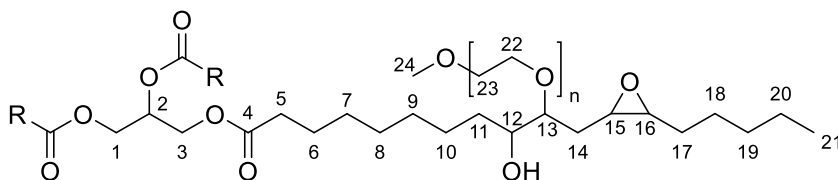
1H NMR (400 MHz, CHLOROFORM-D) δ 5.25 (1H, m, H1), 4.29 (4H, m, H1, H3), 3.65 (34H, s, H22, H23), 3.55 (4H, m, H12, H13), 3.38 (5H, s, H24), 2.31 (6H, t, J = 7.6 Hz, H5), 1.76-1.13 (74 H, m, H6-11, 14, 17-20), 0.88 (9H, m, H21).

^{13}C NMR (101 MHz, CHLOROFORM-D) δ 173.36, 172.95 (C4), 104.95, 104.88, 72.02 (C13), 70.65 (C12), 70.38 (C22, C23), 68.96 (C2), 62.18 (C1, C3), 61.79, 59.13 (C24), 42.94, 42.85, 42.80, 36.10, 34.25, 34.14, 34.08, 32.02, 31.96, 31.91, 31.69, 31.51, 29.79, 29.75, 29.57, 29.46, 29.37, 29.21, 29.16, 29.10, 28.98, 28.17, 28.12, 27.91, 24.95, 24.90, 23.98, 23.89, 23.83, 22.78, 22.67, 22.52, 14.22 (C21).

FTIR-ATR (v_{max} cm^{-1}) – 3476 (O-H stretch), 2925, 2856 (sp^3 C-H stretch), 1742 (C=O stretch).

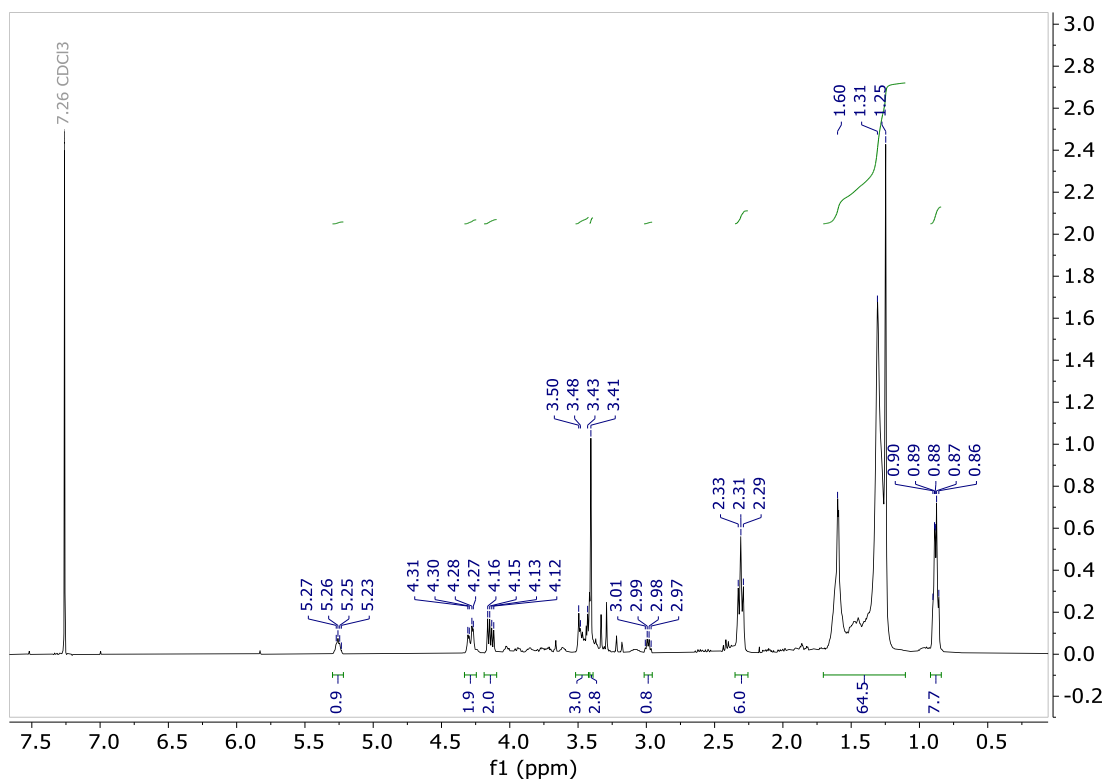*Figure A 4: ^{1}H NMR spectrum of mPEG-ESBO **13.***
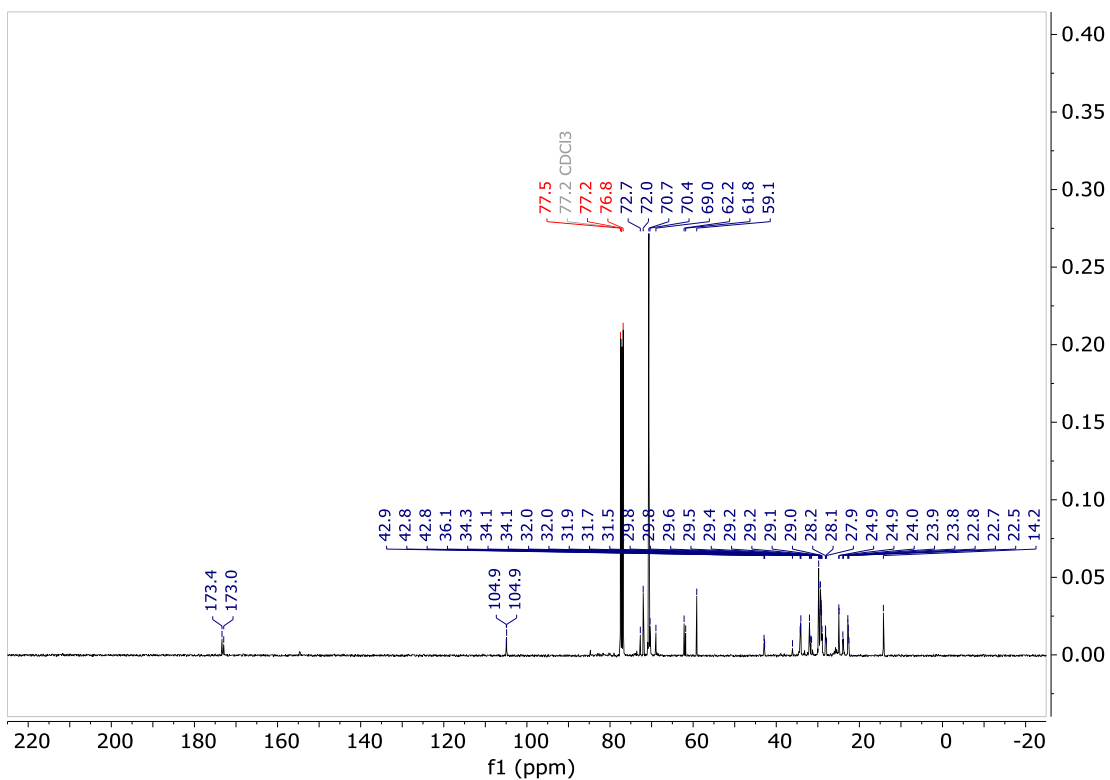
*Figure A 5: ^{13}C NMR spectrum of mPEG-ESBO **13.***
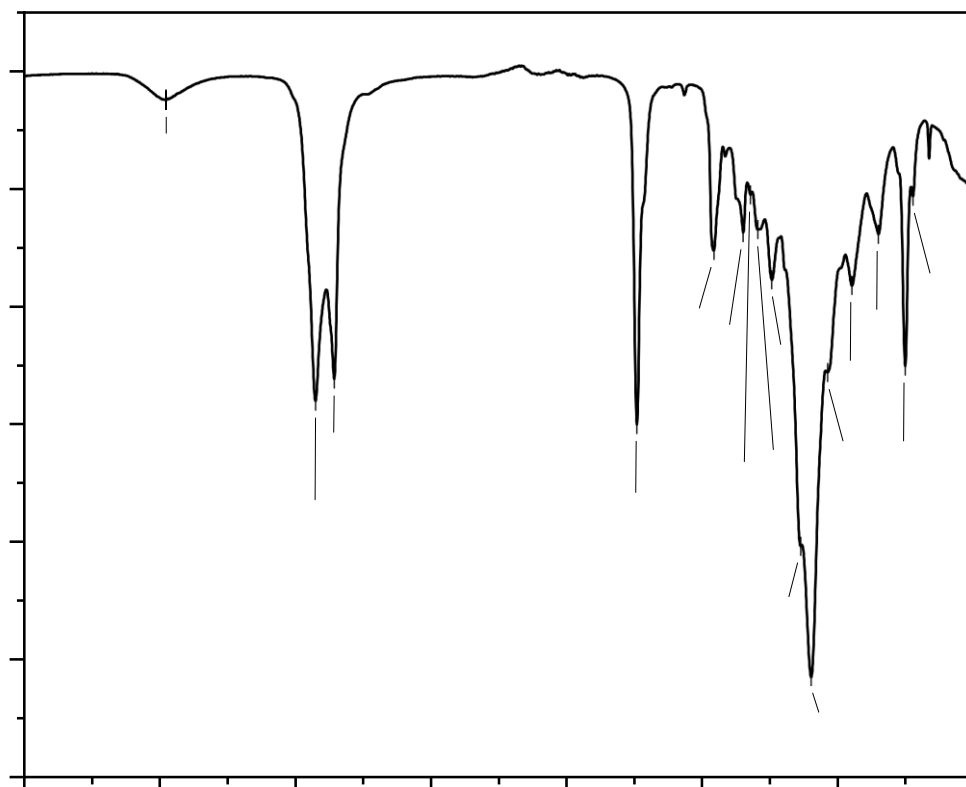
*Figure A 6: FTIR spectrum of mPEG-ESBO **13**.*

Methyl ESBO Furoic Ester - MEFE 14

^{1}H NMR (400 MHz, CHLOROFORM-*D*) δ 7.88 – 7.49 (2H, m, H25, H27), 6.51 (1H, m, H26), 5.25 (1H, m, H2) 4.34 – 4.08 (4H, m, H1, H3), 3.44 (1H, s, C22), 3.41 (2H, s, C22), 2.99 (<1H, m, H15, H16), 2.35 (3H, s), 2.31 (6H, t, J = 7.6 Hz, H5), 2.09 (s, 5H) 1.72 – 1.16 (72H, m, H6-11, H14, H17-20), 0.87 (9H, t, J = 6.9 Hz, H21).

^{13}C NMR (101 MHz, CHLOROFORM-D) δ 173.42, 130.14, 129.44, 129.17, 128.36, 128.15, 126.67, 125.43, 111.93, 68.99, 65.20, 62.21, 34.18, 32.06, 29.84, 29.79, 29.64, 29.50, 29.41, 29.25, 25.82, 24.97, 22.82, 21.59, 14.26, 14.17.

FTIR-ATR (v_{max} cm^{-1}) 3020 (sp^2 C-H stretch), 2927, 2856(sp^3 C-H stretch), 1735 (C=O stretch), 1661 (C=C stretch).

*Figure A 7: ^{1}H NMR spectrum of methyl ESBO furoic ester **14**.*
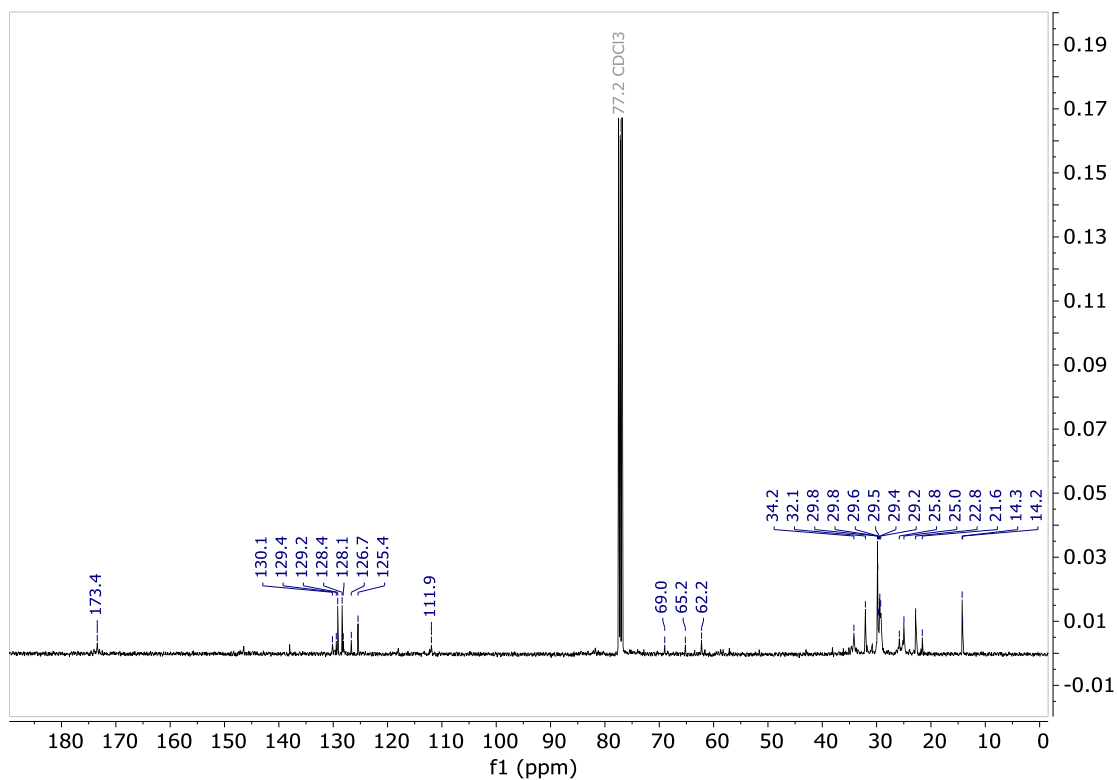
*Figure A 8: ^{13}C NMR spectrum of methyl ESBO furoic ester **14**.*
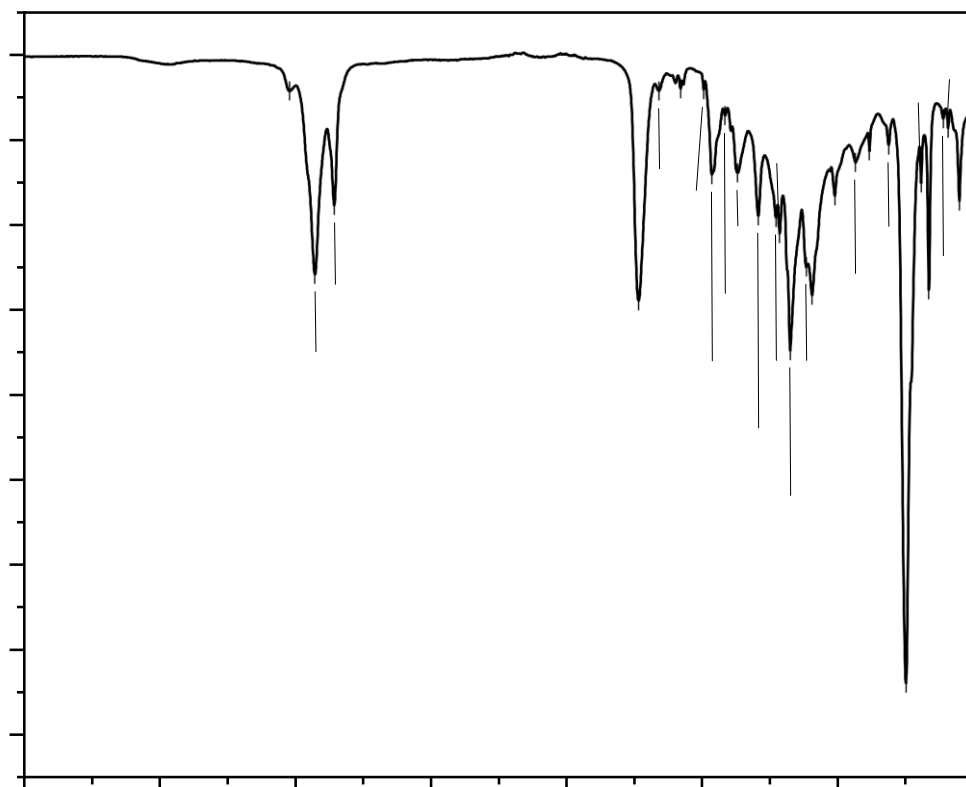
*Figure A 9: FTIR spectrum of methyl ESBO furoic ester **14**.*

Isosorbide Ether ESBO Polyol - IEEP 15

^{1}H NMR (400 MHz, CHLOROFORM-D) δ 5.25 (1H, m, H2), 4.7-4.4 (1H, m), 4.21 (4H, ddd, J = 59.9, 11.7, 5.1 Hz, H1, H3), 4.05 – 3.53 (6H, m, H22-H27), 3.49 – 3.37 (7H, m,), 2.55 (2H, t, J = 7.6 Hz), 2.38 (1H, t, J = 7.4 Hz), 2.31 (6H, t, J = 7.6 Hz, H5), 1.70 – 1.20 (70, m), 0.88 (9H, m, H21).

^{13}C NMR (101 MHz, CHLOROFORM-D) δ 173.46, 104.91, 70.76, 68.98, 62.22, 43.01, 34.29, 34.14, 32.06, 29.84, 29.80, 29.61, 29.51, 29.41, 29.22, 28.18, 26.61, 24.98, 24.02, 22.81, 22.73, 14.28.

FTIR-ATR (v_{max} cm^{-1}) – 3457 (O-H stretch), 2926, 2855 (sp^3 C-H stretch), 1741 (C=O stretch).
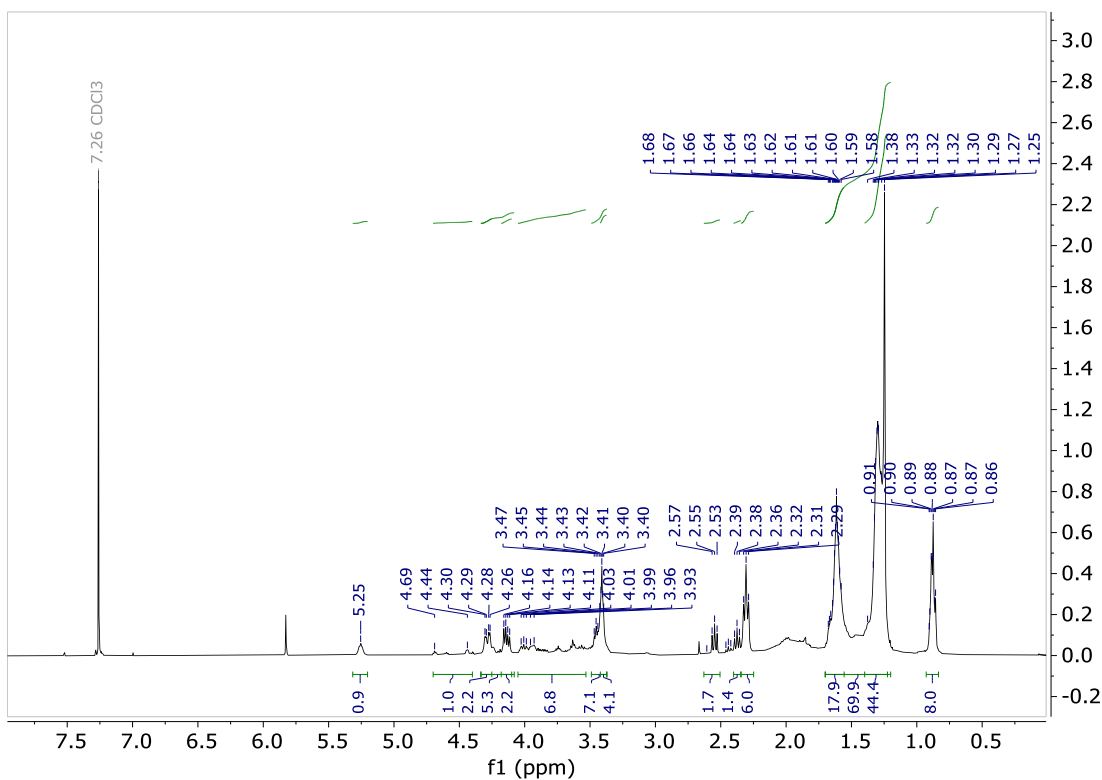
*Figure A 10: ^{1}H NMR spectrum of isosorbide ether ESBO polyol **15**.*
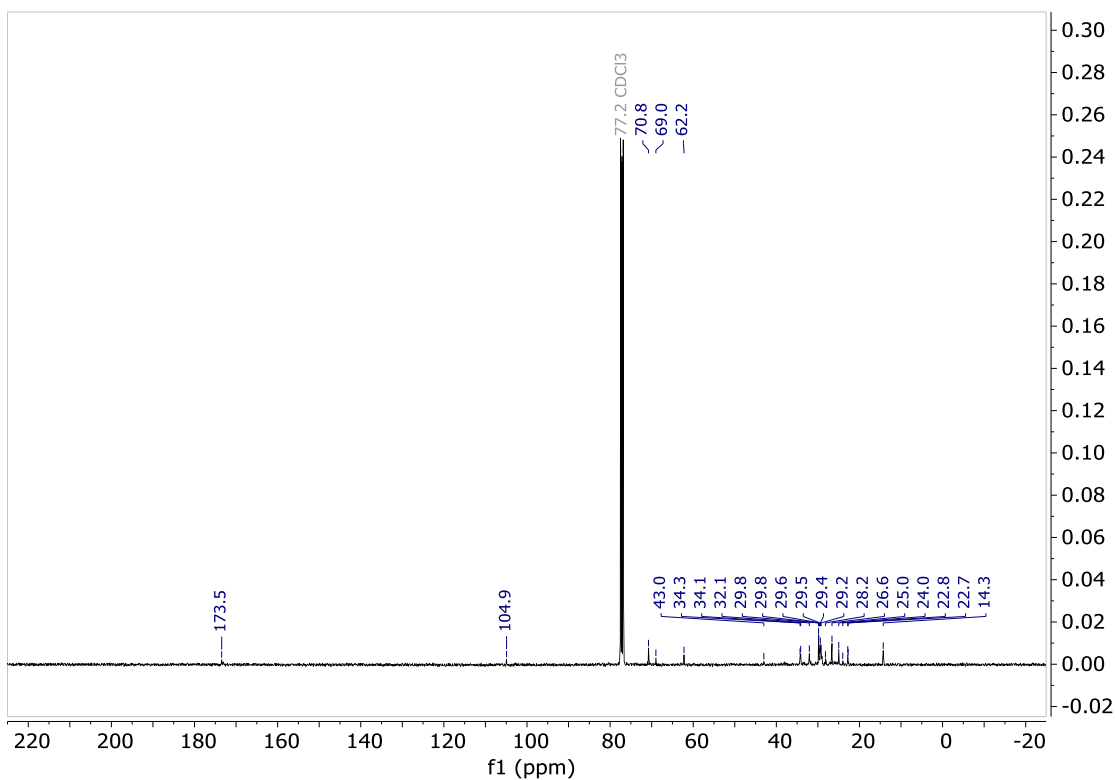
*Figure A 11: ^{13}C NMR spectrum of isosorbide ether ESBO polyol **15**.*
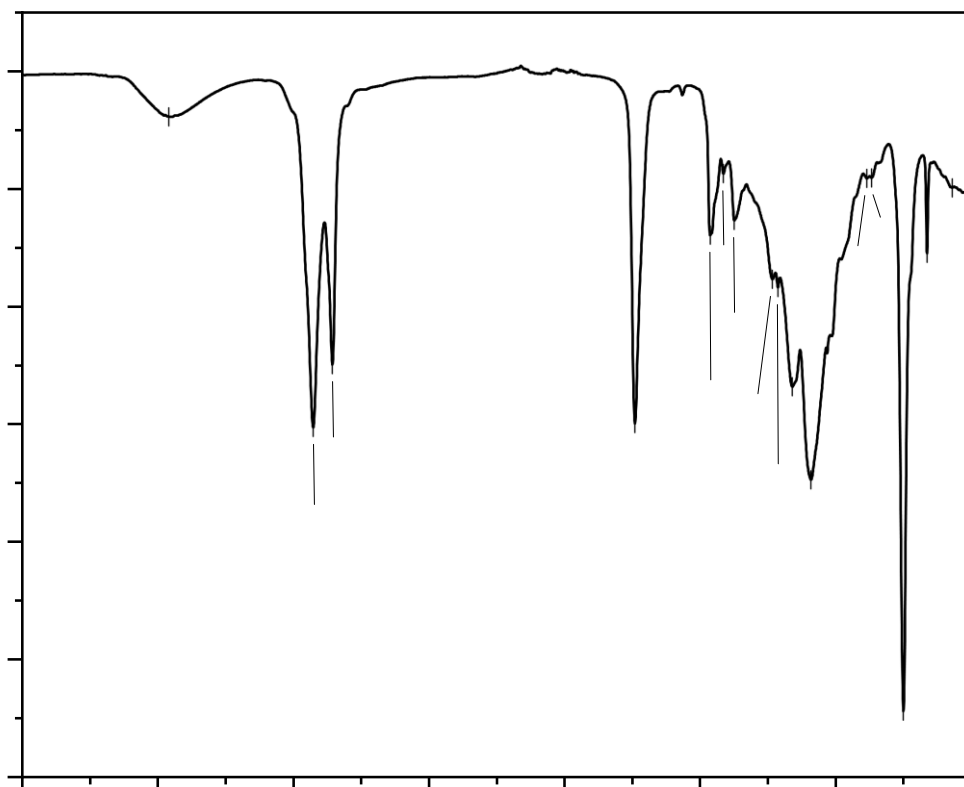
*Figure A 12: FTIR spectrum of isosorbide ether ESBO polyol **15**.*

Hydrophilic-Lipophilic Balance calculations

HLB calculations were carried out according to Davies' method, as follows:

$$HLB = \sum (Hydrophilic\ group\ numbers)$$
$$- n(group\ number\ per\ CH_2\ group) + 7$$

Table A 1: Hydrophilic-Lipophilic balance values for group contribution method.

Group contribution	Group number
Ester	2.4
-O-	1.3
-OH	1.9
C_2H_4O	0.33
CH, CH_2, CH_3, =CH	-0.475

HLB (ESBO)   = 3 x Ester + 5 x -O- + 51 x CH_2 + 7

= (3 x 2.4) + (5 x 1.3) + (51 x -0.475) + 7

= -3.525

HLB (mPEG)   = 1 x -OH + 1 x CH_3 + 8 x C_2H_4O + 7

= 1.9 - 0.475 + (8 x 0.33) + 7

= 11.065

HLB (mPEG-ESBO)   = 3 x Ester + 2 x -OH + 3 x -O- + 53 x CH_2 + 16 x C_2H_4O + 7

= (3 x 2.4) + (2 x 1.9) + (3 x 1.3) + (53 x -0.475) + (16 x 0.33) + 7

= 2.005

Synthesis mass efficiency calculations

$$Atom\ economy\ = \frac{Molar\ mass\ of\ product}{Molar\ mass\ of\ reactants}\ \%$$

$$Reaction\ mass\ efficiency\ = \frac{Mass\ of\ product}{Total\ mass\ of\ reactants}\ \%$$

MEEP (assuming 2 addition reactions per molecule ESBO)

Reactant	Reactant MW	Reactant Mass	Product MW	Product mass
ESBO	933.36	53.67	997.44	53.02
Methanol	32.04	71.28		

ESBO +2 MeOH -> MEEP

AE = 997.44/(933.36+ 2x 32.04) = 100%

RME = 53.02/(53.67+71.28) = 42.43%

mPEG-ESBO

ESBO mass	mPEG mass	mPEG-ESBO mass	RME
15.08	52.15	15.32	22.79

MEFE

Assuming MEEP contains two methyl ether polyols from reaction of epoxide with methanol, and both alcohol groups react with furoic acid to produce MEFE and 2 H_2O:

MEEP MW	Furoic acid MW	MEFE MW	AE
997.44	112.08	1185.56	97.05

MEEP mass	Furoic acid mass	MEFE mass	RME
10.00	6.28	11.21	68.86

IEEP

ESBO mass	Isosorbide mass	IEEP mass	RME
15.01	33.83	19.33	39.58

A Comparative Assessment Of The Use Of Suitable Analytical Techniques to Evaluate Plasticiser Compatibility

A comparative assessment of the use of suitable analytical techniques to evaluate plasticizer compatibility

Katharine Burns[1] | Johannes H. Potgieter[1,2] | Sanja Potgieter-Vermaak[1] |
Ian D. V. Ingram[1] | Christopher M. Liauw[3]

[1]Department of Natural Sciences, Manchester Metropolitan University, Manchester, UK

[2]School of Chemical and Metallurgical Engineering, University of the Witwatersrand, Johannesburg, South Africa

[3]Department of Life Sciences, Manchester Metropolitan University, Manchester, UK

Correspondence
Katharine Burns, Department of Natural Sciences, Manchester Metropolitan University, Manchester, UK.
Email: katharine.burns@stu.mmu.ac.uk

Abstract

The evaluation of novel phthalate-free plasticisers for PVC formulations is hindered by the lack of a reliable quantitative method for testing plasticizer exudation from PVC formulations. Two methods of improving upon the ASTM D3291 exudation test have been trialed using ATR-FTIR and GC–MS. The results of these methods are compared alongside a study of the glass transition temperatures (T_g) by dynamic mechanical analysis (DMA). FTIR is found to be unsuitable for determining plasticizer exudation as the method is not sufficiently sensitive to detect small changes in plasticizer distribution. Carbonyl peak positions in unstressed samples are instead investigated to determine the strength of interaction between the plasticizers and PVC chain. GC–MS is successfully used to quantify plasticizer exudation that could not be observed visually or by FTIR. Furthermore, these methods show limited correlation to each other, which highlights the importance of testing multiple aspects of compatibility when developing novel plasticizers for use in PVC.

KEYWORDS

compatibility, exudation, phthalates, plasticisers, polymers, polyvinyl chloride

1 | INTRODUCTION

PVC is one of the most commonly used polymers, with applications in areas such as construction, food packaging, electrical insulation, clothing and toys.[1] Plasticisers are added to the polymer to soften the material and modify the properties to allow for the wide range of applications in which it is used. The plasticisers most commonly used in PVC are external plasticisers – that is, the plasticizer is not chemically bonded to the polymer.[2] These plasticisers typically have low volatility and low to medium molecular weights. Historically, PVC plasticisation has been dominated by phthalate esters, which were one of the earliest plasticizer types used in PVC.[2] Dioctyl phthalate (DOP or DEHP, Figure 1-**1**) was the most widely used plasticizer in PVC formulations until recent years. As of 2015, it represented only 13% of the EU plasticizer market.[3] This is largely due to safety concerns – studies have suggested that DOP may have carcinogenic and endocrine-disrupting properties.[4,5] The addition of DOP and other phthalates to the REACH (Registration, Evaluation, Authorisation and Restriction of Chemicals) SVHC (Substances of Very High Concern) list,[6] and other legislation such as the Safe Drinking Water and Toxic Enforcement Act of 1986 (also known as Proposition 65) in California, has limited the use of these plasticisers in

Appendices
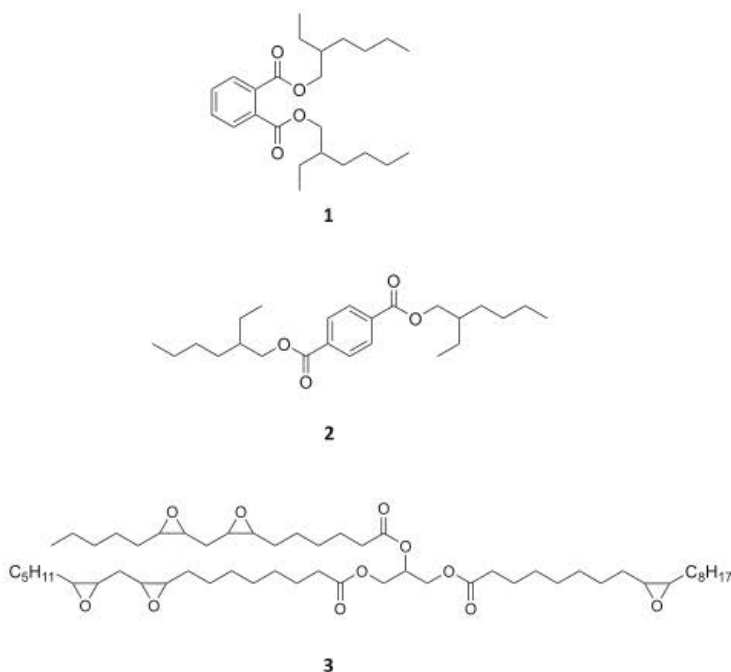
FIGURE 1 Chemical structures of three plasticisers used in PVC formulations – diethylhexyl phthalate (DEHP or DOP, 1), diethylhexyl terephthalate (DOTP, 2) and a representative component of epoxidised soybean oil (ESBO, 3).
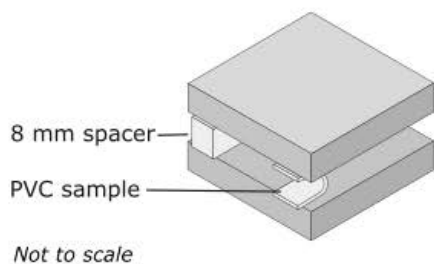
FIGURE 2 Diagram of the ASTM D3291 loop spew test for plasticizer compatibility in PVC.[10]

FIGURE 3 Diagram of compressed PVC sample showing the stressed portion and the target area for FTIR measurement. [Color figure can be viewed at wileyonlinelibrary.com]

PVC compounding.[2] This has created a gap in the market, leading to the development of many alternative plasticisers, such as terephthalates, citrates, adipates and sebacates.[1,2] One widely used terephthalate is the para isomer of DOP, dioctyl terephthalate (DOTP, Figure 1-2).[1,7] Although the two plasticisers are similar in structure, it has been shown that DOTP does not pose the same health risks as DOP due to the difference in metabolites formed by the two compounds in the body.[1,5]

However, both phthalates and terephthalates are largely synthesized from petrochemicals. As environmental pressure increases, the demand for renewable, bio-based plasticisers has grown.[2] Plasticisers can comprise more than 50% of the total weight of a flexible PVC formulation. As such, replacing petrochemical plasticisers with bio-based alternatives can significantly reduce the environmental footprint of the finished product, despite the typically petrochemical-based PVC polymer.

Plant-based oils derived from sunflower oil, castor oil, linseed oil and soybean oil have been used as PVC plasticisers, following an epoxidation reaction.[2] This increases the polarity of the fatty acid chains in the oils and gives rise to a stronger interaction with the PVC chain.[8] Epoxidised oil plasticisers such as ESBO (epoxidised soybean oil, Figure 1-3) are typically used as a secondary plasticizer in combination with a primary plasticizer, as compatibility is thought to be lower.[2] The epoxide functionality provides

165

an additional benefit to the PVC compound, as it acts as an acid scavenger and so improves the thermal stability of the material.[9]

Despite the many developments in alternative plasticisers for PVC, the methods for evaluating these plasticisers have not shown similar progress, particularly regarding plasticizer compatibility. ASTM D3291 "loop spew" test is one method for testing plasticizer compatibility in PVC compounds.[10] This method involves stressing a sample of PVC compound in a loop, as shown in Figure 2. Plasticizer exudation is then judged visually on a scale from 0 (no exudation) to 3 (heavy exudation). This method is based on a subjective judgment which may be unreliable. A more quantitative analytical method would allow PVC compounders to compare and record useful information about the compatibility of different plasticisers. The techniques typically available to laboratories in the PVC compounding industry must be considered – fourier transform infrared (FTIR) and gas chromatography - mass spectrometry (GC–MS) are commonplace, while techniques such as NMR (nuclear magnetic resonance) or UV–Vis spectroscopy are not.

Plasticizer exudation can lead to a number of undesirable properties in a PVC formulation. At low levels it can cause a tacky surface finish and poor clarity, while at higher levels it can lead to environmental contamination of air, water or food p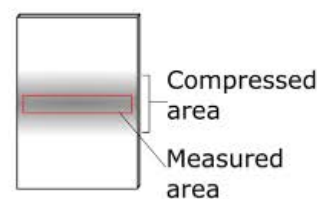roducts as well as a degradation in the properties of the PVC article.[11,12] As such, minimizing plasticizer exudation is of high concern for PVC formulators.

FTIR (Fourier Transform Infrared) spectroscopy has been used in a number of works to examine the strength of the interaction between plasticisers and PVC.[13–17] The most common plasticizer types (phthalates, adipates etc.) all contain carbonyl functional groups. These polar groups are attracted by dipole forces to the polar carbon-chlorine bond in PVC and can also hydrogen bond to the α-hydrogen.[15] These attractive forces hold the polymer and plasticizer molecules together within the PVC compound. This interaction slightly weakens the carbon–oxygen double bond in the plasticizer, and the stronger the attractive force between the molecules, the more this bond is weakened. This weakening of the carbonyl bond can be observed by FTIR spectroscopy as a shifting of the C=O stretching band to a lower wavenumber. Some works have used the magnitude of this weakening as a definition of plasticizer compatibility.[16] However, the strength of the interaction between the plasticizer and PVC is not the only determining factor in plasticizer exudation. The size and shape of the plasticizer molecule, and therefore the ability of the plasticizer to move freely through the polymer matrix, will also affect exudation.

The vast majority of studies on plasticizer loss from PVC are concerned with evaporative loss at elevated temperatures, or loss to a liquid extractant medium.[18–21] Plasticizer loss resulting from mechanical stress (such as in the ASTM D3291 method) is less frequently studied, even though there are numerous applications for plasticised PVC where mechanical stress is far more likely to occur than solvent contact or raised temperatures, for example window gaskets. While the use of GC–MS for plasticizer analysis is well known, for example in measuring plasticizer extracted into solvents or food simulants,[6] it has not yet been explored as a way to add quantification to the loop-spew test for exudation. Investigations into plasticizer compatibility also tend towards studying single-plasticizer systems.

Plasticizer compatibility is also frequently measured by the suppression of the glass transition temperature of the polymer, usually measured by differential scanning calorimetry (DSC) or dynamic mechanical analysis (DMA).[22,23] Effective plasticisation lowers the glass transition temperature of a polymer to below the operating range of the product, allowing for flexible rubbery behavior. Incompatibility between the plasticizer and polymer can cause phase separation within the material, which can be observed by the presence of broad or multiple glass transition temperatures within a sample.[24]

Despite the many works to develop an understanding of PVC technology and evaluate plasticisers in PVC compounds, there is still no generally accepted method to quantitatively determine the amount of exudation by a plasticizer from a PVC matrix, especially not in so far as it concerns the newer, more sustainable plasticisers derived from biobased resources. Neither is there significant work correlating plasticizer exudation to other methods of testing plasticizer compatibility in PVC such as the suppression of glass transition temperature. This investigation therefore aims to find alternative, objective, and qualitative and quantitative instrumental analytical methods to determine the presence and level of exudation of plasticisers from PVC, as well as comparing it with the ASTM D3291 standard method.

2 | MATERIALS

All materials used to produce the PVC samples were provided by Alphagary Ltd. Chemicals used were ethanol (absolute, VWR), 1-Ethyl Naphthalene ($\geq$97%, Aldrich), sodium citrate (99%, Aldrich), dimethyl pimelate (99%, Aldrich), sodium ethoxide (21% in ethanol, Alfa Aesar), Methyl tert-butyl ether (MTBE, 99.8%, Sigma Aldrich), n-hexane (>97%, Honeywell), magnesium sulfate (Laboratory reagent grade, Fisher Scientific).

TABLE 1 PVC formulations based on single and mixed plasticizer systems in PHR (per hundred resin) and percentage (%).

Formulation	1 PVC-DOTP	2 PVC-DOP	3 PVC-ESBO	4 PVC-DOTPESBO	5 PVC-DOPESBO
PVC K70 resin [PHR] [percentage]	100 58.6%	100 58.6%	100 58.6%	100 58.6%	100 58.6%
Ca/Zn heat stabilizer	0.6 0.4%	0.6 0.4%	0.6 0.4%	0.6 0.4%	0.6 0.4%
DOTP	70 41.0%	-	-	35 20.5%	-
DOP	-	70 41.0%	-	-	35 20.5%
ESBO	-	-	70 41.0%	35 20.5%	35 20.5%

3 | EXPERIMENTAL

3.1 | Sample preparation

Samples of plasticised PVC were prepared by cold mixing of plasticisers, PVC resin and heat stabilizer additives, followed by compounding with a Farrel two-roll mill at 155°C for 5 min. The formulations tested are shown in Table 1. Per hundred resin (PHR) is a commonly used convention for PVC compounding, where components are listed relative to 100 grams of PVC resin.

The samples were compression molded in a Mackey-Bowley heated hydraulic press at 170°C and 200 bar pressure for 4 min to produce plaques of 2 mm thickness. The 2 mm thickness pressed plaque was cut into samples with dimensions 25 × 30 mm.

3.2 | Compression loop test

Samples were prepared and stressed in the loop spew test as described in ASTM D3291 (Figure 2). The sample pieces were inserted between metal plates separated by spacers 8 mm thick. The test pieces were compressed over a range of time periods, then removed and tested for plasticizer exudation. Individual sample pieces were prepared for each measurement and discarded after testing. Exudation was measured using visual examination of a test paper as in the ASTM method, by FTIR spectroscopy and by GC–MS analysis.

3.3 | Fourier transform infrared spectroscopy (FT-IR)

FTIR spectra were measured on a Nicolet iS5 with iD5 ATR attachment. FTIR was used to measure the surfaces of the samples stressed by the compatibility test in the area where plasticizer would exude, that is, the compressed face of the looped sample, Figure 3. The sample was removed from the compression plates, the centre of the stressed area was placed on the ATR crystal and clamped in place to ensure good contact with the crystal. Five samples of each formulation were measured for each time point. 16 scans were collected for each spectrum, the spectral resolution was set to 4 cm^{-1} and the data spacing was 0.482 cm^{-1}. FTIR spectra were also collected for the individual plasticisers, as well as representative mixtures of the plasticisers (1:1 DOTP-ESBO and 1:1 DOP-ESBO), corresponding to the mixed plasticizer formulations.

3.4 | Gas chromatography—mass spectroscopy (GC–MS)

GC–MS analysis was used to quantify plasticizer exudation following the loop spew test. The inner surface of each sample, where the exudation occurs, was wiped with an analytical cotton swab in a set pattern covering the surface of the sample. The swabbing procedure ensured that every part of the compressed area was swabbed twice in each of two perpendicular directions. The swab was then immersed in 3 mL ethanol and mechanically agitated for 20 s to dissolve any substances transferred from the sample to the swab. This solution was analyzed directly to quantify DOTP and DOP, as well as transesterified to quantify ESBO.[25] The ethanol contained 5 ppm 1-ethyl naphthalene (1-EN) and 5 ppm dimethyl pimelate (DMPi) as internal standards. Three samples were tested for each time interval and were discarded after swabbing.

To analyze ESBO, the exudate solutions were derivatised using 21% sodium ethoxide/ethanol solution to

convert the triglyceride to ethyl esters. This allows for analysis of ESBO by GC–MS under standard conditions due to the increased volatility of the resulting ethyl esters compared with ESBO. The internal standard DMPi also undergoes transesterification in these conditions, and this is used to monitor the reaction. Sodium ethoxide solution can absorb moisture during storage which can lead to saponification of the esters. The concentration of diethyl pimelate (DEPi) produced from DMPi was monitored to identify any issues with the sodium ethoxide reagent.

1 mL of the ethanol solutions was added to 0.325 mL of sodium ethoxide/ethanol solution, shaken and allowed to react for 5 min. 2 mL MTBE/hexane (60/40%) and 2 mL disodium citrate solution was added. The organic phase was then separated and dried over excess magnesium sulfate and filtered using pipette filters (Fisherbrand, PTFE 0.2 μm) into vials for GC–MS analysis.

GC–MS analysis was carried out on an Agilent 7890B/5977B. 1 μL injection volume, inlet 300°C, split-less, 1 mL/min column flow helium. The column was an Agilent HP-5MS UI, length 30 m, ID 0.25 mm. 60–100°C at 7°C/min, then 15°C/min to 300°C, hold 5 min.

Samples of known concentration were prepared and used as calibration standards. A total of 6 concentration levels were prepared, and 3 repeats were tested. A quadratic fit was used, giving an R^2 value of 0.995 for DOTP and 0.996 for DOP. Method blank samples were prepared by immersing clean swabs in 3 mL ethanol containing the internal standard and were tested alongside the samples and standards. This confirmed that the swabs did

not release any substances that would interfere with the results.

These standards were also derivatised as described to quantify ESBO. This gave rise to a number of peaks due to the mixed composition of the ESBO triglycerides. The peak corresponding to ethyl 9-epoxystearate (Et 9-ES) was chosen for quantification, giving an R^2 of 0.994 with a quadratic fit. This peak was chosen from four potential ESBO derivative peaks as it had sufficient intensity and no overlapping peaks – see Data S1.

3.5 | Dynamic mechanical analysis

DMA was used to investigate the low temperature properties of the samples. Samples were tested on a Perkin Elmer DMA8000 from −130 to 70°C at a rate of 5°C/min in tensile mode. The samples were exposed to an oscillating strain of 0.5 mm at a frequency of 1 Hz.

4 | RESULTS AND DISCUSSION

4.1 | Visual exudation evaluation

Samples were tested in the compatibility loop for 60 min, then removed and wiped with a dry test paper. The paper was examined for exudation visually in accordance with the ASTM D3291 standard. All samples showed no visible exudation, and so would be given a grading of 0 by the ASTM D3291 scale under these conditions.

4.2 | FT-IR spectroscopy

The FTIR carbonyl stretch peak position (1700–1800 cm^{-1}), can be used for qualitative identification of the different plasticisers used in this study (Figure 4). It is expected that interaction of the plasticizer with the PVC matrix will lead to a change in peak position depending on the change in bond properties, as shown in other works.[13–17] To that end, the peak positions for single plasticisers, plasticizer mixtures, the PVC compound samples prior to the loop compression test, and PVC samples after compression, were measured.

The carbonyl peak in the plasticizer shifts to a lower wavenumber, albeit small differences (1–4 wavenumbers) when in the PVC compound (Table 2). This could be ascribed to interactions with the C-Cl bonds in the polymer which weaken the carbonyl bond.[26]

The carbonyl peaks of the individual plasticisers in the plasticizer mixtures (either as free liquids (1:1 DOTP-ESBO and 1:1 DOP-ESBO) or in the PVC compound)
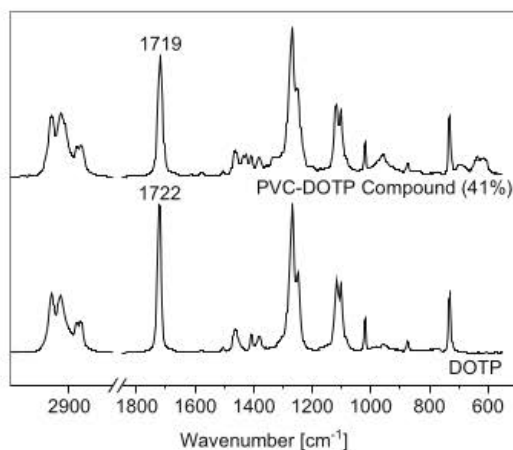

FIGURE 4 FTIR spectra of DOTP and a DOTP-plasticised PVC sample (Formulation 1), with the carbonyl symmetric stretching band indicated.

TABLE 2 Carbonyl peak positions of each plasticizer individually and in the mixtures (DOTP-ESBO) and (DOP-ESBO) investigated, with the difference from the single plasticizer in brackets.

Plasticizer	DOTP carbonyl position (cm^{-1})	DOP carbonyl position (cm^{-1})	ESBO carbonyl position
Single plasticizer	1722.5	1728.5	1742.4
DOTP-ESBO mixture	1720.7 (−1.8)	-	1744.3 (+1.9)
DOP-ESBO mixture	-	1724.8 (−3.7)	1739.8 (−2.6)

TABLE 3 Carbonyl peak positions in PVC formulations, and shift in carbonyl peak position between the free plasticizer (or plasticizer mixtures for Formulations 4 and 5) and the plasticised PVC samples before compression testing.

Sample	Carbonyl peak position (cm^{-1})	Carbonyl shift relative to free plasticizer (cm^{-1})
Formulation 1—DOTP	1719.2	−3.4
Formulation 2—DOP	1724.6	−4.0
Formulation 3—ESBO	1739.9	−2.5
Formulation 4—DOTP	1719.2	−1.6
Formulation 4—ESBO	1742.0	−2.2
Formulation 5—DOP	1723.0	−1.8
Formulation 5—ESBO	1739.2	−0.6

overlapped and therefore deconvolution was used to identify peak positions. The WIRE® software package of the Renishaw Invia Raman spectrometer was used to perform the deconvolution. The optimum deconvolution was achieved by manually providing boundaries for peak positions and a maximum of 3000 iterations, with a tolerance value of 0.001. The model provided a best fit using a mixture of Gaussian and Lorentzian peak shapes.

The peaks found by this method for the plasticizer mixtures were shifted relative to the single plasticisers, as shown in Table 2. These data suggest an interaction between the plasticisers in the mixtures leading to a change in the carbonyl bond energy following mixing. In DOTP and DOP individually, the carbonyl groups will interact most strongly with other carbonyl groups due to the electronegativity of the carbonyl oxygen. However, these groups are relatively sterically hindered by their position next to the aromatic ring, particularly so for DOP where the carbonyl groups are in the ortho position. ESBO contains epoxide groups in addition to ester groups, and these are located on long alkyl chains which are more mobile and may be more able to interact with the para- and ortho-phthalate ester groups. This explanation could explain the corresponding increase in the ESBO carbonyl position in the DOTP-ESBO mixture, if this interaction reduces the number of epoxide groups interacting with ESBO carbonyl groups. However, it

would not explain the negative shift of the ESBO carbonyl bond in the mixture with DOP.

The carbonyl peaks in all formulations tested showed a shift between the free plasticizer(s) and the plasticised PVC samples (Table 3). However, following 60 min compression, the carbonyl peak positions had not changed significantly relative to the resolution of the FTIR instrument. A change in peak position was predicted based on exuded plasticizer dominating the spectra. As the magnitude of the initial shift in carbonyl is already close to the resolution of the FTIR instrument, low levels of exudation such that the FTIR measurement is of a mixture of free and bound plasticizer is likely to be below the detection limit of the method.

The carbonyl shift in the PVC compound corresponds to the strength of the interaction between the PVC and the carbonyl group of the plasticizer.[13] By this measure, in the single plasticizer formulations DOP would be considered the most compatible (strongest interaction) and ESBO the least compatible (weakest interaction).

In Formulation 4 (PVC-DOTPESBO) the carbonyl shift at t = 0 was substantially smaller for DOTP (−1.6 cm^{-1}) compared to Formulation 1 (PVC-DOTP, −3.4 cm^{-1}), while the ESBO carbonyl shift was similar to that of Formulation 3 (PVC-ESBO). This would suggest that the compatibility of DOTP is reduced when mixed with ESBO. In Formulation 5 (PVC-DOPESBO) both DOP and ESBO t = 0 carbonyl shifts are significantly lower compared to each plasticizer alone. ESBO in particular changed by only 0.6 cm^{-1}. However, comparing the absolute carbonyl peak position gives a different picture. In Formulation 4 the DOTP peak has the same wavenumber as in Formulation 1 (1719.2 cm^{-1}) while the ESBO peak shows negligible shift relative to free ESBO (1742.0 and 1742.4 cm^{-1}). DOP is shifted to lower wavenumber in Formulation 5 compared with Formulation 2, while the ESBO peak position is similar to that of ESBO in Formulation 3.

The formulations chosen for this analysis were designed to simplify any analysis, containing only the PVC polymer, plasticisers, and a heat stabilizer. However, in typical PVC formulations, the use of FTIR analysis may be further complicated by the presence of the other components in the material. For example, Linde analyzed

TABLE 4 Exuded plasticizer at t = 60 min measured by GC–MS quantification alongside the plasticizer composition of the tested PVC formulations.

	Plasticizer composition in formulation (%)			Exudation (µg)		
	DOTP	DOP	ESBO	DOTP	DOP	ESBO
Formulation 1—PVC-DOTP	41.2%			83.9	-	-
Formulation 2—PVC-DOP		41.2%		-	7.6	-
Formulation 3—PVC-ESBO			41.2%	-	-	9.8
Formulation 4—PVC-DOTPESBO	20.6%		20.6%	14.5	-	8.0
Formulation 5—PVC-DOPESBO		20.6%	20.6%	-	5.3	3.4

samples containing high levels of carbon black, which made IR analysis impossible due to the strong absorption.[27] Carbon black is relatively common in PVC formulations and so this would limit the method. A number of other common additives in PVC formulations contain carbonyl groups such as acrylic processing aids and copolymers such as vinyl acetate.[28] Calcium carbonate, which is widely used as a filler material in PVC formulation, shows a strong, broad feature in FTIR analysis centred at 1360 cm^{-1} due to the asymmetric stretch in the CO_3^{2-} anion.[29] Calcium carbonate was not used in the formulations tested in this work, however due to the prevalence within PVC formulations it should be considered in future work.

A further limitation of the ATR-FTIR method is that it requires good contact between the sample and the ATR crystal to obtain high quality data. The ATR attachment clamps the sample to the ATR crystal, ensuring close contact. This could be affecting the FTIR results, since the pressure applied by the ATR clamp could force the liquid plasticizer on the sample surface to flow away from the point of contact of the crystal. This would limit the amount of plasticizer that could accumulate between the solid PVC sample and the crystal, and so could potentially affect the accuracy of the results. Additionally, compatibility as measured by initial carbonyl shift may not directly correlate to the overall strength of the plasticizer-polymer solvation, as other parts of the plasticizer molecule may also interact with the polymer.

4.3 | GC–MS analysis

The compounds present in the swab extracts and derivatised samples were quantified using the Agilent MassHunter software. Each plasticizer was quantified by the ion with the highest response, and qualifier ions were chosen to validate the results. The intensity of the qualifier is compared to the quantifier to confirm that the correct target molecule is being measured. For DOTP, the
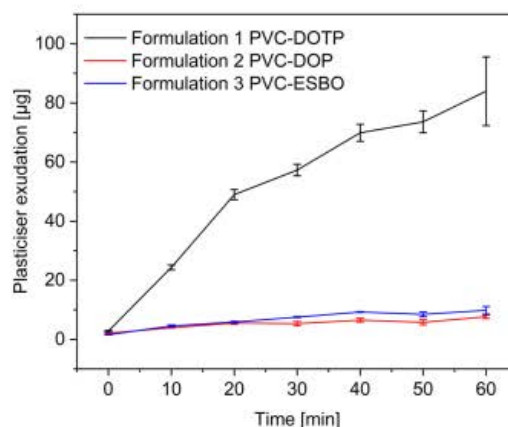

FIGURE 5 Plasticizer exudation by GC–MS for PVC samples containing DOTP, DOP and ESBO, following compression in the 'loop spew test'. [Color figure can be viewed at wileyonlinelibrary.com]

quantifier ion had an m/z value 167, qualifier 261, and for DOP the quantifier ion had an m/z value 149, qualifier 167. For the representative peak for ESBO, Et9-ES, m/z 155 was chosen as quantifier and 69.1 as qualifier.

Table 4 shows the measured exuded plasticizer for each sample alongside the composition of the samples. As seen in Figure 5, DOTP (Formulation 1) gives the highest level of exudation of the single plasticizer samples – ten times more than DOP (Formulation 2) or ESBO (Formulation 3). The exudation appears to follow a non-linear pattern of a steep early gradient followed by a more gradual increase.

Figure 6 shows the exudation of plasticisers in the mixed plasticizer formulations, alongside the relevant single plasticizer formulation. The DOTP exuded from Formulation 4 was 17% of that exuded from Formulation 1, despite the concentration of DOTP in Formulation 4 being 50% of that in Formulation 1. This reduction in exudation contrasts with FTIR analysis, which suggested
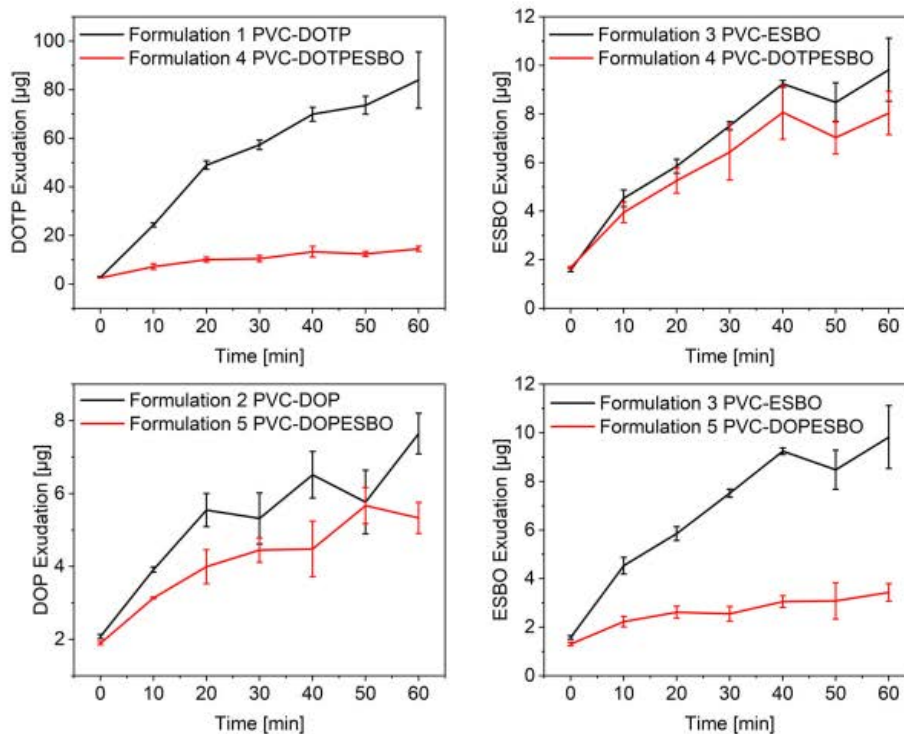
FIGURE 6 Plasticizer exudation from the mixed plasticizer formulations (shown in red) alongside the exudation of the component plasticisers from the single plasticizer formulations (black) following compression in the 'loop spew test'. [Color figure can be viewed at wileyonlinelibrary.com]

that DOTP interacted less strongly with PVC when in a mixture with ESBO. Conversely, the mixture of plasticisers in Formulation 5 appears to increase the exudation of DOP and decrease the exudation of ESBO, relative to the concentration in the PVC sample. In fact, while ESBO exuded more rapidly than DOP in the single plasticizer Formulations 2 and 3, when mixed in Formulation 5 this was reversed, with DOP exuding faster than ESBO. The exudation of plasticizer was quantifiable for all samples tested by GC–MS, which highlights the increased sensitivity of the method.

In addition to quantifying the amount of plasticizer exuded from the PVC matrix, an attempt was also made to determine the kinetics of the exudation for the various plasticisers and combinations thereof. An example is illustrated in Figure 7 for DOTP, where the amount of plasticizer exuded over time was fitted to a first order process with a reasonable degree of success ($R^2 = 0.96$). The other plasticisers and combinations yielded poorer fits to both zero and first order processes. The various attempts
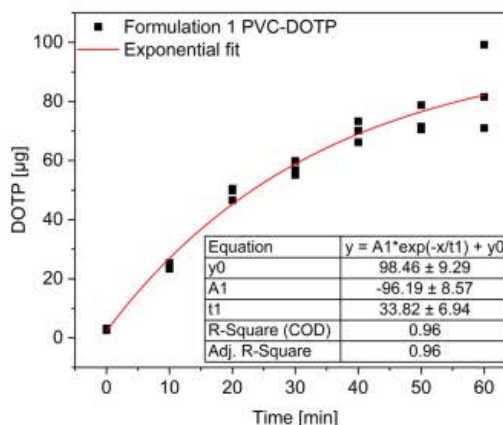

FIGURE 7 Exponential fit of DOTP exudation from Formulation 1 by GC–MS. [Color figure can be viewed at wileyonlinelibrary.com]

TABLE 5 R^2 values for exponential fits to the plasticizer exudation data as measured by GC–MS.

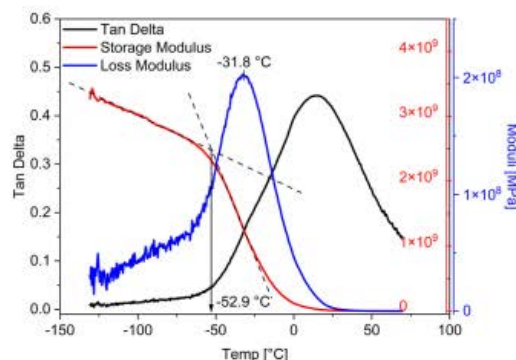| Formulation	Plasticizer	Linear fit R^2	Exponential fit R^2
Formulation 1	DOTP	0.91	0.96
Formulation 2	DOP	0.69	0.72
Formulation 3	ESBO	0.84	0.92
Formulation 4	DOTP	0.79	0.88
Formulation 4	ESBO	0.76	0.85
Formulation 5	DOP	0.79	0.85
Formulation 5	ESBO	0.79	0.84

FIGURE 8   An example of the storage modulus, loss modulus and tan delta data produced by DMA analysis. Measurements of glass transition temperature include the onset of Storage modulus (intersection of tangents) and peak of loss modulus as illustrated. [Color figure can be viewed at wileyonlinelibrary.com]

are summarized in Table 5 and illustrate that for all datasets, the exponential fit gives a higher R^2 than the linear fit.

The results obtained by GC–MS analysis show that this method can be used to quantify plasticizer exudation from PVC. In comparison with the ASTM D3291 standard method of a subjective rating of visible exudation on a 4-point scale, this method is based on an objective measurement and shows greatly improved sensitivity, as no exudation was visually observed within 60 min by the ASTM standard method. The plasticizer exudation results do not correlate strongly with the FTIR compatibility measurement of the weakening of the plasticizer carbonyl bonds. PVC-DOTP showed the highest level of plasticizer exudation by GC–MS, even though this formulation showed the second highest carbonyl peak shift by FTIR. This would suggest that exudation is controlled by other factors, such as interactions between other parts of the plasticizer molecule as well as kinetic factors.

The method of testing plasticizer exudation over time, as used for the GC–MS analysis, is very labour-intensive, and the variance in results was shown to be quite high in some cases. As all samples appeared to follow similar trends in exudation behavior, it could be beneficial to develop a test method based around a single compression interval.

4.4 | DMA analysis

The DMA data was used to produce plots of storage modulus, loss modulus and tan delta for the samples. These plots were examined to determine the glass transition temperature as well as any signs of phase separation which would indicate incompatibility. The storage modulus (E') represents the elastic (glassy) component of the material while the loss modulus (E'') represents the inelastic (rubbery) component. As the sample temperature is increased, the polymer changes from glassy behavior to rubbery behavior. The point at which this change occurs is the glass transition temperature. Storage and Loss modulus are related by the tan delta as calculated in Equation (1).

$$tan\delta = \frac{E''}{E'} \qquad (1)$$

All samples showed similar overall trends in both storage and loss modulus, producing profiles such as the example shown in Figure 8. The samples gave a clear single glass transition temperature, which can be measured by either the onset of the storage modulus decrease, or the peak of the loss modulus curve. These data are presented in Table 6.

The storage modulus onset and loss modulus peak values both show the same trends between the plasticised samples – Formulation 1 (PVC-DOTP) and Formulation 2 (PVC-DOP) gave the lowest T_g values, and Formulation 3 (PVC-ESBO) the highest, with the T_g for the mixtures at approximately the midpoint of those values. This suggests that the ability of the individual plasticisers to solvate and lubricate the PVC chains is unchanged when combined in the mixtures tested. Additionally, no evidence of phase separation (that would indicate poor compatibility) was detected in any sample by DMA.

Table 7 summarizes the methods evaluated for plasticizer compatibility testing. It is clear that there is little correlation between the methods, besides PVC-DOP showing the greatest compatibility by both FTIR and GC–MS. While exudation behavior suggests that DOTP is less compatible than DOP, it is also more effective at

TABLE 6 Glass transition temperatures (and standard deviations) measured by storage modulus onset and loss modulus peak, and the FTIR carbonyl peak shifts representing the strength of the interaction between carbonyl and the PVC C-Cl bonds.

Sample	Storage modulus onset (°C)	Loss modulus peak (°C)	FTIR carbonyl peak shift (cm^{-1})
Formulation 1—PVC-DOTP	−51.2 (0.2)	−32.7 (0.9)	−3.4
Formulation 2—PVC-DOP	−47.3 (2.5)	−29.9 (0.7)	−4.0
Formulation 3—PVC-ESBO	−29.8 (1.0)	−12.8 (0.3)	−2.5
Formulation 4—PVC-DOTPESBO	−38.2 (1.1)	−22.3 (0.2)	−1.6/−2.2
Formulation 5—PVC-DOPESBO	−38.0 (2.7)	−20.9 (0.8)	−1.8/−0.6

TABLE 7 Summary of the outcomes for the four methods of compatibility testing – ASTM D3291, FTIR carbonyl shift, GC–MS of exudation and glass transition temperature by DMA.

Compatibility measure	ASTM D3291 method	FTIR carbonyl shift	Exudation by GC–MS	Glass transition temperature
Most compatible	n.d.	DOP	DOP	DOTP
Least compatible	n.d.	DOP-ESBO	DOTP	ESBO

reducing the glass transition temperature of the PVC, and so is classified as the most compatible by this measurement. This highlights the need to consider the way that compatibility is defined when developing new plasticisers for use in PVC, as clearly the glass transition behavior is only one aspect of the relationship between the polymer and plasticizer.

5 | CONCLUSIONS

Four methods of determining plasticizer compatibility in PVC have been evaluated and compared for PVC formulations containing three plasticisers individually and in combination. GC–MS was used to quantify the plasticizer exudation on the surface of plasticised PVC samples stressed as described in the ASTM D3291 compatibility test. This method was able to detect and quantify plasticizer exudation that was not visible by the ASTM D3291 standard method. DOP displayed greater resistance to exudation than DOTP, while the presence of ESBO in the formulations appeared to enhance DOP migration and decrease DOTP migration. Correspondingly, the presence of DOTP increased ESBO migration, while the presence of DOP reduced ESBO migration. By fitting the data, it was shown that the process of exudation likely follows first order kinetics, however this was not conclusive due to high variance in the data.

FTIR was used to determine the carbonyl peak shift in the PVC compound relative to the free plasticizer (or a representative mixture of plasticisers). This is considered to be a measure of the strength of the interaction of the carbonyl group with the PVC chain, and thus indicative of compatibility. Aside from DOP, which showed the greatest carbonyl peak shift and lowest exudation by GC–MS, minimal correlation was found between the FTIR and GC–MS results. An attempt was made to quantify plasticizer exudation using FTIR, but this method was found to have insufficient sensitivity for this application.

These results were compared with the glass transition temperatures of the materials, as measured by DMA. It was shown that the T_g values do not correlate with the amount of exudation of the plasticisers – Samples 1 and 2, plasticised solely by DOTP and DOP respectively, had very similar T_g values but showed very different amounts of exudation.

GC–MS was shown to be a potentially viable method of improving upon the current ASTM D3291 compatibility test, as it is highly sensitive, repeatable and is based on objective measurement as opposed to subjective classifications. While the other methods for evaluating plasticisers give further information about the interactions between PVC and plasticisers in these PVC compounds, they could not be used as an indication of the tendency of the plasticizer to exude. However, the methods in combination could give a more complete picture of the compatibility of the plasticisers in PVC.

AUTHOR CONTRIBUTIONS

Katharine Burns: Conceptualization (lead); formal analysis (lead); investigation (lead); methodology (lead); writing – original draft (lead). **Johannes H Potgieter:** Conceptualization (supporting); supervision (lead); writing – review and editing (equal). **Sanja Potgieter-Vermaak:** Conceptualization (supporting); supervision (supporting);

writing – review and editing (equal). **Ian D. V. Ingram:** Supervision (supporting); writing – review and editing (equal). **Christopher M Liauw:** Investigation (supporting); supervision (supporting).

DATA AVAILABILITY STATEMENT

The data that support the findings of this study are available from the corresponding author upon reasonable request.

ORCID

Katharine Burns https://orcid.org/0000-0002-8568-0580

REFERENCES

[1] F. Chiellini, M. Ferri, A. Morelli, L. Dipaola, G. Latini, *Prog. Polym. Sci.* **2013**, *38*, 1067.

[2] M. Bocque, C. Voirin, V. Lapinte, S. Caillol, J. J. Robin, *J. Polym. Sci. A. Polym. Chem.* **2016**, *54*, 11.

[3] European Plasticisers. https://www.plasticisers.org/plasticisers/orthophthalates/ **2017**.

[4] J. Doull, R. Cattley, C. Elcombe, B. G. Lake, J. Swenberg, C. Wilkinson, G. Williams, M. van Gemert, *Regul. Toxicol. Pharmacol.* **1999**, *29*, 327.

[5] U. Wirnitzer, U. Rickenbacher, A. Katerkamp, A. Schachtrupp, *Toxicol. Lett.* **2011**, *205*, 8.

[6] M. Al-Natsheh, M. Alawi, M. Fayyad, I. Tarawneh, *J. Chromatogr. B* **2015**, *985*, 103.

[7] A. P. T. Demir, S. Ulutan, *J. Appl. Polym. Sci.* **2013**, *128*, 1948.

[8] M. G. A. Vieira, M. A. da Silva, L. O. dos Santos, M. M. Beppu, *Eur. Polym. J.* **2011**, *47*, 254.

[9] B. Bouchareb, M. T. Benaniba, *J. Appl. Polym. Sci.* **2008**, *107*, 3442.

[10] ASTM D3291-11, *Standard Practice for Compatibility of Plasticizers in Poly(Vinyl Chloride) Plastics Under Compression*, ASTM International, West Conshohocken, PA **2011**.

[11] A. O. Earls, I. P. Axford, J. H. Braybrook, *J. Chromatogr. A* **2003**, *983*, 237.

[12] B. Subedi, K. D. Sullivan, B. Dhungana, *Environ. Pollut.* **2017**, *230*, 701.

[13] M. Beltran, J. C. Garcia, A. Marcilla, *Eur. Polym. J.* **1997**, *33*, 453.

[14] N. Gonzalez, M. J. Fernandez-Berridi, *J. Appl. Polym. Sci.* **2008**, *107*, 1294.

[15] A. Lindstrom, M. Hakkarainen, *J. Appl. Polym. Sci.* **2006**, *100*, 2180.

[16] B. Yin, M. Hakkarainen, *J. Appl. Polym. Sci.* **2011**, *119*, 2400.

[17] N. Gonzalez, M. J. Fernandez-Berridi, *J. Appl. Polym. Sci.* **2006**, *101*, 1731.

[18] L. Audouin, J. Verdu, *Proceedings of the 4th International Conference on Properties and Applications of Dielectric Materials*, Vol. 1-2, Institute of Electrical and Electronics Engineers Inc. Brisbane, Australia **1994**, p. 262.

[19] M. Ekelund, H. Edin, U. W. Gedde, *Polym. Degrad. Stab.* **2007**, *92*, 617.

[20] M. Ekelund, B. Azhdar, U. W. Gedde, *Polym. Degrad. Stab.* **2010**, *95*, 1789.

[21] L. Audouin, B. Dalle, G. Metzger, J. Verdu, *J. Appl. Polym. Sci.* **1992**, *45*, 2091.

[22] D. T. C. Ang, Y. K. Khong, S. N. Gan, *J. Vinyl Addit. Technol.* **2016**, *22*, 80.

[23] P. H. Daniels, A. Cabrera, *J. Vinyl Addit. Technol.* **2015**, *21*, 7.

[24] P. W. Skelly, L. B. Li, R. Braslau, *Polym. Rev.* **2022**, *62*, 485.

[25] S. Biedermann-Brem, M. Biedermann, K. Fiselier, K. Grob, *Food Addit. Contam. A. Chem.* **2005**, *22*, 1274.

[26] D. L. Tabb, J. L. Koenig, *Macromolecules* **1975**, *8*, 929.

[27] E. Linde, T. O. J. Blomfeldt, M. S. Hedenqvist, U. W. Gedde, *Polym. Test.* **2014**, *34*, 25.

[28] G. Wypych, *PVC Formulary*, 2nd ed., ChemTec Publishing, ON, Canada **2015**.

[29] C. Croitoru, C. Spirchez, D. Cristea, A. Lunguleasa, M. A. Pop, T. Bedo, I. C. Roata, M. A. Luca, *J. Appl. Polym. Sci.*, **2018**, *135*, 46317.

SUPPORTING INFORMATION

Additional supporting information can be found online in the Supporting Information section at the end of this article.

A Comparative Assessment of the Use of Suitable Analytical Techniques to Evaluate Plasticiser Compatibility – Supplementary Information

Katharine Burns, Johannes Potgieter*, Sanja Potgieter-Vermaak*, Ian Ingram*, Christopher Liauw*.

GC-MS

Four peaks resulting from derivatisation products of ESBO were detected by GC-MS. These peaks were attributed to ethyl esters of fatty acids, with 0, 1 or 2 epoxide groups. Ethyl 9-epoxystearate (Et 9-ES) was chosen for quantification due to the intensity and minimal overlapping peaks. The components detected are shown in table S1.

Table S1: ESBO derivatives following transesterification with sodium ethoxide, identified by GC-MS.

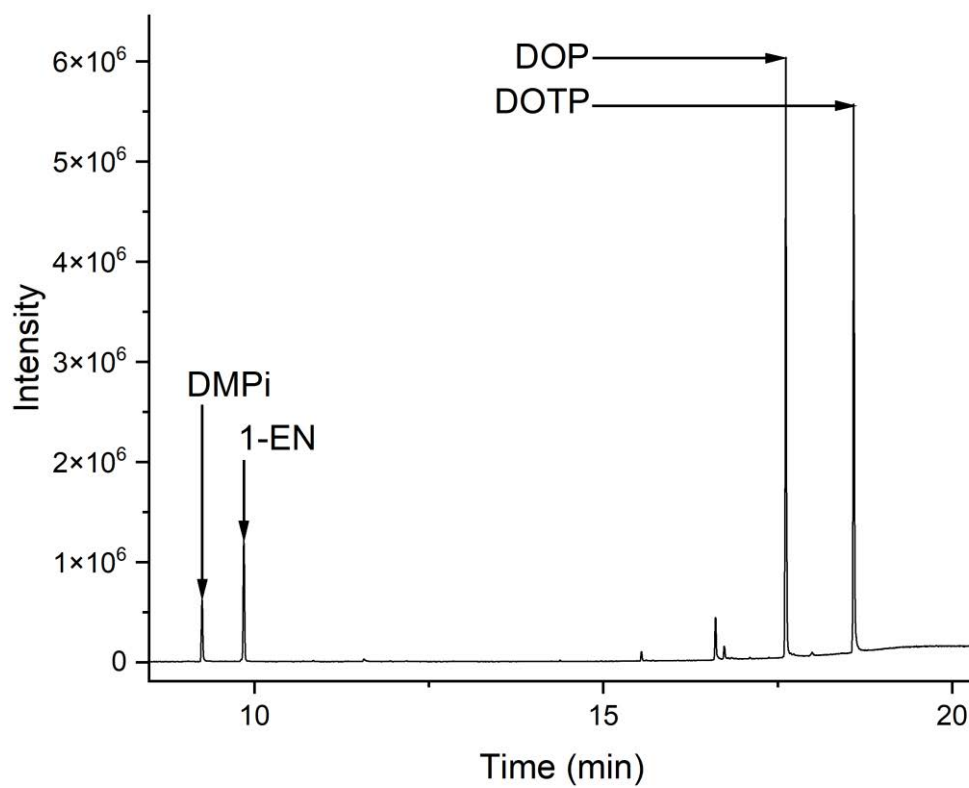| Compound	Retention Time (min)
Ethyl hexadecanoate	14.4
Ethyl octadecanoate	15.6
Ethyl 9-epoxystearate	16.6
Ethyl 9,12-diepoxystearate	17.4

Figure S1. Gas Chromatograph of plasticiser standard, with internal standards DMPi and 1-EN, and plasticisers DOP and DOTP indicated.
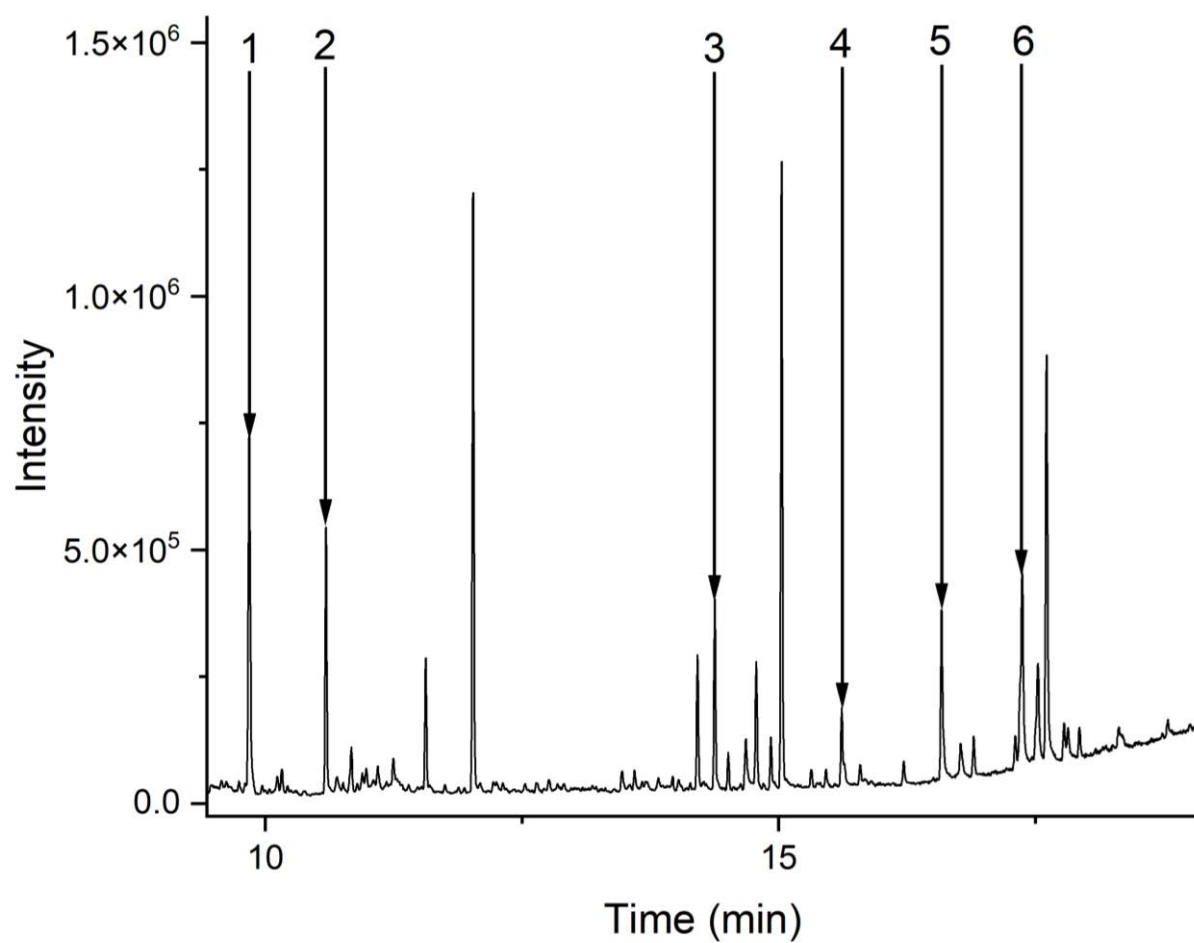
Figure S2. Gas chromatograph of derivatised plasticiser standard with compounds labelled: 1 - 1-EN, 2 – DEPi, 3 - Ethyl hexadecanoate, 4 - Ethyl octadecanoate, 5 - Ethyl 9-epoxystearate, 6 - Ethyl 9,12-diepoxystearate.
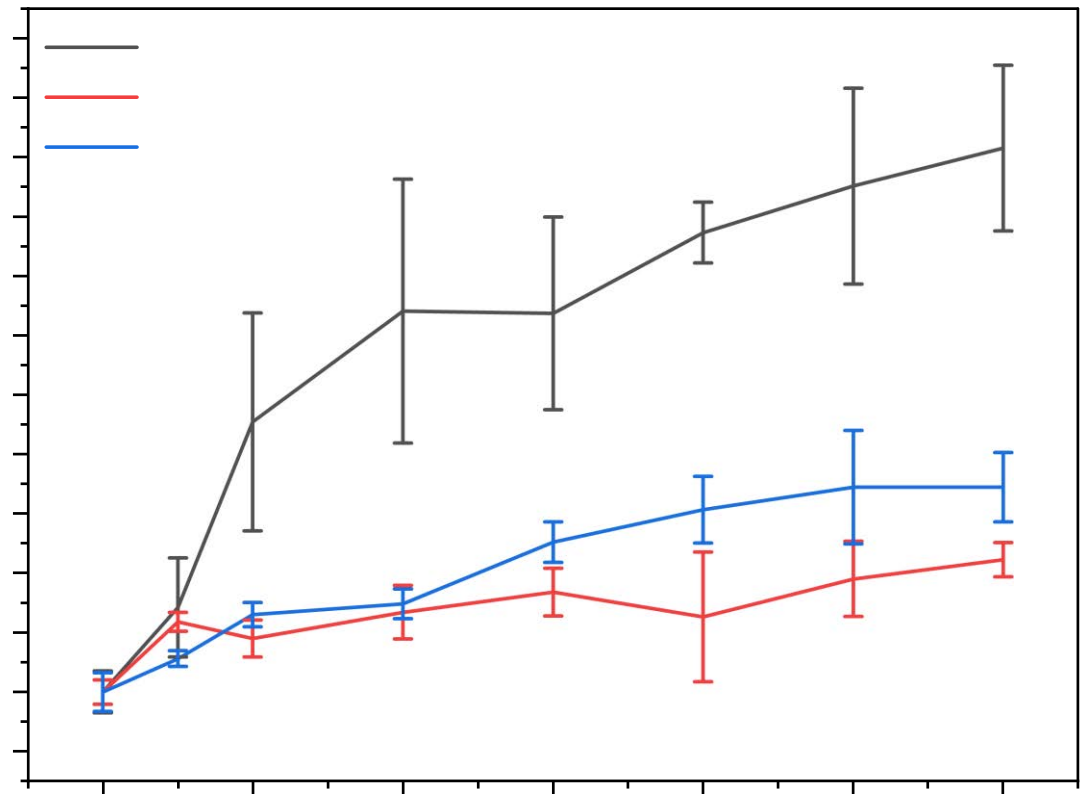
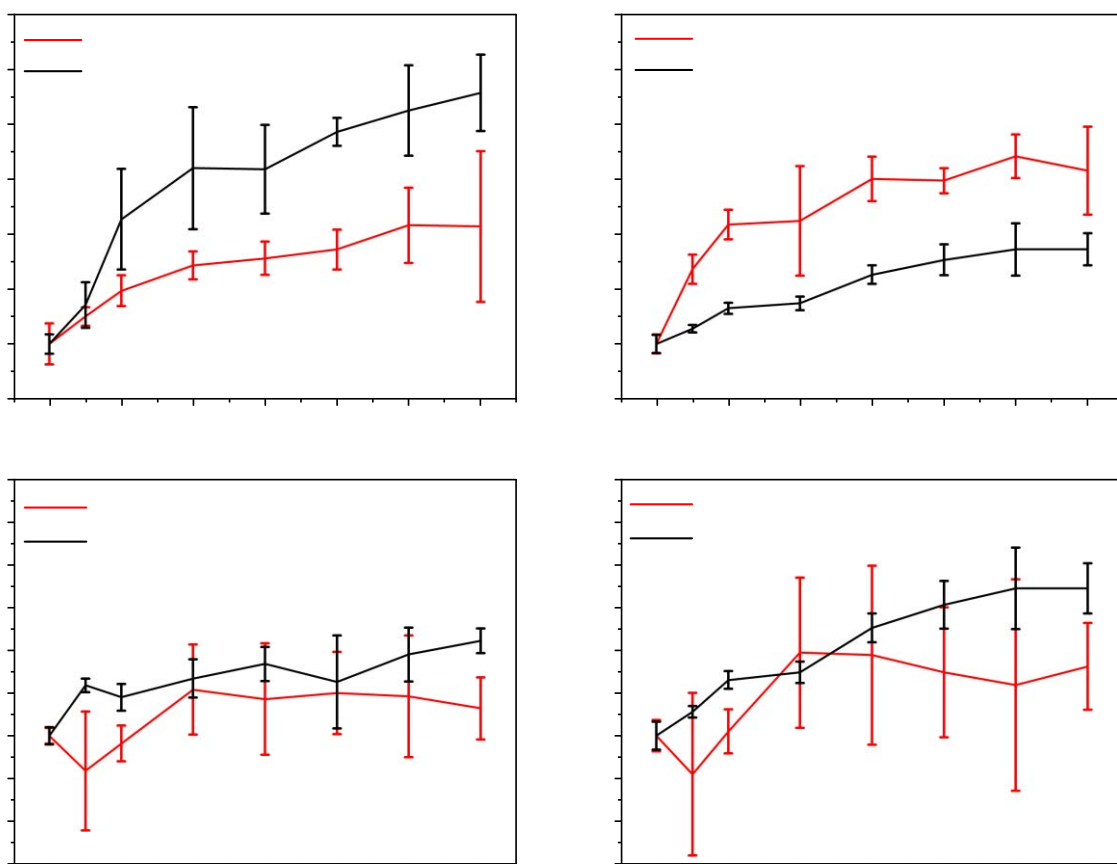**Figure S3.** FTIR - Carbonyl peak position change for the single plasticiser samples.

Figure S4. Carbonyl peak position changes for the mixed plasticiser samples in comparison with the respective single plasticiser samples.

Synthesis and Performance Evaluation of Novel Soybean Oil-Based Plasticisers for Polyvinyl Chloride (PVC)

Synthesis and performance evaluation of novel soybean oil-based plasticisers for polyvinyl chloride (PVC)

Katharine Burns[1] | Ian D. V. Ingram[1] | Johannes H. Potgieter[1,2] | Sanja Potgieter-Vermaak[1]

[1]Department of Natural Sciences, Manchester Metropolitan University, Manchester, United Kingdom

[2]School of Chemical and Metallurgical Engineering, University of the Witwatersrand, PO Wits, South Africa

Correspondence
Ian D. V. Ingram, Department of Natural Sciences, Manchester Metropolitan University, Chester Street, Manchester, M1 5GD, United Kingdom.
Email: i.ingram@mmu.ac.uk

Abstract

Novel bio-based plasticisers for polyvinyl chloride (PVC) are a significant and growing area of interest. These compounds aim to replace toxic and petro-chemical additives in commonly used plastic products. Plasticisers can comprise as much as 50% of the total mass of the PVC product. Epoxidised soybean oil (ESBO) is a commercially available bio-based plasticiser that is typically used at lower levels than traditional phthalates in PVC compounds because it does not show equivalent performance to existing phthalate plasticisers. Four derivatives of ESBO have been synthesized through reaction at the epoxide rings. These compounds have been evaluated in PVC formulations and compared to current petrochemical plasticisers, as well as ESBO. The product of methoxy polyethylene glycol and ESBO shows good plasticising ability, giving a PVC compound with higher tensile strength and elongation than dioctyl phthalate (DOP) and a lower glass transition temperature (Tg) than with the use of ESBO.

KEYWORDS

bio-based plasticizer, epoxidised soybean oil, phthalate, PVC, renewable

1 | INTRODUCTION

PVC (polyvinyl chloride) is used around the world in many different applications, owing to the wide variety of properties that can be obtained through the use of additives such as plasticisers.[1] Unplasticised PVC (U-PVC) is commonly used in construction, for products such as window frames and guttering, while plasticised PVC (pPVC) has uses in medical tubing, electrical insulation, toys and clothing (among others). Plasticisers create flexibility in polymers by increasing the free volume between the polymer chains, which allows the polymer to move and stretch more easily.[2] Plasticisers used in PVC formulations typically contain a mixture of polar and non-polar groups. The polar groups (such as esters) provide noncovalent interactions with the polymer chain, while the non-polar groups (such as alkyl chains) increase the free volume and provide lubrication.[2,3]

The most commonly used plasticisers for PVC are phthalates (e.g., diethyl hexyl phthalate, DOP/DEHP, Figure 1) which are derived from oil and can exhibit toxic and harmful effects on the endocrine system, especially in children.[2] Many petrochemical alternatives to phthalates have been developed and commercialized, such as benzoates (sold under the Benzoflex® brand by Eastman, 4) and Hexamoll® DINCH (BASF, 3). The use of non-
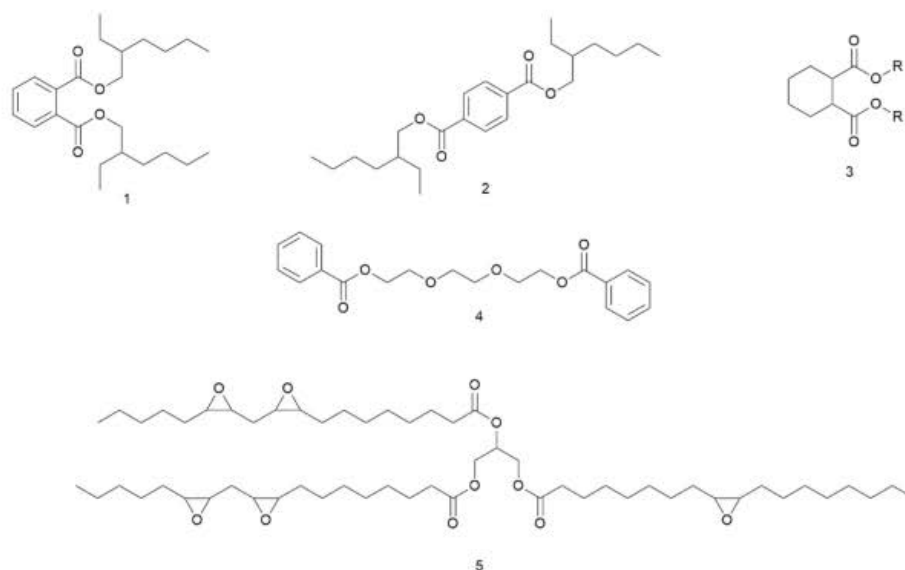
FIGURE 1 Chemical structures of petrochemical plasticisers used in PVC formulations – diethylhexyl phthalate (1), diethylhexyl terephthalate (2), 1,2-cyclohexane dicarboxylates (3, such as DINCH, where R = isononyl), benzoates (4) and representative structure of epoxidised soybean oil (ESBO, 5).

phthalate plasticisers globally has continued to increase, from 12% in 2005 up to 35% in 2017.[4] Terephthalates (e.g., diethyl hexyl terephthalate, DOTP, 2) are the para-isomers of phthalates and are widely used in PVC formulations. Despite the similarity in structure to phthalates, these compounds are non-toxic and approved for use in food-contact plastics and childcare items.[5,6] Plasticised PVC formulations typically contain 15–50% plasticizer and can even contain up to 1.8 times as much plasticizer as PVC resin.[7] As such, replacing petrochemical plasticisers with bio-based alternatives can have a significant impact on the sustainability of the PVC product.

Epoxidised soybean oil (ESBO, 5) is often used at low levels in PVC formulation but is not sufficiently compatible with the polymer to be practical as a primary plasticizer.[2,8] The reactivity of the epoxide ring has been used to functionalize ESBO for a number of bio-based applications.[9,10] By attaching more polar bio-based chemical groups, the compatibility of ESBO with PVC could be improved, allowing for greater bio-based content in PVC products. A typical composition of soybean oil is 53% C18:2 (fatty acid chain length: unsaturation), 22% C18:1, 12% C16:0, 8% C18:3, 5% other, thus giving 4–5 epoxide groups in the resulting ESBO.[11]

The epoxide ring opening reaction of ESBO is well established with a range of nucleophiles such as alcohols, diols and amines, with reports going back as far as 1995.[10,12,13] These reactions have been used to produce
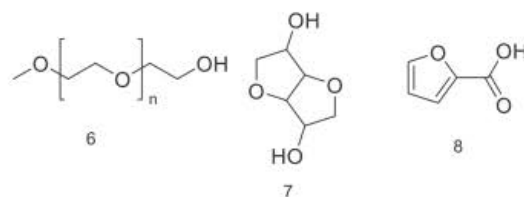

FIGURE 2 Bio-based PEG-methyl ether (6), isosorbide (7) and 2-furoic acid (8) used to prepare modified ESBO plasticisers for PVC.

polyols for applications such as the synthesis of polyurethanes and other bio-based polymer alternatives.[9,14,15] The polyols can also be further functionalized by esterification reactions which can be used to introduce additional polar groups to the molecule.[16] Despite the utility of the epoxide ring as a target for synthetic modification, retaining some epoxide functionality could be desirable, due to the benefits to both compatibility and stability.[17,18] ESBO is often used as a heat stabilizer in PVC, as the epoxide ring scavenges the hydrochloric acid produced by PVC degradation. This prevents the acid from promoting further degradation of the PVC chain.[2]

The target compounds studied in this work aim to improve upon the compatibility between ESBO and PVC to develop a replacement for DOP in PVC formulations. As such, the success of the synthesized plasticisers will be

determined by the degree to which the resulting plasticizer replicates the performance of DOP when combined with PVC. The reactant molecules (Figure 2) were chosen to introduce more polarity into the structure of the plasticizer, thus increasing the intermolecular attraction between the plasticizer and the PVC polymer. Additionally, the ubiquitous phthalate plasticisers in part owe their compatibility to the aromatic ring in their structure, and the introduction of aromaticity into bio-based plasticisers intended to replace phthalates has therefore also been the subject of investigation.[19] In a computational analysis of a series of phthalate plasticisers, the aromatic ring was found to have the largest contribution towards the polymer-plasticizer interaction.[20] Furans can be produced from biomass and are a significant area of renewable chemistry, and importantly are a much more scalable and accessible source of bio-based aromaticity than benzene derivatives which (with some exceptions) are less available from biomass.[21] As such, one target molecule investigated here is the ester of 2-furoic acid (8), with the aim of introducing aromaticity into the ESBO derivative structure. Furoic acid is produced by the oxidation of furfural, which has been produced commercially from biomass for decades.[22] Isosorbide is derived from natural sugars and has shown promise as a component of a bio-based plasticizer for PVC in the form of a diester.[23] Polyethylene glycol and compounds thereof have also been investigated in PVC plasticisation and have the interesting property of both adding a branched, higher-volume morphology to the ESBO backbone, as well as additional polarity.[24–26] In this study, we prepare four different bio-based ESBO derivatives, and evaluate their performance as plasticisers for PVC against both ESBO itself and traditional petrochemical plasticisers DOP and DOTP. A successful bio-based plasticizer will show plasticising properties that are more similar to the petrochemical plasticisers DOP and DOTP, relative to the ESBO starting material.

2 | EXPERIMENTAL

2.1 | Materials

PVC resin (suspension grade, K70), barium-zinc based liquid heat stabilizer and plasticisers (DOP, DOTP and ESBO, industrial grade) were provided by Alphagary Ltd. Additionally, chemicals used were magnesium sulfate (Laboratory reagent grade, Fisher Scientific), methoxypolyethylene glycol (average molecular weight 350, Alfa Aesar), p-toluene sulfonic acid (99%, Acros Organics), zinc trifluoromethane sulfonate (98%, Acros Organics), methanol (≥ 99.9%, Fisher Scientific), D-isosorbide

(98%, Alfa Aesar), 2-furoic acid (98%, Acros Organics), THF (Fisher Scientific, PureSolv purification system), chloroform (Fisher Scientific, >99% lab reagent grade), DCM (Fisher Scientific, >99% lab reagent grade), deuterated chloroform (Sigma Aldrich), diethyl ether (Fisher Scientific, laboratory reagent grade), sodium hydrogen carbonate (Fisher Scientific Laboratory reagent grade), toluene (Fisher Scientific, PureSolv purification system).

2.2 | Characterization

^{1}H, ^{13}C, and DOSY NMR were carried out on a JEOL ECS 400 MHz FT-NMR. Deuterated chloroform was used as solvent and spectra were referenced by the solvent peak. FTIR spectra were measured on a Perkin Elmer Spectrum Two (4000–400 cm^{-1}, resolution 4 cm^{-1}, 16 scans). These techniques were used to analyze the synthetic products formed.

2.3 | Synthesis of novel plasticisers

The reaction of the ESBO epoxide functionality with alcohols was carried out under acidic conditions. The catalyst was chosen to prevent transesterification reactions from occurring. As ESBO is not a single molecule and has approximately 5 possible reaction sites per molecule, calculating precise yields is unlikely to give valid results. As such, yields are expressed by mass. Reaction schemes and product structures are also shown as simplified representations due to the complex structure of ESBO – each triglyceride may contain fatty acids of variable composition as detailed previously, with 0, 1 or 2 epoxide groups present. Furthermore, each nucleophilic attack at an epoxide can occur at either carbon of the epoxide ring, leading to numerous possible products. Assignments and structures are presented in supplementary information.

2.4 | Synthesis of methyl ether ESBO polyol (MEEP, 9)

ESBO (53.67 g) was reacted with excess methanol (90 mL) with zinc triflate catalyst (0.25 g). The reaction mixture was stirred at reflux (65°C) under argon for 20 h. The reaction mixture was cooled to room temperature and the solvent removed in vacuo. The crude product was dissolved in chloroform (50 mL), washed with 1 M sodium bicarbonate solution (50 mL) and deionized water (2 x 50 mL). The organic fraction was dried over magnesium sulfate and concentrated in vacuo to give a yellow oil (53.02 g).

δH (400 MHz, CDCl₃) 5.26 (m), 4.29 (dd, $J = 11.8$, 4.2 Hz), 4.14 (dd, $J = 11.9$, 5.9 Hz), 3.52–3.42 (m), 3.41 (s), 2.99 (q, $J = 5.7$ Hz) 2.31 (t, $J = 7.6$ Hz), 1.61–1.26 (m), 0.88 (m).

δC (101 MHz, CDCl₃) 173.43, 173.01, 84.46, 72.74, 68.98, 62.21, 58.25, 56.75, 50.97, 39.14, 38.83, 38.05, 34.30, 33.63, 33.51, 32.19, 32.05, 32.01, 30.11, 30.02, 29.88, 29.82, 29.60, 29.49, 29.40, 29.24, 29.18, 26.11, 25.90, 25.16, 24.98, 24.93, 22.81, 22.74, 14.25, 14.20.

ν_{max}/cm⁻¹ 3456, 2926, 2855, 1742 cm⁻¹.

2.5 | Synthesis of ESBO-mPEG ether polyol (mPEG-ESBO, 10)

mPEG (methoxy polyethylene glycol, 52.15 g, 0.15 mol) of average molecular weight 350 Da was reacted with ESBO (15.08 g, 0.015 mol) and zinc triflate catalyst (0.022 g, 0.06 mmol) at 150°C under argon with stirring for 2 h. The reaction mixture was cooled to room temperature and triturated with deionized water (3 x 50 mL). The resulting yellow oil was dissolved in chloroform, dried over anhydrous magnesium sulfate, and concentrated in vacuo, giving a mass of 15.32 g.

δH (400 MHz, CDCl₃) 5.25 (m), 4.29 (m), 3.65 (s), 3.55 (m), 3.38 (s), 2.31 (t, J = 7.6 Hz), 1.76–1.13 (m), 0.88 (m).

δC (101 MHz, CDCl₃) 173.36, 172.95, 104.95, 104.88, 72.71, 72.02, 70.65, 70.38, 68.96, 62.18, 61.79, 59.13, 42.94, 42.85, 42.80, 36.10, 34.25, 34.14, 34.08, 32.02, 31.96, 31.91, 31.69, 31.51, 29.79, 29.75, 29.57, 29.46, 29.37, 29.21, 29.16, 29.10, 28.98, 28.17, 28.12, 27.91, 24.95, 24.90, 23.98, 23.89, 23.83, 22.78, 22.67, 22.52, 14.22.

ν_{max}/cm⁻¹ 3476, 2925, 2856, 1742 cm⁻¹.

2.6 | Synthesis of furoic acid ester of methoxylated ESBO (MEFE, 11)

Methyl Ether ESBO Polyol (MEEP, 10.00 g) was reacted with furoic acid (6.28 g) in dry toluene (100 mL) with PTSA catalyst (0.964 g) in a round bottomed flask with a Dean-Stark condenser trap. The mixture was stirred at reflux (110°C) for 18 h and cooled to room temperature and the solvent removed in vacuo. The crude product was dissolved in chloroform (50 mL), washed with 1 M sodium bicarbonate solution (50 mL) and deionized water (2 x 50 mL). The organic fraction was dried over magnesium sulfate and concentrated in vacuo to give a brown oil (11.21 g).

δH (400 MHz, CDCl₃) 7.88–7.49 (m), 6.51 (m), 5.25 (m), 4.34–4.08 (m), 3.41 (s), 2.99 (m), 2.35 (s), 2.31 (t, J = 7.6 Hz), 2.09 (s), 1.72–1.16 (m), 0.87 (t, J = 6.9 Hz).

δC (101 MHz, CDCl₃) 173.42, 130.14, 129.44, 129.17, 128.36, 128.15, 126.67, 125.43, 111.93, 68.99, 65.20, 62.21, 34.18, 32.06, 29.84, 29.79, 29.64, 29.50, 29.41, 29.25, 25.82, 24.97, 22.82, 21.59, 14.26, 14.17.

ν_{max}/cm⁻¹ 3020, 2927, 2856, 1735, 1661 cm⁻¹.

2.7 | Synthesis of Isosorbide ether ESBO polyol (IEEP, 12)

ESBO (15.01 g) was reacted with an excess of isosorbide (33.83 g) in THF (175 mL) with zinc triflate catalyst (0.279 g). The chemicals were dissolved in THF and dried with excess magnesium sulfate, then filtered into a dry round bottomed flask. The mixture was heated to reflux under argon for 20 h with stirring. The reaction mixture was cooled to room temperature and the solvent removed in vacuo. The crude product was dissolved in diethyl ether (50 mL), washed with 1 M sodium bicarbonate solution (50 mL) and deionized water (2 x 50 mL). The organic fraction was dried over magnesium sulfate and concentrated in vacuo to give a yellow oil (19.33 g).

δH (400 MHz, CDCl₃) 5.25 (m), 4.7–4.4 (m), 4.21 (ddd, J = 59.9, 11.7, 5.1 Hz), 4.05–3.53(m), 3.49–3.37 (m), 2.38 (t, J = 7.4 Hz), 2.31 (t, J = 7.6 Hz), 1.70–1.20 (m), 0.88 (m).

δC (101 MHz, CDCl₃) 173.46, 104.91, 70.76, 68.98, 62.22, 43.01, 34.29, 34.14, 32.06, 29.84, 29.80, 29.61, 29.51, 29.41, 29.22, 28.18, 26.61, 24.98, 24.02, 22.81, 22.73, 14.28.

ν_{max}/cm⁻¹ 3457, 2926, 2855, 1741 cm⁻¹.

2.8 | Evaluation of novel plasticisers in PVC compounds

2.8.1 | Solvent casting of plasticised films

Plasticizer (2.5 g) was dissolved in 50 mL THF in a 100 mL round bottomed flask with stirrer bar. 0.05 μL liquid barium-zinc stabilizer was added with stirring, followed by 5 g PVC resin (K70 suspension resin). A condenser was attached, and the mixture was heated to reflux (66°C) under argon for 2 hours until the polymer was fully dissolved. The mixture was allowed to cool to room temperature and then poured into a dry glass petri dish and loosely covered to allow gradual evaporation of the THF for 7 days.

The films were removed from the petri dishes and dried under vacuum at 40°C for 2 hours to remove residual THF. This was shown to be sufficient for the removal of THF by TGA analysis which did not show a mass loss step that could be attributed to THF evaporation.

This method does not replicate the methods of PVC plasticisation used in the PVC industry, however such methods (extrusion, 2-roll milling) would require greater quantities of plasticizer than were available in this study.

2.8.2 | Tensile testing

For the tensile properties testing, 1 mm thickness plaques were prepared using a heated hydraulic press. The cast films were placed in a steel mold which was subjected to 200 bar at 160°C for 4 min and cooled under pressure. Dumbbell shaped pieces in accordance with BS EN ISO 527-2:2012 (Type 5A) were cut from the molded sheets. The thickness of the central portion was measured and recorded. Five test pieces were prepared for each plasticised PVC formulation.

The tensile properties of the molded films were tested in accordance with BS EN ISO 527-1:2019 using a Hounsfield H10KS UTM equipped with a 1000 N load cell and laser extensometer. The speed of the moving grip was set to 100 mm/min. Load and extension were measured, and stress and strain calculated from the sample dimensions.

2.8.3 | Dynamic mechanical analysis

DMA was used to investigate the low temperature properties of the samples. This analysis was carried out using a Perkin Elmer DMA 8000 in tensile mode on samples of dimension 6 x 20 mm cut directly from the cast films. Sample thicknesses were measured to 0.01 mm and were approximately 1 mm. Samples were tested from −130 to 70°C at a rate of 5°C/min. The samples were exposed to an oscillating strain of 0.5 mm at a frequency of 1 Hz.

2.8.4 | Thermogravimetric analysis

Samples of the novel plasticisers and plasticised films were tested by TGA using a Mettler Toledo TGA 1. Samples of approximately 15 mg were weighed into aluminium pans (plasticisers) or alumina crucibles (PVC samples) and heated at 20°C/min to 600°C (plasticisers) or 1000°C (PVC samples) under nitrogen.

2.8.5 | Scanning electron microscopy

PVC samples were cold fractured under liquid nitrogen. The fracture surfaces were sputter coated with gold/palladium (10 nm thickness) and examined by SEM (Zeiss Supra 40VP) at 5000–20,000× magnification, 2 kV acceleration voltage, to investigate the internal structure.

3 | RESULTS AND DISCUSSION

The reactions were carried out as presented in Scheme 1. The synthesis of novel plasticisers was monitored primarily by ^{1}H NMR. As ESBO itself is a mixture with multiple possible reaction sites, the resulting products were themselves mixtures. As such, options for purification of the products were limited since typical routes such as column chromatography were unsuitable.

Methyl ether ESBO polyol (MEEP, **9**) has been synthesized in previous works[9,27] as a precursor for polyurethane synthesis and was primarily prepared here as an intermediate. Zinc triflate, PTSA and sulfuric acid were all evaluated for use as catalysts in the ring opening reaction with methanol based on their use in similar works,[9,14] but zinc triflate was chosen as this gave the greatest conversion and did not lead to significant transesterification, which was observed when sulfuric acid or higher levels of PTSA were used (Figure 3).

The structure was confirmed with FTIR-ATR spectroscopy which showed the broad alcohol O-H stretch at 3400–3500 cm^{-1}, as well as a reduction in the epoxide double peak (828 and 847 cm^{-1}). As both ESBO and mPEG are mixtures, the resulting product will be a statistical mixture of composition and so precise structural determination is not possible. In the case of mPEG-ESBO, the terminal methyl group (3.4 ppm) was used to determine the progress of the reaction. In the final product, the methyl group was measured as 4.85 protons, indicating that on average each molecule of ESBO has reacted with 1–2 mPEG molecules. An excess of mPEG was used to ensure the greatest possible reaction of the epoxide rings. Methyl capped PEG was used to prevent crosslinking between ESBO molecules, as uncapped PEGs have two alcohol functionalities that could both react with epoxide rings. While isosorbide is also a diol with the potential to cause crosslinking, the two alcohol groups exhibit different reactivities. One alcohol group is in an endo- position that leads to hydrogen bonding with the furan ring, while the other alcohol group is in an exo- position and so is significantly more available for reaction.[28]

Purification was first carried out by dissolving the reaction mixture in chloroform and washing with water. However, this did not remove the residual mPEG. This was noted by ^{1}H NMR as integration of the peak corresponding to the terminal methyl of mPEG gave an equivalent of 12 mPEG chains per ESBO molecule despite the theoretical maximum number of epoxide sites being 5–6.
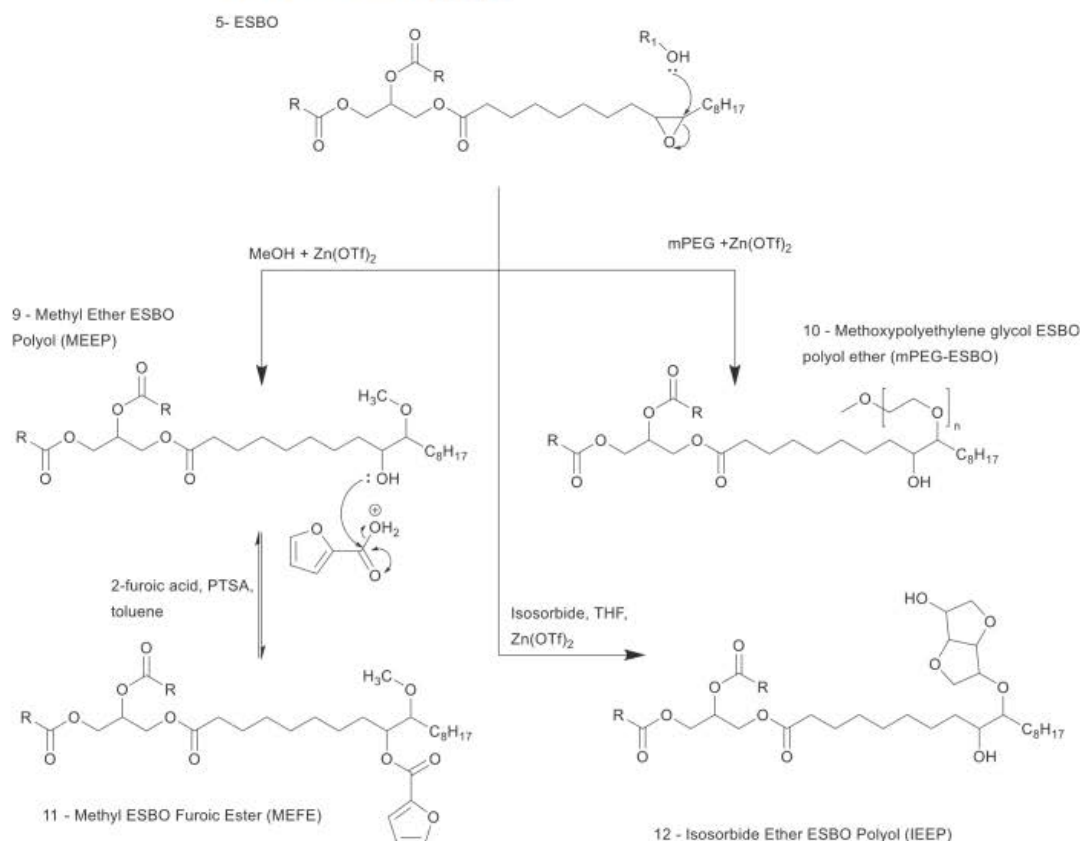
SCHEME 1 Reaction scheme showing the synthesis routes for four bio-based derivatives of ESBO, 9- Methyl Ether ESBO Polyol (MEEP), 10 – methoxy polyethylene glycol ESBO polyol ether (mPEG-ESBO), 11 - Methoxylated ESBO Furoic Ester (MEFE), 12- Isosorbide Ether ESBO Polyol (IEEP).

Purification was instead carried out by trituration in water. The composition of the resulting product was confirmed by Diffusion-Ordered NMR Spectroscopy (DOSY). DOSY can be used to determine the composition of samples by separating the 1H-NMR signals based on the diffusion properties of the molecules. Comparison of a mixture of ESBO and mPEG with the reaction product showed the difference following reaction. The two components are separated by their diffusion behavior in Figure 4, while Figure 5 shows a single diffusion coefficient, indicating that the product has been formed. FTIR-ATR also indicated that the product was formed, due to an alcohol O-H stretch at 3485 cm^{-1}, reduction in epoxide (828 and 847 cm^{-1}) and a peak at 1108 cm^{-1} corresponding to the C-O-C asymmetric stretch of the ether groups.

In the synthesis of isosorbide ether ESBO polyol (IEEP, **12**), initial reactions showed a disappearance of the epoxide ring signals by NMR, without new signals appearing which would correspond to the isosorbide structure. It was thought that this could be due to moisture and so all reactants were dried over magnesium sulfate prior to reaction and dry solvent was used. ^{1}H NMR peaks consistent with isosorbide were observed in the region 4–3.5 ppm, and the reaction was confirmed by DOSY NMR (Figure 6), which confirmed that the isosorbide was attached to ESBO, and FTIR, which showed alcohol formation, and hence conversion of epoxides, by the O-H stretch at 3452 cm^{-1}.

The esterification of the alcohol groups formed by epoxide ring opening in MEEP (**9**) was attempted with furoic acid to introduce aromaticity into the plasticizer structure. Initial reaction attempts using a single vessel were unsuccessful, and so a Dean-Stark apparatus was used to remove water formed by the reaction. By using

this method, methoxylated ESBO furoic ester (MEFE, **11**) was produced. The MEFE product **11** was confirmed by ¹H NMR, which showed peaks corresponding to the furan ring at 7.8, 7.2 and 6.5 ppm. DOSY analysis showed a single diffusion behavior confirming that the furan

signals were attached to the larger molecule and FTIR showed the inclusion of an sp^2 C-H stretch at 3019 cm⁻¹ as well as the disappearance of the O-H stretch observed in MEEP **9** which confirms that the alcohol group has reacted.

3.1 | Tensile testing

The tensile elongation and stress at the ultimate breakpoint for all samples are shown in Figure 7, and values including 100% modulus are presented in Table 1. The plasticised PVC films prepared by solvent casting were compression molded prior to tensile testing to give an even sample thickness throughout. However, both MEEP **9** and IEEP **12** showed delamination of the molded PVC samples, where the material did not fuse together when molded and instead separated into layers. This is an indication of poor compatibility, as delamination can be caused by plasticizer exudation which forms an oily layer on the surface, preventing fusion.

Tensile testing of flexible PVC samples typically shows a trend of increasing elongation and decreasing tensile stress at breakpoint with higher plasticisation. This is demonstrated with the three commercial plasticisers – DOP is known to be a more efficient plasticizer than DOTP (giving a softer product at the same weight percentage)
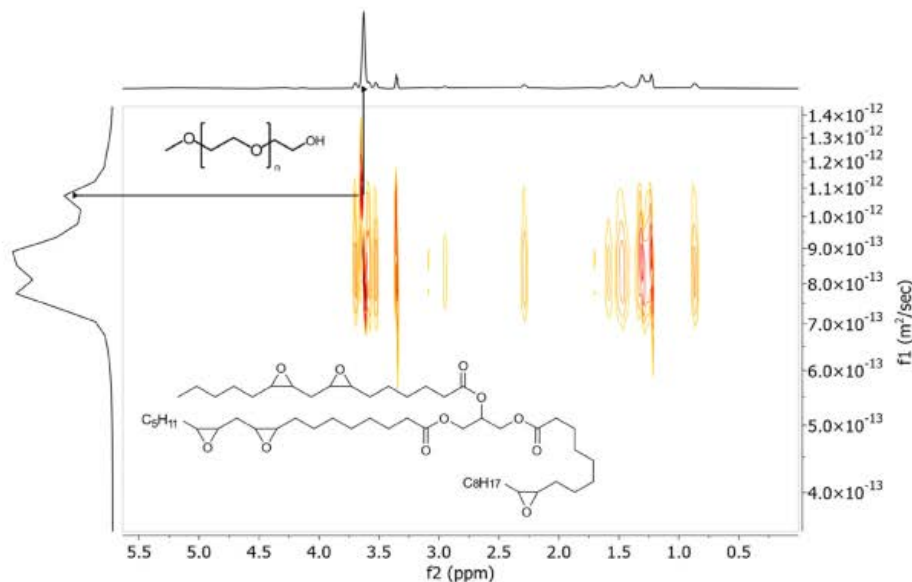

FIGURE 3 Catalyst comparison for the methoxylation of ESBO measured by 1H NMR, showing conversion and selectivity of epoxide to methyl ether and glycerol esters to methyl esters (calculations listed in ESI). [Color figure can be viewed at wileyonlinelibrary.com]

FIGURE 4 DOSY NMR for a mixture of ESBO and mPEG showing the separation of the signals for the components. [Color figure can be viewed at wileyonlinelibrary.com]
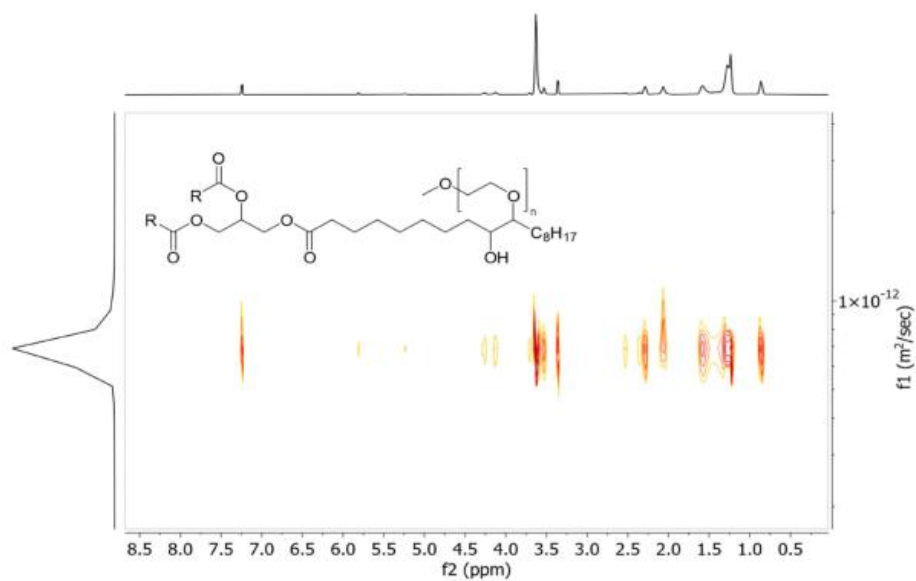
FIGURE 5 DOSY NMR for the product of ESBO and mPEG (mPEG-ESBO **10**) showing a single diffusion behavior, indicating that the reaction has occurred. [Color figure can be viewed at wileyonlinelibrary.com]
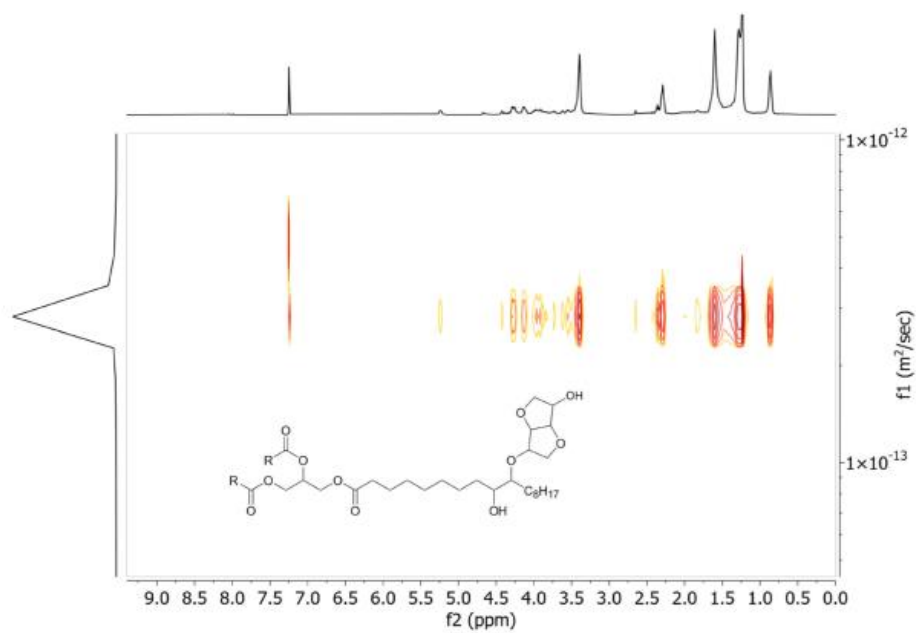

FIGURE 6 DOSY NMR of IEEP (product of ESBO and isosorbide) showing a single diffusion behavior, indicating that all peaks are from the same molecule. [Color figure can be viewed at wileyonlinelibrary.com]
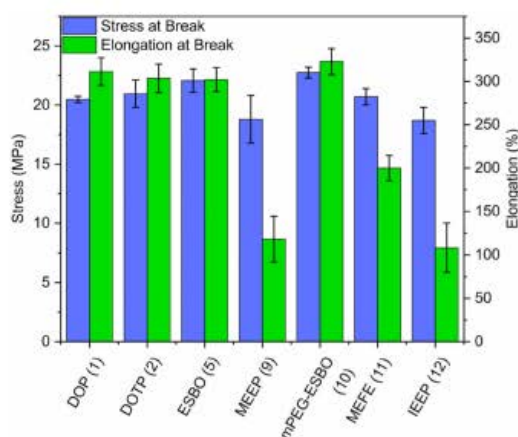
FIGURE 7 Tensile Stress and Elongation at breakpoint for PVC samples produced with commercial and novel plasticisers. [Color figure can be viewed at wileyonlinelibrary.com]

TABLE 1 100% Tensile Modulus, Tensile Stress and Elongation at breakpoint for the plasticised PVC samples.

Plasticizer	100% modulus (MPa)	Stress at breakpoint (MPa)	Elongation at breakpoint (%)
DOP (1)	10.3	20.5	311.4
DOTP (2)	11.9	21.0	303.6
ESBO (5)	12.75	22.1	302.0
MEEP (9)	14.6	18.8	118.2
mPEG-ESBO (10)	12.6	22.8	322.9
MEFE (11)	16.7	20.7	200.0
IEEP (12)	8.4	18.7	108.3

and correspondingly DOP shows greater elongation and lower stress at breakpoint than DOTP or ESBO.

The mPEG-ESBO **10** product shows the highest elongation at breakpoint and tensile stress at breakpoint of all samples, which indicates that this new bio-based plasticizer gives greater strength and flexibility to the PVC product than the commercial plasticisers.

The other synthesized plasticisers show signs of less effective plasticisation, with lower stress and elongation at break than the commercial plasticisers. This indicates that these plasticisers do not as effectively lubricate the polymer chains to move within the polymer matrix and allow the test pieces to elongate under load. In fact, the stress–strain curves for the novel plasticisers show very different behavior for MEEP **9**, MEFE **11** and IEEP **12** as shown in Figure 8. mPEG-ESBO **10** is the only one of our

bio-based plasticisers that gives a similar profile of stress–strain behavior to the commercial PVC plasticisers. These samples displayed ductile behavior prior to break, with no necking of the sample, followed by a brittle fracture as indicated by SEM images (supplemental data). The other novel plasticisers also show ductile deformation behavior; however, this was followed by an early yield point leading to 'necking' of the sample. This necking creates a region of very high stress as the cross-section narrows, and thus leads to early fracture with low elongation and stress at breaking point. The fracture surfaces of these samples indicate a combination of brittle and ductile behavior.

3.2 | Dynamic mechanical analysis

DMA was used to measure the response of the plasticised samples to an oscillating deformation over a temperature range. The glass transition temperature T_g of the material can be determined by the point at which the response changes from 'glassy' elastic behavior to 'rubbery' inelastic behavior. The loss modulus is a measure of the inelastic component of the material response. The effect of a plasticizer on the glass transition temperature of PVC is a common metric of plasticizer compatibility and performance.[29–31] Effective plasticisation leads to a lower T_g, while poor plasticisation can also give rise to phase separation which is shown through multiple or poorly defined glass transitions.

The T_g of plasticised PVC samples was determined by the peak of the loss modulus (Figure 9, see supplementary information for plots of storage modulus and tan delta). All novel compounds gave a lower T_g than ESBO, however the loss modulus peaks were generally broader and less well defined. IEEP showed the lowest average T_g, but the peak width was more than double that of ESBO (FWHM of 82.2°C compared with 39.7°C). The peak width of mPEG-ESBO **10** was also broad, despite this plasticizer generally showing good performance in other material properties. It is possible that this could be due to the broader composition of this product than the other novel plasticisers, as both ESBO and mPEG starting materials are composed of mixtures of chain lengths and molecular weights.

3.3 | Thermogravimetric analysis

Thermogravimetric analysis was carried out on the plasticisers and plasticised PVC samples. For the plasticisers alone, the data shows the volatility of the plasticizer, while for the plasticised PVC samples this technique also
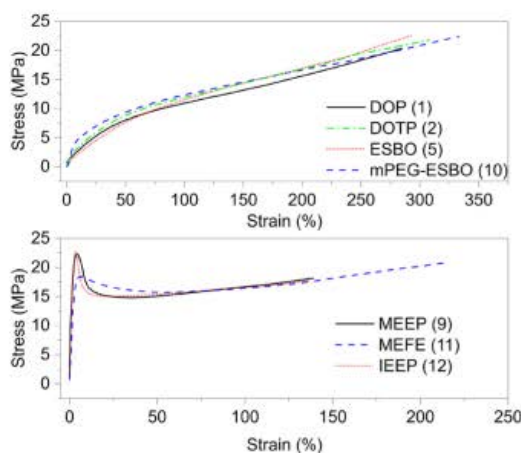
BURNS ET AL.

FIGURE 8 Stress–strain curves for tensile elongation of plasticised PVC samples. [Color figure can be viewed at wileyonlinelibrary.com]
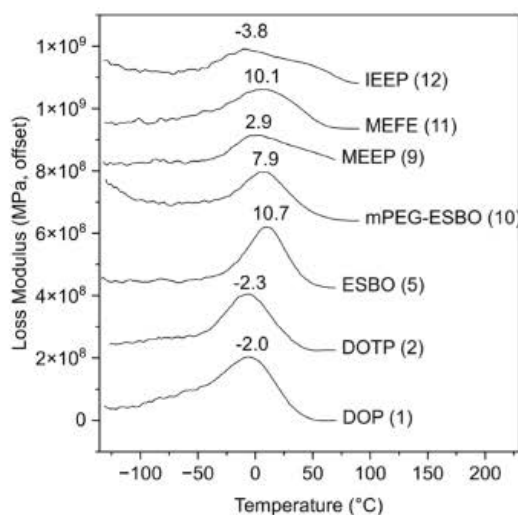

FIGURE 9 Loss modulus against sample temperature by DMA for samples of plasticised PVC prepared by solvent casting.

shows the effect of the plasticizer on the degradation of the PVC. Figure 10 shows the mass loss of the plasticisers by TGA. All of the modified-ESBO plasticisers showed an earlier onset of evaporation than ESBO itself. The mass loss also progressed in multiple distinct steps for MEEP **9**, MEFE **11** and IEEP **12**, whereas for mPEG-ESBO **10** the mass loss occurred gradually throughout the experiment. The temperatures of 5% and 50% mass loss ($T_{95\%}$ and $T_{50\%}$) are presented in Table 2.
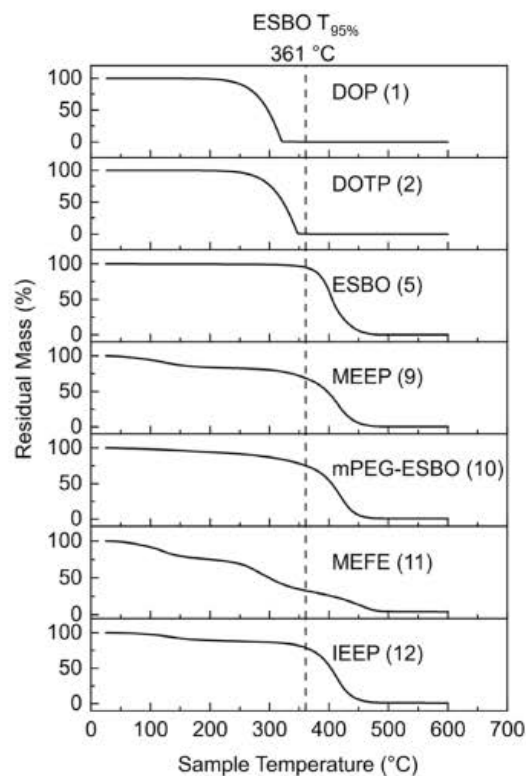
FIGURE 10 Thermogravimetric analysis of commercial and modified-ESBO plasticisers.

TABLE 2 Temperature of 5% and 50% mass loss for plasticisers by TGA.

Plasticizer	$T_{95\%}$	$T_{50\%}$
DOP (1)	236	297
DOTP (2)	260	323
ESBO (5)	361	406
mPEG-ESBO (10)	185	405
MEEP (9)	95	397
MEFE (11)	82	300
IEEP (12)	126	403

MEFE showed the earliest onset of mass loss, losing 5% by 82°C. The other novel plasticisers showed a lower $T_{95\%}$ than ESBO, but comparable $T_{50\%}$ values. As such, while the major component of these plasticisers appears to have similar volatility to ESBO, these also contain more volatile or unstable minor components.
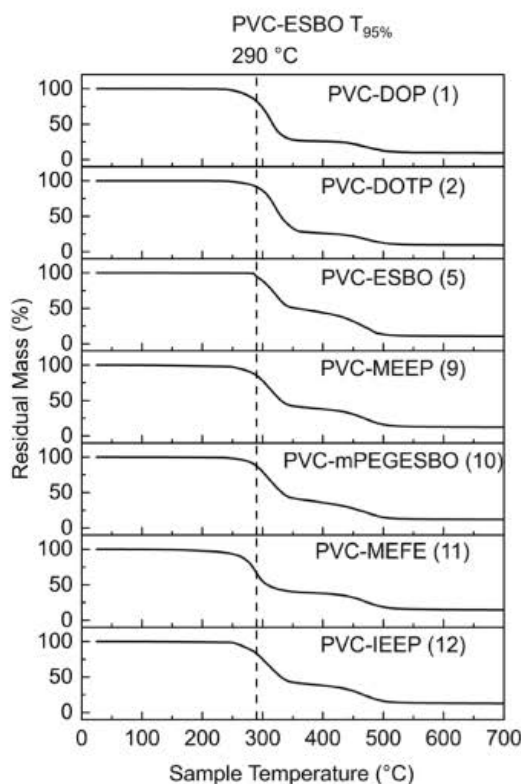
189

FIGURE 11 Thermogravimetric analysis of plasticised PVC samples.

these processes could not be specifically and separately identified in the data. The onset temperature and percentage mass loss for the two steps is presented in Table 3. Onset temperatures were calculated by the intersection of tangents using the Mettler Toledo STARe Evaluation software.

The effect of ESBO on PVC decomposition is observable in the Step 1 mass loss. PVC-DOP and PVC-DOTP lose 73.9 and 73.7% of the total sample mass in this step, while PVC-ESBO loses only 54.1%. This is likely to be a combination of the reduction in dehydrochlorination as described, as well as the lower volatility of ESBO. All of the synthesized plasticizer samples retained some degree of this behavior, with mass loss ranging from 61.2% to 63.2%. This suggests that unreacted epoxide rings remain present in the compounds and may function as PVC stabilizers. ^{1}H NMR measurement of the epoxide signals in the novel plasticisers supports this, as some residual epoxide could be detected in all products.

However, the onsets of degradation in the samples prepared with the synthesized plasticisers are lower than with ESBO, showing that these plasticisers produced from ESBO do not stabilize the PVC to the same extent. This is expected, as the epoxide functionality that provides the stabilization effect is also the functionality that has been exploited in this synthesis. As Table 3 shows, the $T_{95\%}$ for the novel plasticisers are comparable to the petrochemical plasticisers (with the exception of MEFE **11** which is somewhat lower) and so these plasticisers are suitably non-volatile for use in PVC compounds. mPEG-ESBO **10** shows the highest $T_{95\%}$ of the ESBO-derived plasticisers.

3.4 | Scanning electron microscopy

SEM images of plasticised PVC samples are shown in Figure 12. The samples containing commercial plasticisers DOP **1** and ESBO **5** both show smooth planes in the fractured surfaces, indicating good solvation of the PVC grains. There is no evidence of phase separation identifiable in these images. PVC-MEEP **9** shows mainly smooth plans with some inclusions observed. PVC-mPEG-ESBO **10** is the most similar in appearance to the commercial plasticisers, however there are some features visible that appear fibrous. Features of this sort are sometimes seen as a result of localized crystallization of the plasticizer, however this phenomenon is difficult to characterize and was not investigated further. PVC-MEFE **11** displays a very uneven microstructure, with large irregular regions visible. The surface of the fracture planes also appears to be rougher than in PVC-DOP or PVC-ESBO. PVC-IEEP **12** also shows signs of roughness on the fracture planes

The TGA results for the plasticised PVC samples (Figure 11) show the effect of the plasticizer on the decomposition of PVC. These data also confirm that there is no significant residual THF present in the samples, as this would be notable by a mass loss step at approximately 65°C. All samples contained the same amount of liquid heat stabilizer additive. PVC decomposition occurs in two stages – first dehydrochlorination, forming conjugated polyenes and hydrochloric acid, followed by cyclisation to form benzene and other aromatic compounds.[32] The epoxide rings in ESBO react with chloride ions that are released during PVC decomposition.[33] This slows the degradation as the hydrochloric acid produced by the PVC decomposition acts as a catalyst for this decomposition. Epoxides can also replace labile chlorine atoms to form α-chloro-ethers which prevents the dehydrochlorination reaction.[33] Two main mass loss steps were identified for all samples of plasticised PVC. As well as the PVC decomposition, these steps will also include volatilization and decomposition of the plasticizer, however

TABLE 3 Thermogravimetric analysis of plasticised PVC samples.

Plasticizer	Step 1 onset (°C)	Step 1 mass loss (%)	Step 2 onset (°C)	Step 2 mass loss (%)	Final residue (%)	$T_{95\%}$
DOP (**1**)	284	73.9	452	15.9	8.2	262
DOTP (**2**)	296	73.7	442	16.7	8.3	278
ESBO (**5**)	291	54.1	447	34.5	7.2	290
MEEP (**9**)	266	61.8	442	22.9	13.8	261
mPEG-ESBO (**10**)	278	63.2	450	23.6	10.2	272
MEFE (**11**)	277	61.5	440	25.7	11.8	240
IEEP (**12**)	272	61.2	439	25.3	10.2	263

PVC-DOP (**1**) 5 μm   PVC-ESBO (**5**) 5 μm

PVC-MEEP (**9**) 5 μm   PVC-mPEG-ESBO (**10**) 5 μm

PVC-MEFE (**11**) 5 μm   PVC-IEEP (**12**) 5 μm
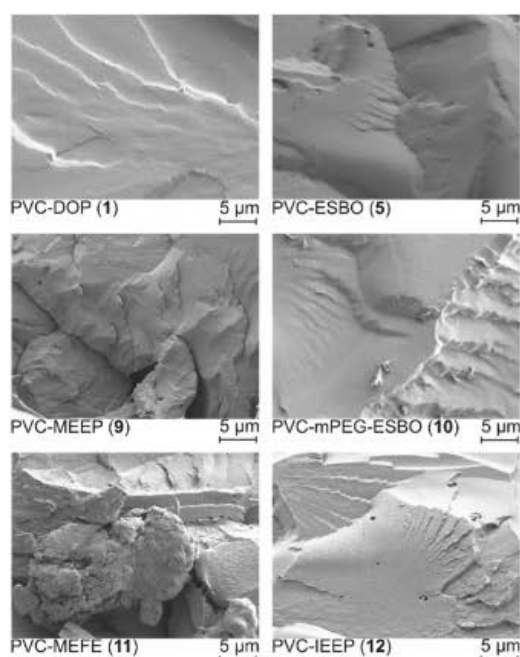
FIGURE 12 SEM images of cold fractured plasticised PVC sample surfaces, showing the effect of plasticizer on the morphology of the PVC-plasticizer blend.

as well as voids which could be caused by areas of plasticizer accumulation due to poor compatibility with PVC.

4 | CONCLUSIONS

Four derivatives of ESBO **5** were synthesized through epoxide ring opening reactions (and subsequent modification in the case of MEFE **11**). Analysis of these products showed that the epoxide ring opening reaction did not go to completion, with typically 1–3 addition reactions occurring per ESBO molecule (of approximately 4–5 epoxide groups per molecule).

These products were evaluated as potential bio-based plasticisers for PVC compounding, with the aim of matching the performance of the petrochemical plasticizer DOP. mPEG-ESBO showed the greatest plasticising behavior as measured by T_g suppression and tensile properties. The tensile strength and elongation of PVC-mPEG-ESBO exceeds that of PVC-DOP. The other ESBO derivatives showed poor elongation at breakpoint, indicating that they do not plasticise the PVC chains effectively. IEEP and MEEP both showed delamination after molding which indicates poor compatibility of the plasticisers. The loss modulus peaks by DMA were also wider for all derivatives of ESBO, which can also indicate poor compatibility. The peaks for IEEP **12** were particularly irregularly shaped, suggesting that there may be multiple glass transitions due to phase separation in the material. mPEG functionalised ESBO has been shown to be a very promising candidate for the drop-in replacement of conventional petrochemical PVC plasticisers with a bio-based, non-toxic alternative which can be efficiently prepared from commercially available ESBO whilst substantially retaining some heat-stabilizing performance.

AUTHOR CONTRIBUTIONS
Katharine Burns: Conceptualization (equal); investigation (lead); visualization (lead); writing – original draft (lead). **Ian D. V. Ingram:** Conceptualization (equal); investigation (supporting); supervision (lead); writing – review and editing (lead). **Johannes H. Potgieter:** Supervision (supporting); writing – review and editing (supporting). **Sanja Potgieter-Vermaak:** Supervision (supporting).

Applied Polymer WILEY | 13 of 13

CONFLICT OF INTEREST STATEMENT

This work was funded by Alphagary Ltd., with whom K Burns was previously employed. Alphagary Ltd. had no further influence on the investigation or findings.

DATA AVAILABILITY STATEMENT

The raw data required to reproduce these findings are available to download from https://doi.org/10.23634/MMU.00632240.

ORCID

Katharine Burns https://orcid.org/0000-0002-8568-0580
Ian D. V. Ingram https://orcid.org/0000-0002-3153-9637
Johannes H. Potgieter https://orcid.org/0000-0003-2833-7986
Sanja Potgieter-Vermaak https://orcid.org/0000-0002-1994-7750

REFERENCES

[1] L. M. De Espinosa, A. Gevers, B. Woldt, M. Grass, M. A. R. Meier, *Green Chem.* **2014**, *16*, 1883.
[2] M. Bocque, C. Voirin, V. Lapinte, S. Caillol, J. J. Robin, *J. Polym. Sci., Part A: Polym. Chem.* **2016**, *54*, 11.
[3] M. G. A. Vieira, M. A. Da Silva, L. O. Dos Santos, M. M. Beppu, *Eur. Polym. J.* **2011**, *47*, 254.
[4] I. A. Sheikh, M. A. Beg, *Reprod. Toxicol.* **2019**, *83*, 46.
[5] U. Wirnitzer, U. Rickenbacher, A. Katerkamp, A. Schachtrupp, *Toxicol. Lett.* **2011**, *205*, 8.
[6] F. Chiellini, M. Ferri, A. Morelli, L. Dipaola, G. Latini, *Prog. Polym. Sci.* **2013**, *38*, 1067.
[7] G. Wypych, *PVC Formulary*, 2nd ed., ChemTec Publishing, ON, Canada **2015**.
[8] K. Burns, J. H. Potgieter, S. Potgieter-Vermaak, I. D. V. Ingram, C. M. Liauw, *J. Appl. Polym. Sci.* **2023**, *140*, e54104.
[9] A. Guo, Y. J. Cho, Z. S. Petrovic, *J. Polym. Sci., Part A: Polym. Chem.* **2000**, *38*, 3900.
[10] B. Dahlke, S. Hellbardt, M. Paetow, W. H. Zech, *J. Am. Oil Chem. Soc.* **1995**, *72*, 349.
[11] G. Knothe, J. Krahl, J. V. Gerpen, *6.7 Soybean Oil Composition for Biodiesel, Biodiesel Handbook*, 2nd ed., AOCS Press, Urbana, IL, **2010**, p. 248.
[12] R. Turco, R. Tesser, R. Vitiello, V. Russo, S. Andini, M. Di Serio, *Catalysts* **2017**, *7*, 309.
[13] B. Lin, L. T. Yang, H. H. Dai, A. H. Yi, *J. Am. Oil Chem. Soc.* **2008**, *85*, 113.
[14] L. C. Bailosky, L. M. Bender, D. Bode, R. A. Choudhery, G. P. Craun, K. J. Gardner, C. R. Michalski, J. T. Rademacher, G. J. Stella, D. J. Telford, *Prog. Org. Coat.* **2013**, *76*, 1712.
[15] B. Zhong, C. Shaw, M. Rahim, J. Massingill, *J. Coat. Technol.* **2001**, *73*, 53.
[16] H. H. Dai, L. T. Yang, B. Lin, C. S. Wang, G. Shi, *J. Am. Oil Chem. Soc.* **2009**, *86*, 261.
[17] Y. F. Ma, F. Song, J. Yu, N. N. Wang, P. Y. Jia, Y. H. Zhou, *J. Polym. Environ.* **2022**, *30*, 2099.
[18] P. Karmalm, T. Hjertberg, A. Jansson, R. Dahl, *Polym. Degrad. Stab.* **2009**, *94*, 2275.
[19] B. Mehta, B. Kathalewar, A. Sabnis, *Polym. Int.* **2014**, *63*, 1456.
[20] C. S. Coughlin, K. A. Mauritz, R. F. Storey, *Macromolecules* **1991**, *24*, 1526.
[21] R. Bielski, G. Grynkiewicz, *Green Chem.* **2021**, *23*, 7458.
[22] K. J. Zeitsch, *The Chemistry and Technology of Furfural and its Many By-Products*, Elsevier, Amsterdam **2000**.
[23] B. M. Lee, J. Jung, H. J. Gwon, T. S. Hwang, *J. Polym. Environ.* **2022**. https://doi.org/10.21203/rs.3.rs-1275145/v1
[24] L. Chen, C. Sheng, Y. Duan, J. Zhang, *Polym.-Plast. Technol. Eng.* **2011**, *50*, 412.
[25] Z. He, Y. Y. Lu, C. Q. Lin, H. H. Jia, H. L. Wu, F. Cao, P. K. Ouyang, *Polym. Test.* **2020**, *91*, 106793.
[26] J. Tan, B. Liu, Q. Fu, L. Wang, J. Xin, X. Zhu, *Polymer* **2019**, *11*, 779.
[27] A. Campanella, L. M. Bonnaillie, R. P. Wool, *J. Appl. Polym. Sci.* **2009**, *112*, 2567.
[28] M. Rose, R. Palkovits, *ChemSusChem* **2012**, *5*, 167.
[29] P. H. Daniels, A. Cabrera, *J. Vinyl Addit. Technol.* **2015**, *21*, 7.
[30] D. T. C. Ang, Y. K. Khong, S. N. Gan, *J. Vinyl Addit. Technol.* **2016**, *22*, 80.
[31] Y. Yang, J. C. Huang, R. Y. Zhang, J. Zhu, *Mater. Des.* **2017**, *126*, 29.
[32] H. Pi, Y. Xiong, S. Y. Guo, *Polym.-Plast. Technol. Eng.* **2005**, *44*, 275.
[33] W. H. Starnes, *Prog. Polym. Sci.* **2002**, *27*, 2133.

SUPPORTING INFORMATION

Additional supporting information can be found online in the Supporting Information section at the end of this article.

How to cite this article: K. Burns, I. D. V. Ingram, J. H. Potgieter, S. Potgieter-Vermaak, *J. Appl. Polym. Sci.* **2023**, e54656. https://doi.org/10.1002/app.54656

Synthesis and performance evaluation of novel soybean oil-based plasticisers for polyvinyl chloride (PVC) Supplementary Information

K. Burns, I. D. V. Ingram, J.H. Potgieter and S. Potgieter-Vermaak

Calculations used for Figure 1

Peaks were identified in the ^{1}H NMR spectra corresponding to the epoxide groups (3.2-2.8 ppm), glycerol esters (5.2 and 4.2 ppm), methyl ether (3.4 ppm) and methyl ester (3.6 ppm). The spectra were integrated and normalised to the fatty acid alpha-carbonyl ester peak at 2.3 ppm, which was set to 6 (as in a triglyceride structure). The values presented in Figure 1 were calculated as follows.

Conversion of Epoxide = 100 – (Epoxide peak area (3.2-2.8 ppm)/ESBO epoxide peak area [%])

Number of opened Epoxides = (ESBO epoxide area – Epoxide area)/2 [†]

New Methyl Ether groups = Methyl ether area (3.4 ppm)/3

Selectivity to Methyl Ether = New methyl ether groups / Opened epoxide groups [%]

Conversion of Glycerol Esters = (ESBO Glycerol ester area (5.2, 4.2 ppm, 5H) – glycerol ester area)/ESBO glycerol ester area [%]

Selectivity to methyl Ester = (Methyl ester peak (3.6 ppm)/9[‡]) * Conversion of glycerol esters

---

[†] 2 protons per epoxide group

[‡] As 9 is the maximum proton count for methyl esters relative to 6H present in triglyceride structure.

Analysis and structural determination of the synthetic products

All structures and assignments presented herein are shown as a simplified form of the ESBO triglyceride, based on a fatty acid chain with a single epoxide group. The true products will contain a statistical mixture of original ESBO composition with 0, 1 or 2 epoxide groups per fatty acid chain, of which some will have undergone reaction and some will remain intact. The structures are shown as the product of a reaction in a chain with a single epoxide functionality. Peak areas were normalised to 6H at the α-carbonyl position (2.3 ppm).

Methyl Ether ESBO Polyol - MEEP 9
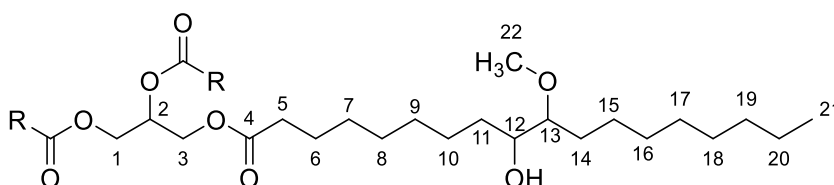
Methyl Ether ESBO Polyol, **9**

Simplified structural representation (R- groups may vary in chain length and contain 0, 1 or 2 reacted and unreacted epoxide groups).

^{1}H NMR (400 MHz, CHLOROFORM-*D*) δ 5.26 (1H, m, H2), 4.29 (2H, dd, *J* = 11.8, 4.2 Hz, H1,H3), 4.14 (2H, dd, *J* = 11.9, 5.9 Hz, H1, H3), 3.52 − 3.42 (3H, m, H12,13), 3.41 (3H, s, H22), 2.99 (1H, q, J = 5.7 Hz, unreacted epoxide, not shown) 2.31 (6H, t, *J* = 7.6 Hz, H5), 1.61 - 1.26 (64H, m, H6-11, 14-20), 0.88 (9H, m, H21).

^{13}C NMR (101 MHz, CHLOROFORM-D) δ 173.43, 173.01 (C4), 84.46, 72.74 (C13), 68.98 (C2), 62.21 (C1, C3), 58.25 (C22), 56.75 (C15,16), 50.97, 39.14, 38.83, 38.05, 34.30, 33.63, 33.51, 32.19, 32.05, 32.01, 30.11, 30.02, 29.88, 29.82, 29.60, 29.49, 29.40, 29.24, 29.18, 26.11, 25.90, 25.16, 24.98, 24.93, 22.81, 22.74, 14.25, 14.20 (C21).

FTIR-ATR (v_{max} cm^{-1}) − 3456 (O-H stretch), 2926, 2855 (sp^3 C-H stretch), 1742 cm^{-1} (C=O stretch).
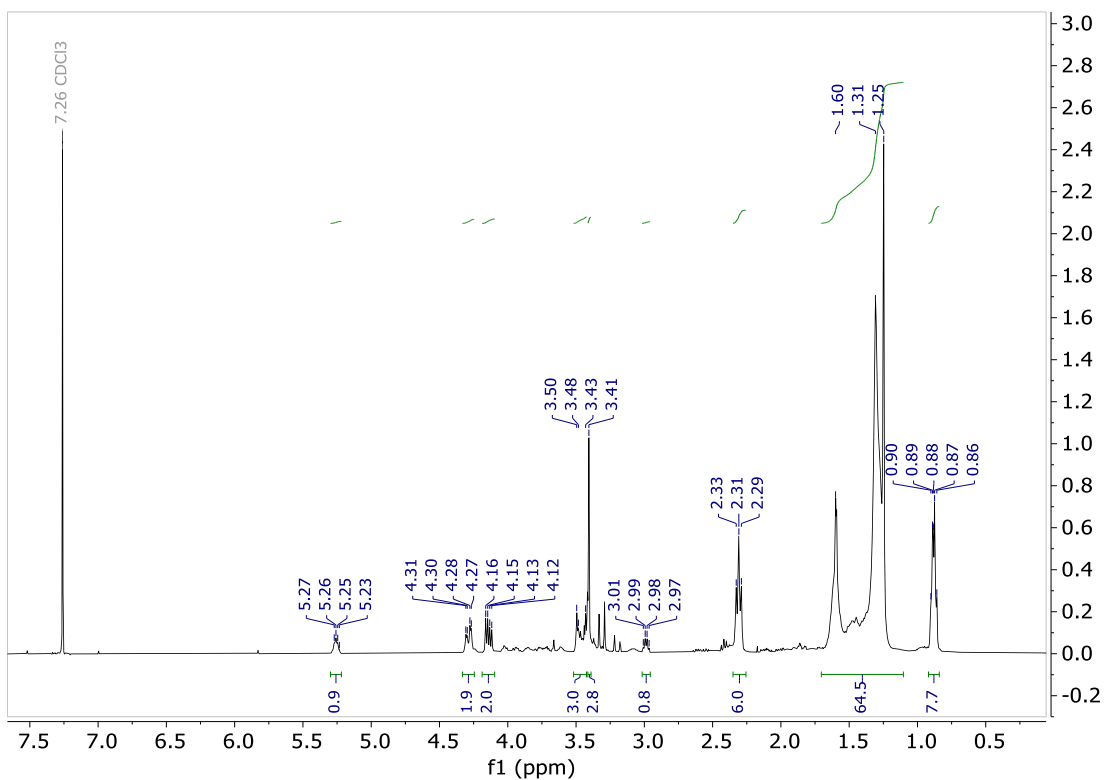
Figure S1: ^{1}H NMR of methyl ether ESBO polyol
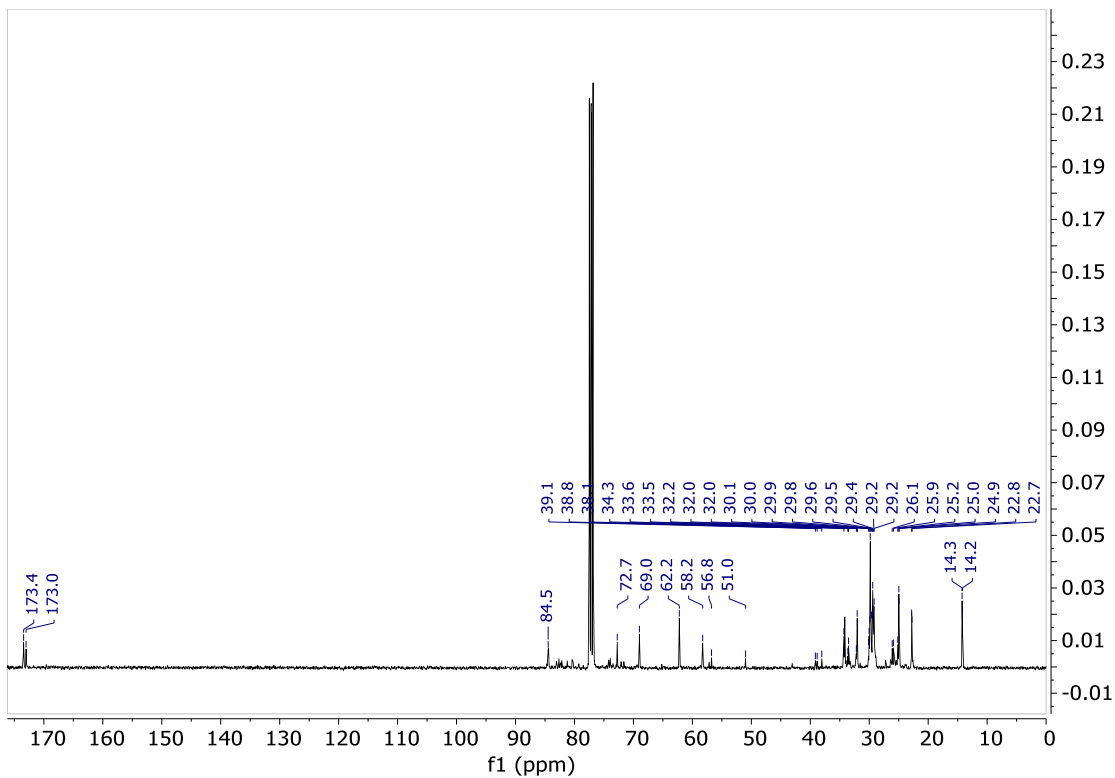
Figure S2: ^{13}C NMR of methyl ether ESBO polyol
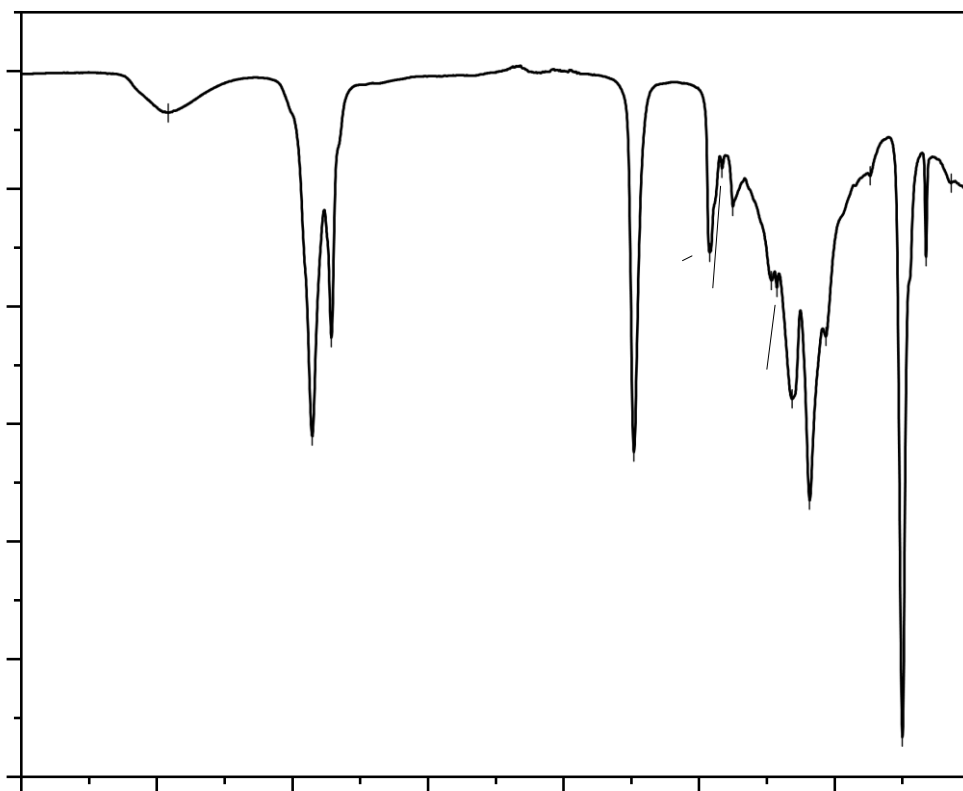
Figure S3: FTIR-ATR of methyl ether ESBO polyol

Methoxy polyethylene glycol ESBO ether - mPEG-ESBO, 10
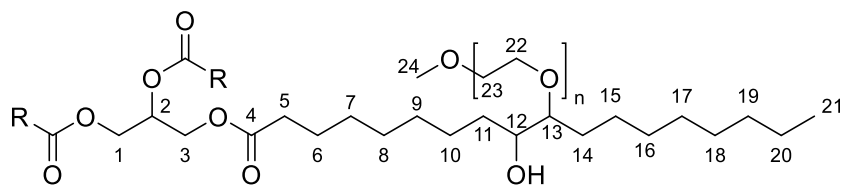
mPEG-ESBO, **10**

Simplified structural representation (R- groups may vary in chain length and contain
0, 1 or 2 reacted and unreacted epoxide groups).

1H NMR (400 MHz, CHLOROFORM-D) δ 5.25 (1H, m, H2), 4.29 (4H, m, H1, H3), 3.65 (34H, s, H22, H23), 3.55 (4H, m, H12, H13), 3.38 (5H, s, H24), 2.31 (6H, t, J = 7.6 Hz, H5), 1.76-1.13 (74 H, m, H6-11, 14-20), 0.88 (9H, m, H21).

^{13}C NMR (101 MHz, CHLOROFORM-D) δ 173.36, 172.95 (C4), 104.95, 104.88, 72.02 (C13), 70.65 (C12), 70.38 (C22, C23), 68.96 (C2), 62.18 (C1, C3), 61.79, 59.13 (C24), 42.94, 42.85, 42.80, 36.10, 34.25, 34.14, 34.08, 32.02, 31.96, 31.91, 31.69, 31.51, 29.79, 29.75, 29.57, 29.46, 29.37, 29.21, 29.16, 29.10, 28.98, 28.17, 28.12, 27.91, 24.95, 24.90, 23.98, 23.89, 23.83, 22.78, 22.67, 22.52, 14.22 (C21).

FTIR-ATR (v_{max} cm^{-1}) – 3476 (O-H stretch), 2925, 2856 (sp^3 C-H stretch), 1742 (C=O stretch).
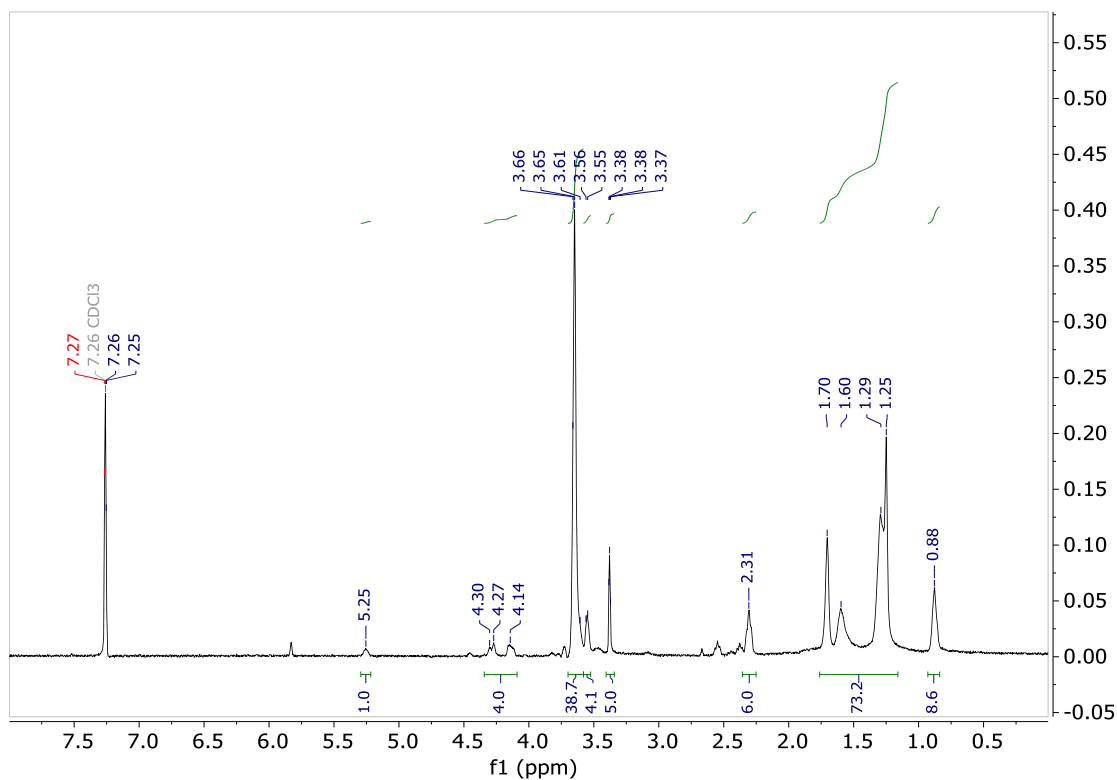
Figure S4: ^{1}H NMR of Methoxy polyethylene glycol ESBO ether
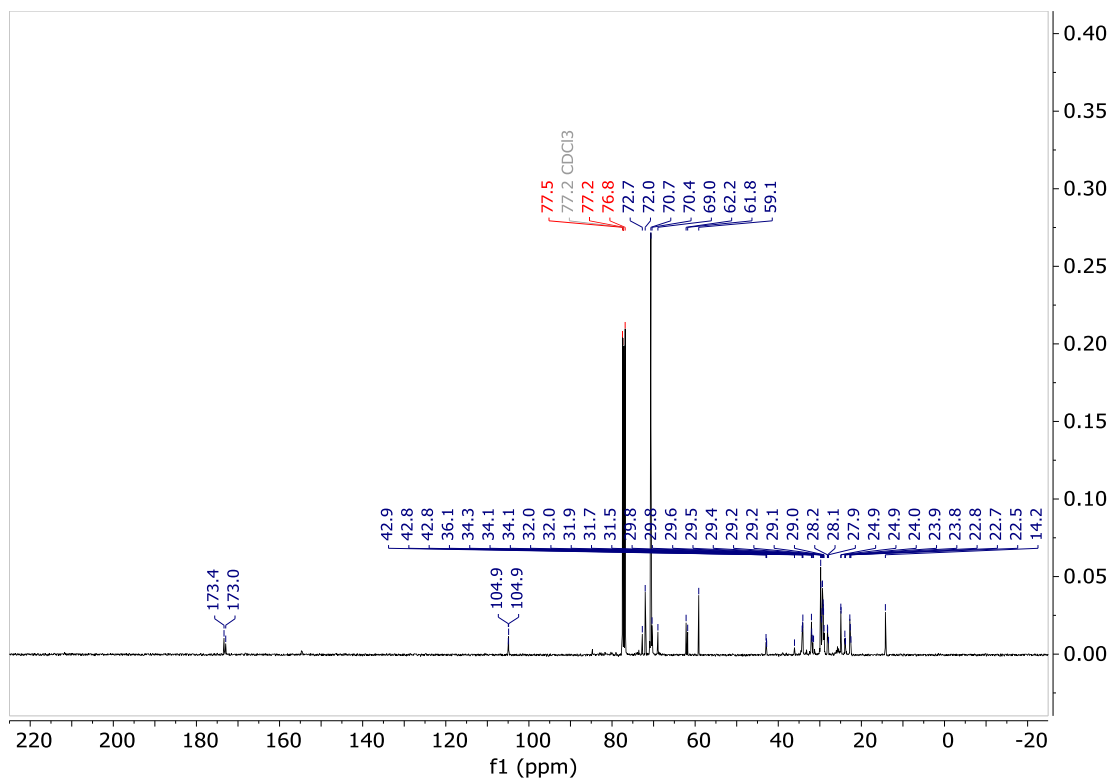
Figure S5: ^{13}C NMR of Methoxy polyethylene glycol ESBO ether
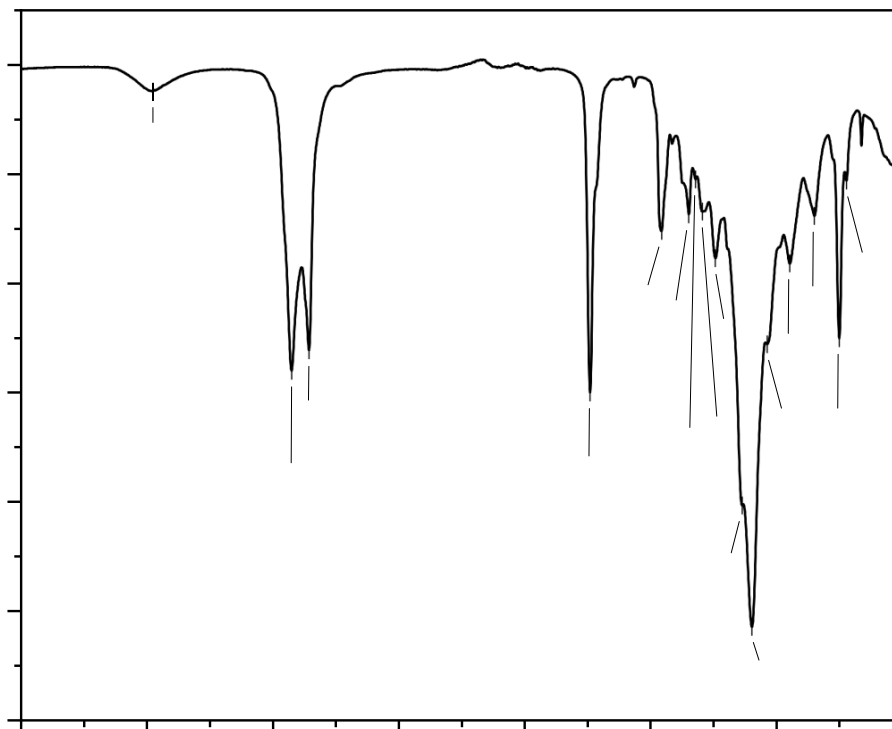
Figure S6: FTIR-ATR of Methoxy polyethylene glycol ESBO ether

Methyl ESBO Furoic Ester - MEFE 11
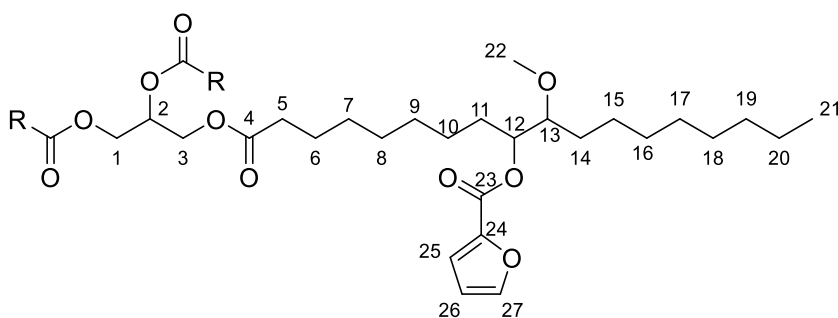
Methoxylated ESBO Furoic Ester, **11**

Simplified structural representation (R- groups may vary in chain length and contain 0, 1 or 2 reacted and unreacted epoxide groups).

^{1}H NMR (400 MHz, CHLOROFORM-*D*) δ 7.88 – 7.49 (2H, m, H25, H27), 6.51 (1H, m, H26), 5.25 (1H, m, H2) 4.34 – 4.08 (4H, m, H1, H3), 3.41 (2H, s, C22), 2.99 (<1H, m, unreacted epoxide, not shown), 2.35 (3H, s), 2.31 (6H, t, J = 7.6 Hz, H5), 2.09 (s, 5H) 1.72 – 1.16 (72H, m, H6-11, H14 -20), 0.87 (9H, t, J = 6.9 Hz, H21).

^{13}C NMR (101 MHz, CHLOROFORM-D) δ 173.42, 130.14, 129.44, 129.17, 128.36, 128.15, 126.67, 125.43, 111.93, 68.99, 65.20, 62.21, 34.18, 32.06, 29.84, 29.79, 29.64, 29.50, 29.41, 29.25, 25.82, 24.97, 22.82, 21.59, 14.26, 14.17.

FTIR-ATR (v_{max} cm^{-1}) 3020 (sp^2 C-H stretch), 2927, 2856(sp^3 C-H stretch), 1735 (C=O stretch), 1661 (C=C stretch).
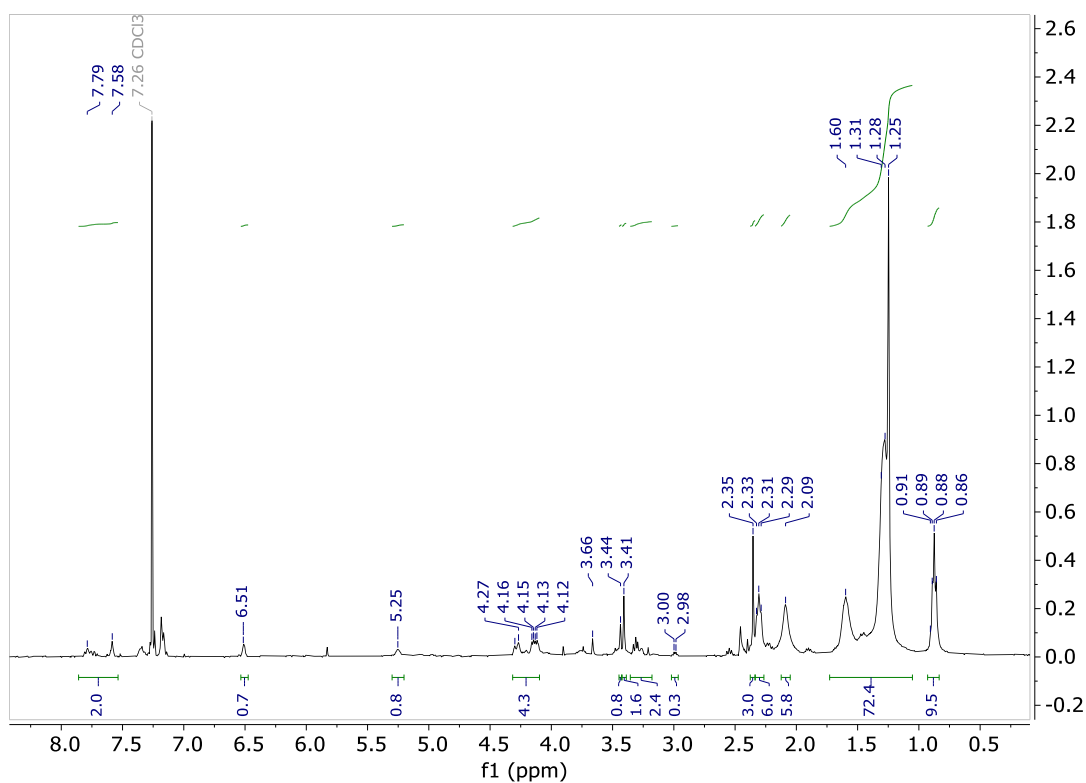
Figure S7: ^{1}H NMR of Methyl ESBO Furoic Ester
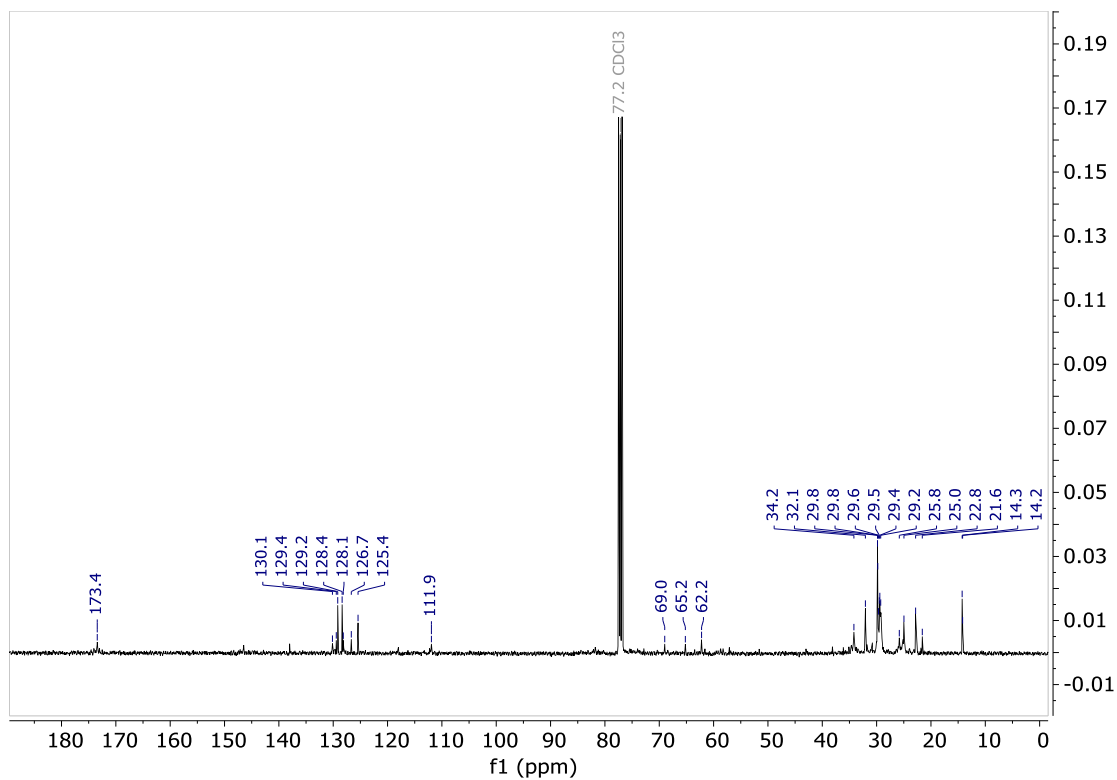
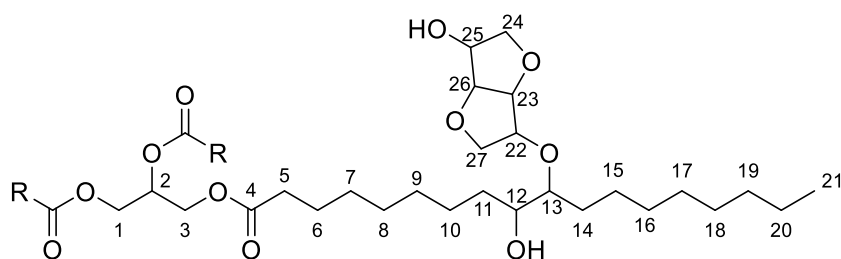Figure S8: ^{13}C NMR of Methyl ESBO Furoic Ester
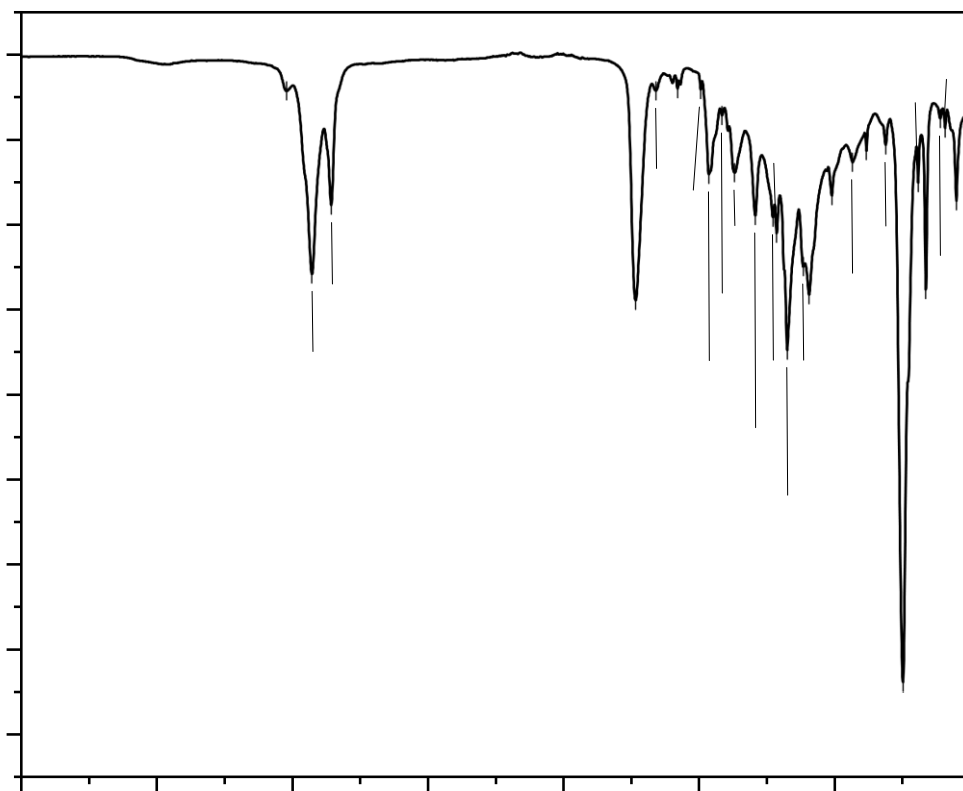
Figure S9: FTIR-ATR of Methyl ESBO Furoic Ester

Isosorbide Ether ESBO Polyol - IEEP 12

Isosorbide Ether ESBO Polyol, **12**

Simplified structural representation (R- groups may vary in chain length and contain 0, 1 or 2 reacted and unreacted epoxide groups).

^{1}H NMR (400 MHz, CHLOROFORM-D) δ 5.25 (1H, m, H2), 4.7-4.4 (1H, m), 4.21 (4H, ddd, J = 59.9, 11.7, 5.1 Hz, H1, H3), 4.05 – 3.53 (6H, m, H22-H27), 3.49 – 3.37 (4H, m, H12, H13), 2.31 (6H, t, J = 7.6 Hz, H5), 1.70 – 1.20 (70, m, H6-11, H14-20), 0.88 (9H, m, H21).

^{13}C NMR (101 MHz, CHLOROFORM-D) δ 173.46, 104.91, 70.76, 68.98, 62.22, 43.01, 34.29, 34.14, 32.06, 29.84, 29.80, 29.61, 29.51, 29.41, 29.22, 28.18, 26.61, 24.98, 24.02, 22.81, 22.73, 14.28.

FTIR-ATR (v_{max} cm^{-1}) − 3457 (O-H stretch), 2926, 2855 (sp^3 C-H stretch), 1741 (C=O stretch).
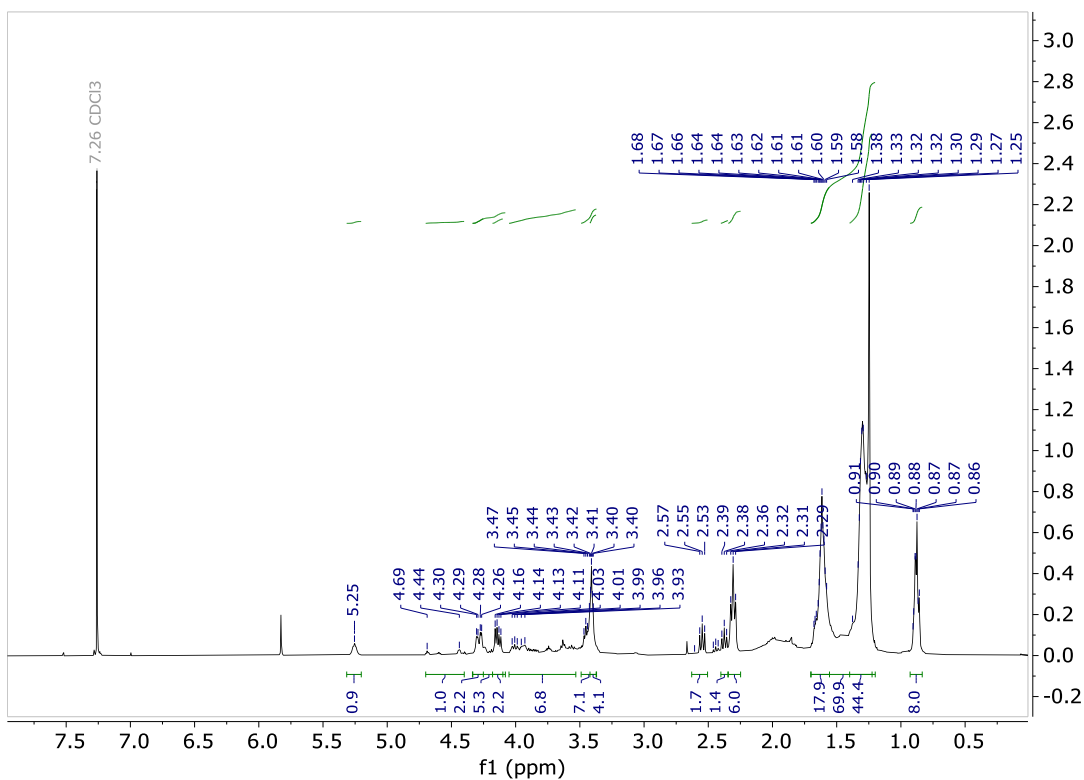
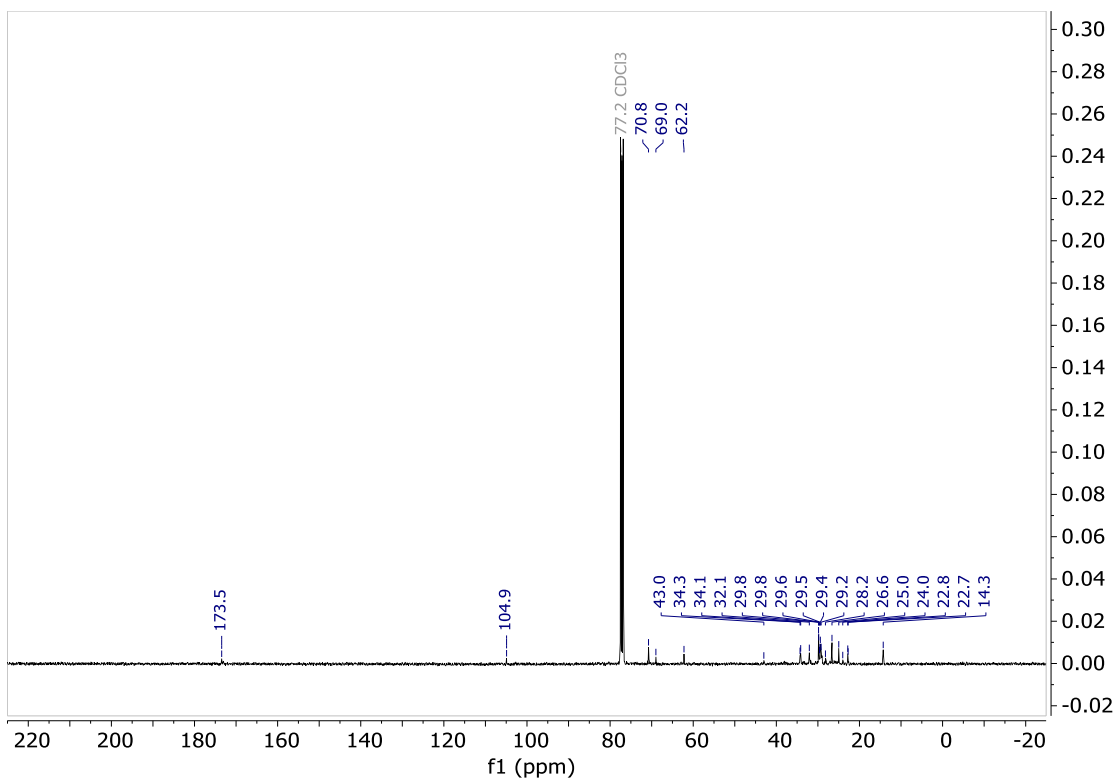Figure S10: ^{1}H NMR of Isosorbide Ether ESBO Polyol

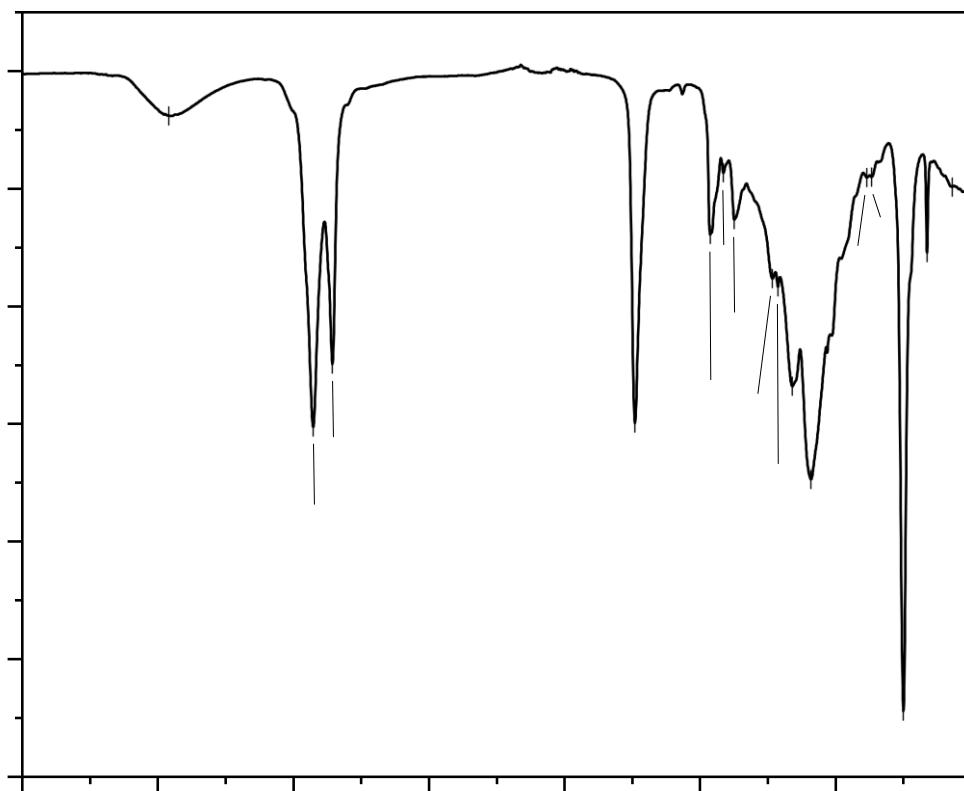Figure S11: ^{13}C NMR of Isosorbide Ether ESBO Polyol

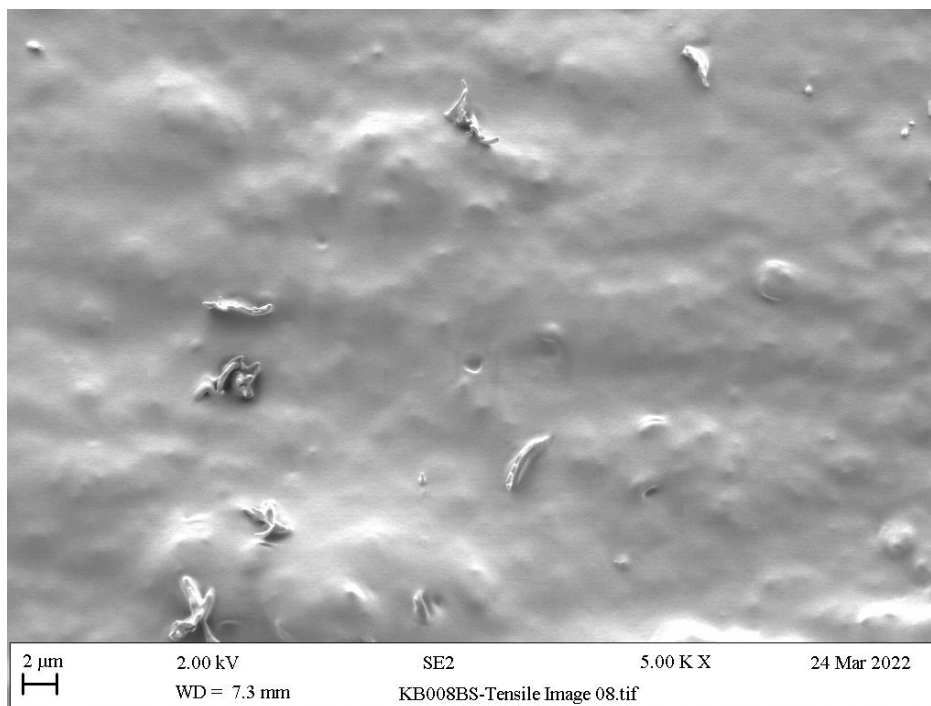Figure S12: FTIR-ATR of Isosorbide Ether ESBO Polyol

Figure S13: SEM micrograph of PVC-mPEG-ESBO (**10**) fracture surface showing a largely flat surface indicating brittle failure.
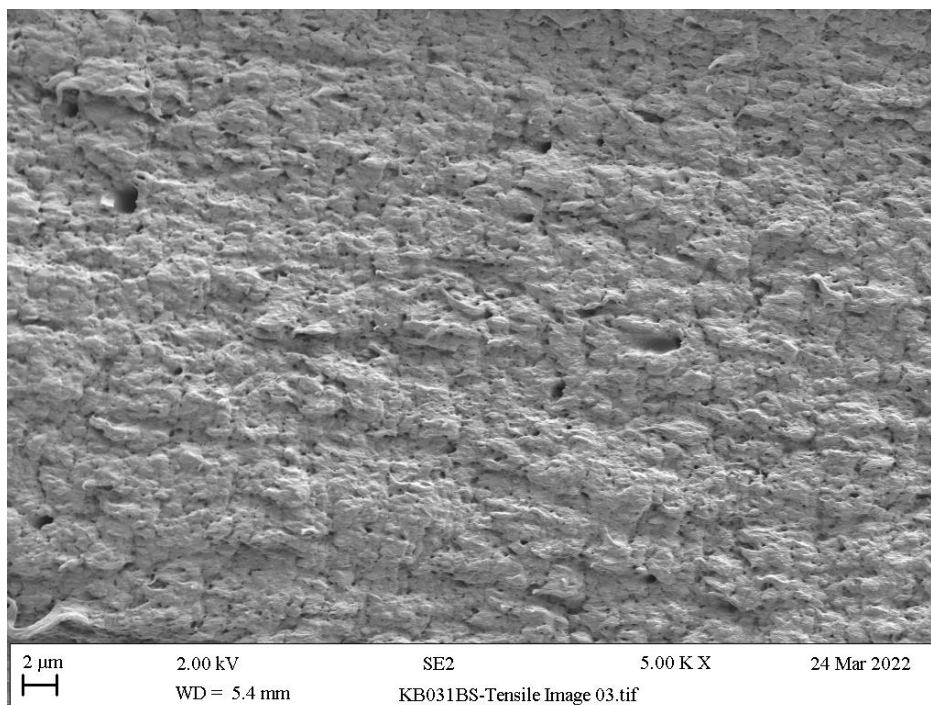

Figure S14: SEM micrograph of PVC-IEEP (**12**) fracture surface showing a rough surface indicating brittle-ductile failure.
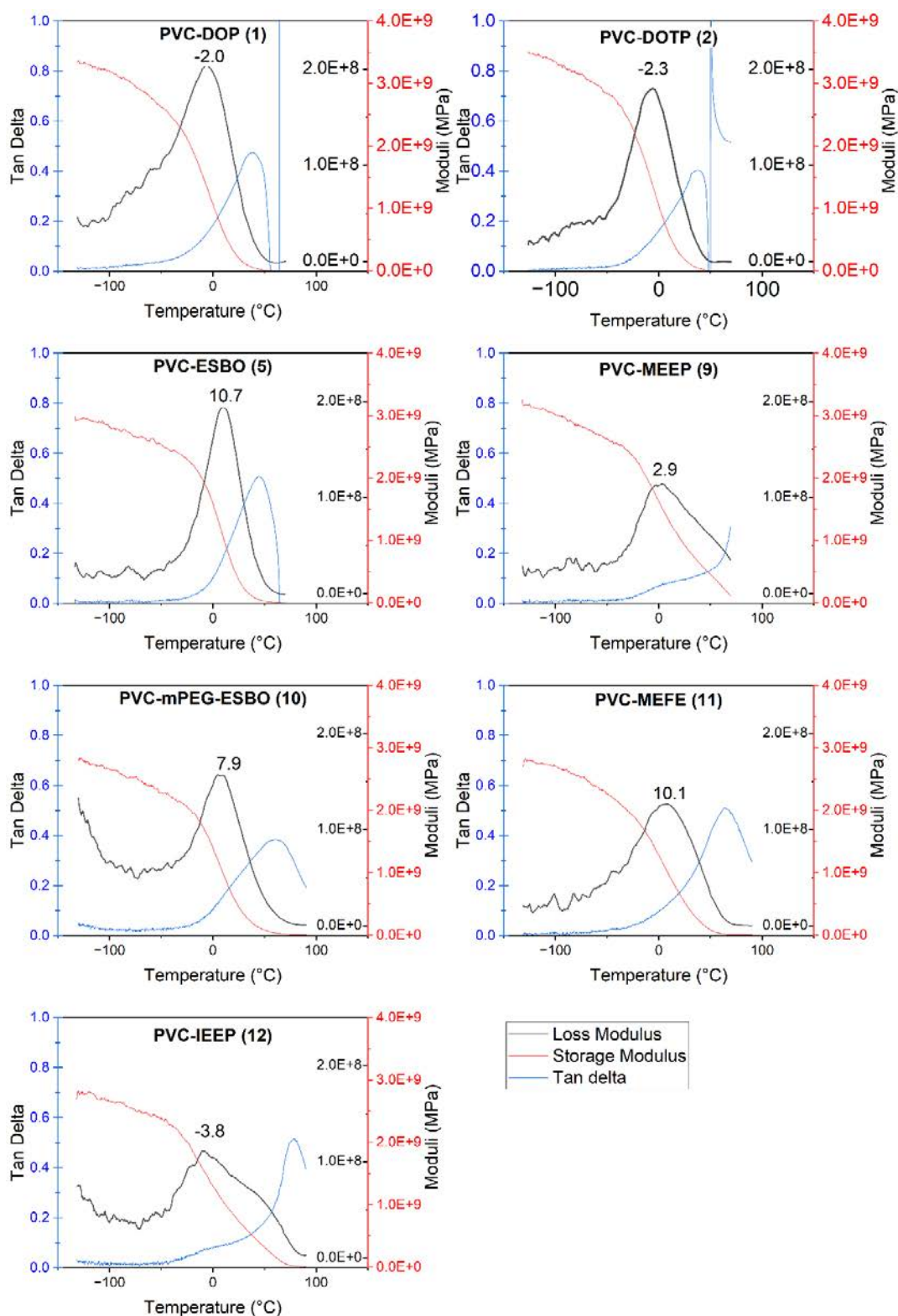
Figure S15: TGA analysis of plasticised PVC samples showing storage modulus, loss modulus and tan delta, with the loss modulus peak indicating glass transition temperature labelled.